FORECASTING FUTURES - THE EFFECT OF AGE, ABUNDANCE, AND HARVESTING ON THE LONG-TERM SUSTAINABILITY OF MARINE FISHES

by

David M. Keith

Submitted in partial fulfillment of the
requirements for the degree of
Doctor of Philosophy

at

Dalhousie University
Halifax, Nova Scotia
August 2014

To my mum who is probably the only person that will ever read this whole thing!

Table of Contents

List of Tables

List of Figures

Abstract

In the first part of this thesis I attempt to address some of the concerns regarding the stock-recruitment relationship that have been voiced over the last 50 years. In chapter 2 I revisit the shape of the stock-recruitment relationship at low abundance. I show that at these low abundances an increase in productivity is not ubiquitous. In many populations the dynamics are essentially density independent after the populations decline below 40% of maximum historic SSB, and in some species the productivity actually starts to decline below this threshold. Given the weakening of compensation in many populations, in chapter 3 I examine how per capita harvest mortality changes with abundance. The results show that in the majority of populations, per capita mortality continues to increase with declines in abundance. In Chapter 4, I attempt to address concerns that have been raised about the effect of age structure on recruitment. Here, I break down the relationship to determine whether there is an effect of first time (virgin) or repeat spawners in terms of average size, and the relative abundance of large and small fish. The results suggest that these age-specific components of the spawning stock contribute differentially to recruitment across a wide range of species and populations. In Chapters 5 and 6 I change the focus and use a technique widely used in terrestrial ecology to estimate both the risk of collapse and the probability of persistence for numerous populations of Atlantic cod (*Gadus morhua*) and Atlantic herring (*Clupea harengus*). In chapter 5 the models indicate that periods of unusually elevated recruitment are vital to the persistence of all the populations analyzed. In Chapter 6, I look specifically at the potential impact that different management actions and environmental variability may have on population recovery for an endangered Atlantic cod population in the Gulf of St. Lawrence. Throughout this thesis, I attempt to address problems in fisheries science from a more ecological perspective than that traditionally used in fisheries science. More collaboration between ecologist scientists and fisheries scientist will only help to improve our understanding of population dynamics in both marine and terrestrial ecosystems.

Acknowledgements

First and foremost I want to thank Dr. Jeff Hutchings for taking a chance on me and giving me the opportunity to work with so many world class scientists (and to hang out in Santa Barbara once in a while!). I am also indebted to the many scientists from across the globe for providing the data used in this thesis. In this vein I especially would like to acknowledge Dan Ricard and Coilin Minto for their guidance during the early phase of this project. I also must thank my great lab-mates over the past several years, first Paul Debes thanks for being German, hours of statistical rants, and lots of great discussion about fisheries science. Nancy Roney for your craziness, all the help putting together the database, and for being Nancy. Rebekah Oomen thank you for picking such a wonderful husband and supplying us with endless baked goods and chocolate. Njal Rollinson for... I have no idea exactly, but your awesome. Meghan McBride for being an ear to lean on when science went bad. Finally, thanks to Steph Mogensen for showing me the ropes around during my early daze at Dalhousie. From a previous life, thanks to Ellen Lea for showing me that I could take a different path and Dr. John Post for helping me find it. The biggest thanks of all of course goes to Nadine for putting up with all the foolish of my decade long return to school. Finally, thanks to Kaden for giving me eleven years of epic distractions. Extra-finally, I should also thank my funders at NSERC for giving me enough money to get Kaden through 4 years of being a goalie and still being able to eat.

Chapter 1

Introduction

The underpinnings of fisheries science in the latter half of the 20th century can be traced back to the concept of maximum sustainable yield (MSY), first proposed in the late 1940's [15]. The theoretical biological assumptions underlying the MSY concept is that there is a density dependent compensatory decline in mortality within a population when its abundance is reduced. Although this concept had been discussed since the 1930's, the seminal works in fisheries science that directly incorporated compensation can be traced to the stock-recruitment models developed in the 1950's [10,27,89].

From the outset, when these stock-recruitment models were being developed, there were several concerns about their general applicability. Ricker [89] hypothesized that the strength of compensation in iteroparous spawners is dependent on the number of age classes; if the number of age classes declines, compensatory mechanisms will be weakened by random environmental fluctuations. He further suggested that a depression in reproductive rates at low abundances is likely to be fairly common in commercially harvested marine fishes, a suggestion that was not revisited in any significant way for several decades [78]. Within a few years, Ricker [90] proposed that, in highly variable environments, depensation (termed 'Allee effect' in non-fisheries literature) has the potential to lead to population collapse and that fishing pressure must be reduced when recruitment is weak in these populations. He went on to suggest that highly variable quotas are necessary to ensure fisheries do not collapse. He also noted that, when a fishery captures more than one species, MSY management could lead to the extinction of less productive species. Ricker clearly recognized the limitations of his model and already noted that "poor resistance to exploitation at low stock densities" [90, p. 999] was evident in some Pacific salmon (Oncorhynchus spp.) populations. Despite these caveats, the fisheries science community adopted the MSY cause with considerable enthusiasm and not always with an appropriate degree of caution throughout the following decades [27, 59].

In the first half of this thesis, I attempt to address some of the concerns voiced by Ricker over half a century ago. Chapter 2 revisits the shape of the stock-recruitment relationship at low abundance. Instead of addressing this question using standard stock-recruitment relationships, I developed a hierarchical ANOVA that assumes no functional relationship between recruitment and spawning stock biomass (SSB). At low abundances, the models typically employed by fisheries scientists have generally assumed population dynamics increasingly become more "productive" (i.e. per capita recruitment rate will increase). I show that at these low abundances an increase in productivity is not ubiquitous. In many populations the dynamics are essentially density independent after they decline below 40% of maximum historic SSB, and in some species the productivity actually starts to decline below this threshold. Thus, I provide strong evidence that one of the primary assumptions of traditional fishery models does not hold for all populations at low abundance.

Given the weakening of compensation in many populations, I next examined how per capita harvest mortality changes with abundance. As suggested by Ricker [90], if per capita harvest mortality does not decline when production is low this can have serious consequences for the harvested population. In Chapter 3 I explore the relationship between harvest mortality and abundance and how this relationship varies with age, taxonomic group, and management agency. I find that, in the majority of populations, per capita mortality continues to increase with declines in abundance.

In Chapter 4, I address Ricker's concern about the effect of age structure on recruitment [89]. Traditional stock-recruitment models combine age, abundance, and fecundity (mass) into a single variable (SSB) and these models implicitly assume that none of these factors influence recruitment differentially [39]. Here, I break down the relationship to determine whether there is an effect of first time (virgin) or repeat spawners in terms of average size, and the relative abundance of large and small fish. The results suggest that different components of the spawning stock contribute differentially to recruitment across a wide range of species and populations.

In Chapters 5 and 6 I change the focus from a retrospective analysis, attempting to understand the processes controlling population dynamics, to forecasting the long-term viability of several populations of Atlantic cod (*Gadus morhua*) and Atlantic herring (*Clupea harengus*). I borrow a technique widely used in terrestrial biology

to estimate both the risk of collapse and the probability of persistence for numerous populations of both species. Population viability analysis (PVA) has been used for decades in terrestrial ecosystems to estimate the risk of extinction, but it has rarely been used for harvested marine populations to estimate their long-term fate [3]. I utilize sensitivity analysis to determine how small changes in survival and fertility of any one age class influences the probability of persistence of these populations. These models were also used to identify the central role that periods of unusually elevated recruitment have on persistence in all the populations analyzed. In Chapter 6, I look specifically at the potential impact that different management actions could have on population recovery for an endangered Atlantic cod population in the Gulf of St. Lawrence. In addition, I explore the effect of environmental variability in terms of the strength, frequency, and duration of unusually elevated recruitment events and how this influences the potential for recovery in this population.

The questions addressed in Chapters 3-6 required the development of a novel database which includes time series of age-specific measures of abundance, individual mass, maturity, and harvest rates for over 100 populations. The development of this database was a critical component of this thesis and I believe that the database will be a very useful tool for exploring how age might influence harvested populations in both terrestrial and marine ecosystems for many years.

Chapter 2

Population dynamics of marine fishes at low abundance

2.1 Introduction

Numerous marine fishes have experienced unprecedented fishing-induced declines over the last half-century [50]. Despite considerable reductions in fishing mortality [124] many stocks have not recovered at the rate that would have been predicted based on classical and stationary population dynamics [22, 45, 53].

Historically, studies of the population dynamics of commercially exploited fishes, including numerical responses to changes in fishing mortality, have relied on Ricker and Beverton Holt stock-recruitment (S-R) models to describe the relationship between abundance and offspring production [10, 89, 90]. Both of these formulations predict that per capita recruitment (recruitment is the number of offspring that survive to enter a fishery) will increase as abundance declines. The compensatory (negative density-dependent) relationship between per capita recruitment and abundance has underlain much of fisheries management, although even Ricker [90] acknowledged the limitations of his model, remarking that "poor resistance to exploitation at low stock densities" [90, p. 999] was evident in some Pacific salmon (*Oncorhynchus* spp.) populations. More recently, the use of these models has been questioned because of the observation that non-parametric models can provide more robust alternatives to the fitting of a stock-recruitment relationship when the actual relationship is unknown [74]. Despite these caveats there has been little effort to account for a lack of strong compensation at low abundance, in part because of an absence of strong empirical support for the existence of Allee effects, or depensation, in meta-analyses of marine fishes [62, 78]. Slow or absent recovery in many depleted populations [44], despite reductions in fishing mortality [45], has led to suggestions that Allee effects might comprise a more important component of marine fish population dynamics than previously thought [28, 54, 99].

Thus, the question of whether per capita recruitment generally increases with

declining abundance when populations are at very low abundance is a fundamentally important one from a conservation and resource management perspective. Although previous research has generally failed to detect an Allee effect in marine fishes, the statistical power of these analyses was comparatively low, primarily because of the paucity of recruitment data available at low levels of spawning stock abundance [62, 78]. Additionally, Allee effects at the population level may be undetectable when these population data are aggregated across several populations [28].

The theoretical impact of Allee effects on population dynamics is well established and numerous mechanisms that might affect offspring production at low abundance have been hypothesized [104, 105], including difficulties in mating success [8, 25, 93], cultivation induced changes to food webs [120], and increased predator-related mortality resulting from increased aggregation at low abundance [19, 84].

My objective here is to quantitatively analyze the relationship between recruitment and spawning stock biomass (SSB) in commercially exploited marine fishes. Analytically, I develop a simple Bayesian hierarchical model to determine how recruitment changes with SSB. The change in recruitment per spawner biomass ($\frac{Recruits}{SSB}$) was then modelled for various levels of SSB for 207 stocks. The results show a range of dynamics between $\frac{Recruits}{SSB}$ and SSB. Although $\frac{Recruits}{SSB}$ increases with decreasing SSB for many species, the S-R dynamics of a substantial number of species exhibits weak compensation, density independence or an Allee effect as stock size declines.

2.2 Methods

Using data collated in the RAM II-SRDB [88] I analyzed commercially exploited teleost marine fishes for which there were more than 10 years of data on both recruitment (thousands of individuals) and SSB (tonnes), and for which stock size and recruitment were estimated by commonly employed fisheries models (e.g. Virtual Population Analysis (VPA), Statistical Catch-at-Age(SCA)). There were 207 stocks (representing 104 species within 7 orders) with time series ranging between 10 and 96 years in duration (median of 32 years), resulting in a total of 7290 data points (Table A1) with approximately 22% (46) of the stocks having data in the lowest SSB bin. The Statistical Catch-at-Age models included in this analysis are fit using an underlying stock-recruitment curve which assumes a compensatory relationship between

recruitment and SSB. A complementary analysis was run on the subset of data that excluded the SCA stocks to determine what effect their exclusion might have on the results. This analysis included 99 stocks, representing 59 species within 7 orders, and the results of the non-SCA analysis are summarized in appendix A (Figs. A.1-A.6).

The response variable was the number of recruits per kg of spawning stock biomass ($\frac{Recruits}{SSB}$). Spawning stock biomass is often used as a proxy for a populations total fecundity. Thus no change in $\frac{Recruits}{SSB}$ with changing SSB would suggest that the recruitment was independent of total fecundity (i.e. density independent). In fisheries stock recruitment models $\frac{Recruits}{SSB}$ is assumed to increase as SSB declines, and an Allee effect would be manifested by a decrease in $\frac{Recruits}{SSB}$ with declining SSB (Fig. 2.1).

To facilitate the meta analysis the $\frac{Recruits}{SSB}$ and SSB metrics were standardized. The ratio of SSB to the historical maximum SSB was grouped into one of seven SSB percentage categories, $< 10\%$, 10-20%, 20-30%, 30-40%, 40-60%, 60-80%, and 80-100%, a binning of S-R data which follows that applied by Myers and Barrowman [77] in their study of the relationship between stock size and recruitment. These particular categories were chosen to provide for more detailed contrasts of the relationship between $\frac{Recruits}{SSB}$ and SSB at low abundance, while retaining sufficient data within the respective categories to allow for the characterization of general trends throughout the entire range of data. This categorization enables us to estimate the shape of the stock recruitment relationship without the constraints of a parametric model. This method assumes that the maximum biomass observed for each stock is a good estimate of the stocks carrying capacity (K), and that there is equal variance between the stock's SSB categories.

The $\frac{Recruits}{SSB}$ data were initially log transformed to normalize the data. These log transformed $\frac{Recruits}{SSB}$ data were standardized (Z) so that species with highly variable $\frac{Recruits}{SSB}$ could be compared in common units of standard deviations from $\overline{ln(\frac{Rec}{SSB})}$.

$$Z_{ij} = \frac{\ln\left(\frac{Rec}{SSB}\right)_{ij} - \left(\overline{\ln\frac{Rec}{SSB}}\right)_j}{sd\left(\ln\frac{Rec}{SSB}\right)_j} \tag{2.1}$$

where i represents the individual data point, and j is the species. This analysis tests how deviations of $\frac{Recruits}{SSB}$ from the species log-mean $\frac{Recruits}{SSB}$ vary with changes in SSB. The standardization also permits comparison between stocks both within and

between higher taxonomic levels.

We constructed a multilevel Bayesian Analysis of Variance (ANOVA) framework for analytical purposes primarily because this modeling approach provides flexibility to develop a model with no strong assumptions about the relationship between $\frac{Recruits}{SSB}$ and SSB, thus avoiding problems that can occur when attempting to determine the shape of specific S-R models at low abundance [62, 78]. SSB category, the interaction between species and SSB category, and the interaction between order and SSB category were included in the model;

$$\begin{aligned} y_i &= \gamma_{ssb} + \delta_{ssb,species} + \eta_{ssb,order} + \epsilon_i \\ \delta_{ssb,species} &\sim N(\mu_\delta, \sigma_\delta^2) \\ \eta_{ssb,order} &\sim N(\mu_\eta, \sigma_\eta^2) \end{aligned} \tag{2.2}$$

where i is an individual data point, y is $Z_{\ln\left(\frac{Rec}{SSB}\right)}$ (hereafter $\mathrm{Z}_{\frac{\mathrm{Recruits}}{\mathrm{SSB}}}$, standardized number of log transformed $\frac{Recruits}{SSB}$ is used), γ_{ssb} the mean of each SSB category and was treated as a fixed effect, $\delta_{ssb,species}$ is the interaction term between species and SSB category, and $\eta_{ssb,order}$ is the interaction term between order and SSB category. Each interaction (species and order) in the model was treated as a random variable and assigned a normal distribution with its mean (μ_δ and μ_η, fixed effects) and variance (σ_δ^2 and σ_η^2) estimated from the data. The priors for each μ was a zero mean normal prior with σ^2 estimated from the data, for the variance priors an identical vague uniform prior was set on each standard deviation, e.g. $\sigma_\delta \sim U(0, 5)$ [33]. Models including other taxonomic levels (e.g. stock, genus, family) were also investigated, but these more complex models had to be excluded from further consideration because of data limitations.

Analyses were conducted using R, version 2.14, while Markov chain Monte Carlo (MCMC) sampling was performed using the R2WinBUGS package, and WinBUGS Version 1.4.3 [65, 87]. The model was run for 80,000 time steps, with an initial burn in period of 5000. To eliminate auto-correlation in the MCMC chains, they were thinned, such that only every 200^{th}data point was used. In addition three separate chains were run to check for non-convergence of each parameter. Model convergence was assessed via a visual inspection of the MCMC sampling chains, and using the Gelman and Rubin convergence diagnostic $\hat{R}$. The highest value of $\hat{R}$ that was observed for any parameter was 1.024 which is less than the threshold value of 1.1

suggesting there is little evidence of non-convergence for any of the parameters [33]. Posterior predictive checks (PPC's) were used to visually assess the model fit; (Fig. A.8a) the model produced reasonable estimates for each species and SSB category within the model [33]. Additionally, a Bayesian p-value of 0.50 was estimated based on the model results. A well fit model will have a Bayesian p-value near 0.5, while a poorly fit model would have Bayesian p-values skewed towards 0 or 1 [57]. Standard residual plots were checked to ensure the error terms were homoscedastic. Finally, a sensitivity analysis was performed to test the influence of individual stocks on the results for each species (Fig. A.9a). In the vast majority of cases removing one stock had little influence on the model estimates, with exceptions noted in the text.

Bayesian hierarchical models have several advantages over a traditional modelling framework. Using these methods, the variance explained for each hierarchical level can be estimated. This allows for a better understanding of the influence of each level on the model fit [33]. These models also allow for a partial pooling of the results, thus allowing for multiple comparisons without an additional penalty [34]). The final advantage is the ability to estimate coefficients for terms at each hierarchical level, allowing for an accurate estimate of the size and direction of any effect at each level in the model [32, 34]).

Several different comparisons were made when analyzing these data. The primary analysis looked at the contrast between the lowest and second lowest SSB categories on a species by species basis. Ad hoc comparisons were also made among species for which there were obvious trends that the primary analysis did not account for. Strong evidence for either an Allee effect or compensation was based upon the 95% Bayesian credible intervals (BCI's); a second level of weaker dynamics was based on the species' 50% BCI. Negative values for each contrast are indicative of an Allee effect, while positive values reflect compensation.

An additional issue that arises when analyzing these data is that of time-series bias [121]. However, the effects of time-series bias here will be somewhat mitigated by our use of long term time-series which include data at extremely low abundances and across a wide range of fishing mortalities [121]. Also, the effect of this bias would tend to increase $\frac{Recruits}{SSB}$ at low abundance, and to reduce $\frac{Recruits}{SSB}$ at high abundance, rendering our analysis a conservative test for an Allee effect.

2.3 Results

The total variance explained by the model is approximately 35% (Fig. 2.2). Overall the SSB term explains 22% of the total variance, the species × SSB interaction explains approximately 12%, while the order × SSB interaction explains less than 1% of the total variance. The pattern of change in $Z_{\frac{\text{Recruits}}{\text{SSB}}}$ with decreasing SSB varies considerably among species and between SSB categories (Fig. 2.2), while there is little effect of order across the SSB levels (Fig. 2.3).

Combining data for all species results in a linear increase in $Z_{\frac{\text{Recruits}}{\text{SSB}}}$ with declining SSB. This is consistent with a linear increase in the $Z_{\frac{\text{Recruits}}{\text{SSB}}}$ vs. SSB relationship as would be predicted from fitting a Ricker stock recruit model (Fig. 2.4) on the entire dataset. At the lowest SSB level, there is a slight reduction in the $Z_{\frac{\text{Recruits}}{\text{SSB}}}$ rate of increase. This is the only situation in which the 50% Bayesian credible intervals overlap between any two SSB categories (Fig. 2.4). This suggests that the influence of compensatory dynamics (i.e. negative density-dependence) may have slightly weakened in the lowest SSB category.

A comparison of the raw data and model coefficients ($\delta_{ssb,species} + \gamma_{ssb}$) for two species for which I have the most data (Atlantic cod, *Gadus morhua* and Atlantic herring, *Clupea harengus*) shows how the relationship between $Z_{\frac{\text{Recruits}}{\text{SSB}}}$ and SSB can differ between species. Although the most dramatic differences are observed in the lowest SSB class (Fig. 2.5), in which the cod show evidence of an Allee effect, there are also substantive differences at higher relative SSB's. As SSB declined from 60-80% of maximum SSB to 20%, the herring $Z_{\frac{\text{Recruits}}{\text{SSB}}}$ increased by approximately 0.69 standard deviations (an increase in $\frac{Recruits}{SSB}$ from 3.9 to 13.7), whereas for cod $Z_{\frac{\text{Recruits}}{\text{SSB}}}$ increased by only 0.39 standard deviations (an increase in $\frac{Recruits}{SSB}$ from 0.53 to 1.0) over the same range. Additionally, for the Atlantic cod stocks the evidence for an Allee effect is largely due to the Western Atlantic stocks (DFO/NAFO), as only 5 of the data points in the lowest SSB category come from stocks in the Eastern Atlantic (ICES). A subsequent analysis with the cod stocks split into Eastern and Western stocks indicates that in the Western Atlantic $Z_{\frac{\text{Recruits}}{\text{SSB}}}$ weakens below 30% of max SSB, whereas in the Eastern Atlantic it is only in the lowest SSB category where compensation in $Z_{\frac{\text{Recruits}}{\text{SSB}}}$ weakens (Fig. A.7).

In addition to the Atlantic herring, the Pacific herring *Clupea pallasii* also exhibit

compensatory dynamics at SSB's below 40% (Fig. 2.3a). Notably, two of the other clupeiformes, Peruvian anchoveta *(Engraulis ringens)* and Pacific sardine *(Sardinops sagax)*, do not exhibit similar compensatory dynamics at their lowest abundances.

Within the order Gadiformes, the results at low SSB are dominated by both the Atlantic cod and haddock *(Melanogrammus aeglefinus)* which exhibit diverse responses to declines in SSB (Fig. 2.3b). As discussed above, an Allee effect is evident for cod at their lowest historical SSB; the model estimate for $Z_{\frac{\text{Recruits}}{\text{SSB}}}$ at $< 10\%$ of historical maximum is virtually identical (difference of 0.004) to that for cod abundance levels between 80 and 100% of maximum SSB. The relationship between $Z_{\frac{\text{Recruits}}{\text{SSB}}}$ and SSB is relatively weak in cod as it increased by only 0.76 standard deviations before an Allee effect becomes evident; this is roughly half of the increase experienced for an average species. The sensitivity analysis indicated that the Allee effect in cod is robust to the removal of any cod stock in the dataset, though removal of either of the 2 stocks with the most data in the $< 10\%$ SSB category (NAFO-SC-COD3NO and NAFO-SC-COD3M) did increase the modelled $Z_{\frac{\text{Recruits}}{\text{SSB}}}$ estimate in this category (Fig. A.9a). In haddock, $Z_{\frac{\text{Recruits}}{\text{SSB}}}$ is unusually low in the 10-20% SSB category, followed by a relatively high $Z_{\frac{\text{Recruits}}{\text{SSB}}}$ in the $< 10\%$ category. Across all SSB categories there is little evidence of a strong relationship between $Z_{\frac{\text{Recruits}}{\text{SSB}}}$ and SSB in haddock, and the sensitivity analysis confirms that these patterns are robust to the removal of any one stock from the analysis.

The trend for most Perciforms (Fig. 2.3c-d) species is similar to that of the overall trend (Fig. 2.4), although only 9 of 35 Perciform species included data for more than 1 stock. Atlantic Bluefin tuna *(Thunnus thynnus)* exhibited the strongest deviation. Its $Z_{\frac{\text{Recruits}}{\text{SSB}}}$ was highest (0.40, sd = 0.18) when the population was between 60 and 80% of its historical SSB. As the population declined from this SSB level, the $Z_{\frac{\text{Recruits}}{\text{SSB}}}$ also declined, (0.05, sd = 0.25) in the 40-60% SSB category, and thereafter remained largely unchanged with further declines in SSB. For this species the sensitivity analysis (Fig. A.9a) indicates that the high $Z_{\frac{\text{Recruits}}{\text{SSB}}}$ in the 60 to 80% categories is strongly influenced by the western Atlantic stock (ICCAT-ATBTUNAWATL). When analysed separately neither stock (Fig. A.9a, ICCAT-ATBTUNAWATL and ICCAT-ATBTUNAEATL) appears to show strong compensatory dynamics at low SSB (Fig. A.9a).

There are several Pleuronectiform species that exhibit a weak relationship between $Z_{\frac{\text{Recruits}}{\text{SSB}}}$ and SSB as SSB declines below approximately 20-30% of historical maximum. Above this SSB level the species show a relatively robust increase in $Z_{\frac{\text{Recruits}}{\text{SSB}}}$ with declining SSB (Fig. 2.3e). The Scorpaeniformes are characterized by a large percentage of species having data available for only one stock (16/22). Although there is little evidence of an Allee effect for any Scorpaeniform species, there are several species for which there is little evidence of a relationship between $Z_{\frac{\text{Recruits}}{\text{SSB}}}$ and SSB at low abundance (Fig. 2.3f). These include Dusky rockfish *(Sebastes variabilis)* and one genus of *Sebastes* sp. (this "population" was only identified to the genus level in the database).

The contrast between the lowest and second lowest SSB categories (based on the model posterior estimates) for each species suggests that there is strong evidence of an Allee effect for only 1 of 104 species at their lowest recorded SSB category. Strong compensatory dynamics is found in 25 species at their lowest recorded abundance (Fig. 2.6 based on 95% Bayesian credible intervals). There is weak evidence of an Allee effect in another 3 species, and weak evidence for compensation in another 40 species (Fig. 2.6, based on 50% Bayesian credible intervals). For the remaining 35 species, there is no good evidence of either compensatory dynamics or of an Allee effect. While this may be attributable to low statistical power (because of low sample size and high variability), it also suggests that there is little evidence for compensation in these species when reduced to their lowest historical abundance. Indeed the median difference between the lowest and second lowest recorded SSB categories was negative for approximately 19% of the species (n = 20). Intriguingly, of the 22 species in this analysis whose minimum SSB was in either the 40-60% or 60-80% categories, only one had a negative estimate in this analysis (4.5%), and this estimate was only very slightly negative (*Katsuwonus pelamis*, mean difference = -0.02), while of the remaining 82 species that declined below 40% of their maximum SSB 19 had negative estimates (23%). Additionally, I looked at the trends in the raw data at the stock level, these results largely mirror those found in the model, for example of the stocks that have declined below 40% of maximum SSB, the lowest SSB category has a lower mean $Z_{\frac{\text{Recruits}}{\text{SSB}}}$ estimate than the second lowest SSB category in 34 (24%, n = 143) of the stocks.

A coarser set of contrasts compared $Z_{\frac{\text{Recruits}}{\text{SSB}}}$ when SSB was below 20% with $Z_{\frac{\text{Recruits}}{\text{SSB}}}$ when SSB was between 20 and 40% of historic maximum. These data suggest that there is little compensation, or a weak Allee effect, in 22% of the species (12/55, note that only 55 of the species had SSB values below 20%). Strong evidence for an Allee effect is not evident when applying this type of contrast (i.e. all 95% BCI's include 0 when the mean estimate is less than 0). The difference between this and the previous contrast analysis can be attributed to the sharp decline in the lowest SSB category for Atlantic cod (in which strong Allee effects were detected).

In several species this contrast helps clarify the patterns observed in Figs. 2.3 and 2.6. For example, while haddock show a strong increase between the lowest and second lowest SSB classification, evidence at the coarser scale suggests there may be a weak Allee effect in this species (Fig. 2.7). Using this contrast, the dynamics of haddock and Atlantic cod appear similar. Although there are other stocks in which the fine-scale analysis above suggests that the stocks may be experiencing an Allee effect or appear density independent, this complementary analysis indicates that the $Z_{\frac{\text{Recruits}}{\text{SSB}}}$ for these species did increase significantly in the lowest two SSB classes. However, for these species further reductions in SSB below the 10-20% category lead to no increase in $Z_{\frac{\text{Recruits}}{\text{SSB}}}$, e.g. *Eopsetta jordani and Engraulis ringens*. This contrast also confirms the observation that Atlantic bluefin tuna $Z_{\frac{\text{Recruits}}{\text{SSB}}}$ exhibits no compensatory recruitment when when SSB is below 40% of maximum.

The analysis on the subset of data that excluded stocks which used a statistical catch at age model (SCA) yielded similar results to the full analysis (Figs. A.1-A.6 and Table A.1). The most notable exception is the trend for Atlantic herring at low abundance. At abundances below 40% of historical maximum there is no strong evidence for compensation in Atlantic herring (VPA model) when looking at the stocks fit without an SCA model (Figs. A.4-A.6). Additionally, the overall estimate of $Z_{\frac{\text{Recruits}}{\text{SSB}}}$ in the lowest SSB category is actually lower than the second lowest category when using this subset of data (Fig. A.3). Of the 59 species in this analysis, 12 had negative estimates (21%), and none of the species (n=16) whose minimum occurred in the either the 40-60% or 60-80% categories had negative estimates. Thus better than 1 in 4 (12/43) species whose abundance declined below 40% of historical maximum had a declining $Z_{\frac{\text{Recruits}}{\text{SSB}}}$ estimate at their lowest historical abundances.

2.4 Discussion

2.4.1 Allee effects in marine fishes

This analysis suggests that the assumption of an increase in $\frac{Recruits}{SSB}$ as SSB declines is well founded for many species across much of their historical range in SSB. Overall there is a steady increase in $Z_{\frac{\text{Recruits}}{\text{SSB}}}$ as SSB declines, although this trend slows at the lowest values of SSB. At their lowest historical abundances, there is an estimated decline in $Z_{\frac{\text{Recruits}}{\text{SSB}}}$ in over 20% of species. While in the majority of cases the difference between $Z_{\frac{\text{Recruits}}{\text{SSB}}}$ in the two lowest SSB categories is not significantly different from zero, this pattern certainly suggests a decline in the strength of compensation. Such a weakening in compensation might be indicative of an Allee transition region (illustrated by the boxed region in Fig. 1; discussed below), where further reductions in abundance would result in a continued slowing of population growth and an inhibition of recovery.

By examining data at the species level, the amount of information available often grows substantially, enabling greater resolution of patterns in $\frac{Recruits}{SSB}$ at low abundance, but this could lead to biases in the results based upon the number of time series available for a species (61% of species in the present analysis are represented by a single stock). Species represented by a single stock accounted for 14 of the 26 species classified as having strong dynamics (either compensatory or depensatory), 25 of the 43 species classified with weaker dynamics, and 24 of 35 classified as having density-independent dynamics (68%). Somewhat surprisingly, given the high percentage of single stock species (61%), there is minimal evidence that these species are more likely to be classified as density-independent (68%). Evidence of strong compensation was found in a number of species represented by a single time series. Eleven of the 20 species whose $Z_{\frac{\text{Recruits}}{\text{SSB}}}$ declined from their second-lowest to lowest SSB categories were classified as being density-independent based on species represented by a single stock. For these species, there was evidence of a weakening in $Z_{\frac{\text{Recruits}}{\text{SSB}}}$ at low SSB, but the inference was rather weak.

Atlantic cod, a species for which considerable stock level data were available, exhibited weak compensatory dynamics at moderate SSBs and the strongest evidence for Allee effects among the species examined here at low SSB. Upon closer inspection

of these results it is clear that the Allee effect is driven by cod stocks in the Western Atlantic where compensation in $Z_{\frac{\text{Recruits}}{\text{SSB}}}$ is weak across all SSB categories, and the Allee effect becomes evident as SSB declines below 30%. In the Eastern Atlantic the cod stocks have not generally been driven to as low abundance as the Western stocks, but the evidence suggests that there is compensation in $Z_{\frac{\text{Recruits}}{\text{SSB}}}$ across most SSB categories (although it is approximately 30% weaker than the average species). For these Eastern cod stocks the contrast between the lowest and second lowest SSB categories does suggest a weakening of the $Z_{\frac{\text{Recruits}}{\text{SSB}}}$ -SSB relationship.

These results suggest that the lack of recovery evident in many of these cod stocks [53] is related to a decrease in the $Z_{\frac{\text{Recruits}}{\text{SSB}}}$ relationship at low SSB. This work is consistent with suggestions made by Walters [120] who, based on a visual inspection of stock recruitment data, concluded that evidence of an Allee effect was strongest in the Gadiformes. Notably, the two other Gadiformes for which there are the most data - Atlantic haddock and Alaskan Pollock (*Theragra chalcogramma*) - show a weak relationship between $Z_{\frac{\text{Recruits}}{\text{SSB}}}$ and SSB when the SSB is below 40% of historical maximum.

The mechanism by which $Z_{\frac{\text{Recruits}}{\text{SSB}}}$ is reduced at low SSB cannot be determined by this type of analysis, but there are a number mechanisms that could result in reproductive Allee effects in Atlantic cod. At low densities, there is experimental evidence to suggest that male cod experience low success and high variability in fertilization rates [93]. Additionally, a sex bias in the Northeast Arctic cod population is thought to have contributed to a reduction in total egg production that may have resulted in an Allee effect for this population [69]. Sex bias has also been shown to induce Allee effects in sessile marine broadcast spawners by reducing fertilization efficiency [31].

The collapse of a fish stock generally results in the truncation of the population's age structure as fishing generally targets older, larger individuals [9]. With very few older fish surviving, their contribution to recruitment can decline by orders of magnitude, thus substantially increasing the relative contribution to recruitment by younger fish (e.g., northern cod [52]). Hatching success, length of breeding season, and frequency of batch spawning by first-time spawners are much lower than that of experienced spawners for Atlantic cod [112], and younger spawners may also be less

successful than older spawners because of increased variability in recruitment [51]. Additionally, in longer lived species, the influence of older fish on reproductive rate is greater than for species with faster life-histories [117]. Finally, the number of eggs produced per unit biomass (specific fecundity) has been shown to increase with increasing fish mass, potentially leading to a reduction in recruitment in populations with truncated age structure [70].

At the ecosystem level the lack of recovery in Atlantic cod has been linked to cultivation-induced changes in food webs, or an emergent Allee effect [29, 116]. In these types of ecosystems cod would have been a dominant predator, controlling the abundance of various forage fishes. This top-down control of the food web weakens as cod populations are reduced, allowing the abundance of forage fishes to potentially increase by orders of magnitude. Many of these forage fishes feed on planktonic fish larvae, potentially contributing to high mortality of larval cod [110].

The other species for which there were considerable data at low SSB were Pacific and Atlantic herring. Herring stock population dynamics appear rather robust to massive declines in abundance, a finding that concurs with conclusions drawn elsewhere [37, 44, 119]. Nash [81] attributed strong compensation at low abundance in Atlantic herring to density-dependent effects on mortality during the egg stage, while [66] found that predation on eggs could lead to such compensatory dynamics . At high adult abundance, spawning grounds can become saturated with eggs (which are spawned on gravel or on plants), leading to high egg mortality. Conversely, at lower spawner abundance, intra-specific competition is relaxed and egg mortality is reduced. There is also evidence that density-dependent mortality during the larval stage could lead to these patterns in herring [80]. Finally, in comparison to Atlantic cod, herring species longevity and age at maturity is relatively low. Thus, any fishery induced-truncation in age structure would be less likely to affect reproductive rate [117].

The Allee effect in some species could also be influenced by environmental regime shifts that negatively affect the number of recruits produced per unit of spawning stock biomass [35]. These regime shifts can lead to periods of low productivity in which both recruitment and SSB are low. I looked for these trends in several of the Western Atlantic cod stocks and found mixed evidence for such a relationship.

The strongest support for a regime shift comes from the $\frac{Recruits}{SSB}$ of the Gulf of St. Lawrence cod (DFO-4TVn) which declined rapidly in the 1980's when its SSB was at its peak, and while SSB has not recovered since, the $Z_{\frac{\text{Recruits}}{\text{SSB}}}$ since 1993 has been higher than during the peak SSB period of the 1980's. In this stock these patterns are consistent with a productivity shift in this region, but they are also consistent with a dome shaped relationship between $\frac{Recruits}{SSB}$ and SSB. Evidence for a regime shift in other Western Atlantic cod stocks (e.g. NAFO-3NO, and NAFO-3M) is not as strong, but in all of these cases a dome shaped relationship is found between $\frac{Recruits}{SSB}$ and SSB. Additionally, the low SSB's in Western Atlantic cod across all stocks did not coincide with environmental conditions known to be particularly detrimental to $\frac{Recruits}{SSB}$ in any specific stock. In the Northwest Atlantic, for example, periods of low SSB (late 1980s to present day) have encompassed periods of comparatively warm and cold temperatures [48]. Clearly, a better understanding of the processes (be they biological, environmental, or, more likely, the interaction between the two) that underlie any relationship between abundance and recruitment are vital to the proper management of marine fishes.

2.4.2 Allee transition region

Certain combinations of life-history traits might render some species or populations more susceptible to Allee effects than others [19]. For a given life-history strategy, there is some abundance (range) at which the population dynamics transition from compensatory through density independence and enter the realm in which an Allee effect could be manifested. Determining how different life-history strategies influence the location and shape of this transition, hereafter referred to as the "Allee transition region", has implications for both species conservation and management. Conservation efforts for populations found to be below the Allee transition region would need to be more intensive for a species or population that experienced Allee effect. Alternatively, a population far below its Allee transition region may have such low potential for rescue that limited conservation funds might be better focused on other populations for which management is more likely to be effective. While the magnitude of Allee effect is obviously critical, as a first approximation, knowledge of where classical compensatory population dynamics begin to weaken would be exceedingly

useful for both species conservation and fisheries management strategies.

2.4.3 Using stock recruit relationships to estimate recovery rates

The approach taken in the present analysis does not assume a functional relationship between $\frac{Recruits}{SSB}$ and SSB. Thus the approach adopted here avoids the difficulties associated with estimating depensation-related model parameters [78]. An additional advantage is that this analysis can differentiate the species-specific shape of the $\frac{Recruits}{SSB}$ -SSB relationship, which might be spuriously interpreted as simply a poor model fit when using a one-size-fits-all stock-recruitment model. Using the relative SSB enables a comparison of populations having very different population sizes, although this assumes that the maximum SSB in the time series is a good proxy for the maximum SSB of a stock. This pooling of data increases the power of the analysis, especially at low spawning stock sizes for which recruitment data are relatively few, but comes at the cost of having to ensure that one does not mask important stock specific responses.

When rendering predictions about recovery, stock recruitment relationships are often fitted for stocks to estimate their maximum per capita rate of growth at low population size [79]. This metric is then used to determine how populations will respond to population declines. However, these fits are often performed when there is little information at low abundance (e.g. minimum SSB in available data exceeds 40% of maximum SSB). I show that fitting a classical fisheries model (a Ricker type) would lead to incorrect inferences for at least two species in the present study, indeed those species having the greatest data availability. For Atlantic herring, the model fit would greatly underestimate the $Z_{\frac{\text{Recruits}}{\text{SSB}}}$ at low abundance, while the opposite is evident for cod. Based on the Ricker model, one would predict greater compensation in $\frac{Recruits}{SSB}$ for Atlantic cod at low SSB, the opposite of what is suggested when analyzing the entire range of data. Clearly, fitting a population dynamics model to stocks (species) that have not been reduced to low abundance to predict what the dynamics are at low abundance can result in serious errors and incorrect management decisions. For species lacking data at low abundance, a more appropriate approach might be to use species with similar life-histories strategies that have been reduced to low abundances to infer putative population dynamics. Additionally, there are few species (bluefin tuna being one notable exception) whose $Z_{\frac{\text{Recruits}}{\text{SSB}}}$ decreases with declining SSB

when SSB is relatively high (above 40-60% of historical maximum), suggesting that the overwhelming majority of species (for which I have data) exhibit compensatory recruitment dynamics even when their SSB has been reduced by approximately 50%.

Previous meta-analysis of the stock recruitment relationship have had limited success in determining the shape of this relationship at low abundance, largely due to a dearth of of data at low abundance [62, 78]. Myers et al. [78] found evidence for depensation in only 3 of 128 stocks, but his data set had very few data at low abundances, which necessarily led to extrapolating curves into regions in which there was no information. Liermann and Hilborn [62] also found that for the majority of species there is a dearth of strong evidence for either hyper-compensation or an Allee effect because the variance in the parameter estimates are so large that it is difficult to determine if a stock is showing evidence for an Allee effect or hyper-compensation. The interpretation of our model results suggests that in the majority of species evidence for compensation is relatively strong at high SSB, but at lower relative SSB's greater than 1 in 3 species show signs of either an Allee effect or density independent dynamics. While our analysis does not include any Salmonids for which Liermann [62] found the best evidence for an Allee effect, they also suggest that the Pleuronectiformes and Gadiformes exhibited weaker evidence for compensatory dynamics than Clupeiformes. This is similar to our findings in which no Clupeiform species' show evidence of an Allee effect, while a number of Pleuronectiform and Gadiform species exhibited evidence of an Allee effect.

2.4.4 Future directions

The present analysis looked solely at the relative changes in $\frac{Recruits}{SSB}$ with SSB. Although outside the scope of this study, one extension of our work would be to examine absolute changes in $\frac{Recruits}{SSB}$ on a stock-by-stock basis to provide estimates of recruitment strength (and associated error) at different levels of abundance. Comparing these estimates to those obtained from the literature would be instructive (e.g. [79]). Additionally, our analysis excluded other potentially relevant covariates (life-history traits, environmental conditions, age structure) which could be included in the model to determine if there is a relationship between these covariates and $Z_{\frac{\text{Recruits}}{\text{SSB}}}$. Based on the results for the cod and herring, it appears that one covariate worth exploring

further is the species reproductive strategy.

The present study provides estimates of the trends in $\frac{Recruits}{SSB}$ vs. SSB for many commercially harvested marine fishes. For some species, there is evidence that as SSB declines the relationship between $\frac{Recruits}{SSB}$ and SSB weakens, and in some cases an Allee effect is evident. For these species abundances should be kept above their respective Allee transition regions to minimize the probability of a collapse. In 39 of the 104 species, there is no evidence of compensatory dynamics in the $Z_{\frac{\text{Recruits}}{\text{SSB}}}$ vs SSB relationship between the lowest SSB and second lowest SSB categories. These relationships can vary substantially within an order with some species showing strong compensatory dynamics at less than 10% of their historical maximum abundance (e.g. Atlantic herring), while others show no evidence for compensatory dynamics below 30% of historical maximum SSB (e.g. Pacific sardine).

As data at low levels of abundance become increasingly available, it appears that compensation, while strong in some species, is comparatively weak or non-existent in others, thus providing an explanation for why the recovery of some depleted stocks, despite reductions in fishing mortality, has been considerably slower than what classic models of population growth would otherwise suggest.

2.5 Figures and Tables

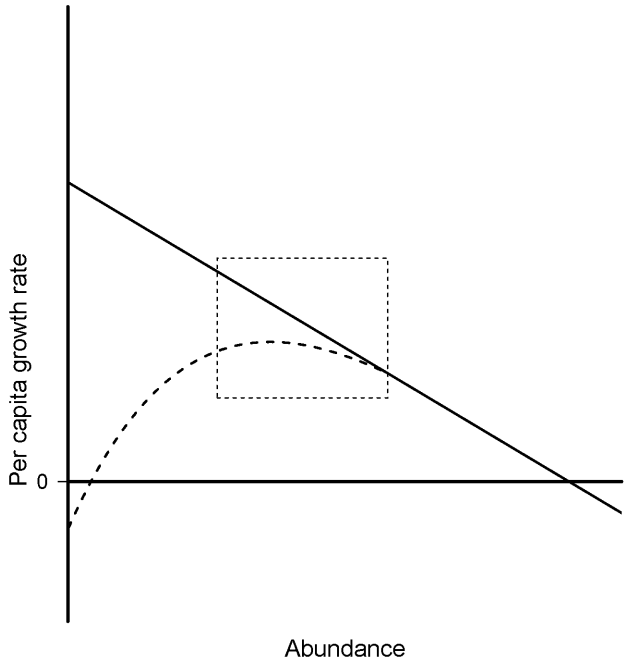

Figure 2.1: Solid line represents theoretical relationship between per capita growth rate and population abundance (density) assuming classical compensatory dynamics (negative density dependence). The y-intercept represents the maximum rate of population growth, while the x-intercept is the populations carrying capacity. The dashed line represents a species with an Allee effect, where this line crosses the x-axis is the "Allee threshold", below this point population growth is negative. The boxed region represents the "Allee transition region", where classical compensatory dynamics weaken, and transition through apparent density independence to a region of positive density dependence (Allee effect).

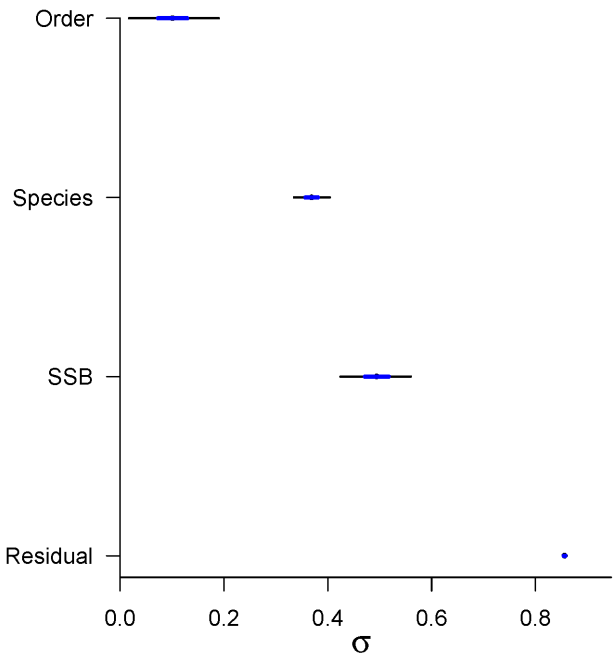

Figure 2.2: The variance explained (σ) by the fixed effect (γ_{ssb}), random effects ($\delta_{ssb,species}, \eta_{ssb,order}$), and residual error ($\epsilon_i$) terms in the hierarchical model.

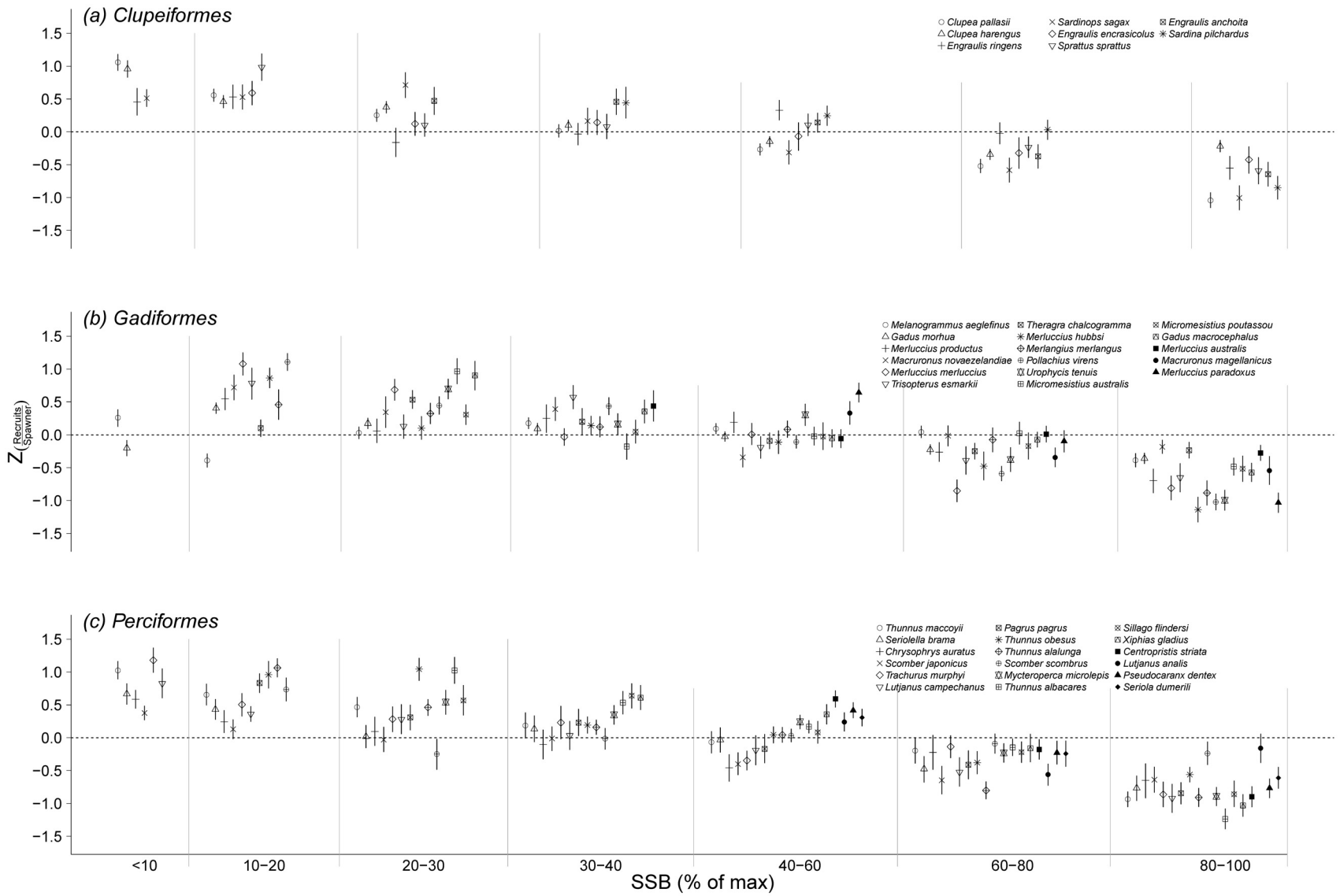

Figure 2.3: Estimated model coefficients of the term $\delta_{ssb,species} + \gamma_{ssb}$ with 50% Bayesian credible intervals sorted by order. a: Clupeiformes, b: Gadiformes, c: Perciformes, d: Perciformes (cont) , e: Pleuronectiformes, f: Scorpaeniformes. This figure excludes the orders for which there is data for 2 or fewer species (i.e. the Beryciformes and Zeiformes).

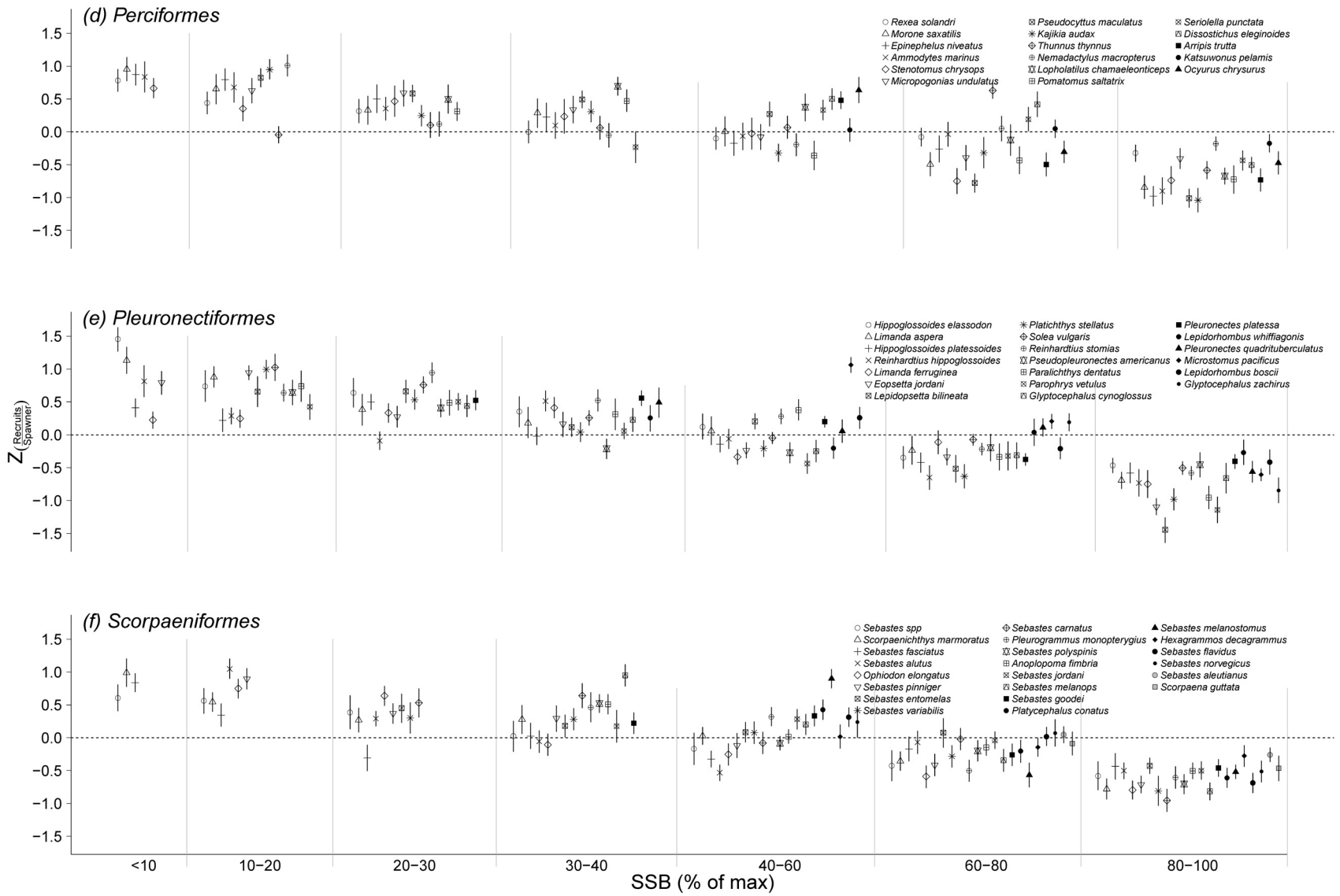

Figure 2.3: Estimated model coefficients of the term $\delta_{ssb,species} + \gamma_{ssb}$ with 50% Bayesian credible intervals sorted by order. a: Clupeiformes, b: Gadiformes, c: Perciformes, d: Perciformes (cont) , e: Pleuronectiformes, f: Scorpaeniformes. This figure excludes the orders for which there is data for 2 or fewer species (i.e. the Beryciformes and Zeiformes).

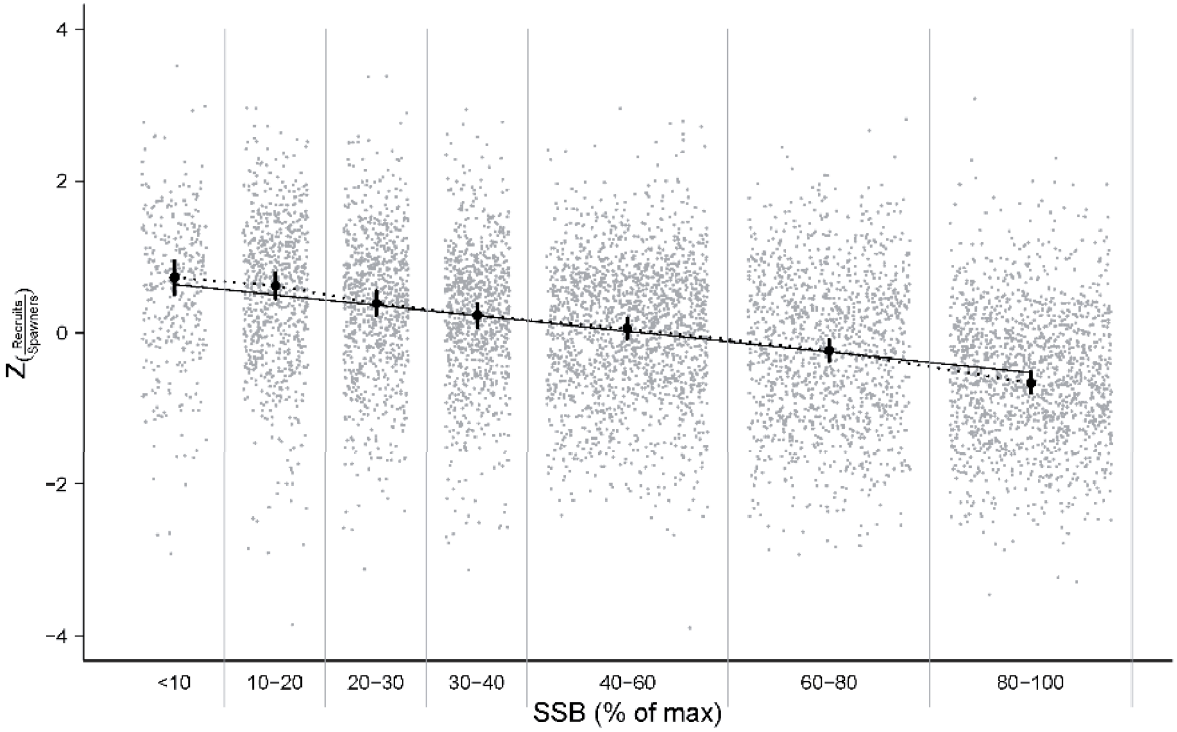

Figure 2.4: Modelled relationship between $Z_{\ln\left(\frac{Rec}{SSB}\right)}$ and SSB. Grey points represent individual data points. Model means with 95% Bayesian credible intervals connected with dotted line. A Ricker model based on the entire dataset is shown with the solid black line.

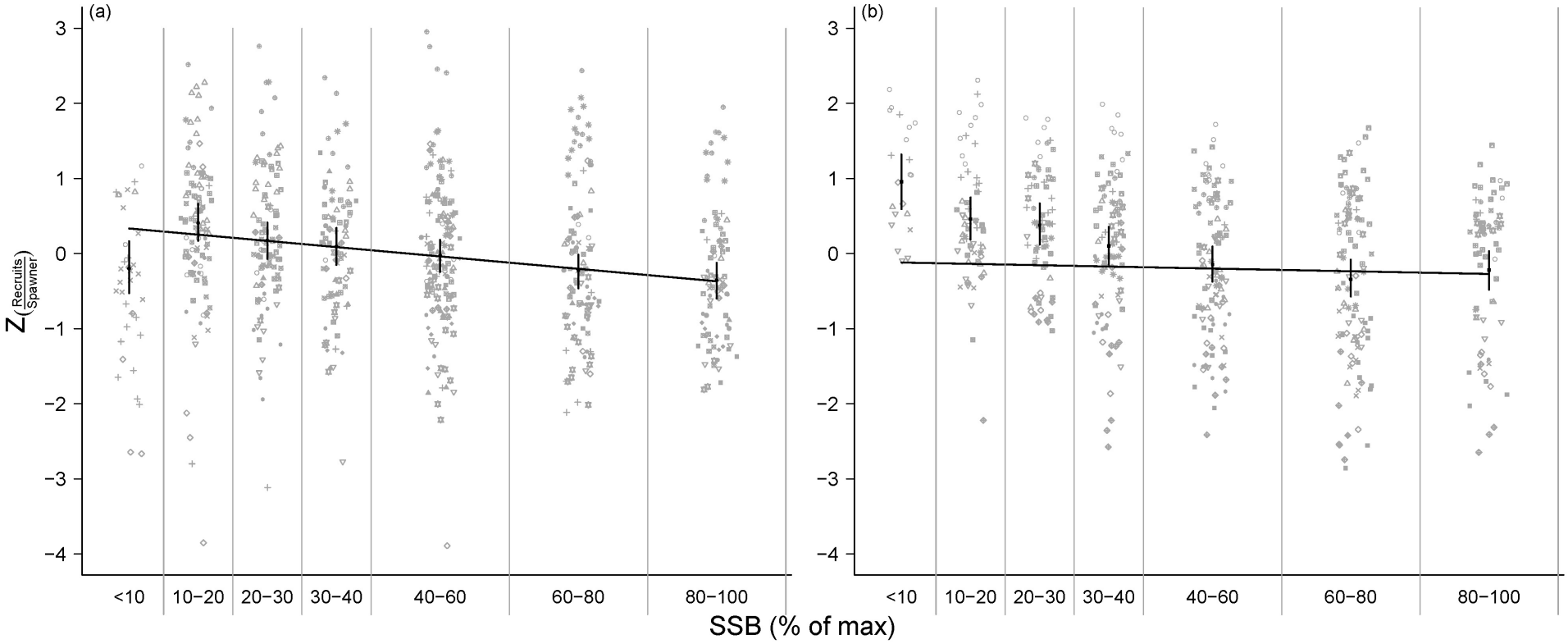

Figure 2.5: Estimated model coefficients of the term $\delta_{ssb,species} + \gamma_{ssb}$ for a: Atlantic cod (*Gadus morhua*) and b: Atlantic herring (*Clupea harengus*). Symbols represent individual data points for individual stocks. Model means with 95% Bayesian credible intervals connected with dotted line. A Ricker model based on the data > 40% of maximum historic SSB is shown with the solid black line for each species.

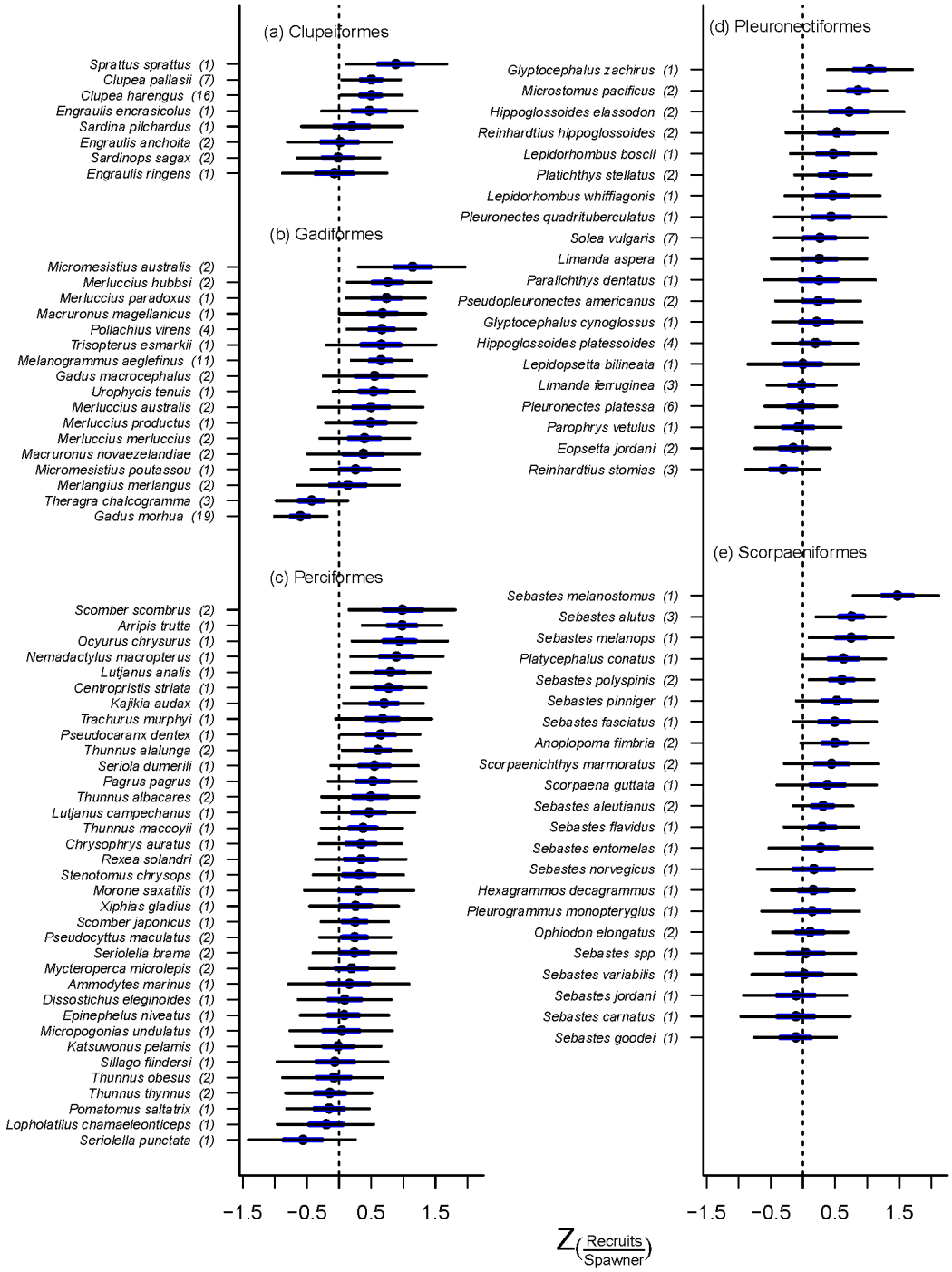

Figure 2.6: Contrast of $Z_{\ln\left(\frac{Rec}{SSB}\right)}$ between lowest and second lowest SSB category for each species, sorted by order. Negative values represent a lower $Z_{\frac{\text{Recruits}}{\text{SSB}}}$ in the lowest SSB category. Thick lines represent 50% Bayesian credible intervals, thin lines represent 95% BCI. a: Clupeiformes, b: Gadiformes, c: Perciformes, d: Pleuronectiformes, e: Scorpaeniformes. Number of stocks included in analysis for each species in brackets after species name. This figure excludes the orders for which there is data for 2 or fewer species (i.e. the Beryciformes and Zeiformes).

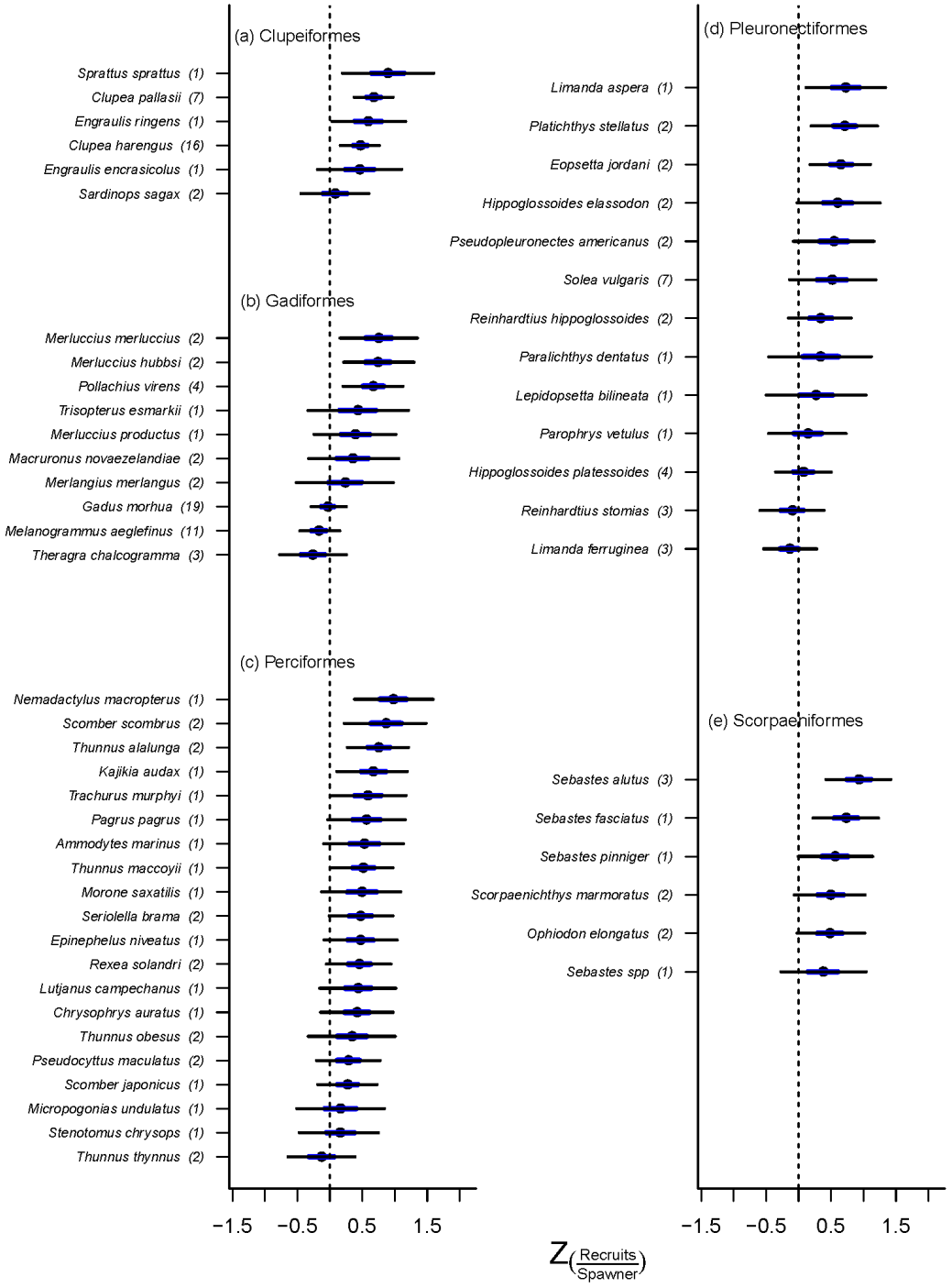

Figure 2.7: Contrast of $Z_{\ln\left(\frac{Rec}{SSB}\right)}$ between SSB $< 20\%$ and SSB between 20-40% for each species sorted by order. Negative values represent a lower $Z_{\frac{\text{Recruits}}{\text{SSB}}}$ in the $< 20\%$ SSB category. Thick lines represent 50% Bayesian credible intervals, thin lines represent 95% BCI. a: Clupeiformes, b: Gadiformes, c: Perciformes, d: Pleuronectiformes, e: Scorpaeniformes. Number of stocks included in analysis for each species in brackets after species name.This figure excludes the orders for which there is data for 2 or fewer species (i.e. the Beryciformes and Zeiformes).

Chapter 3

Functional response of fisheries

3.1 Introduction

Many commercially exploited marine populations have experienced unprecedented reductions despite efforts to maintain viable populations [44, 124]. The primary means by which managers have attempted to sustain these populations is through the control of harvest mortality. From the perspective of the harvested population, a fishery is analogous to the introduction of a novel predator. In terrestrial ecosystems, numerous theoretical and empirical studies have examined how predator-induced mortality is influenced by changes in prey abundance [42, 101, 102], although few have identified a harvest regime as the predator [26, 100]. Since these functional response (FR) relationships were first discussed by Solomon [101] and generalized by Holling ([42, 43]), several theoretical relationships have been derived, based on different interactions between predator and prey [1]. Here our focus is to understand how fishing mortality changes with predator abundance in harvested populations. To achieve this I utilize three simple yet commonly studied FRs that can accurately depict the nature of the relationship between fishing mortality and prey abundance: Type I, Type II, and Type III FRs [30].

The simplest relationship is the Type I FR for which per capita mortality attributable to predation is independent of prey abundance up to a critical abundance threshold, above which per capita mortality declines with further increases in abundance [71]. Below the threshold, the relationship is density independent; irrespective of prey abundance, the predator takes the same proportion of the population (Fig. 3.1a). This is manifest by a positive linear relationship between the number of prey consumed and the number of prey in the population below the critical abundance threshold. In a fishery, this would be akin to a harvest strategy for which the same proportion of the population is caught irrespective of abundance [58].

A Type II FR describes reductions in per capita mortality with increasing prey

abundance (Fig. 3.1b; [42]). As prey abundance declines, however, the proportion of prey captured continually increases, resulting in what can be termed a component Allee effect (i.e., a positive relationship between a component of individual fitness and population abundance [19]). From a fishery perspective, this type of FR contributes to a relatively low inter-annual variability in total catch, which is highly desired from an economic perspective, and can be achieved by a constant harvest strategy [58].

The Type III FR is characterized by a peak in per capita prey mortality at intermediate population sizes. This occurs because predators are increasingly unable to capture available prey when prey are abundant (Fig. 3.1c). At low prey abundances, per capita mortality also declines (below some threshold) because of "predator switching", i.e., the targeting of more abundant prey, or because of the availability of a set number of refugia within which prey are not vulnerable to predation [43, 63, 76]. In a harvested population, intentional management actions can result in a Type III FR. In harvested populations it is also possible that the fishery captures an ever increasing proportion of the prey up to the maximum observed abundance, but at low abundances the harvest switches to other species (Fig. 3.1d). This is essentially the behaviour of the Type III FR when prey abundances are below the peak and it would have a strong stabilizing effect on the prey population. Given this similarity to the Type III FR I have dubbed this a Type IIIL FR. It is somewhat akin to the concept of a threshold harvest (catch is taken only when abundance is above a threshold) in which harvesting rates could be highly variable, possibly due to expansion and contraction of the fishing fleet or effort [58].

There is also potential for variability in the FR within a given population when harvesting targets individuals with specific characteristics. In terrestrial ecosystems these can include large horns and large size in some mammals [18]. In fisheries the largest fish are often targeted directly and gear selectivity can also lead to exploitation rates varying with size of the fish [39]. These factors may result in variability of both the functional response and exploitation rate between age classes. If harvesting significantly alters either the magnitude and structure of mortality between age classes from the unharvested state the population may also experience significant and rapid evolutionary changes [49, 60].

My objectives are four-fold. First I describe the relationship between fishing mortality and abundance of more than 90 fished populations using the FR relationships. Second, I quantify the average exploitation rate at various levels of prey population abundance. Third, I determine if there are differences in the functional responses or exploitation rates between the youngest and oldest age classes. Finally, I determine whether our findings are influenced by either taxonomy or management agency.

3.2 Methods

Data for this analysis were collated from publicly available fisheries stock assessment analyses from around the world. The data include time series of abundance, biomass, weight, maturity, fishing mortality, natural mortality, and/or catch for each age class in 134 different marine fish populations. The data sources include Europe (ICES, International Council for the Exploration of the Sea), Canada (DFO, Department of Fisheries and Oceans), the USA (NOAA, National Oceanic and Atmospheric Administration), and the High Seas (NAFO, North Atlantic Fisheries Organization, and ICCAT, International Commission for the Conservation of Atlantic Tunas). Six taxonomic orders (Clupeiformes, Gadiformes, Osmeriformes, Perciformes, Pleuronectiformes, and Scorpaeniformes) are represented in the database.

3.2.1 Functional responses

As I was interested only in the FR while a fishery was in operation data from years during which a moratorium was in place (meaning that there was no quota for a fishery targeting the population in question) have been excluded (4 populations). For the overall analysis both the catch and number of individuals was summed across each age class in each year to obtain the total catch (C) and total abundance (N) for each year. To determine which FR best represented the data the per capita mortality rates ($\frac{C}{N}$) were calculated for all years in the time series.

A Bayesian model fitting procedure was employed to avoid difficulties with non-convergence and the estimation of numerous starting conditions required for typical frequentist maximum likelihood estimation methods. Three different models were compared to determine the shape of the FR; the first was a linear model;

$$p(h) = k + aN \tag{3.1}$$
$$C \sim Binomial(N, p(h))$$

where C is the catch in numbers, N is the total abundance in numbers, $p(h)$ is the probability of an individual fish being harvested and is constrained to be between 0 and 1, k is the intercept of the relationship between per capita harvest mortality and number, and a is the slope of this relationship. Using this general equation three separate models were fit, the first was an intercept only model in which a was constrained to be 0 (a Type I FR; Fig. 1a). In the second model a was constrained to be positive ($a \sim U(0.001, 10)$), this model is the Type IIIL model in which mortality declines linearly with abundance (Fig. 1d). Finally, in the third model, I constrained a to be negative ($a \sim U(-10, -0.001)$), this model was classified as a Type II FR since mortality increased as abundance declined (Fig. 1b). I also used a classic non-linear Type II FR parameterization;

$$p(h) = \frac{k}{b + N} \tag{3.2}$$
$$C \sim Binomial(N, p(h))$$

where k and b are both shape parameters determining the steepness of the relationship as depicted in Fig. 1b. The Type III FR parameterization used was;

$$p(h) = \frac{kN}{D^2 + N^2} \tag{3.3}$$
$$C \sim Binomial(N, p(h))$$

where k and D are both parameters which determine the location of the peak and overall shape of the relationship (Fig. 1c). Uninformative priors were used for k, ($ln(k) \sim N(0, 10)$), b had a normal prior ($a \sim N(0, 10)$), while D was constrained so that the peak per capita mortality was never at an abundance lower than the minimum abundance found in the time series ($D \sim U(N_{min}, 10)$.

Markov chain Monte Carlo (MCMC) sampling was performed using the R2WinBUGS package and WinBUGS version 1.4.3 [65]. Each model was run for 100 000 time steps,

with an initial burn-in period of 50 000. I thinned the MCMC chains to eliminate auto-correlation, using only every 50^{th}data point. The best fit model was selected using the Deviance Information Criteria (DIC); the model receiving the lowest DIC for each population being the model with the best fit [33]. When the best fit model chosen was a linear model with a very small slope (less than $\pm$ 0.05) it was classified as a Type I due to the weak relationship between abundance and exploitation rate.

Three separate chains were run to check for non-convergence of each parameter. Model convergence was assessed by visual inspection of the MCMC sampling chains and using the Gelman and Rubin convergence diagnostic ($\hat{R}$). When the parameters from a populations FR relationship had poor convergence ($\hat{R} > 1.1$) it was excluded, and the FR with the next lowest DIC was chosen, if no FR relationships had an $\hat{R} < 1.1$ that population was excluded from further analysis [33]. The model fits for each population can be found in Electronic Supplement A.

3.2.2 Age-specific analysis

To determine the functional response for the oldest and youngest age classes the catch and abundance data were partitioned into 4 age quartiles for each population. The upper quartile contained the oldest age classes, while the lower quartile contained the youngest age classes. The data in these two age quartiles (i.e. the oldest and youngest age classes) were summed to determine the total catch and population size for both old and young fish in a given year. The functional response of the old and young age classes was determined in the manner described above. The age-specific model fits for each population can be found in Electronic Supplement B.

3.2.3 Subsequent analysis

Functional responses were further classified (*Class*) by the abundance at which the per capita prey mortality (PCM) peaks. Type I FRs were classified as having no relationship between PCM and abundance, hereafter referred to as the density independent (DI) classification. The Type IIIL FRs were classified as having peak PCM at high abundance, hereafter referred to as the positive density dependence (PDD) classification. The Type II FRs were classified as having a peak PCM at low abundance which is subsequently referred to as the negative density dependence (NDD)

classification. Based on previous work indicating that per capita productivity can remain constant or even decline at parental population sizes (i.e. spawning stock biomass (SSB)) lower than $\approx 40\%$ of maximum SSB [56], I classified Type III FRs with a peak PCM at less than 40% of peak abundance as having a peak at low abundance (NDD classification), and the Type III FRs with a peak PCM above 40% as having a peak at high abundance (PDD classification). Using the FR model fits I estimated exploitation rate (ER) at minimum abundance, ER at maximum abundance, the maximum ER (Pk_{ER}), the absolute change in ER (Abs_{ER}, which was calculated as $ER_{\text{min abundance}} - ER_{\text{max abundance}}$), and the relative change in ER (Rel_{ER}, which was calculated as $(\frac{ER_{\text{min abundance}}}{ER_{\text{max abundance}}})$.

The relationship between the response variables (see below), taxonomy, management, and age were modeled using frequentist linear models with the following basic model form;

$$y_i = \gamma_{tax} + \delta_{man} + \eta_{tax \times man} + \epsilon_i \tag{3.4}$$

$$y_i = \gamma_{tax} + \delta_{man} + \phi_{age} + \eta_{tax \times man} + ... + \varphi_{tax \times man \times age} + \epsilon_i \tag{3.5}$$

Equation 3.4 was used for the aggregated ER analyses, while equation 3.5 was used for the age-specific analyses. Here γ_{tax} was the estimate for the taxonomic main effects, δ_{man} was the estimate for the management main effects, ϕ_{age} was the estimate for the age main effects, $\eta_{tax \times man}$ was the interaction between taxonomy and management, and $\varphi_{tax \times man \times age}$ was the three way interaction. Additionally all two way interactions were also included in equation 3.5 (but not shown explicitly). For the models that incorporate a continuous response variable the error term (ϵ_i) is assumed to follow a normal distribution ($\epsilon_i \sim N(0, \sigma^2)$) on the scale of the response variable. Depending on the analysis the response variable y_i is either $Class$, Pk_{ER}, Abs_{ER}, or the Rel_{ER}. The residuals from the full models (Equations 3.4 and 3.5) were visually inspected to ensure there were no serious violations of the assumptions of these analyses.

Model selection was performed using an information theoretic model selection process; all possible model combinations were investigated and compared using the Akaike Information Criterion (AIC [2]), corrected for small sample size (AICc) along

with AICc weights [13]. The model parameter estimates were based on the model with the lowest AICc score rather than using full model averaging techniques. Given that I did not account for model selection uncertainty when estimating the parameters, the 95% confidence intervals associated with each parameter will be somewhat non-conservative [13]. All models with a $\Delta AICc < 2$ of the best model are discussed, given that these models are essentially equivalent in terms of explanatory power, but I generally will focus on the simplest model within this subset. When this set includes the null model (i.e., the model having only an intercept), I suggest that the evidence for any of the more complex models is very weak. I note that all models with a $\Delta AICc < 10$ should not be dismissed outright. The full model selection tables are given in Appendix B. Additionally, where appropriate, the variance explained (R^2) by a particular model will be used to better understand the model fit. Populations were excluded from these analyses if they contained only a single datum in either the taxonomic class or management unit (2 populations).

3.3 Results

3.3.1 The Functional response

In 57% of populations in this analysis the abundance declines by 80% or more. The most common functional response was the Type II FR (42%), followed by Type III FR and Type I FR occurring 30% and 20% of the time, respectively (Fig. 3.2). A FR in which prey mortality increased linearly with increasing abundance (a Type IIIL FR) was uncommon, occurring in only 8% of the populations. The peak mortality occurs at an abundance of less than 40% of maximum abundance in exactly 50% of the Type III populations (median abundance at peak ER was 13% of maximum abundance in these populations). Across all FRs peak ER occurred at low abundance in 58% of the populations. In only 23% of populations was ER found to decline with reductions in abundance.

The likelihood of being in a particular FR category (i.e., no relationship, peak mortality at low abundance, and peak mortality at high abundance) was not significantly influenced by management body or taxonomic order. The null model (AICc weight = 0.94; Table B.1) received the greatest support. Despite this, parameter estimates

for the management model did vary substantially, with approximately 71% of DFO populations having their peak ER at low abundances and 59% of ICES populations having this negative density dependent relationship.

3.3.2 Exploitation rate

At peak ER (Pk_{ER}) across all populations, approximately 17% (15-20; 95% CI) of individuals in a population were removed annually. There was little evidence for any relationship between the Pk_{ER} and either management body or taxonomy (null model AICc weight = 0.77; Table B.3). Although inclusion of management body in the model did have some support (AICc weight =0.17, $R^2 = 0.04$), it explained little of the overall variation in these data (Fig. 3.3a).

Across populations, the ER at maximum abundance was 0.13, and the Abs_{ER} model results indicate that, on average, ER increased by 0.07% (0.04-0.09; 95% CI) at the minimum abundance. The model selection criteria again suggested that the most parsimonious model was the null model (AICc weight = 0.75; Table B.4). Here the model that included taxonomy had support similar to that of the null model (AICc weight = 0.19, $R^2 = 0.04$; Fig. 3.3b) but explained little of the variation in these data. The Rel_{ER} model results largely mirrored those expressed above, although models that included taxonomy had greater support than the null model (Table B.5; Fig. 3.3c).

3.3.3 Age-specific functional response

The most common functional response when considering either the youngest or oldest fish was again the Type II FR, although it was more common in the older age classes (57% vs 33%; Fig. 3.4). The Type I and Type III FRs were more common in the youngest age classes (Type I old = 14%, young = 23% and Type III old =18%, young = 32%). The Type IIIL FR, while present in both age groups, was observed relatively infrequently (11% for old and 12% for young).

The likelihood of being in a particular category was a function of both taxonomy and age class (AICc weight = 0.74; Table B.6). Both the older and younger fish had a high percentage of the Type III populations classified as NDD (59% and 47% respectively) and overall there were more NDD populations for the old age classes

(68% compared to 48% for the young ages; Fig. 3.5). The effect of taxonomy is largely driven by the youngest aged pleuronectiformes which have a high percentage of populations in which harvesting mortality declines with declines in abundance (Fig. 3.5).

3.3.4 Age-specific exploitation rate

For the Pk_{ER} models, the most support was for a model with an interaction between management and taxonomy and an interaction between age class and taxonomy (AICc weight = 0.55, $R^2 = 0.48$), although a simpler model in which the second interaction is replaced by an additive effect of age class is essentially equivalent (Fig. 3.6; Table B.7). The top four models all contained some combination of management, taxonomy, and age class, and these models had a cumulative AICc weight of 0.97. On average the Pk_{ER} was 199% higher for older fish (ER_{young} = 0.08 (0.06-0.12; 95% CI), ER_{old} = 0.25 (0.19-0.33; 95% CI); Fig. 3.7a). The interaction between management body and taxonomy was influenced by a single NOAA clupeiform population for which the Pk_{ER} estimate was extremely high (Fig. 3.6). Removing this population weakens the support for the interaction (AICc weight = 0.18), with a more parsimonious additive model now has essentially identical support as more complex models (AICc weight = 0.18); nonetheless the suite of models favored remained largely unchanged (Table B.8, Fig. B.1).

The best Abs_{ER} model suggested that as abundance declines the ER increases more for older age classes (Fig. 3.7b, AICc weight = 0.66; Table B.9; AICc weight = 0.11) but it explained only 4.7% of the variation in the data. Model selection generally supported the inclusion of a taxonomy term (AICc weight = 0.39, R^2 = 0.09; Fig 3.7c), although the exact nature of the model was difficult to discern because numerous models, including the null model, could not be dismissed (Table B.10) and none of the models explained much of the overall variation in the data.

3.4 Discussion

3.4.1 The functional response

The most commonly expressed functional response for commercially harvested marine fishes is one in which fishing induced morality continually increases as prey abundance declines (median minimum abundance = 17% of maximum in these Type II FR populations). Even for the more conservative Type III FR peak fishing mortality occurred at prey abundance levels below 40% of maximum abundance in half of the populations (50% of the Type III FRs). Peak exploration rate in these Type III populations occurred at a median abundance corresponding to just 13% of maximum abundance; this is approximately 66% below both the abundance at which per capita population productivity starts to weaken and the recommended biomass limit reference point used in many jurisdictions [38, 56].

The Type II functional response can destabilize population dynamics in simple two-species models and represents one of the best examples of a component Allee effect [19,30,63]. Although the potential for harvesting to produce a component Allee effect has been acknowledged, it has typically been considered more the exception than the rule in marine fisheries [39]. In freshwater fisheries, however, there is evidence that a Type II functional response can lead to collapse, instability, and a lack of recovery [85]. Given the high proportion of populations in the present analysis for which harvest-induced mortality is associated with a component Allee effect, it is reasonable to conclude that the aforementioned problems observed for freshwater fisheries are also a potential problem in marine fisheries.

There is little evidence in our analysis for any influence of management body or taxonomy on the level of fishing mortality, suggesting that, on average, fisheries have been prosecuted in a similar manner, irrespective of the fisheries management agency or taxonomic group, at some time in the past. That is, fisheries agencies have tended to adjust fishing mortality in a similarly problematic fashion in association with reductions in fish abundance. There is a small effect of management body on peak ER, with European-managed populations having a higher peak ER (0.19 (0.16-0.23; 95% CI)) than those in the United States (0.14 (0.1-0.18; 95% CI)), a finding consistent with a previous cross-jurisdictional comparison of over-fishing [88].

In terms of absolute number of fish harvested, there is a surprising number of instances for which a given fishery removes approximately the same number of (or more) fish when abundance is less than half of historical maximum abundance, as when the populations were near their maximum level (Electronic Supplement A). In most of these populations, such as Icelandic capelin (*Malottus villosus)* and Southern Gulf Canadian Atlantic cod (*Gadus morhua*), although absolute catch declined with further reductions in abundance, in almost all instances, these populations were driven to very low levels where they are vulnerable to the uncertainties in future population trajectory associated with demographic and environmental stochasticity [29, 35, 69, 116]. Such large populations declines are common in commercially exploited marine fishes [44], indeed 57% of species in our analysis had their abundance reduced 80% or more, relative to their maxima.

I do not have information on how either the fishing effort (analogous to the number of predators) or efficiency have changed over time in these fisheries, although there is reason to believe it would increase as the fishery matures [52]. Given that I am interested in the general relationship between abundance and fishing mortality and not whether the assumptions behind functional response theory are fully realized in this analysis I do not believe this influences our findings. Irrespective of the number of fishers involved in the fishery I believe it is troubling that in the majority of cases the mortality within these fisheries is peaking when abundances are at or near their minimum. In addition, both the catch and abundance will be measured with an unknown amount of error which I am unable to quantify, these "errors in variables" problems are well known when studying fisheries data [121]. In the context of this analysis random variability in these two metrics would tend to increase the uncertainty in the data and would bias our results towards favouring Type I models (i.e density independence). More systematic errors, such as abundance being overestimated at lower abundances, and being underestimated at high abundances, could bias our results towards favouring either PDD or NDD, but I have no evidence for such systematic measurement errors in these data.

If these data were collected prior to the development of full scale fisheries the observed negative density dependence might be the default expectation since fishing mortalities will typically be extremely low when at the start of the fishery when the

population is a high abundance. It is clear this is not generally the case (see Electronic Supplement A and B), these populations are all subjected to a relatively intense fishery from the beginning of the time series. Given that the detailed data I have compiled is only available for economically important species this should not come as a surprise; many of these populations have been harvested for decades-centuries before these detailed fisheries data began to be collected.

3.4.2 Age effects

There is a small effect of age on the functional response with NDD fisheries being even more common (68%) in the oldest age class than in either the youngest age class (48%), or the aggregated data. For the majority of populations the ER peaks when the abundance of the age class is at or approaching historically low levels. This is the case irrespective of management agency or taxonomy. Thus, even the young fish are often being harvested in a manner than is likely to de-stabilize these populations, although the consequences of these types of FRs on a structured population have received scant theoretical attention to date. It seems that the Pleuronectiformes are harvested in a more sustainable fashion with PDD and DI being more common in this taxonomic group; this is especially evident for the youngest age classes.

Each of taxonomy, management, and age class has an influence on the peak exploitation rate. For the oldest individuals in each population 25% are removed every year, approximately three times the harvest mortality of fish in the youngest age classes. Additionally, the increase in ER between the maximum and minimum abundance is significantly higher for the oldest fish; the increase being 155% (0.04 vs. 0.1) higher for the oldest fish. On average a typical fishery removes an additional 10% of old fish when a population is at its minimum abundance. Given that typical natural mortality is $\approx$ 10-20% for the majority of fish in examined here, the average fishery has elevated adult mortality to unprecedented levels. Even for the youngest age classes, in which management agency attempt to minimize the impacts of fishing, there is an approximate doubling of mortality. While an overall doubling of natural mortality is often suggested to be sustainable in fisheries science, this level of mortality is occurring in the component of the population with the lowest harvest mortality rate of any age group and when these populations have declined to low abundances.

These changes in mortality will have consequences not just for the life history and population dynamics of the fish being harvested, but will be felt across the ecosystem, especially if a harvested species has a central role in ecosystem processes, e.g. a keystone species [83]

Increasingly marine management is moving away from managing populations using single-species models and towards ecosystem level management [16]. These models can account for the complex interaction between species in the ecosystem, and often incorporate functional response theory to deal with predatory-prey interactions [17]. Incorporating the FR of the fishery into these models to account for mortality variability should improve these models given that (i) ER is often equivalent or higher than natural mortality rates, (ii) both FR and ER vary significantly between age classes, (iii) ER increases substantially as abundance declines, and (iv) quantitative measures of ER differ between taxonomy and management agency.

3.5 Conclusion

The most common means by which fisheries are prosecuted results in a pattern of association between fishery-induced mortality and prey abundance that will almost certainly increase the likelihood of collapse and instability for declining populations, eventually contributing to delayed and uncertain recovery [82]. Concomitant with a Type II functional response maximum per capita predator-induced mortality typically occurs when prey abundance is at less than 20% of historical maxima. When coupled with per capita harvest mortality being on par with natural mortality rates for many of the youngest individuals and upwards of 2 times greater than natural mortality rates for the oldest individuals it should come as no surprise that over-exploitation, collapse, and slow recovery are relatively common in marine ecosystems. The realized functional responses associated with exploitation provide an instructive means of exploring the stability of predator-prey interactions within a fisheries context. The utility of incorporating such patterns of association into single-species and ecosystem models merits attention.

3.6 Figures and Tables

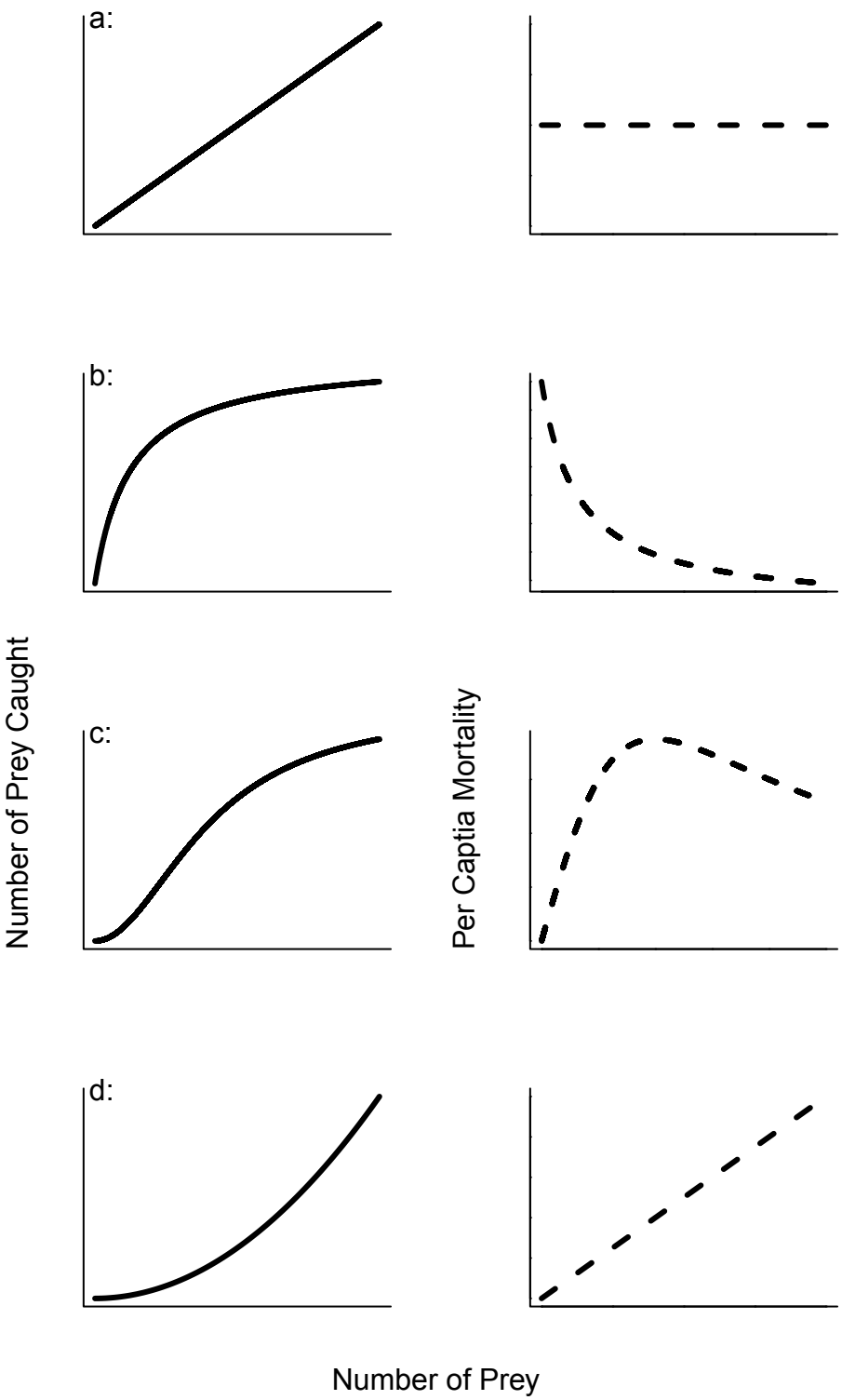

Figure 3.1: Examples of the four functional responses (FRs) used in this study, the figures on the left show the theoretical relationships between number of prey caught and prey abundance, while the right side is the relationship between the per capita prey mortality and prey abundance. a: the Type I FR, b: the Type II FR, c: the Type III FR, d: the Type IIIL FR.

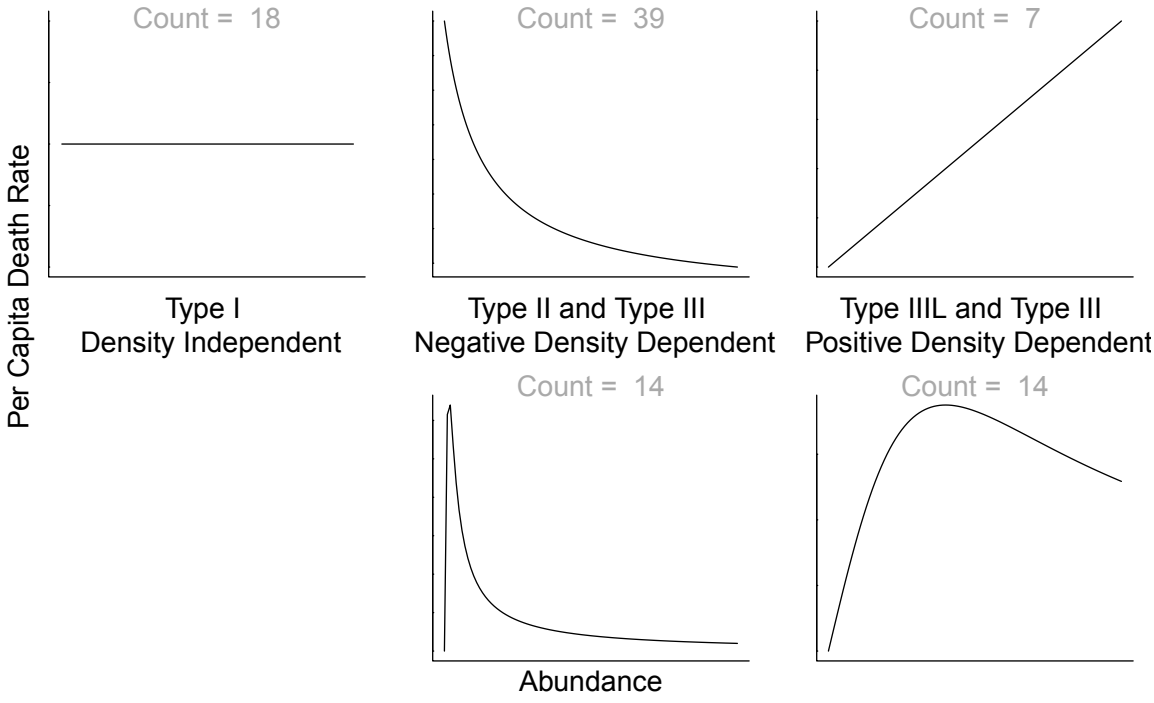

Figure 3.2: The types of functional responses and the number of populations found with a given FR.

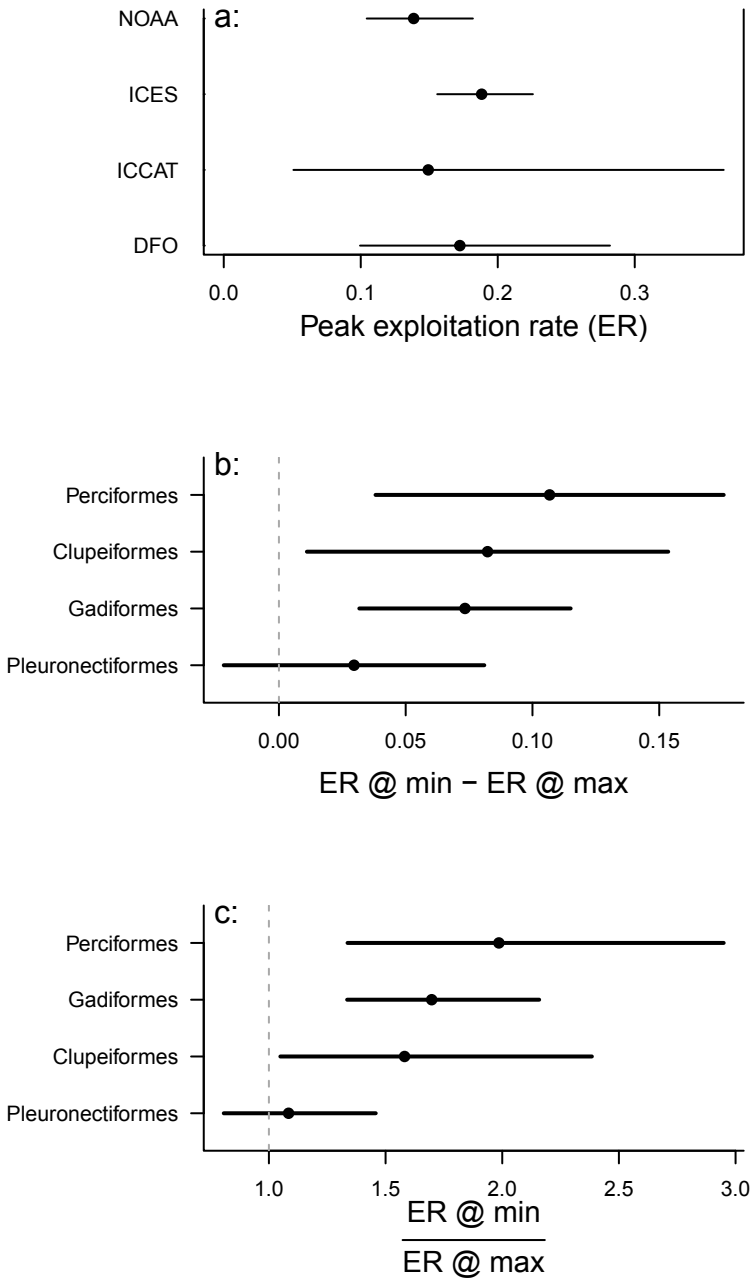

Figure 3.3: a: Model estimated peak exploitation rate ($Peak_{ER}$) with 95% confidence intervals across the four management agencies (National Oceanic and Atmospheric Administration (NOAA), the International Council for the Exploration of the Sea (ICES), the International Commission for the Conservation of Atlantic Tunas (ICCAT), and the Department of Fisheries and Oceans (DFO)). b: Estimated absolute change in exploitation rate (Abs_{ER}), with 95% confidence intervals, across the taxonomic orders, positive values indicate that exploitation rate is higher at minimum abundance than the exploitation rate at maximum abundance. c: Estimated relative change in mortality (Rel_{ER}), with 95% confidence intervals across the taxonomic orders.

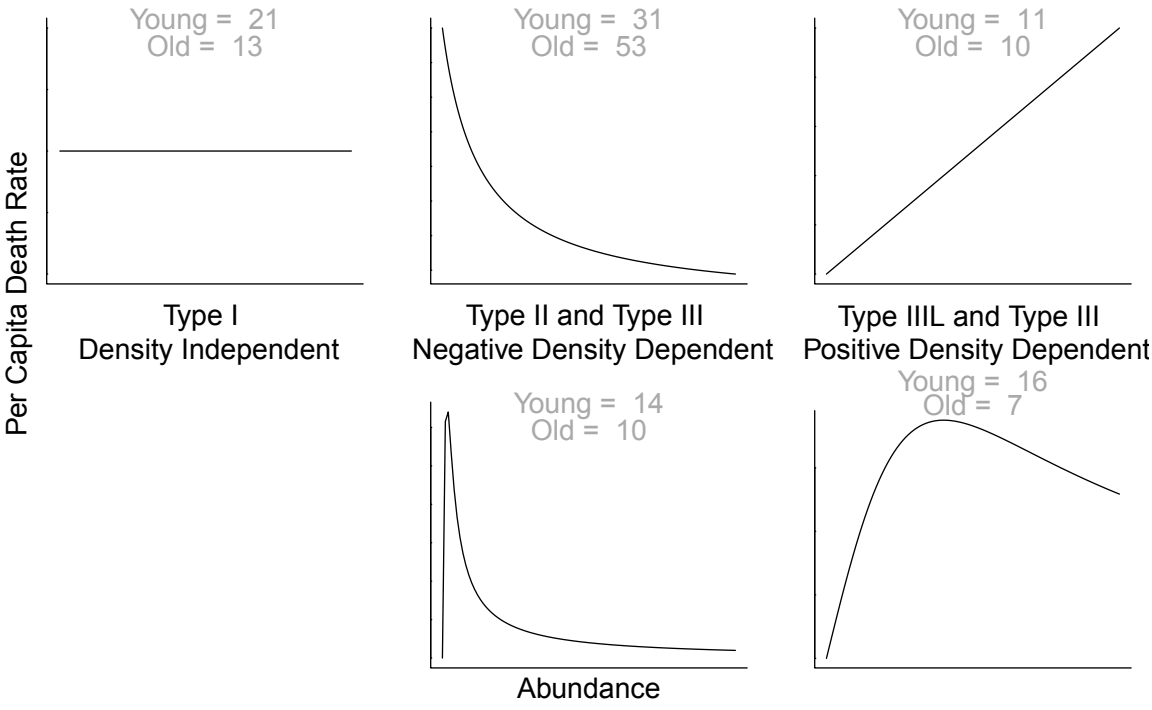

Figure 3.4: The number of populations found in each FR and each age class using the age-specific data.

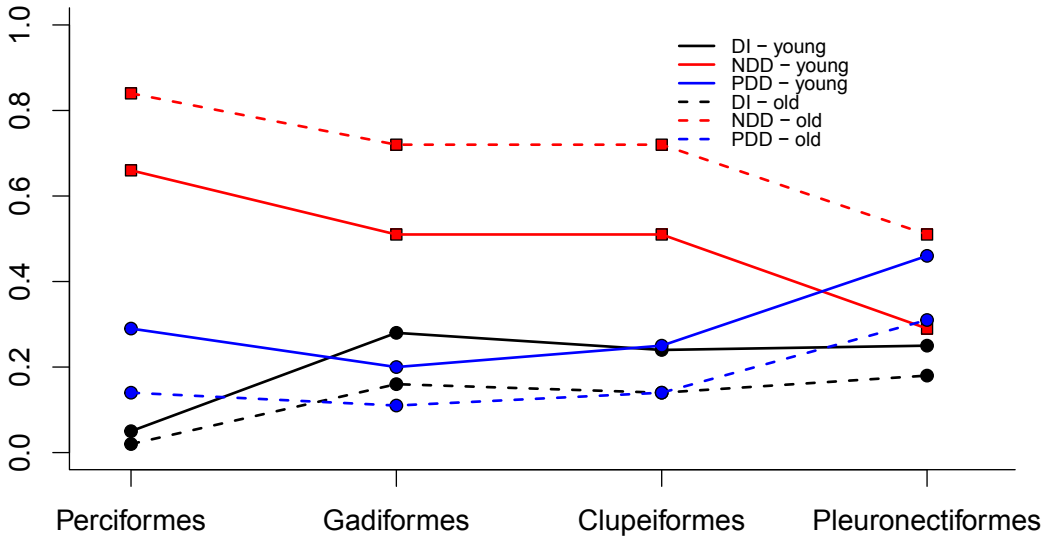

Figure 3.5: Model estimates of probability of being in given FR classification (DI, NDD, PDD) between the young and old age classes.

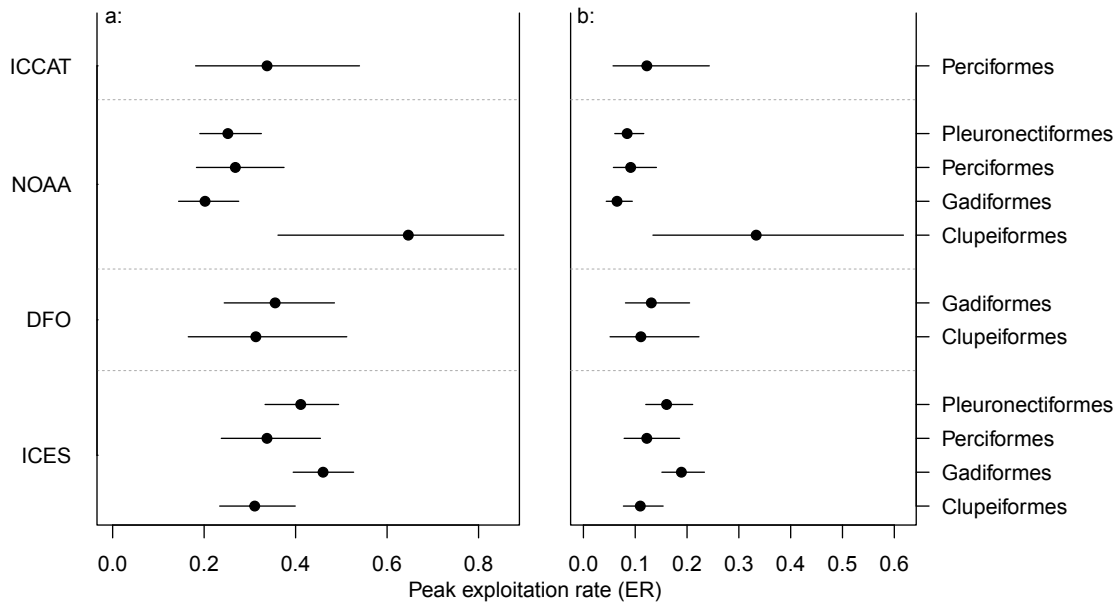

Figure 3.6: Model estimated peak exploitation rate ($Peak_{ER}$) with 95% confidence intervals for both taxonomy and management body of the the a: old age classes and b: young age classes.

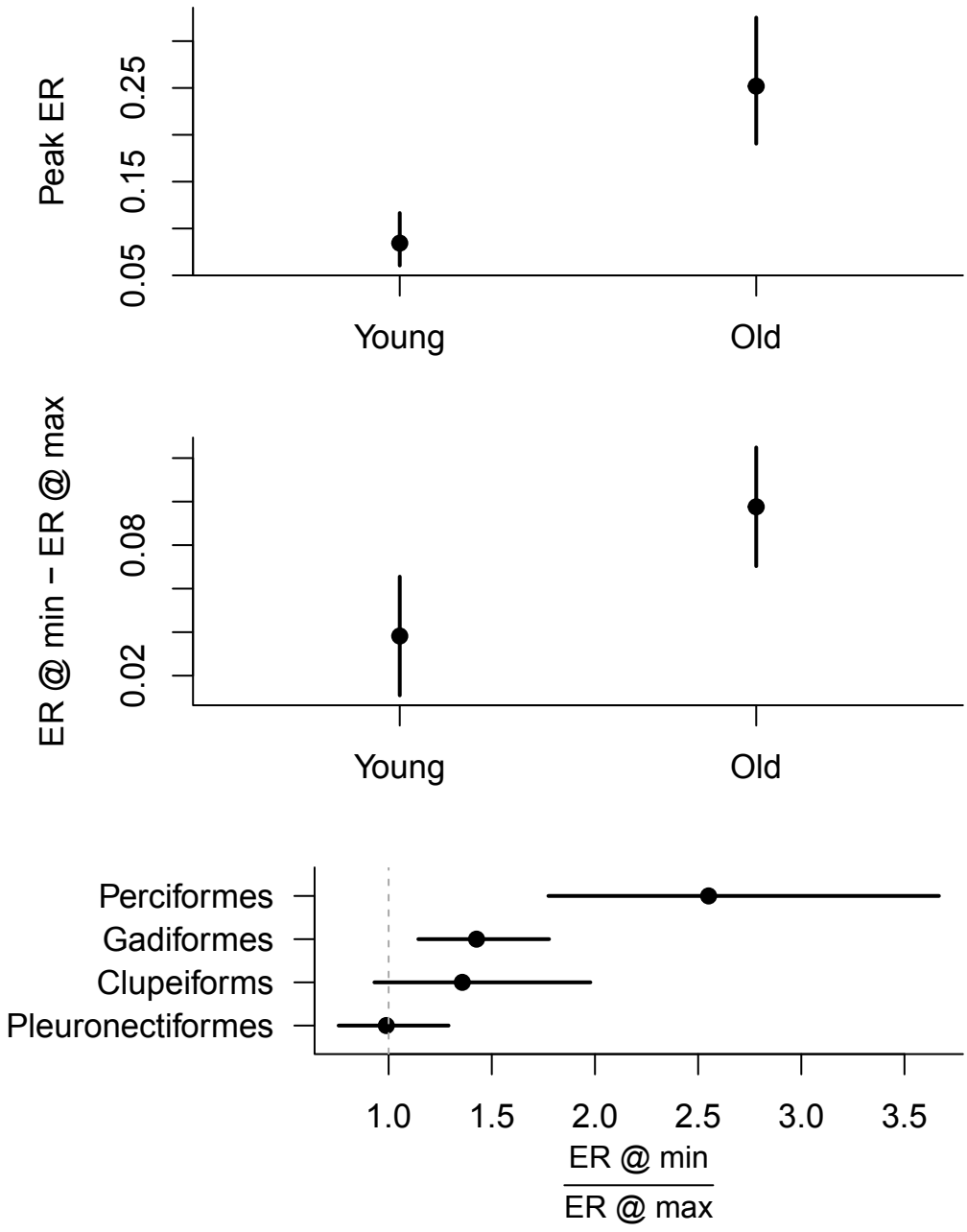

Figure 3.7: Model estimated (a) peak exploitation rate ($Peak_{ER}$) with 95% confidence intervals for each age class; (b) absolute change in exploitation rate (Abs_{ER}) with 95% confidence intervals for each age class; (c) relative change in exploitation rate (Rel_{ER}) with 95% confidence intervals for the taxonomic orders using the age-specific data.

Chapter 4

The impact of age structure on recruitment

4.1 Introduction

Predicting recruitment (the number of offspring which survive to enter a fishery) has long been a central goal of fisheries science, and spawning stock biomass (SSB) has long been the measure used to predict recruitment [89]. From its inception, it has been recognized that the SSB-recruitment relationship is a simplification of complex biological processes and that more knowledge of the underlying biological processes is needed [10]. Despite this, and the relatively poor fit of stock-recruit models in many populations, this relationship has become a central tenet of fisheries science [121].

SSB is actually a composite metric made up of the number of adult fish and the weight of these fish; it integrates the impact of density dependence (abundance) and reproductive potential (mass) into a single variable. Moreover, SSB-recruitment models do not account for a population's age structure; they treat each unit of mass as being identical. However, there is a growing literature suggesting that age can have a significant impact on offspring production and hence recruitment [9, 112]. While utilizing SSB might provide a good first approximation to estimate recruitment variability, the integration of these different processes may result in SSB being too coarse of a metric to identify some of the underlying biological processes that lead to recruitment variability [98].

Density dependent dynamics are generally assumed to be a function of SSB and not the actual quantity of fish [121]. This approach is likely not problematic if there are no major changes in either the age or size structure of a fished population. However, if age or size structure changes significantly over time, models that incorporate SSB alone will be unable to account for the potential confounding impacts of having an equivalent SSB comprised of either a small number of large fish or a large number of small fish. A shift to populations dominated by smaller fish is common in harvested

populations, but the impacts of such shifts cannot easily be assessed when using traditional SSB-recruitment models [52, 60]. In such populations, shifts towards more numerous assemblages of small fish might lead to more direct intra-specific competition both within and among age classes. It may also result in elevated inter-specific competition with species that may have formerly been the prey for the largest individuals in the population becoming their predator [116]. For cannibalistic species, smaller adults might also be more likely to exhibit juvenile cannibalism given the increased likelihood that juveniles will be closer to the optimal prey size of the adults, this could result in major changes to the underlying population dynamics [115]. For territorial species, such as salmonids, an increase in the abundance of small adults could lead to a reduction in the availability of high-quality territories, especially if egg quality declines with parental size, leading to a reduction in per capita recruitment [72].

There is compelling evidence that the number of recruits can be a function of the age, and thus size, of the parental fish [9, 114]. For example, in Atlantic cod (*Gadus morhua*), egg production per kilogram has been reported to be up to an order of magnitude lower in first-time (virgin) spawners [112]. In some species, as individuals grow and mature the number of eggs produced can increase per kilogram of fish (size-specific fecundity), therefore a kilogram of older fish would be predicted to produce more recruits than a kilogram comprised of younger fish [23,70]. Thus, when there is a high percentage of large parental fish in a population, recruitment would be expected to be elevated while a high percentage of either virgin or small parental fish would likely result in low offspring production and in-turn low recruitment.

An age-independent SSB-recruitment relationship has traditionally been used because information on population age structure is often limited. More detailed studies on the effects of age were typically limited to single populations, which raises questions about the applicability of these results to other populations and species [70]. However, during the last several years numerous fisheries stock assessments containing detailed age-specific information have become publicly available. I have compiled these stock assessments for 85 populations to determine the influence of age-specific metrics on recruitment and to understand how this varies between species and across populations. My objectives are three-fold: (a) determine how the potential fecundity

(mass) of virgin and repeat spawners influences recruitment ($\frac{Recruits}{SSB}$); (b) determine how density dependence (abundance) of virgin spawners influences $\frac{Recruits}{SSB}$; and (c) determine the extent to which any effects of age structure on recruitment can be generalized among different species and populations.

4.2 Methods

We collated the data for this analysis from publicly available stock assessments. The data set includes time series of abundance, biomass, average weight, probabilities of maturity, fishing mortality, natural mortality, and/or catch for each age class in 134 different populations. The data originated from fisheries stock assessments undertaken for harvested fish stocks in from Europe (ICES [International Council for the Exploration of the Sea]), Canada (DFO [Department of Fisheries and Oceans]), the USA (NOAA), and the High Seas (NAFO [Northwest Atlantic Fisheries Organization and ICCAT [International Council for the Conservation of Atlantic Tunas]), and includes populations from 6 taxonomic orders (Clupeiformes, Gadiformes, Osmeriformes, Perciformes, Pleuronectiformes, and Scorpaeniformes). I extracted age-specific estimates of abundance, average individual mass, and maturity probabilities for the 85 populations for which these data were available.

To undertake the analysis, a number of metrics needed to be calculated from the database. The number of first-time spawners (hereafter, virgin spawners; N_{vir}) was calculated using abundance data and maturity ogives. For the first year of data, it was assumed the maturity ogive was the same as in the previous year. The number of virgin spawners in each age class was calculated as:

$$N_{vir}[i,j] = \begin{cases} N[i,j] \times Mat[i,j] & i = 1 \quad j = m \\ N[i,j] \times (Mat[i,j] - Mat[i,j-1]) & i = 1 \quad j > m \\ N[i,j] \times Mat[i,j] & i > 1 \quad j = m \\ N[i,j] \times (Mat[i,j] - Mat[i-1,j-1]) & i > 1 \quad j > m \end{cases} \tag{4.1}$$

where $Mat[i,j]$ was the proportion of mature individuals in the j^{th}age class and the i^{th}year, m was the youngest age class in which maturity was > 0. This assumes that mortality between years is independent of maturity and the increase in maturity is not

due to a disproportionately high mortality rate of immature fish. If this assumption does not hold it would result in a elevated estimate of the number of virgin spawners. To obtain the total number of virgin spawners, N_{vir} was summed across all mature age classes in each year:

$$N_{vir}[i] = \sum_{j=m}^{n} N_{vir}[i,j] \tag{4.2}$$

where n was the number of age classes. I then calculated the number of repeat spawners (N_{rep}) (not used in our models):

$$N_{rep}[i] = \sum_{j=m}^{n} N_{mat}[i,j] - N_{vir}[i,j] \tag{4.3}$$

where $N_{mat}[i,j]$ is the total number of mature individuals. N_{rep} represents the number of spawners who have spawned at least once.

The next covariate used in the models was Spawning Stock Biomass (SSB); it was calculated from the data as:

$$SSB[i] = \sum_{j=m}^{n} N_{mat}[i,j] \times MA[i,j]) \tag{4.4}$$

where $MA[i,j]$ is the average mass of individuals in each age class in each year. The next covariate was the average mass of virgin spawners (M_{vir}) and was calculated as:

$$M_{vir}[i] = \frac{\sum_{j=m}^{n}(N_{vir}[i,j] \times MA[i,j])}{N_{vir}[i]} \tag{4.5}$$

Similarly the average mass of repeat spawners (M_{rep}) was calculated for each year as:

$$M_{rep}[i] = \frac{\sum_{j=m}^{n}(N_{rep}[i,j] \times MA[i,j])}{N_{rep}[i]} \tag{4.6}$$

The proportion of virgin spawners (P_{vir}) was the next covariate and was calculated as:

$$P_{vir}[i] = \frac{N_{vir}[i]}{N_{mat}[i]} \tag{4.7}$$

Finally, metrics of the relative number of large and small repeat spawners were calculated. The average annual mean weight of the two oldest age classes was calculated. I then determined the year in which the median weight was observed (meant to represent an average year). Using the frequency distribution for this year, mass-specific quartiles were calculated. All fish in the data that were smaller than the lower quartile of this distribution were classified as 'small', while all fish larger than the upper mass quartile were classified as 'large'. In each year for each population the proportion of repeat spawners that were classified as small (P_{small}) was calculated as:

$$P_{small}[i] = \frac{\sum_{j=1}^{small} N_{rep}[i,j]}{N_{rep}[i]} \tag{4.8}$$

where *small* includes the age classes in which mass is less than the lower quartile as calculated above. The proportion of large repeat spawners (P_{large}) was calculated as:

$$P_{large}[i] = \frac{\sum_{j=large}^{n} N_{rep}[i,j]}{N_{rep}[i]} \tag{4.9}$$

where *large* includes the age classes in which mass is greater than the upper quartile mass as calculated above. To facilitate the analysis among populations, these covariates and the response variable, recruits per spawner $\frac{Recruits}{SSB}$ (hereafter referred to as $\mathrm{Z}_{\frac{\mathrm{Recruits}}{\mathrm{SSB}}}$), were standardized using the general equation:

$$Z_{bk} = \frac{X_{bk} - \overline{X}_k}{sd\,(X)_k} \tag{4.10}$$

where Z is the standardized data, X is the data on the original scale, b is the individual data point, and k is the population.

4.2.1 Overall analysis

The full model was:

$$\begin{aligned} y_i = \gamma_{(SSB)[i]} + \Gamma_{(SSB,pop)[i]} + \upsilon_{(M_{vir})[i]} + \Upsilon_{(M_{vir},pop)[i]} + \\ \lambda_{(M_{rep})[i]} + \Lambda_{(M_{rep},pop)[i]} + \psi_{(P_{small})[i]} + \Psi_{(P_{small},pop)[i]} + \\ \omega_{(P_{large})[i]} + \Omega_{(P_{large},pop)[i]} + \phi_{(P_{vir})[i]} + \Phi_{(P_{vir},pop)[i]} + \epsilon_i \end{aligned} \tag{4.11}$$

where i is an individual data point and y_i is $\mathrm{Z}_{\frac{\text{Recruits}}{\text{SSB}}}$. The model terms $\gamma_{(SSB)}$, $\upsilon_{(M_{vir})}$, $\lambda_{(M_{rep})}$, $\psi_{(P_{small})}$, $\omega_{(P_{large})}$, and $\phi_{(P_{vir})}$ are the fixed effect terms. For each fixed effect term, there is also a random effect term which estimates the coefficient for each population; these are represented by the terms in the model with the capitalized Greek letters (e.g. $\Gamma_{(SSB,pop)}$ contains the estimate of the coefficients of the effect of SSB for each population) and the error is assumed to be normally distributed $\epsilon_i \sim N(0, \sigma)$

Model selection was performed using a frequentist information theoretic model selection process as model selection using a Bayesian paradigm in complex random effects models has yet to find a satisfactory solution. Starting with the full model, the random and fixed terms were removed sequentially, using Akaike Information Criteria (AIC; [2]), corrected for small sample size (AICc). Restricted maximum likelihood estimators were used to compare the random terms (while comparing models with the same fixed effects), and maximum likelihood estimates for the fixed terms comparing models with the same random effects [13, 125]. In this model, a fixed term that explains an important component of variation suggests there is a strong relationship overall. The retention of random terms indicates that there is significant variation at the stock level for that component. In cases in which either the fixed or random term (but not both) accounted for an insignificant portion of the variation, I have retained both terms so I can fully interpret the influence of the term at each hierarchical level. After model selection a multilevel Bayesian multiple regression framework was used to estimate the regression coefficients and their uncertainty at the stock, species, and overall levels. After model selection, the final model chosen was:

$$\begin{aligned} y_i = \gamma_{(SSB)[i]} + \Gamma_{(SSB,pop)[i]} + \upsilon_{(M_{vir})[i]} + \Upsilon_{(M_{vir},pop)[i]} + \\ \lambda_{(M_{rep})[i]} + \Lambda_{(M_{rep},pop)[i]} + \phi_{(P_{vir})[i]} + \Phi_{(P_{vir},pop)[i]} + \epsilon_i \end{aligned} \tag{4.12}$$

$$\begin{aligned} \Gamma_{(SSB,pop)} &\sim N(\mu_\Gamma, \sigma^2_\Gamma) \\ \Upsilon_{(M_{vir},pop)} &\sim N(\mu_\Upsilon, \sigma^2_\Upsilon) \\ \Phi_{(P_{vir},pop)} &\sim N(\mu_\Phi, \sigma^2_\Phi) \\ \Lambda_{(M_{rep},pop)} &\sim N(\mu_\Lambda, \sigma^2_\Lambda) \end{aligned}$$

Each random model term was assigned a prior normal distribution with its mean (μ) and variance (σ^2) estimated from the data. The priors for each μ was a zero mean normal prior with σ^2 estimated from the data; for the variance priors, an identical vague uniform prior was set on each standard deviation (e.g. $\sigma_\Gamma\, U(0,1)$ [33]). Additionally, for species with multiple populations, the species level estimates were calculated. For Atlantic cod, I also estimated the coefficients for both the Western Atlantic and Eastern Atlantic populations separately as the relationship between recruitment and SSB differs between these populations [56].

Analyses were conducted using R, version 2.15, while Markov chain Monte Carlo (MCMC) sampling was performed using the R2WinBUGS package, and WinBUGS Version 1.4.3 [65, 87]. The model was run for 100,000 time steps, with an initial burn in period of 50,000. To eliminate auto-correlation in the MCMC chains, they were thinned, such that only every 50^{th}data point was used. In addition, three separate chains were run to check for non-convergence of each parameter. Model convergence was assessed via a visual inspection of the MCMC sampling chains and using the Gelman and Rubin convergence diagnostic $\hat{R}$. The highest value of $\hat{R}$ that was observed for any parameter was 1.004, which is less than the threshold value of 1.1, suggesting there is little evidence of non-convergence for any of the parameters [33]. Posterior predictive checks (PPCs) were used to visually assess model fits; the model produced reasonable estimates for each species and SSB category within the model [33]. Additionally, a Bayesian p-value of 0.5 was estimated based on the model results which indicates a well fit model [57]. Standard residual plots were checked to ensure there were no serious violations of the model assumptions.

Bayesian hierarchical models have several advantages over a traditional modelling framework. Using these methods, the variance explained for each hierarchical level can be estimated. This allows for a better understanding of the influence of each level on the model fit [33]. These models also allow for a partial pooling of the results, thus allowing for multiple comparisons without an additional penalty [34]. An additional advantage is the ability to estimate coefficients for terms at each hierarchical level, allowing for an accurate estimate of the size and direction of any effect at each level in the model [32, 34].

4.3 Results

4.3.1 Overall model

The best model retained four of the terms and explains approximately 27.5% of the total variance (Tables 4.1 - 4.4). Although none of the terms explains an overwhelming amount of the total variance (Fig. 4.1), the model does account for 32.2% more of the variation in these data than a Ricker stock-recruit model. SSB has the largest estimated effect, $\mu_{(N_{Rep})}$ = -0.4 (-0.45:-0.34, 95% Bayesian Credible Interval (BCI)) and the largest inter-population variability ($\sigma_{(SSB)} = 0.18$ (0.13:0.24, 95% BCI); Figs. 4.1 and 4.2). There is also a relatively consistent relationship between the proportion of virgin spawners and $Z_{\frac{\text{Recruits}}{\text{SSB}}}$, $\mu_{(P_{Vir})} = 0.08$ (0.03:0.13, 95% BCI) with slightly less inter-population variability in this metric, $\sigma_{(P_{Rec})} = 0.15$ (0.1:0.21, 95% BCI) than for SSB. There is a weak overall relationship between $Z_{\frac{\text{Recruits}}{\text{SSB}}}$ and the average mass of repeat spawners, $\mu_{(M_{Rep})} = 0.02$ (-0.03:0.08, 95% BCI), but the inter-population variability was relatively high which likely led to the retention of this term in the model $\sigma_{(M_{Rep})} = 0.16$ (0.11:0.22, 95% BCI). Finally, the mass of virgin spawners appears to have approximately the opposite effect of M_{rep} , $\mu_{(M_{Vir})}$ = -0.05 (-0.1:0, 95% BCI), with approximately the same amount of inter-population variability ($\sigma_{(M_{Vir})} = 0.14$ (0.08:0.2, 95% BCI); Figs. 4.1 and 4.2).

4.3.2 Spawning stock biomass

On average an increase of one standard deviation in SSB is associated with a decline in $Z_{\frac{\text{Recruits}}{\text{SSB}}}$ of -0.4 (-0.45:-0.34, 95% (BCI); Fig. 4.3). For species with multiple populations, the size of this effect is smallest for Western Atlantic cod (Fig. 4.4). When looking at the population level, three of the Western Atlantic cod populations (i.e., COD3NO, COD3Pn4RS, and COD4TVn) exhibit weak relationships between $\frac{Recruits}{SSB}$ and SSB (Fig. 4.5). The Eastern Atlantic cod stocks also have a lower than average effect (Fig. 4.4) although the effect is generally stronger than the Western Atlantic populations with several populations exhibiting a strong negative effect (i.e., CODICE, CODNEAR, and CDOFAPL); Fig. 4.5). For the other species represented by multiple populations there is generally less intra-species variability than found in the cod populations (Fig. 4.5).

4.3.3 Mean Mass of Virgin Spawners

The mass of virgin spawners M_{vir} has the lowest inter-population variance of the terms retained in the model (Fig. 4.1). On average an increase of one standard deviation in M_{vir} is associated with a decline in $Z_{\frac{\text{Recruits}}{\text{SSB}}}$ of -0.05 (-0.1:0, 95% BCI; (Fig. 4.3). At the species level, there is a relatively weak, but consistent, negative relationship between M_{vir} and $Z_{\frac{\text{Recruits}}{\text{SSB}}}$ Fig. 4.4). *M. aeglefinus* is the one exception as there is a relatively consistent increase in $Z_{\frac{\text{Recruits}}{\text{SSB}}}$ when M_{vir} is large (Fig. 4.6). In the eastern Atlantic cod populations, the effect is negative in the majority of cases, while in the western Atlantic the trend seems to be somewhat more inconsistent (Fig. 4.6).

4.3.4 Mean mass of repeat spawners

The average mass of repeat spawners M_{rep} has a moderate inter-population variance (Fig. 4.1) although on average a one standard deviation in M_{rep} is associated with an increase in $Z_{\frac{\text{Recruits}}{\text{SSB}}}$ of only 0.02 (-0.03:0.08, 95% BCI (Fig. 4.3). For most species there is no clear overall trend suggesting that the majority of the variability is occurring at the population level (Figs. 4.4 and 4.7). The one exception appears to be Atlantic cod in which most populations exhibit a weak positive relationship between M_{rep} and $Z_{\frac{\text{Recruits}}{\text{SSB}}}$. Over 80% of the Atlantic cod populations have positive estimates, including several of the largest estimates in the entire analysis (although there is a large negative estimate for COD3NO). For the remaining populations there are no consistent intra-species trends (Fig. 4.7).

4.3.5 Proportion of virgin spawners

The proportion of virgin spawners (P_{vir}) has the second largest effect size, though only a moderate amount of inter-population variance (Figs. 4.1, 4.3). A one standard deviation change in P_{vir} is associated with an increase in $Z_{\frac{\text{Recruits}}{\text{SSB}}}$ of 0.08 (0.03:0.13, 95% BCI;. The estimated effect is positive for most species with the largest effects found in Atlantic cod and winter flounder while the size of the effect is essentially zero for most herring and yellowtail flounder populations (Figs. 4.4, 4.8).

4.4 Discussion

4.4.1 Virgin spawners

There is a consistent and relatively strong relationship between P_{vir} and $\frac{Recruits}{SSB}$. If there is high proportion of virgin spawners in the population $\frac{Recruits}{SSB}$ is generally elevated. Taken together these results suggest that $\frac{Recruits}{SSB}$ can be strongly influenced by not just SSB, but also the number of virgin spawners in a population. In general $\frac{Recruits}{SSB}$ will be unusually elevated when virgin spawners make up a larger than usual proportion of the population. For population in which there is a strong relationship between $\frac{Recruits}{SSB}$ and P_{vir} , there is generally a strong relationship with SSB. Thus, while traditional stock-recruitment dynamics are in play in these populations, there is also a relationship between recruitment and the virgin spawners that has not been explored in great detail.

Somewhat surprisingly there is a weak inverse relationship between the mass of virgin spawners (M_{vir}) and $\frac{Recruits}{SSB}$, this suggests that when virgin spawners are small, SSB is larger than would be expected. *M. aeglefinus* is the one species in which there may be a small positive effect of (M_{vir}) on $\frac{Recruits}{SSB}$, but even for this species there is a large degree of inter-population variability.

4.4.2 Repeat spawners

There is no evidence that an increase in the average size of repeat spawners,(M_{rep}) , has any effect on $\frac{Recruits}{SSB}$ for the majority of species in this analysis. This suggests that there is no benefit to having large repeat spawners. Additionally, there is little evidence that having a large proportion of either large or small repeat spawners (P_{large} and P_{small} respectively) has an consistent effect on $\frac{Recruits}{SSB}$. Thus when there is a higher than usual proportion of either large or small repeat spawners $\frac{Recruits}{SSB}$ remains largely unchanged. These lines of evidence imply that the variability in fecundity (size) of small fish is not a significant factor in recruitment dynamics. This is consistent with the hypothesis that virgin spawners' direct contribution to offspring production is smaller than that of repeat spawners [112].

Contrary to several other lines of evidence, there is little evidence that maintaining a population of old, large, individuals increases recruitment rates [9, 98]. This may

be due to the low abundance of these spawners in these populations due to their rapid removal in harvested systems, or may be due to the limitations of the covariates chosen. It may also be that age effects are not due to old large fish, but are influenced by interactions between different cohorts during their first few years of maturity. These interactions may include competitive interactions between cohorts, such as cannibalism, or may simply be a function of poor reproductive performance in the first years of maturation [112, 115]

4.4.3 Atlantic cod

Atlantic cod is the most obvious example of a species in which the relationship between $\frac{Recruits}{SSB}$ and SSB is depressed. The Eastern Atlantic populations exhibit somewhat stronger relationships between $\frac{Recruits}{SSB}$ and SSB than Western Atlantic populations, yet in both groups these relationships are weaker than for the other species. This suggests that density-dependent compensation in cod is weaker than for other species. One consequence of this is that when the number of spawners is low, recovery may not be as rapid as for other species. In the Western Atlantic populations this effect is somewhat mitigated by the relatively strong positive effect of the mass of the repeat spawners which indicates larger fish, on average, produce more offspring surviving to recruitment. Unfortunately, in many of these stocks the average size of the fish have been steadily declining [53, 111]. Given that the effect of M_{rep} is relatively large in these populations, it would appear that maintaining the size structure of these populations would have a larger influence on recruitment than for the majority of stocks [9].

4.4.4 Management implications

Somewhat surprisingly, I show that virgin spawners (which comprise on average 45% of total abundance, and 32% of total SSB) can have a relatively large effect on the relationship between $\frac{Recruits}{SSB}$ and SSB. These results imply that recruitment is often influenced by a different component of the population than has traditionally be assumed and suggests that there are additional mechanisms influencing recruitment dynamics than have traditionally been the focus of fisheries science. Thus, the implicit assumption of typical stock-recruit models that there is no effect of age on spawner

biomass is likely to often be incorrect. Most recent research has focused on the effect of large, fecund spawners, this analysis suggests that young spawners may also play an under-appreciated role in recruitment dynamics [9, 98, 103].

4.5 Conclusion

I provide evidence that different components of the spawning stock contribute differentially to recruitment across a wide range of species and populations. The underlying assumption that age has no influence on the recruitment process appears to represent an oversimplification of a complex interaction between age, fecundity, and developmental status. I have identified several empirically meaningful trends, especially with regard to first time spawners, that suggest fruitful avenues for further research. Primarily, I believe continued research into the underlying biological mechanisms, especially with respect to young spawners, that influence recruitment success are paramount to improve our understanding of recruitment variability in marine fishes.

4.6 Figures and Tables

Table 4.1: Model selection table for removing (one of) the random effect of SSB, proportion of small individuals, proportion of large individuals, mean mass repeat spawners, mean mass virgin spawners, and proportion of virgin spawners

Modnames	K	AICc	Delta_AICc	ModelLik	AICcWt	Res.LL	Cum.Wt
Percent Small Removed	14.00	7518.78	0.00	1.00	0.57	-3745.32	0.57
Full Model	15.00	7520.80	2.02	0.36	0.21	-3745.32	0.78
Percent Large Removed	14.00	7521.42	2.64	0.27	0.15	-3746.64	0.94
Mean Mass Repeat Removed	14.00	7523.20	4.42	0.11	0.06	-3747.53	1.00
Mass Virgin Removed	14.00	7534.90	16.12	0.00	0.00	-3753.38	1.00
Percent Virgin Removed	14.00	7542.15	23.37	0.00	0.00	-3757.00	1.00
SSB Removed	14.00	7547.60	28.82	0.00	0.00	-3759.73	1.00

Table 4.2: Model selection table for removing (one of) the random effect of the proportion of small individuals, proportion of large individuals, mean mass repeat spawners, mean mass virgin spawners, and proportion of virgin spawners

Modnames	K	AICc	Delta_AICc	ModelLik	AICcWt	Res.LL	Cum.Wt
+ Percent Large Removed	13.00	7519.99	0.00	1.00	0.53	-3746.93	0.53
Percent Small Removed	15.00	7520.80	0.81	0.67	0.36	-3745.32	0.89
+ Mean Mass Repeat Removed	13.00	7523.21	3.22	0.20	0.11	-3748.54	1.00
+ Mass Virgin Removed	13.00	7530.26	10.28	0.01	0.00	-3752.07	1.00
+ Percent Virgin Removed	13.00	7541.15	21.17	0.00	0.00	-3757.51	1.00

Table 4.3: Model selection table for removing (one of) the random effect of the proportion of both small and large individuals, mean mass repeat spawners, mean mass virgin spawners, and proportion of virgin spawners

Modnames	K	AICc	Delta_AICc	ModelLik	AICcWt	Res.LL	Cum.Wt
Percent Small + Large Removed	13.00	7519.99	0.00	1.00	1.00	-3746.93	1.00
+ Mass Virgin Removed	12.00	7530.86	10.87	0.00	0.00	-3753.38	1.00
+ Mean Mass Repeat Removed	12.00	7536.08	16.10	0.00	0.00	-3755.99	1.00
+ Percent Virgin Removed	12.00	7541.27	21.28	0.00	0.00	-3758.58	1.00

Table 4.4: Model selection table for removing the fixed effect of the proportion of both small and large individuals and each term individually

Modnames	K	AICc	Delta_AICc	ModelLik	AICcWt	LL	Cum.Wt
Percent Small + Large Removed	11.00	7478.33	0.00	1.00	0.37	-3728.12	0.37
Percent Large Removed	12.00	7478.43	0.09	0.95	0.35	-3727.16	0.73
Percent Small Removed	12.00	7480.23	1.90	0.39	0.14	-3728.06	0.87
Full Model	13.00	7480.42	2.09	0.35	0.13	-3727.15	1.00

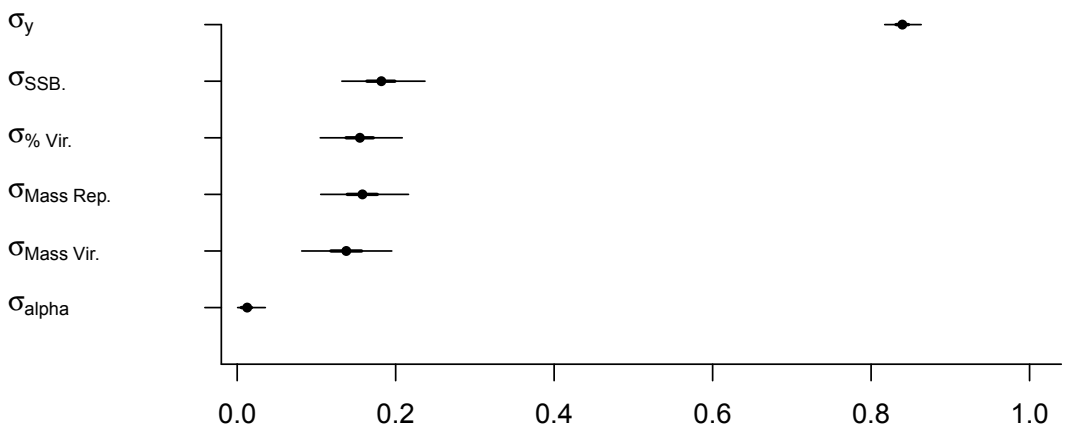

Figure 4.1: Variance explained by each random effect and the overall unexplained variance (σ_y in the model, the thin line is 95% BCI, thick line is the 50% BCI.

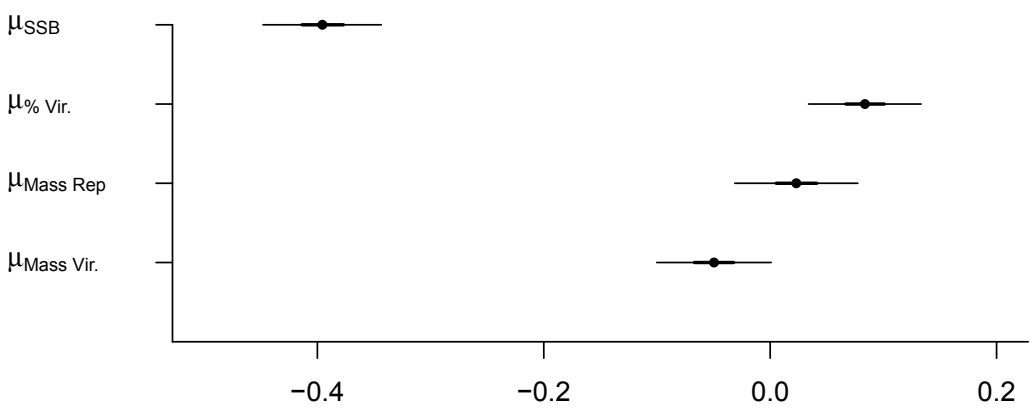

Figure 4.2: The overall model estimates for each term in the model, thin line is 95% BCI, thick line is the 50% BCI. (a) Relationship between $\frac{Recruits}{SSB}$ and spawning stock biomass (SSB); (b) Relationship between $\frac{Recruits}{SSB}$ and percent of virgin spawners; (c) Relationship between $\frac{Recruits}{SSB}$ and mean mass of repeat spawners; (d) Relationship between $\frac{Recruits}{SSB}$ and mean mass of virgin spawners.

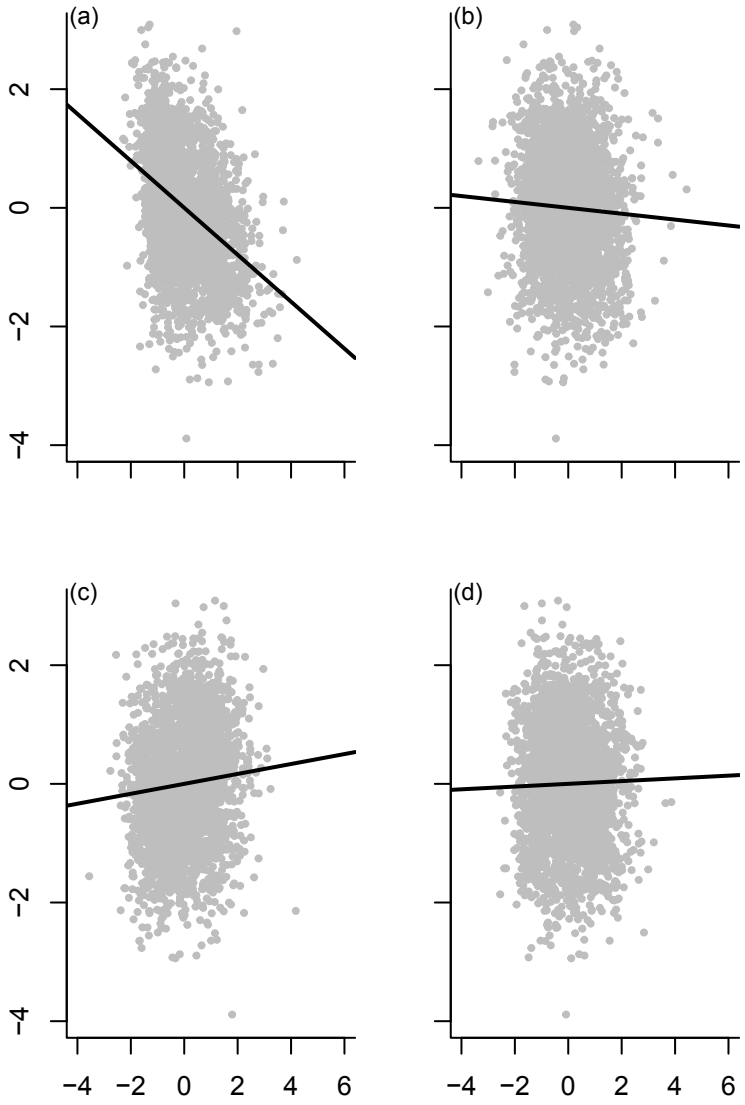

Figure 4.3: The fit of the overall model estimates for each term in the model to the overall data. (a) Relationship between $\frac{Recruits}{SSB}$ and Spawning Stock Biomass (SSB); (b) Relationship between $\frac{Recruits}{SSB}$ and mean mass of virgin spawners; (c) Relationship between $\frac{Recruits}{SSB}$ and percent of virgin spawners; (d) Relationship between $\frac{Recruits}{SSB}$ and mean mass of repeat spawners.

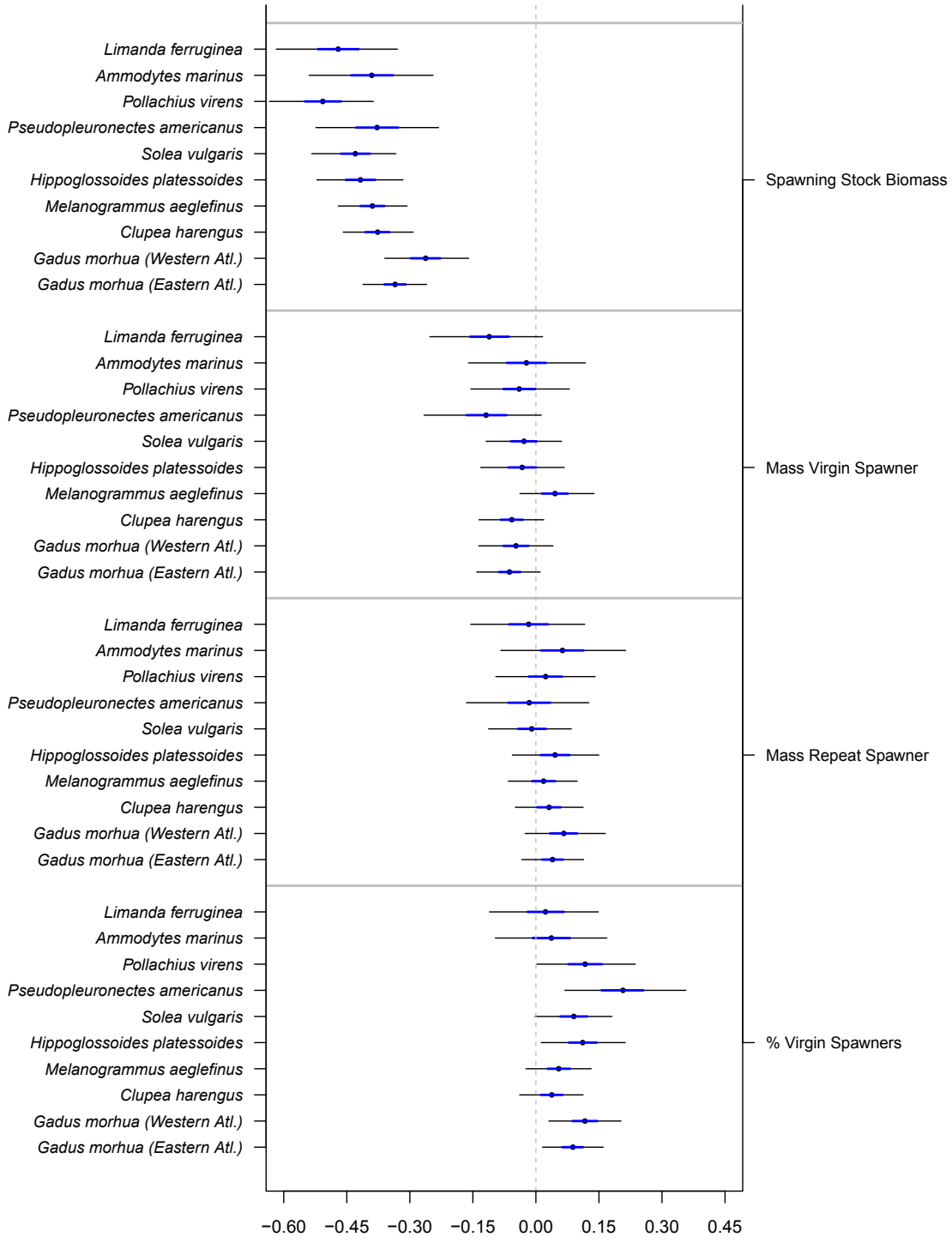

Figure 4.4: The model estimates from the final model for each species with multiple populations. The thin line is 95% BCI, thick line is the 50% BCI.

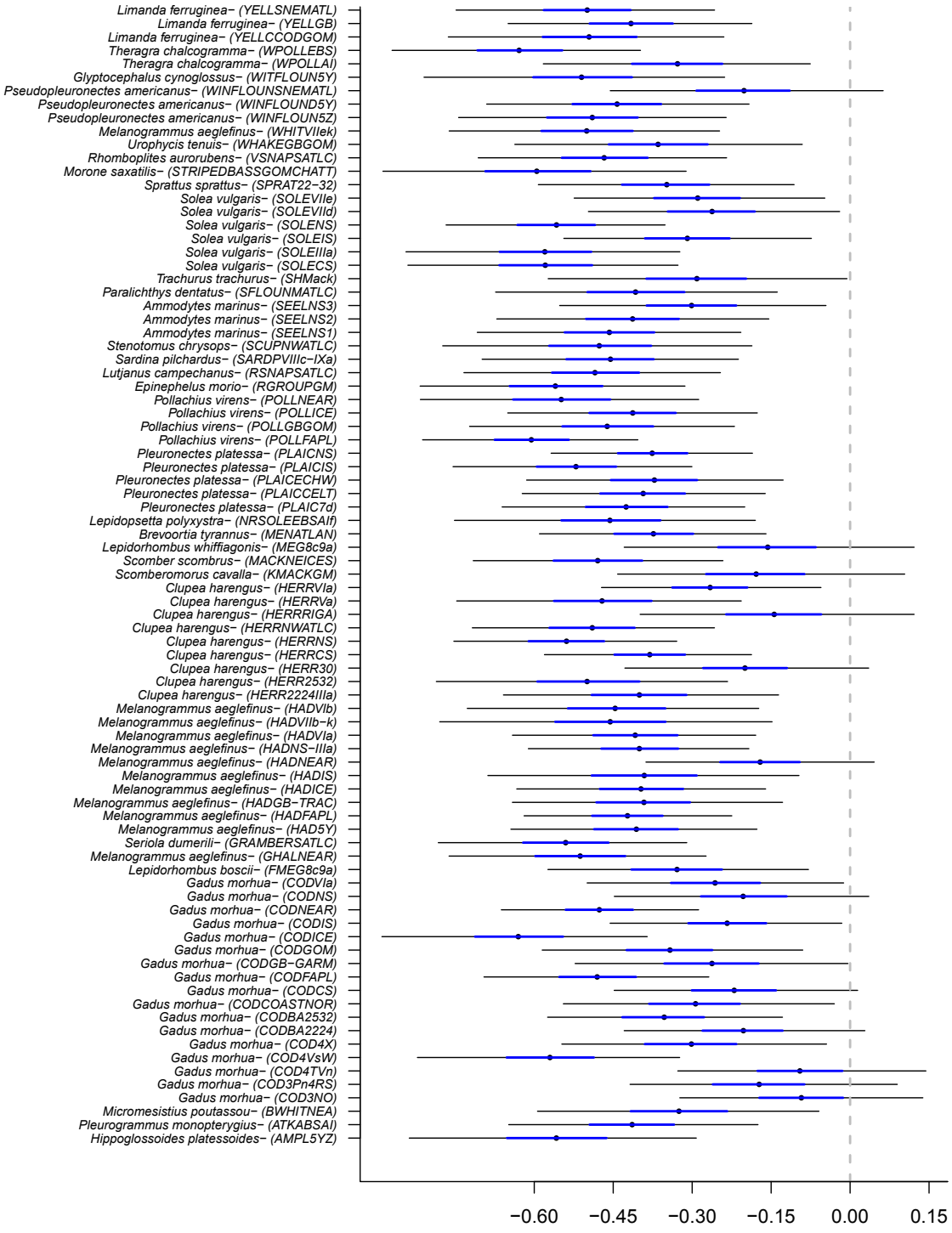

Figure 4.5: The estimated effect of spawning stock biomass (SSB) for each population in the database. The thin line is 95% BCI, thick line is the 50% BCI.

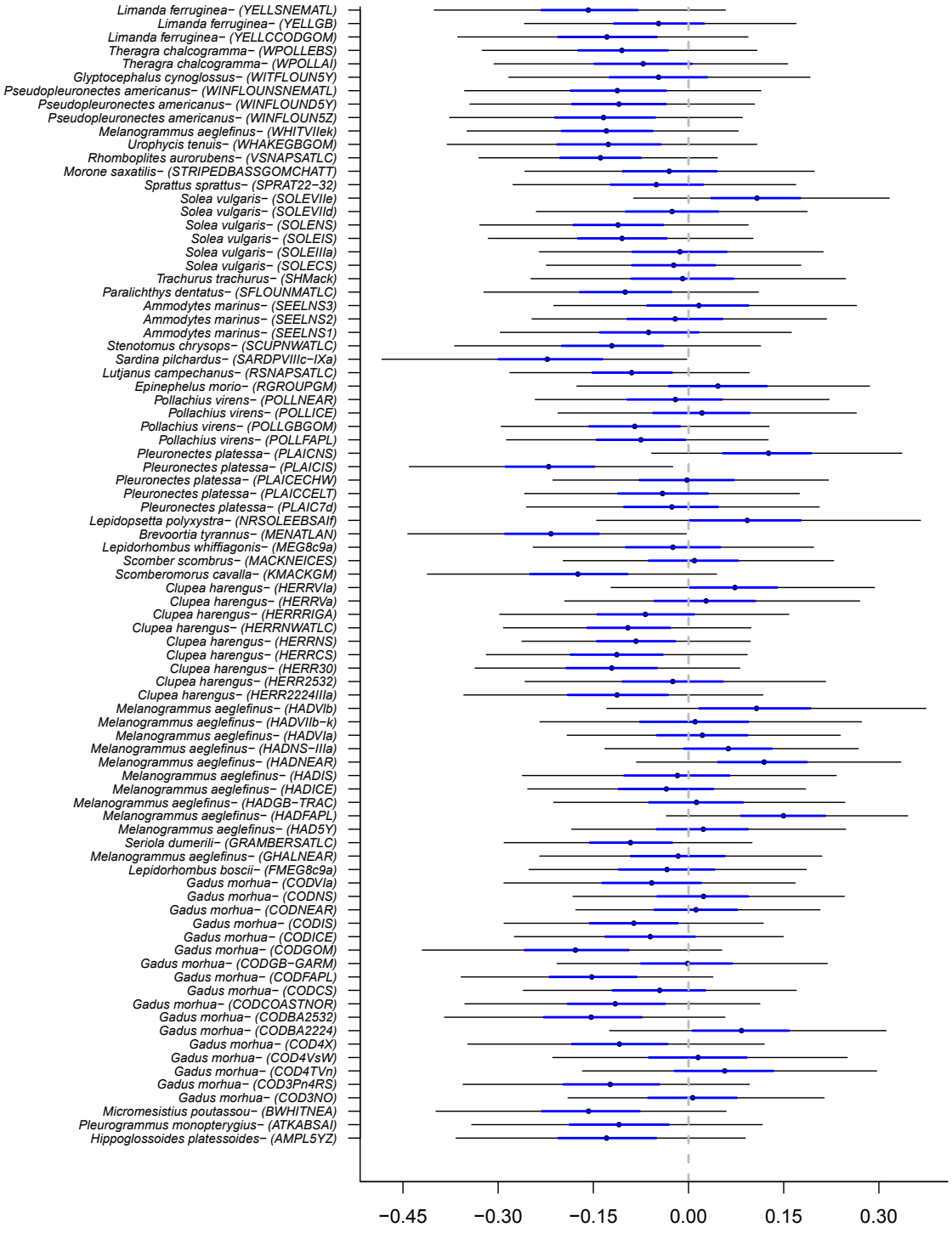

Figure 4.6: The estimated effect of mass of virgin spawners for each population in the database. The thin line is 95% BCI, thick line is the 50% BCI.

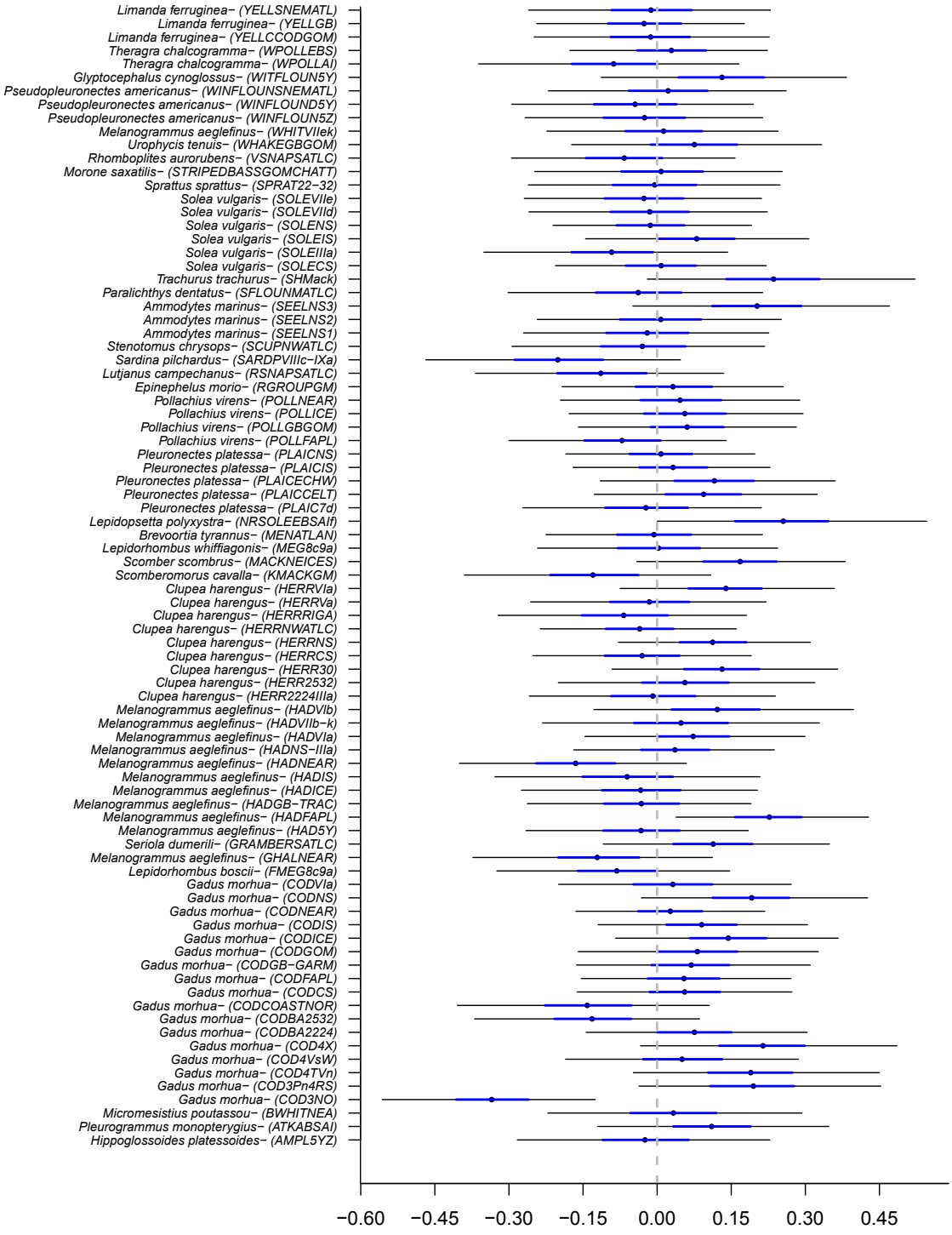

Figure 4.7: The estimated effect of mean mass of repeat spawners for each population in the database. The thin line is 95% BCI, thick line is the 50% BCI.

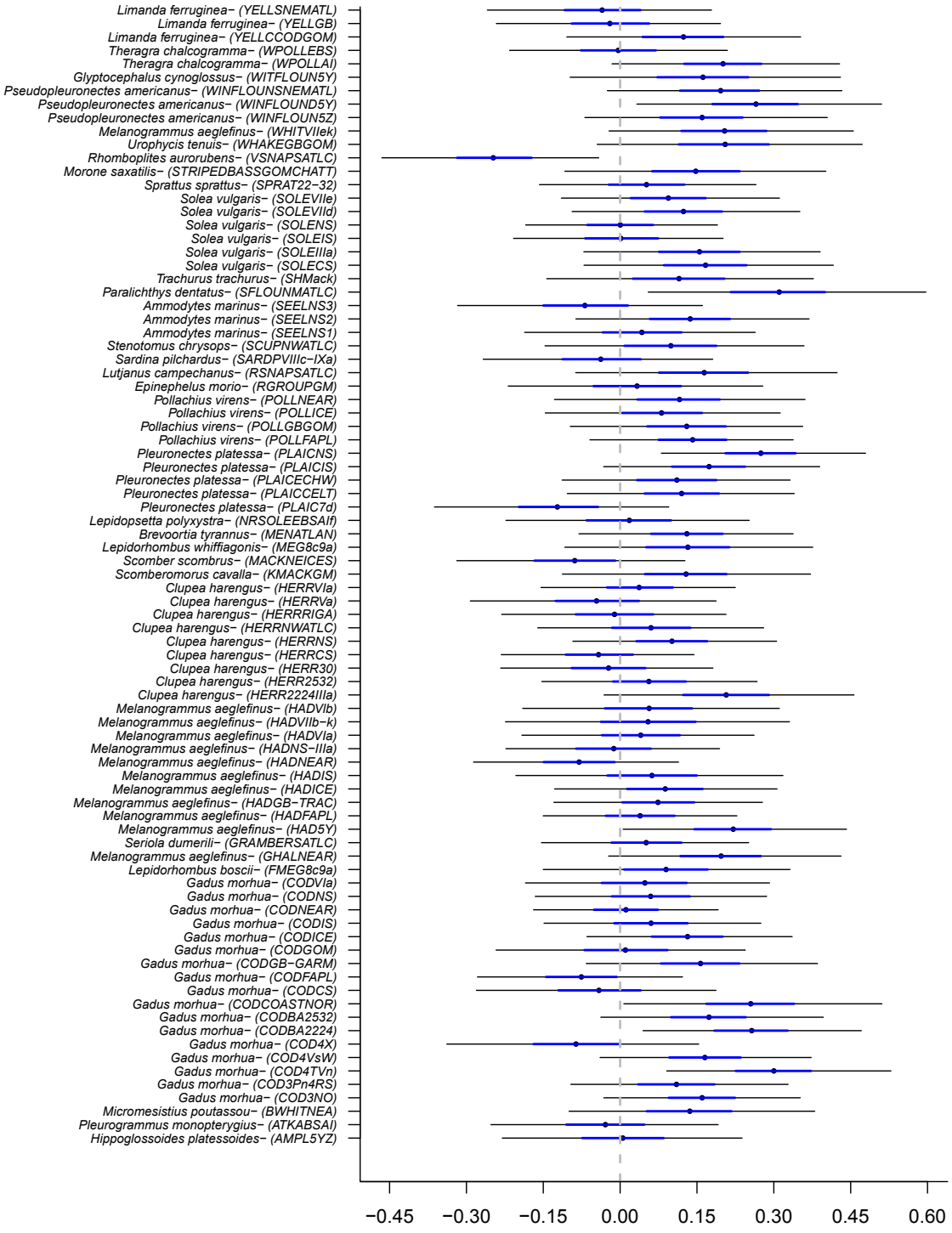

Figure 4.8: The estimated effect of percent of virgin spawners for each population in the database. The thin line is 95% BCI, thick line is the 50% BCI.

Chapter 5

The effect of age-specific vital rates on population persistence

5.1 Introduction

Although it is widely accepted that many harvested marine populations have declined considerably in recent decades [50, 64], the long-term outlook has been the subject of rigorous debate [41, 75, 123, 124]. Forecasted population trends are often based on simple extrapolations of past catch and abundance trajectories and necessarily make assumptions that can be viewed as problematic [75]. In contrast to these simple methods, there exist more complex stock assessment models (e.g. virtual population analysis and Statistical Catch at Age) that are often used to guide managers in setting sustainable harvesting rates [86]. Although these methods generally use (and generate) a great deal of data, they make numerous and often untested assumptions about the biological processes driving population dynamics [121]. However, despite a wealth of detailed data these models often fail to accurately project population size over even short periods, and are usually limited to providing information about the current and past state of the population [122].

In terrestrial systems, the projection of population trajectories has long depended on demographic data generated collected from intensive field studies [14, 96]. The quantity of demographic data available is often relatively sparse due to the difficulty in collecting the necessary data [73]. To overcome these data limitations, assessments of population status have necessarily focused more on probabilistic projections rather than the highly parameterized stock assessments used in fisheries science [3]. The focus has predominately been on determining the risk of extinction, using a class of analyses collectively known as population viability analysis (PVA). This modelling framework has become an integral part of global efforts to assess terrestrial species at risk status [36, 58].

Early PVAs utilized total population abundance trends, specifically the mean and variance of the population growth rate, to project the probability of extinction over some time period [96]. These early efforts were somewhat analogous to the aforementioned attempts to extrapolate fish population trends over time, in that the count-based PVAs assumed that past trends will continue into the future and they treat all individuals within a population as identical. However, for species in which individuals differ significantly in size, age, development, or other characteristics that influence population dynamics, there can be a benefit to accounting for the population structure [73,113]. These more complex models, known as demographic PVAs, utilize stochastic simulations, the annual age-specific mortality and fertility vital rates, the variability in these vital rates, and the correlation between vital rates to predict the probability of being above or below a threshold abundance after a given time period and to determine how sensitive these results are to changes in mortality and fertility vital rates [14,68].

The data necessary to parameterize demographic PVAs are difficult to obtain, and in terrestrial ecosystems they are only available when detailed multi-year demographic studies have been undertaken; a minimum of four years of data is recommended [73]. Data encompassing ten or more years would be preferable but time periods of this length are often unavailable for many terrestrial systems [73]. Conversely, in closely monitored fisheries, there are typically 20-50 years of age-specific demographic data available. Developing PVAs, using these long-term data, would enable fisheries managers to assess both the short- and long-term implications of introducing alternative harvesting strategies on the likelihood of maintaining the population above some target reference point [67]. Rather than having only a near-term view of the population health, the PVA methodology enables managers to perform risk assessments of any harvest strategy across a range of time horizons. Despite the potential advantages of utilizing demographic PVA to complement traditional stock assessment analyses, it has yet to find widespread use by fisheries managers [3].

My objectives are three-fold: (1) develop a model that utilizes age-specific survival and fertility vital rates to estimate the (i) per capita population growth rate (r), (ii) probability of collapse and (iii) probability of persistence; (2) determine which survival and fertility vital rates have the largest effect on these probabilities; and (3)

determine how these results vary between populations of Atlantic cod (*Gadus morhua*) and Atlantic herring (*Clupea harengus*), two species that have experienced depletions throughout their respective ranges and that differ considerably in life history.

5.2 Methods

5.2.1 The data

We collated the data for this analysis from publicly available stock assessments. The data-set includes time series of abundance, biomass, average weight, probabilities of maturity, fishing mortality, natural mortality, and/or catch for each age class in 24 different populations. The data originated from stock assessments undertaken for harvested fish stocks in Europe (ICES [International Council for the Exploration of the Sea]), Canada (DFO [Department of Fisheries and Oceans]), the USA (US), and the High Seas (NAFO [Northwest Atlantic Fisheries Organization). The age-specific abundance, average individual mass, and maturity data was extracted for 16 Atlantic cod *Gadus morhua* and 8 Atlantic herring *Clupea harengus* populations.

5.2.2 Vital rates

To estimate the average contribution of an individual in an age class to fecundity, I first assume that potential fecundity is a linear function of the weight of a mature individual. I can then calculate the relative individual fecundity (RIF) for each year:

$$RIF_{x,y} = \frac{W_{x,y} \times M_{x,y}}{min(W_{mat})} \tag{5.1}$$

where x is the age class, y is the year, $W_{x,y}$ is the weight in age class x and year y, $M_{x,y}$ is the percent of individuals in age class x and year y which are mature, and W_{mat} is the weight of the smallest age class having some mature individuals (across all years and age classes). As an example, the smallest mature individual age class ($\frac{W_{x,y}}{min(W_{mat})} = 1$) with 10% of individuals mature ($M_{x,y} = 0.1$) would have a RIF of 0.1, while an individual in an age class that was fully mature ($M_{x,y} = 1$) and was 3 times larger ($\frac{W_{x,y}}{min(W_{mat})} = 3$) would have a RIF of 3.

Next I calculate the total potential fecundity (TPF) for each year:

$$TPF_y = \sum (RIF_{x,y} \times N_{x,y}) \tag{5.2}$$

where $N_{x,y}$ is the number of individuals in age class x and year y. The actual percent fertility (APF) is the ratio of the actual number of offspring produced to the total potential fecundity:

$$APF_y = \frac{N_{1,y}}{TPF_y} \tag{5.3}$$

where $N_{1,y}$ is the number of individuals in the first age class in year y. The APF is not a measure of the number of offspring produced, rather it is a measure of the number of offspring produced that survive to recruit to the fishery (i.e. the first age class in the stock assessment). Finally, assuming that there is no age effect (over and above the influence of weight), I can now calculate the number of offspring produced by the average individual in each age class across all years, i.e. the actual individual fertility (F):

$$F_{x,y} = APF_y \times RIF_{x,y} \tag{5.4}$$

Survival (S) was estimated from the number of individuals that survived to reach the subsequent age class in the following year:

$$S_{x,y} = \frac{N_{(x+1),(y+1)}}{N_{x,y}} \tag{5.5}$$

where $S_{x,y}$ is the survival of age class x during year y, and $N_{x,y}$ is the number of individuals in age class x in year y. In the stock assessments, given that the final age class combines the estimated number of individuals from all the remaining age groups, I was unable to obtain an estimate of survival in the oldest age class so I assumed that the survival of the second oldest age class was equivalent to that of the oldest age class.

We utilized a stochastic projection matrix model which accounted for correlation in survival and fertility vital rates between and within years [73]. To properly utilize age-specific survival and fertility vital rates, there are three basic classes of parameters needed. The first is the mean vital rate:

$$\bar{S}_x = mean(S_{x,y})$$
$$\bar{F}_x = geomean(F_{x,y}) \tag{5.6}$$

where $\bar{S}_x$ and $\bar{F}_x$ and the mean survival and fertility vital rates for each age averaged across all years. The fecundity means were calculated as geometric means because of the skewed nature of these data. The second parameter class is the variability in each vital rate:

$$S_{var_x} = var(S_{x,y})$$
$$F_{var_x} = var(F_{x,y}) \tag{5.7}$$

where S_{var_x} and F_{var_x} are the variance in survival and fertility vital rates for each age class.

And the third parameter class is the correlation between both the survival and fertility vital rates in a given year:

$$VR_{cor_{x,y}} = cor(S_{x,y}, F_{x,y}) \tag{5.8}$$

In addition to the within year correlation between survival and fertility vital rates, I also account for the cross-correlation between adjacent years. The within and between year survival and fertility covariance matrix was based upon the correlation between vital rates found in each populations' time series. The within year covariance matrix was needed to ensure that vital rates chosen for each age classes in a given year was consistent with what was found in the population. The between year co-variance matrix was used to mimic the historic pattern of change in vital rates over time, e.g. if vital rates tended to change slowly over time the vital rates should not fluctuate between high and low values year-over-year in the simulation. The full computation details can be found in Chapters 8-9 of Morris and Doak [73].

5.2.3 Stochastic simulation

The mean, variance, and correlation of the survival and fertility vital rates form the foundation for the PVA [73]. However, the exact combination these vital rates will

not persist in the future. To perform a stochastic simulation, I need to select the appropriate statistical distribution to sample from, using the mean and variance of these vital rates. By utilizing these data and an appropriate statistical distribution, I can develop the stochastic PVA to simulate the population growth trajectory. The most appropriate distribution to use when simulating vital rates that are the outcome of binary events, such as the survival vital rates, is the beta distribution (B_x) which is bounded by 0 and 1 [73]:

$$B_x = \frac{\Gamma(a+b)}{\Gamma(a)\Gamma(b)} x^{a-1}(1-x)^{b-1} \tag{5.9}$$

where Γ is the Gamma function, x is a value between 0 and 1, and a and b are shape parameters which are related to the mean and variance:

$$\begin{aligned} a &= \bar{S}_x \left(\frac{\bar{S}_x(1-\bar{S}_x)}{S_{var_x}} - 1 \right) \\ b &= (1-\bar{S}_x) \left[\frac{\bar{S}_x(1-\bar{S}_x)}{S_{var_x}} - 1 \right] \end{aligned} \tag{5.10}$$

For the fertility vital rates, a stretched beta distribution is the preferred sampling distribution as it allows for an upper limit to the fertility rates, unlike other distributions (such as the log-normal distribution) in which there is no upper bound [73]. $\bar{F}_x$ and F_{var_x} and the maximum and minimum values of the fertility vital rates for each age class (f_{max} and f_{min}) are then used to parameterize a beta distribution that is bounded by 0 and 1:

$$\begin{aligned} M_B &= \left(\frac{\bar{F}_x - f_{min}}{f_{max} - f_{min}} \right) \\ V_B &= F_{var_x} \left(\frac{1}{f_{max} - f_{min}} \right)^2 \end{aligned} \tag{5.11}$$

The beta-distributed mean M_B and variance V_B are then used to obtain the beta-distributed random value B_x. The stretched beta value is then back calculated from B_x:

$$S_x = B_x(f_{max} - f_{min}) + f_{min} \tag{5.12}$$

5.2.4 Elevated recruitment

For many populations the fertility rates are highly variable, and the distributions typically are either bi-modal or extremely skewed. The years with high fertility represent years, or runs of years, during which recruitment is elevated. As a result of these elevated periods there is no simple distribution that can represent the actual range and frequency of the fertility vital rates. For this reason, I treated the years with unusually elevated fertility vital rates as being separate from the majority of the years. Any age class that had a fertility vital rate greater than 2 standard deviations larger than the geometric mean fertility vital rate (averaged across the entire time series) was considered an outlier:

$$F_{out[x,y]} >= \bar{F}_x + 2 \times sqrt(F_{var_x}) \tag{5.13}$$

If more than 50% of the age-specific fertility vital rates in a given year were outliers it was deemed a year with unusually elevated recruitment. Using this criterion, I mapped out the historic patterns of unusually elevated recruitment and used the duration and frequency of these periods as parameters within the model for each population. The mean, variance, and correlation of the survival and fertility vital rates, along with the sampling distributions, were calculated separately for elevated recruitment and typical recruitment periods. In addition to enabling accurate sampling distributions to be developed, this parameterization also enabled us to determine how the populations were influenced by changes to the duration and frequency of unusually elevated recruitment rates for each population. Finally, to ensure that the population abundances did not increase to biologically unrealistic levels, the populations would exit the period of elevated recruitment if the population abundance was greater than twice the maximum historic abundance.

5.2.5 Population growth, collapse, and persistence

For each population, the PVA was run for 100 years and with 5 005 replicate simulations. The stochastic per capita population growth rate (r) was calculated for

each population at the end of the simulation. A decline to 20% of the biomass at maximum sustainable yield (B_{msy}) has been defined as a collapse in fisheries [82], and B_{msy} is generally between 30-40% of the unfished biomass, thus collapse can be approximated by a decline to an abundance of 6-8% of unfished biomass [38]. For the present analysis, I defined collapse to be a decline to $< 7\%$ of the maximum population abundance. The percentage of replicates that have declined to an abundance of $< 7\%$ of maximum historic abundance was calculated over short (10 years), medium (30 years), and long (50 years) periods to provide an estimate of the probability of collapse. Finally, the probability of a population being at a sustainable level of abundance, defined as the percentage of the replicates having a population abundance of $> 40\%$ (i.e. $> B_{msy}$) of maximum historic abundance, was calculated over the same intervals, this was termed the probability of 'persistence' [38].

5.2.6 Sensitivity and elasticity

To determine which parameters have the most influence on population growth rate, the probability of collapse, and probability of persistence, a sensitivity and elasticity analysis was performed on both the mean and variance of each vital rate for each population. The sensitivity is simply the effect of changing the vital rate on the response variable of interest;

$$\Sigma_{\bar{S}_x} = \frac{\partial r}{\partial \bar{S}_x} \tag{5.14}$$

where Σ_{S_x} is the sensitivity for the parameter, here I use the mean survival vital rate for age class x as an example, but this can be calculated for any parameter in the model, e.g. F_{var_x}, $VR_{cor_{x,y}}$, etc. $\partial \bar{S}_x$ is the size of the perturbation to the model parameter and ∂r is the change in the population growth rate. Again this could be any response variable of interest such as probability of collapse or persistence. Alternatively, the elasticity is the proportional change in the response variable which results from a proportional change in a model parameter;

$$E_{\bar{S}_x} = \frac{\bar{S}_x}{r} \frac{\partial r}{\partial \bar{S}_x} \tag{5.15}$$

where E_{S_x} is the elasticity of a parameter (again mean survival used as an example) and r is the population growth rate.

To perform the sensitivity analysis, each vital rate was sequentially subjected to a perturbation of 5% and the PVA run for 100 years with 5005 replicate simulations [73]. For the survival and fertility vital rates, the perturbation is an increase of 5%. For the periods of elevated recruitment both the duration of these events was reduced by 5% (for convenience I reverse the sign of this effect to make the direction of the effect consistent with the other perturbations). The results of the sensitivity and elasticity analyses are very similar and, for simplicity, only the elasticity results are discussed. In addition, the sensitivity analysis of the variance parameters and co-variance matrices indicate that these parameters have a very small effect on the simulation results and are not discussed further. The full computational details for the PVA analysis can be found in Electronic supplement C.

5.3 Results

5.3.1 Population growth rate

For the vast majority of populations, realized per capita population growth (r) is negative during periods of typical recruitment (mean = -0.072) and positive during periods of elevated recruitment (mean = 0.19; Fig.5.1). Per capita population growth rate is significantly higher during the periods of elevated recruitment (paired t-test,$p < 0.001$,T = 11, df= 23) and the magnitude of this effect (mean difference = 0.26 (0.22-0.31; 95% CI)) suggests that population growth is entirely dependent on periods of unusually elevated recruitment for most populations given historic mortality rates. In several populations, however, growth is slow even during these periods of elevated recruitment. Baltic herring (HERR2532), coastal Norwegian cod (COD-COASTNOR), Icelandic cod (ICECOD), and Western Scotian Shelf cod (COD4X), all have an r during these periods of elevated recruitment which is less than 0.05, meaning that population growth will be relatively slow even under ideal conditions, given historic mortalities.

5.3.2 Population growth rate elasticity

The magnitude of trait elasticities differed between typical and elevated recruitment periods, with the effect of changing a vital rate generally being larger during periods

of typical recruitment. The elasticity of survival on r was higher during a typical recruitment period (Table 5.1; Figs. 5.2a-5.2c and C1a-C1b). Increasing the survival of any one age class usually resulted in an increase in r, with the largest effect being evident among the youngest individuals (Figs. 5.2a-5.2c).

The effect of fertility is smaller than the effect of survival; fertility vital rates have approximately one-third the effect on r as survival elasticities (Table 5.1). The size of the fertility effect peaks for second- or third-time spawners in almost all populations (Fig.5.2a-5.2c); after these ages, however, increased reproductive output has little effect. For herring, the magnitude of the fertility elasticity was approximately the same as that of cod, but it typically peaks for the youngest age classes and falls off thereafter. Increasing the reproductive potential in these younger age classes should result in a higher r but the effect was subtly different between species. The full time

Altering the survival or fertility vital rates during periods of elevated recruitment has much less effect on r (Table 5.1). Where these vital rates do have an effect, the pattern is generally quite similar to that of periods of typical recruitment, with increases in survival of the youngest age classes having the largest impact (Fig. C1a-C1b). Not surprisingly, for most populations, changing the frequency or duration of the period of elevated recruitment has a relatively large effect on r, and is comparable to the highest fertility elasticities evident during periods of typical recruitment. Finally, increasing the duration of the elevated recruitment events usually has a larger effect on r than does changing the frequency of these events (Fig. C1a - C1b).

5.3.3 Collapse

By year 10, the probability of collapse is less than 50% for most populations (Fig.5.3a). The likelihood of collapse increases for most populations by year 30 and overall the average probability of collapse is 40% (Fig.5.3b). The probability of collapse for cod populations generally exceeds 20%, and for some, it exceeds 50% (Fig.5.3b).

In year 50, there is greater than 50% likelihood of collapse for 58% of populations; notably, 79% of these are cod populations. On average, there is a 53% probability of collapse across all populations. For 21% of the populations, the probability of collapse is less than 10% (Fig.5.3c). This group includes four Atlantic herring populations and comprises half of the herring populations in our analysis.

5.3.4 Collapse elasticity

There is a great deal of uncertainty and variability in the elasticity of several of the populations during the first several decades because collapse is a relatively rare event (Figs. C2a- C2v). Changes to either survival or fertility vital rates can have very large effects on the probability of collapse during these transient periods, although there are few general trends even within populations.

After this transient period, it is clear that changes to either survival or fertility vital rates during the periods of typical recruitment have a larger impact on the probability of collapse (Table 5.2). A decline in survival for most age classes will often lead to an increase in the probability of collapse. The strongest effect is usually evident when changing the survival of the youngest age classes; typically there are diminishing returns if increasing survival in older ages. Additionally, in a number of populations, there is a weak, but positive, elasticity in the oldest age classes, indicating that increasing the survival of these older individuals would actually increase the probability of collapse (Figs. C2a- C2v). However, these changes in survival or fertility vital rates have more impact on short-term dynamics, and in the long run these small changes will not greatly reduce the probability of collapse.

The elasticities of the fertility vital rates are smaller than those of survival. A decline in fertility vital rates usually leads to an increase in the probability of collapse in year 50 (Table 5.2; Figs. C2a- C2v). At earlier periods, there are numerous populations for which a decline in fertility rates actually leads to a lower probability of collapse. Unlike the survival vital rates, this positive relationship is observed for changes to both young and old ages with no clear trends between populations or across species.

5.3.5 Persistence

Within the next 10 years, 25% of the populations have a greater than 50% probability of persistence (Fig.5.4a). In 33% of the populations, the probability of persistence is less than 10%, and there is again a clear dichotomy between the herring and cod populations with the cod populations having a lower probability of being in a healthy state 17% (7.9-31; 95% CI) than the herring 57% (36-77; 95% CI). Over time, the probability of persistence declines or is unchanged for most populations, dropping to

just 12% (4.4-24; 95% CI) for cod, while for herring it declines to 44% (24-66; 95% CI) by year 50 (Fig.5.4c).

5.3.6 Persistence elasticity

As with the collapse elasticities, it is clear that changes to either survival or fertility vital rates during periods of typical recruitment have a larger impact on the probability of persistence, although for persistence elasticities it is a positive relationship (Table 5.3; Figs.C3a- C3x). In most populations, the elasticity of the survival vital rates increases over time, suggesting that the full benefits of reducing mortality will not be realized in the short term.

The fertility elasticities are generally much smaller than those for survival (Table 5.3; Figs.C3a- C3x) and the age-specific patterns of these elasticities largely mirrors the patterns observed for the collapse elasticities, although there are some subtle differences. For cod, it is not the fertility of the youngest or the oldest spawners that has the largest elasticities. Most often it is the middle-aged cod for which changes in fertility have the largest effect (Figs. C3a- C3p). In herring, the strongest positive effect is observed in the youngest age classes (Figs. C3q- C3x). Finally, in a number of herring populations there is almost no impact on the probability of persistence of altering either survival or fertility vital rates (HERR30, HERR4TFA, and HERRRIGA). In these populations, there is a very small probability of falling below the persistence threshold, meaning that small deviations in one vital rate will not seriously affect the populations' probability of persistence.

5.4 Discussion

5.4.1 Population growth, persistence, and collapse

In all but one of the cod and herring populations examined, the realized per capita population growth rate (r) differed considerably between years of unusually elevated recruitment and the more common time periods. During typical recruitment events, r was negative (average of -7.2% per annum). By contrast, during periods of unusually elevated recruitment, r was never negative, averaging a very robust 19% per annum. Clearly, if harvesting were to continue at the same rate as it has in the past, the

long-term viability of these populations would be dependent on the infrequent bursts of elevated recruitment.

While this analysis has assumed that periods of elevated recruitment will be of similar magnitude, frequency, and duration as they were historically, there are two processes which could invalidate this assumption and could greatly influence population growth rates. First, fisheries-induced ecosystem shifts could lead to alternative ecosystems dynamics in which elevated rates of recruitment are much less common than they have been in the past [29,116]. Secondly, there is a great deal of uncertainty surrounding the impacts of climate change on marine ecosystems [24,48,55,91,92]. In both cases ecosystem-specific changes could lead to very different dynamics in these systems than those that predominated in the past [4–6, 95].

In the near term, the probability of collapse is forecast to be very low for many of the populations examined here. However, as the time window is extended, there are a number of populations for which the risk of collapse increases rather dramatically. These are dominated by cod populations, primarily those in the Northwest Atlantic. This is in accordance with studies that have identified cod populations as being among the most vulnerable harvested populations [53, 56, 116, 120].

5.4.2 Parameter variability

Despite the great importance of elevated periods of recruitment on maintaining population persistence in the presence of fishing, increasing either the survival or fertility vital rates during typical recruitment events appear to have the biggest influence on population persistence. For survival parameters, I find that increasing the survival of young spawners has the largest impact on population dynamics, underscoring the necessity of ensuring that harvest rates on young individuals are low. As illustrated in Chapter 3, as fisheries mature and the abundance of fish declines, the mortality rate on the youngest recruits increases. By increasingly targeting the most susceptible component of the population, fisheries can increasingly place populations at an elevated risk of collapse and reduced potential for recovery.

Fertility vital rates have much lower elasticities than survival vital rates, with little impact for the oldest spawners in the population. In the majority of Atlantic

cod populations, there is a marked increase in the elasticity of second- to fourth-time spawners, while for herring it is the youngest age classes that have the highest elasticities. Increasing the individual fertility in these age classes can lead to an increase in population growth. There are two biological mechanisms which could lead to an increase in these fertility rates. The first would be an increase in the size of the fish in these age classes, thus leading to more egg production per individual and higher fertility. Unfortunately, such a life history strategy would also decrease the survivorship of a harvested species because these larger fish would have an elevated risk of being harvested in any given year.

The second mechanism would be to increase the proportion of the population that is maturing at these younger ages. There is a wealth of evidence for this type of change in life history for exploited marine fishes [47,60,97,112], especially cod [53,111]. It appears that given the constraints introduced by the high mortality imposed by fisheries earlier maturation might be occurring as a means of increasing the per-capita population growth rate relative to what it would be under fishing pressure in the absence of life-history change [46, 61].

Over time the elasticity of either class of vital rates can change quite substantially. This is partially due to uncertainty in the simulations when there are very few (or conversely very many) replicate populations in which a particular state (i.e. collapse or persistence) has been reached. Aside from these effects, changes in the elasticities with time follow expected patterns, with increases in these vital rates (particularly those for survival) generally resulting in an increase in the probability of persistence and reduced probability of collapse.

The effect of parameter change decays over time for the probability of collapse but increases for the probability of persistence. For collapse, the parameter changes have the greatest effect in the short term, meaning that small increases in survival can retard the rate of collapse. However, given high total mortality effected by harvesting, these results suggest that many populations will eventually reach extremely low abundances if past harvesting rates are not substantially reduced. For the persistence elasticities the effect of changing the vital rate typically increases with time, implying that an increase in survival will have the greatest impact if maintained for an extended period of time. Small increases in either class of vital rates will not

result in a rapid return to sustainable abundances, but will, over time, increase the probability of reaching or maintaining persistent abundances.

In a number of populations, the elasticity of survival vital rates for the oldest age classes actually has the opposite effect on the probability of collapse. In most of these cases, these elasticities decline with time, and are somewhat influenced by the elasticities during the first few years of the simulation. Nevertheless, increasing the survival of the oldest age classes would actually slightly increase the probability of collapse in many populations. This effect may be related to the low future contribution of these age classes to population growth, and the small number of individuals that survive to reach the oldest age classes. A similar trend is evident for the fertility of several age classes for cod populations, when focusing on the probability of persistence. Nonetheless, for the survival vital rates of the oldest age classes, the magnitude of the elasticity is quite small. Given the small magnitude and lack of consistency in the pattern, it is doubtful whether these elasticities actually have much influence on the population dynamics.

5.4.3 Future directions

While the elasticity analyses illustrates the effects of proportionally small changes in survival and fertility vital rates on probabilities of population persistence and collapse, it would be beneficial to further explore the management implications of larger changes across multiple age classes for both survival and fertility vital rates. It would be particularly useful, for example, to ask whether focusing on increasing a particular group of vital rates (e.g. survival of the youngest individuals) has a larger influence on the long-term prognosis of these populations. Additionally, I can estimate the extent to which fishing mortality needs to be reduced in populations for which recovery is unlikely.

The current models incorporate the assumption that both survival and fertility vital rates are density independent. However, as shown in earlier chapters, age-specific vital rates for both survival and fertility are density dependent in some populations. While the effect of mortality was more ubiquitous across populations and ages, utilizing the abundance data to alter the survival and fertility vital rates is a logical next step of biological realism to include in these models. Finally, the influence of

environmental variability on the population dynamics can be explored using these models. Changes in the magnitude, frequency, and duration of elevated recruitment events can be altered to determine how these populations would respond to specific changes in the environment. Indeed, one of the great benefits of these probabilistic models is the ability to perform numerical experiments using the model parameters to determine how these populations may respond to a myriad of future environmental scenarios [14].

5.5 Figures and Tables

Table 5.1: Estimated elasticty of the fertility and survival vital rates on population growth rate (r) in both the elevated and typical recruitment periods. The confidence intervals represent the upper and lower 95% CI's.

	Mean	Lower Confidence Interval	Upper Confidence Interval
Fertility - Elevated Recruitment	0.008	0.003	0.013
Fertility - Normal Recruitment	0.016	0.011	0.021
Survival - Elevated Recruitment	0.007	0.001	0.012
Survival - Normal Recruitment	0.048	0.043	0.053

Table 5.2: Estimated elasticty of the fertility and survival vital rates on the probability of collapse in both the elevated and typical recruitment periods. The confidence intervals represent the upper and lower 95% CI's.

	Mean	Lower Confidence Interval	Upper Confidence Interval
Fertility - Elevated Recruitment	-0.20	-0.67	0.27
Fertility - Normal Recruitment	-0.56	-1.03	-0.09
Survival - Elevated Recruitment	-0.23	-0.70	0.24
Survival - Normal Recruitment	-1.51	-1.98	-1.04

Table 5.3: Estimated elasticty of the fertility and survival vital rates on the probability of persistence in both the elevated and typical recruitment periods. The confidence intervals represent the upper and lower 95% CI's.

	Mean	Lower Confidence Interval	Upper Confidence Interval
Fertility - Elevated Recruitment	0.36	-0.04	0.75
Fertility - Normal Recruitment	0.53	0.13	0.92
Survival - Elevated Recruitment	0.44	0.05	0.84
Survival - Normal Recruitment	1.71	1.31	2.10

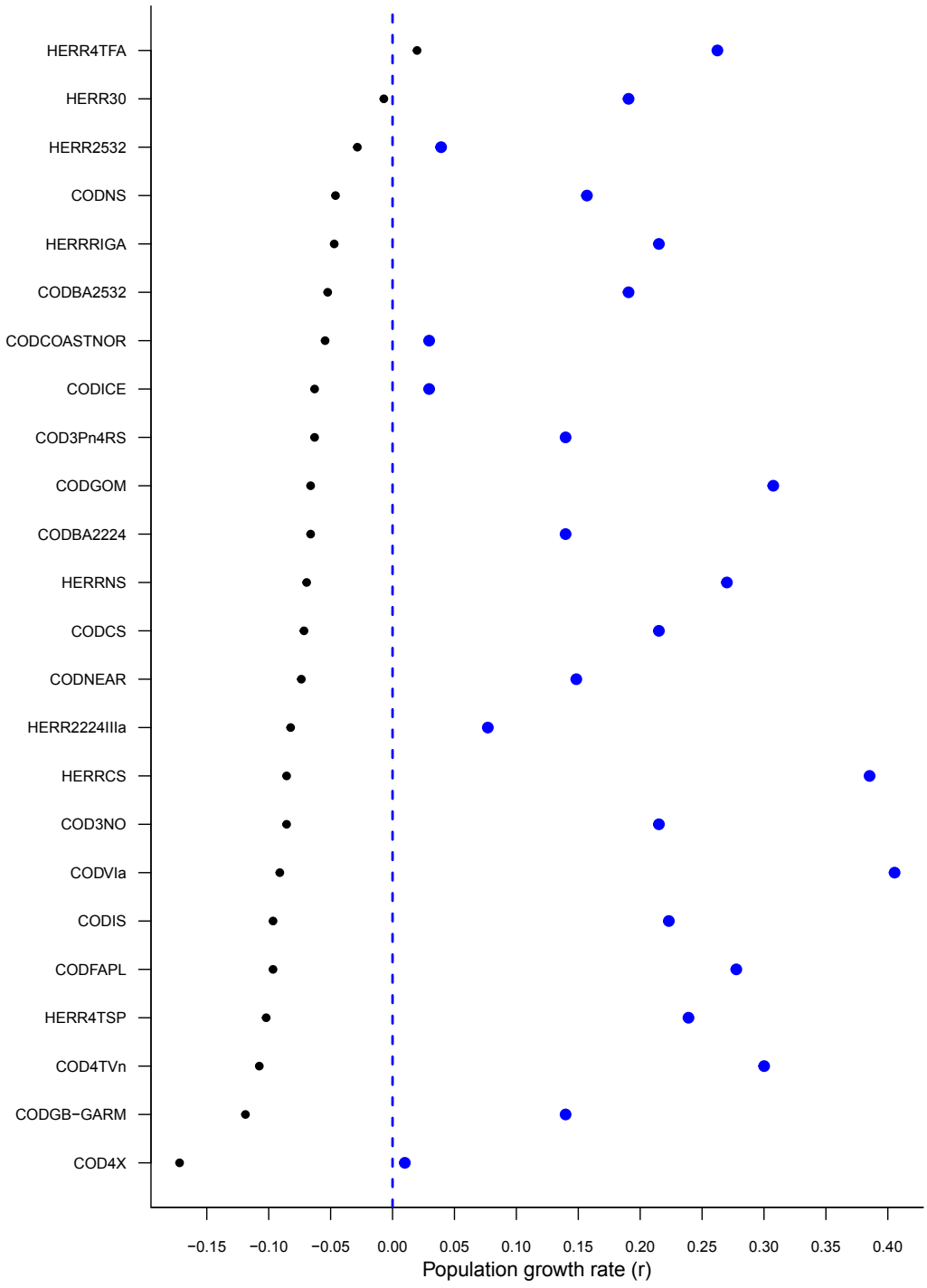

Figure 5.1: The population growth rate during typical recruitment (black) and elevated recruitment (blue) periods .

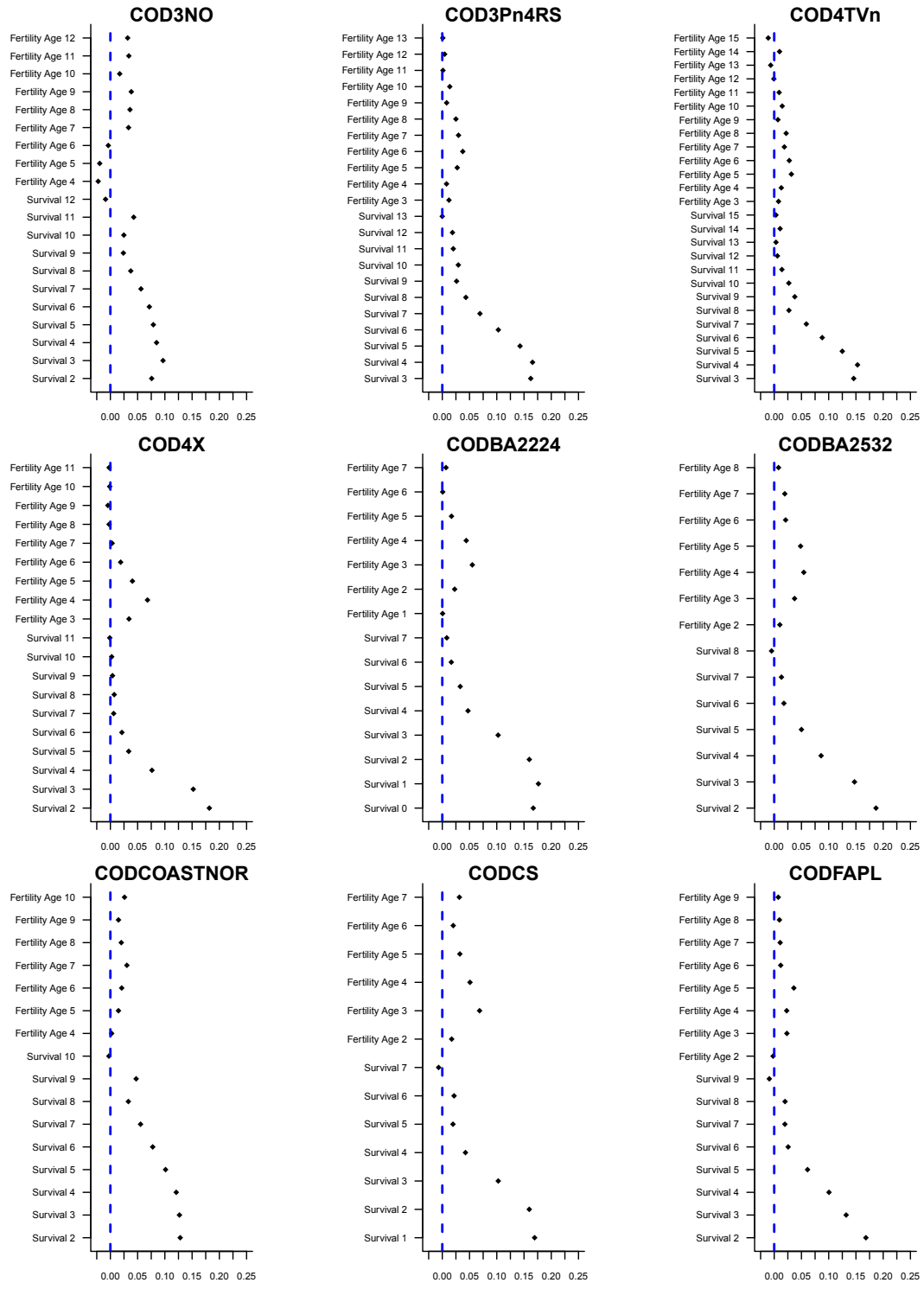

Figure 5.2a: The elasticity of the population growth rate for each population.

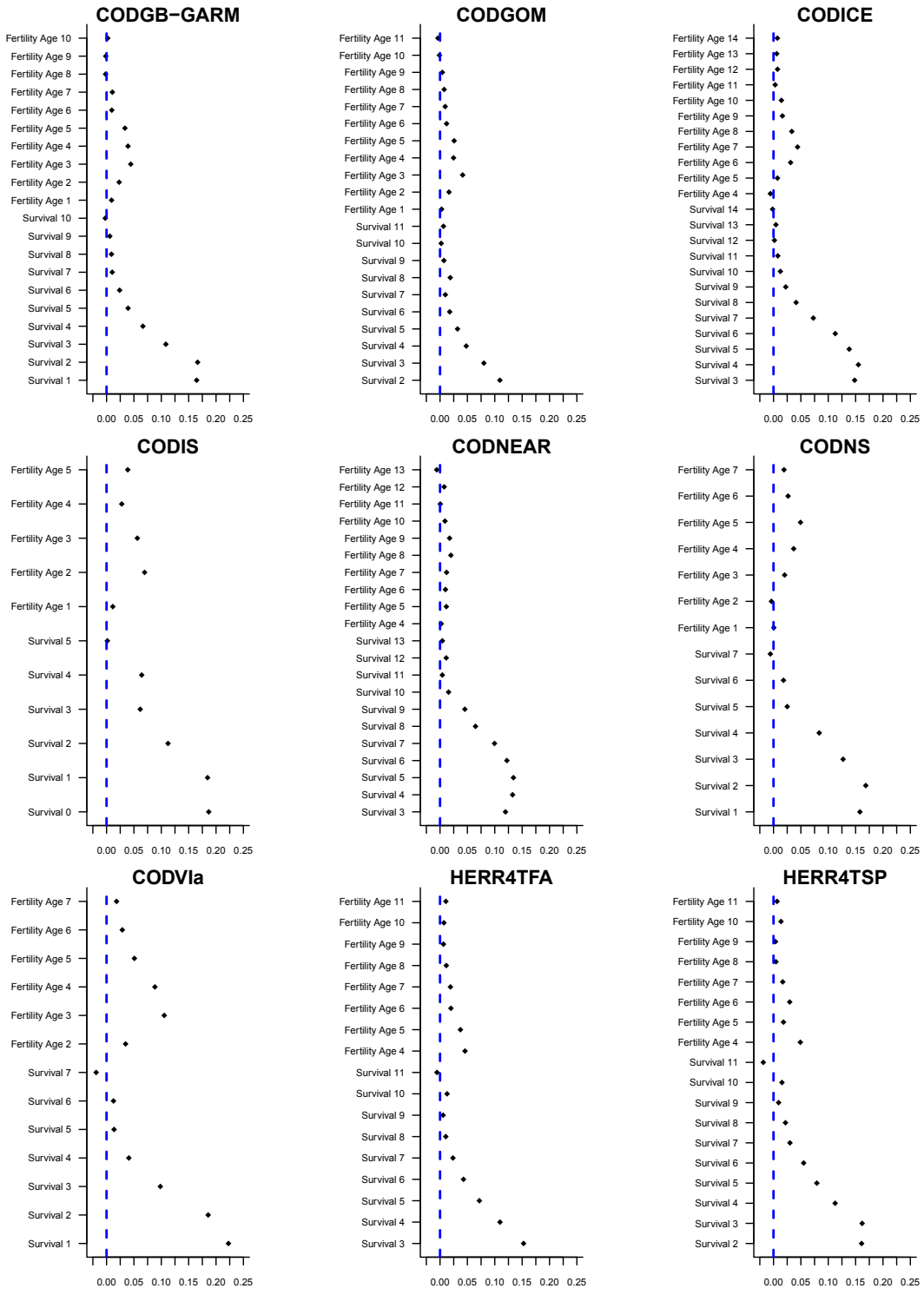

Figure 5.2b: The elasticity of the population growth rate for each population.

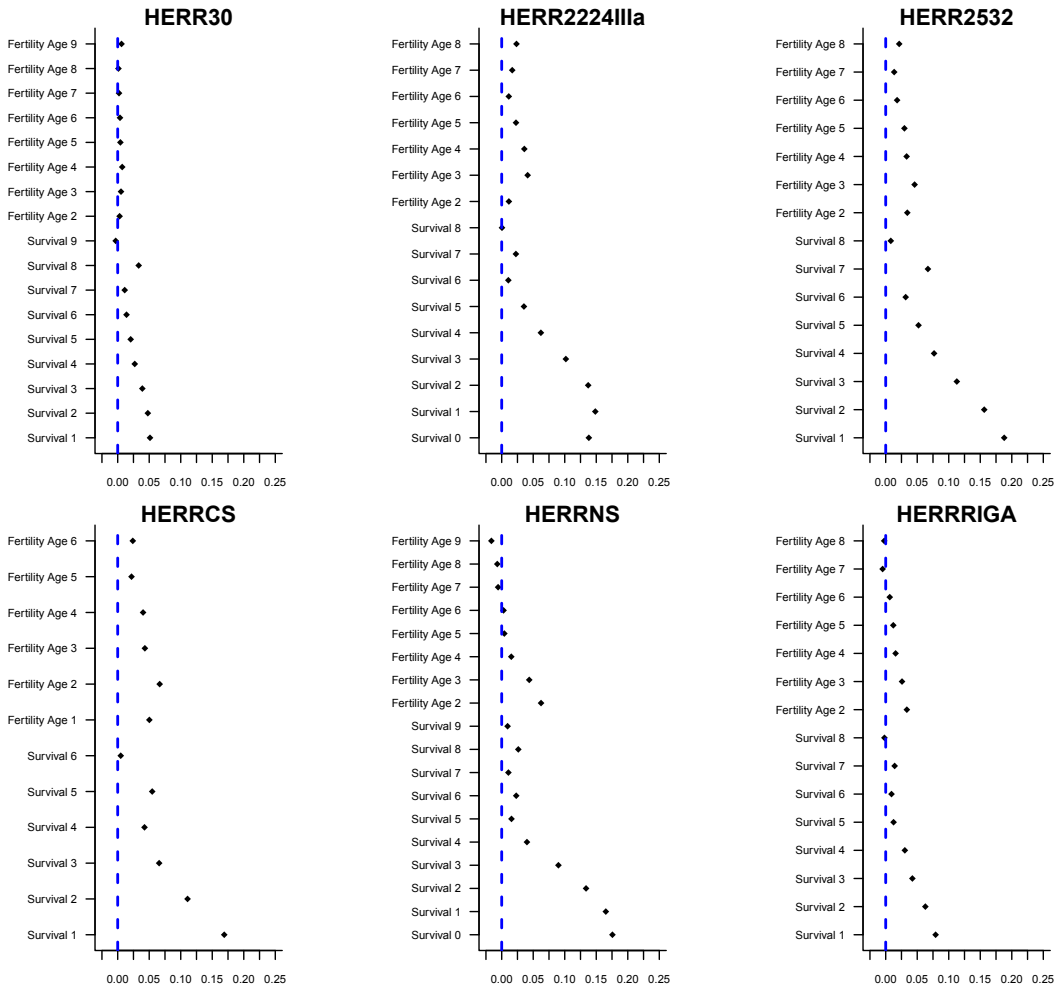

Figure 5.2c: The elasticity of the population growth rate for each population.

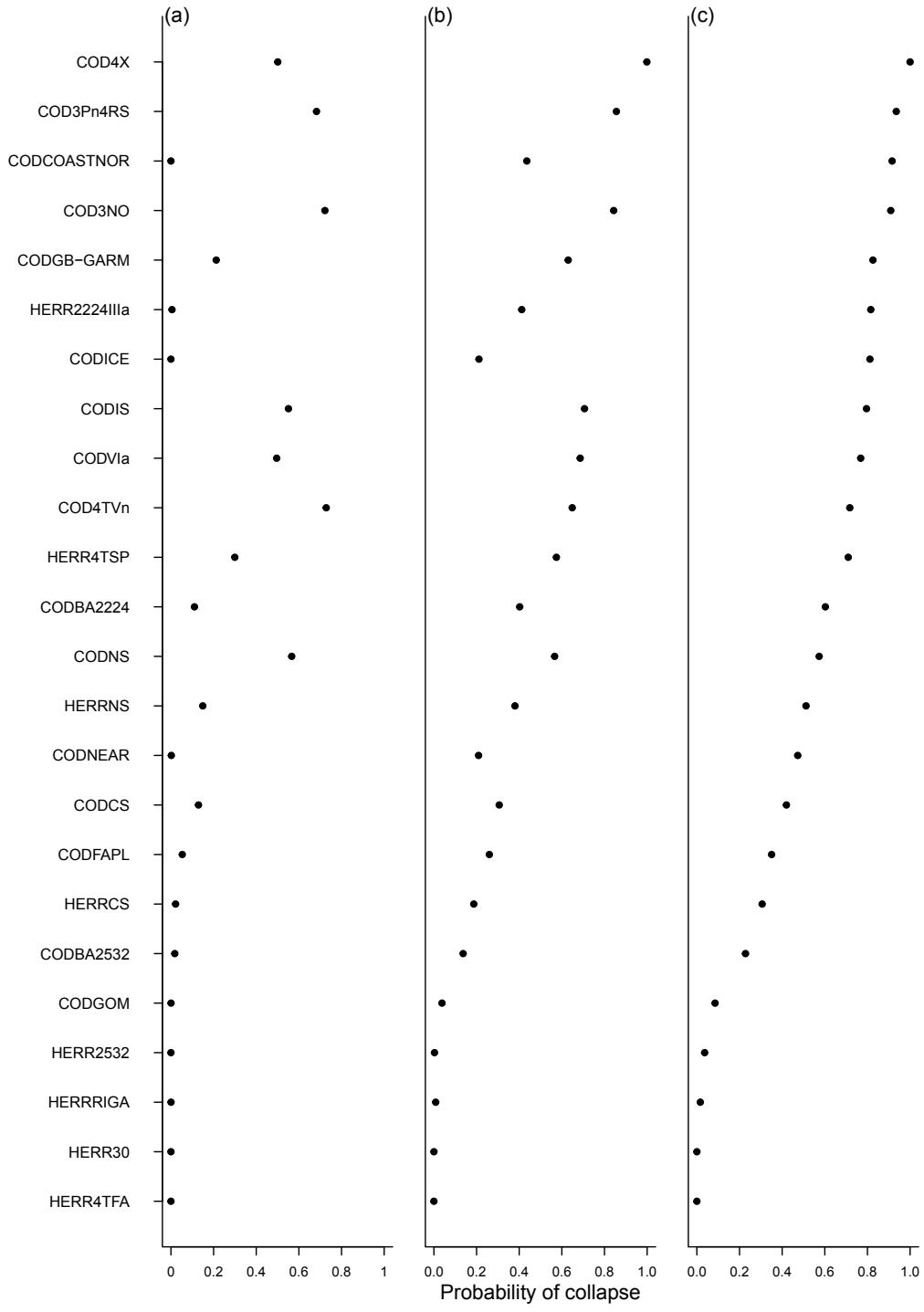

Figure 5.3: The probability of collapse at (a) year 10, (b) year 30, and (c) year 50.

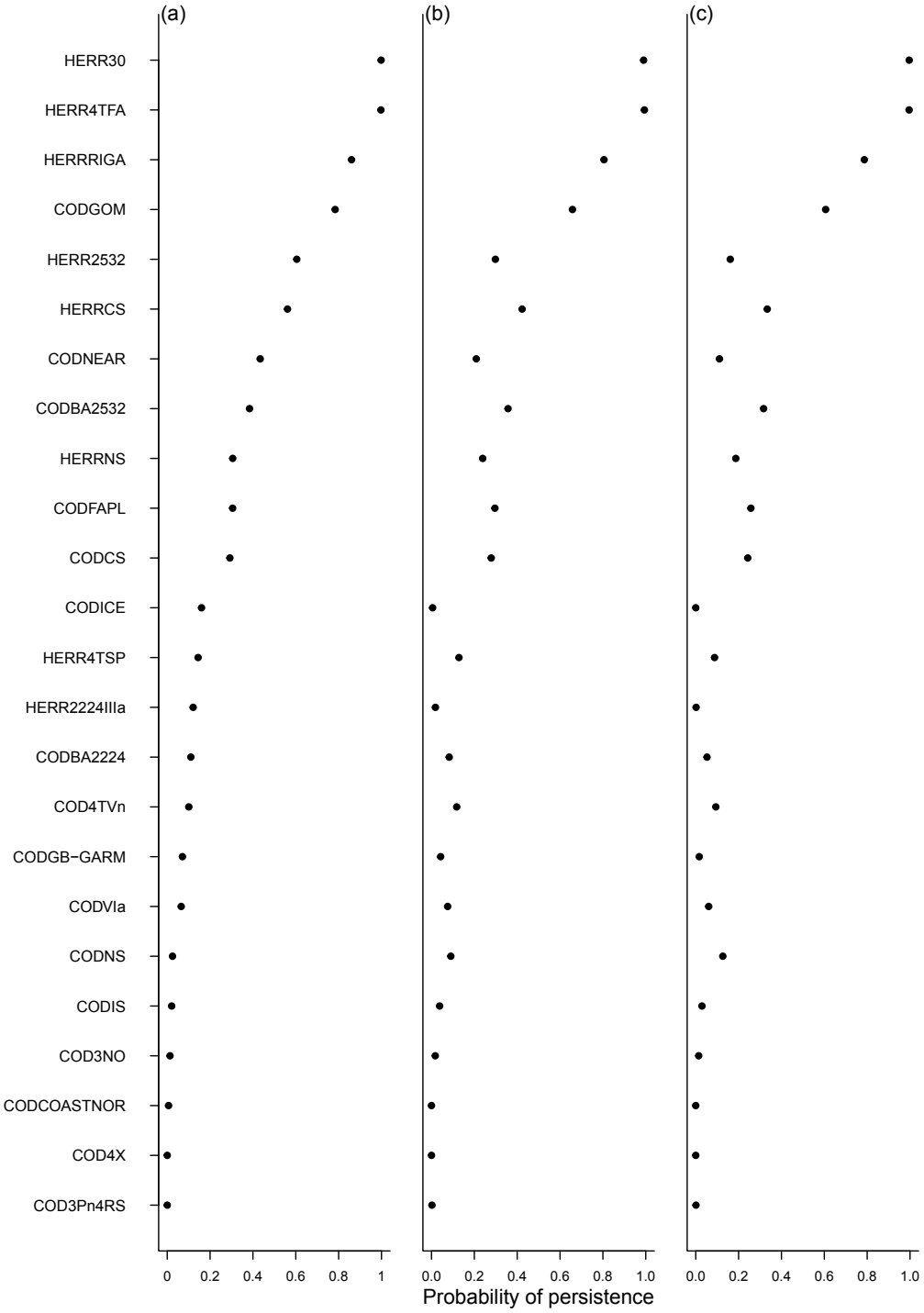

Figure 5.4: The probability of persistence for the base case at (a) year 10, (b) year 30, and (c) year 50.

Chapter 6

Likelihood of recovery for endangered Atlantic cod in the Southern Gulf of St. Lawrence

6.1 Introduction

Conservation biologists have been using population viability analysis (PVA) to predict the future state of populations for decades [14, 96]. These models have the potential to accurately predict the status of the population [12], diagnose what is affecting populations deemed to be in an unhealthy state [40], prescribe an intervention based on the component of the life cycle most sensitive to change [20], and determine the fate of the population given a specific intervention [21]. While these models have played a central role in global efforts to assess terrestrial species at risk status [36, 58], they have received scant attention in fisheries science (but see [3]).

As I have shown in the previous chapter, probabilistic models, such as PVA, are an ideal tool for estimating the likelihood of collapse and recovery in data-rich populations, such as those that have been commercially exploited for long periods of time. These models can also be used by managers to: (a) undertake risk assessment of specific management strategies, (b) determine both the short- and long-term effects of harvesting policy on population status, (c) ascertain which age classes most influence the population dynamics, and (d) quantify the influence of vital rate variability [14, 58].

In many marine fish, there is significant between-year variability in both offspring production and survival (hereafter referred to as recruitment; the abundance of offspring at the age at which they are first vulnerable to fishing). Recruitment can vary by orders of magnitude between years and, despite numerous hypotheses regarding the processes that control recruitment, prediction of both the timing and magnitude of large year classes has proven largely unsuccessful [121]. The uncertainty surrounding the magnitude, duration, and frequency of these unusually large

recruitment events makes long-term predictions difficult for marine species. Despite this, much of fisheries management is predicated on these events occurring more frequently as populations decline and with similar frequency, duration, and intensity as they have occurred in the past. Environmental or ecosystem shifts may alter the frequency and strength of future recruitment events, but we have little knowledge of how these changes could impact both the short- and long-term population dynamics in these populations [29, 35, 116].

Southern Gulf of St. Lawrence Atlantic cod (*Gadus morhua*) had been subjected a major fishery for several centuries before the population collapsed over the course of the latter half of the 20th century. Despite a near-moratorium on harvesting since the early 1990s, the population has continued to decline and, as I also show in Chapter 5, it is at a high risk of extinction within the next half century [108]. The current elevated mortality rates have been linked to an increase in seal predation [7] and has led to a decision to undertake a large scale cull of the grey seal (*Halichoerus grypus*) herd in an effort to lower the mortality of adult cod [94]. The estimated percent of adult cod mortality attributable to grey seals is highly uncertain, ranging from 20-70% of the total mortality, and the efficacy of the cull is highly dependent on the true mortality rate, among numerous other factors [107]. The scientific uncertainty surrounding the factors slowing recovery in Canadian Atlantic cod stocks, the general public interest in both species, and the scale of the potential cull have sparked a great deal of debate about the appropriateness of this management action both within the scientific community and the general public [7, 29, 109].

My objectives are five-fold: (a) determine how much mortality needs to be lowered to increase the probability of recovery in Southern Gulf of St. Lawrence (SGSL) Atlantic cod to greater than 50% in 50 years; (b) determine how much mortality needs to be lowered to reduce the probability of collapse to less than 10% in 50 years; (c) explore how changes in mortality for specific age classes influences the probability of recovery and collapse; (d) determine how changes in frequency, duration, and strength of unusually large recruitment events influences the probability of recovery and collapse; and (e) discuss how a large scale removal of grey seals may influence recovery.

6.2 Methods

6.2.1 The data

We collated the data for this analysis from publicly available stock assessments. The data-set includes time series of abundance, biomass, average weight, probabilities of maturity, fishing mortality, natural mortality, and/or catch for each age class in 134 different populations. The data originated from stock assessments undertaken for harvested fish stocks in Europe (ICES [International Council for the Exploration of the Sea]), Canada (DFO [Department of Fisheries and Oceans]), the USA (US), and the High Seas (NAFO [Northwest Atlantic Fisheries Organization and ICCAT [International Council for the Conservation of Atlantic Tunas]), and includes populations from 6 taxonomic orders (Clupeiformes, Gadiformes, Osmeriformes, Perciformes, Pleuronectiformes, and Scorpaeniformes). From this database I extracted age-specific abundance, average individual mass, and maturity data for Southern Gulf of St. Lawrence (NAFO region 4TvN) Atlantic cod).

6.2.2 Vital rates

To estimate the average contribution of an individual in an age class to fecundity, I first assume that potential fecundity is a linear function of the weight of an individual. I can then calculate the relative individual fecundity (RIF) for each year:

$$RIF_{x,y} = \frac{W_{x,y} \times M_{x,y}}{min(W_{mat})} \tag{6.1}$$

where x is the age class, y is the year, $W_{x,y}$ is the weight in age class x and year y, $M_{x,y}$ is the percent of individuals in age class x and year y which are mature, and W_{mat} is the weight of the smallest age class having some mature individuals (across all years and age classes). As an example, the smallest mature individual age class ($\frac{W_{x,y}}{min(W_{mat})} = 1$) with 10% of individuals mature ($M_{x,y} = 0.1$) would have a RIF of 0.1, while an individual in an age class that was fully mature ($M_{x,y} = 1$) and was 3 times larger ($\frac{W_{x,y}}{min(W_{mat})} = 3$) would have a RIF of 3.

Next I calculate the total potential fecundity (TPF) for each year:

$$TPF_y = \sum (RIF_{x,y} \times N_{x,y}) \tag{6.2}$$

where $N_{x,y}$ is the number of individuals in age class x and year y. The actual percent fertility (APF) is the ratio of the actual number of offspring produced to the total potential fecundity:

$$APF_y = \frac{N_{1,y}}{TPF_y} \tag{6.3}$$

where $N_{1,y}$ is the number of individuals in the first age class in year y. The APF is not a measure of the number of offspring produced, rather it is a measure of the number of offspring produced that survive to recruit to the fishery (i.e. the first age class in the stock assessment). Finally, assuming that there is no age effect (over and above the influence of weight), I can now calculate the number of offspring produced by the average individual in each age class across all years, i.e. the actual individual fertility (F):

$$F_{x,y} = APF_y \times RIF_{x,y} \tag{6.4}$$

Survival (S) was estimated from the number of individuals that survived to reach the subsequent age class in the following year:

$$S_{x,y} = \frac{N_{(x+1),(y+1)}}{N_{x,y}} \tag{6.5}$$

where $S_{x,y}$ is the survival of age class x during year y, and $N_{x,y}$ is the number of individuals in age class x in year y. In the stock assessments, given that the final age class combines the estimated number of individuals from all the remaining age groups, I was unable to obtain an estimate of survival in the oldest age class so I assumed that the survival of the second oldest age class was equivalent to that of the oldest age class.

We utilized a stochastic projection matrix model which accounted for correlation in both the survival and fertility vital rates between and within years [73]. To properly utilize age-specific vital rates, there are three basic classes of parameters needed. The first is the mean vital rate:

$$\begin{aligned} \bar{S}_x &= mean(S_{x,y}) \\ \bar{F}_x &= geomean(F_{x,y}) \end{aligned} \tag{6.6}$$

where $\bar{S}_x$ and $\bar{F}_x$ and the mean survival and fecundity vital rates for each age averaged across all years. The fecundity means were calculated as geometric means because of the skewed nature of these data. The second parameter class is the variability in each vital rate:

$$\begin{aligned} S_{var_x} &= var(S_{x,y}) \\ F_{var_x} &= var(F_{x,y}) \end{aligned} \tag{6.7}$$

where S_{var_x} and F_{var_x} are the variance in survival and fecundity vital rates for each age class.

And the third parameter class is the correlation between both the survival and fertility vital rates in a given year:

$$VR_{cor_{x,y}} = cor(S_{x,y}, F_{x,y}) \tag{6.8}$$

In addition to the within year correlation between survival and fertility vital rates, I also account for the cross-correlation between adjacent years. The within and between year survival and fertility covariance matrix was based upon the correlation between vital rates found in each populations' time series. The within year covariance matrix was needed to ensure that vital rates chosen for each age classes in a given year was consistent with what was found in the population. The between year co-variance matrix was used to mimic the historic pattern of change in vital rates over time, e.g. if vital rates tended to change slowly over time the vital rates should not fluctuate between high and low values year-over-year in the simulation. The full computation details can be found in Chapters 8-9 of Morris [73].

6.2.3 Stochastic simulation

The mean, variance, and correlation of the survival and fertility vital rates form the foundation for the PVA. However, the exact combination these vital rates will not persist in the future. To perform a stochastic simulation, I needed to select the appropriate statistical distribution to sample from, using the mean and variance of the survival and fertility vital rates. By utilizing these data and an appropriate statistical distribution, the stochastic PVA can be developed to simulate the population growth

trajectory. The most appropriate distribution to use when simulating vital rates that are the outcome of binary events, such as the survival vital rates, is the beta distribution (B_x) which is bounded by 0 and 1 [73]:

$$B_x = \frac{\Gamma(a+b)}{\Gamma(a)\Gamma(b)} x^{a-1}(1-x)^{b-1} \tag{6.9}$$

where Γ is the Gamma function, x is a value between 0 and 1, and a and b are shape parameters which are related to the mean and variance:

$$\begin{aligned} a &= \bar{S}_x \left(\frac{\bar{S}_x(1-\bar{S}_x)}{S_{var_x}} - 1 \right) \\ b &= (1-\bar{S}_x) \left[\frac{\bar{S}_x(1-\bar{S}_x)}{S_{var_x}} - 1 \right] \end{aligned} \tag{6.10}$$

For the fertility vital rates, a stretched beta distribution is the preferred sampling distribution as it allows for an upper limit to the fertility rates, unlike other distributions (such as the log-normal distribution) in which there is no upper bound. $\bar{F}_x$ and F_{var_x} and the maximum and minimum values of the fertility vital rates for each age class (f_{max} and f_{min}) are then used to parameterize a beta distribution that is bounded by 0 and 1:

$$\begin{aligned} M_B &= \left(\frac{\bar{F}_x - f_{min}}{f_{max} - f_{min}} \right) \\ V_B &= F_{var_x} \left(\frac{1}{f_{max} - f_{min}} \right)^2 \end{aligned} \tag{6.11}$$

The beta-distributed mean M_B and variance V_B are then used to obtain the beta-distributed random value B_x. The stretched beta value is then back calculated from B_x:

$$S_x = B_x(f_{max} - f_{min}) + f_{min} \tag{6.12}$$

6.2.4 Elevated recruitment

For this population the fertility rates are highly variable, and the distributions typically are either bi-modal or extremely skewed. The years with high fertility represent years, or runs of years, during which recruitment is elevated. As a result of these elevated periods there is no simple distribution that can represent the actual range and frequency of the fertility vital rates. For this reason, I treated the years with unusually elevated fertility vital rates as being separate from the majority of the years. Any age class that had a fertility vital rate greater than 2 standard deviations larger than the geometric mean fertility vital rate (averaged across the entire time series) was considered an outlier:

$$F_{out[x,y]} >= \bar{F}_x + 2 \times sqrt(F_{var_x}) \tag{6.13}$$

If more than 50% of the age-specific fertility vital rates in a given year were outliers it was deemed a year with unusually elevated recruitment. Using this criterion, the historic patterns of unusually elevated recruitment was mapped and the duration and frequency of these periods was used as parameters within the model. The mean, variance, and correlation of the survival and fertility vital rates, along with the sampling distributions, were calculated separately for elevated recruitment and typical recruitment periods. In addition to enabling accurate sampling distributions to be developed, this parameterization also enabled us to determine how the population was influenced by changes to the duration and frequency of elevated recruitment rates. Finally, to ensure that the abundance did not increase to biologically unrealistic levels, the simulation would exit the period of elevated recruitment if the abundance was greater than twice the maximum historic abundance.

6.2.5 Collapse and recovery

The PVA was run for 100 years and with 7000 replicate simulations. The stochastic population growth rate (r) was calculated at the end of the simulation. A decline to 20% of the biomass at maximum sustainable yield (B_{msy}) is often defined as a collapse in fisheries, and B_{msy} is generally between 30-40% of the unfished biomass, thus collapse is a decline to an abundance of 6-8% of unfished biomass [38]. For

this analysis collapse was defined as a decline to $< 7\%$ of the maximum population abundance. Finally, the probability of population recovery, defined as the percentage of the replicates having a population abundance of $> 40\%$ (i.e. $> B_{msy}$) of maximum historic abundance, was calculated [38]. For several of the scenarios, the variability in the population trajectories was calculated using population prediction intervals [58, PPIs;] these trajectories are used to define the likelihood of the population abundance being below a threshold abundance level across time (e.g. the 95% PPI indicates the abundance for which 95% of the simulations had a lower abundance).

To determine how much mortality needed to change to lead to (a) a probability of collapse of less than 10% in 50 years and (b) a probability of recovery greater than 50% in 50 years, the survival of every age class was incrementally increased and the simulation re-run until these thresholds were obtained. The maximum survival allowed in any age class was 0.78 (i.e. an instantaneous mortality of approximately 20%). In addition to uniformly altering the survival of all age classes, three sets of simulations were developed to focus on changing the survival of the youngest, middle aged, and the oldest mature individuals in the population. In the first simulations the survival of 4-6 year old fish was incrementally increased up to a ceiling survival of 0.78. In the second set of simulations, the survival of the fish aged 7 through 9 was incrementally increased, while in the third simulations the survival of the 11-13 year old fish was increased in the same fashion.

6.2.6 Recruitment variability

Simulations were performed to determine the influence of the unusually large recruitment events on the probability of recovery and collapse. Using the mortality rates that resulted in a 50% probability of recovery in year 50, I determined how a decline in (a) the average total time spent with recruitment elevated, (b) frequency, (c) duration, and (d) strength of the elevated recruitment periods influenced the probability of recovery and collapse. The effect of reducing both the mean frequency and the mean duration of the elevated recruitment period was determined by reducing these values in 2% increments until they reached 0. To determine the effect of elevated recruitment, the mean fertility of each age class during these periods was reduced

in 1% increments until the average fertility was identical to typical periods of non-elevated recruitment (to ensure that reasonable sampling distributions were chosen for the stochastic simulation the variances were reduced in the same fashion). The full computational details for the PVA analysis can be found in Electronic supplement C.

6.3 Results

6.3.1 Baseline trajectories

Per capita population growth (r) when recruitment is at typical levels is negative (r =-0.1), but growth is very robust during periods of elevated recruitment (r = 0.35). The average population trajectory crosses the collapse threshold within a few years, although decline slows briefly in 20-30 years because of the influence of periods of elevated recruitment (Fig. 6.1a). In approximately 25% of the simulations there is evidence for stabilization or recovery in the population over the next half century, but in all cases this recovery is temporary; by the end of the simulation, 91% of the replicate populations have declined below the collapse threshold (Fig. 6.1).

The probability of recovery ($P_{recovery}$) slowly increases until year 2028, peaking at just 13% (Fig. 6.1b), after which it declines towards 0. The probability of collapse ($P_{collapse}$) increases rapidly within the first decade, peaking at 77% in year 2016 (Fig. 6.1b). This initial peak is due to the population being near the collapse threshold at the start of the simulation and the low population growth rate when recruitment is not elevated. In the medium-term (2017 - 2033), $P_{collapse}$ declines as a number of populations that have not fallen too far below the collapse threshold are rescued by periods of elevated recruitment. In the long term this drop in $P_{collapse}$ is shown to be a transient event, with the probability peaking in the final year of the simulation at 91%.

6.3.2 Sustainable mortality

Significant reductions in the mortality across all age classes have a strong effect on both $P_{recovery}$ and $P_{collapse}$ (Figs. 6.2 and 6.3a). To achieve a 50% probability of recovery in year 50 ($P_{rec[50]}$), the average mortality across age classes must be reduced

to 0.41, which represents a 19% decline from the average historical mortality rates (Fig. 6.4). To reduce the $P_{collapse}$ to 10% in year 50 ($P_{col[50]}$), the average morality must decline to 0.38 (a 25% decline from the average mortality rates; Fig. 6.2b). Even in these sustainable mortality scenarios, the short-term population dynamics are very uncertain. The population prediction intervals (PPIs) indicate there is a high likelihood that the population persists at, or below, the collapse abundance level for at least the next 10-20 years (Fig. 6.4). Once the population escapes from these low abundances, it steadily increases and appears to asymptote near the peak abundance observed.

Both $P_{rec[50]}$ and $P_{col[50]}$ vary logistically with declines in mortality (Fig. 6.3a). The most rapid improvement in $P_{rec[50]}$ occurs as mortality declines from approximately 0.48 down to 0.35 ($P_{rec[50]}$ increases by 70%), while the most rapid declines in $P_{col[50]}$ occur as the mortality drops from 0.5 and 0.4 ($P_{col[50]}$ declines by 60%).

In both cases, the population growth rate when recruitment is at typical levels remains negative for the sustainable mortality case ($r_{rec[sus]}$ = -0.037, $r_{col[sus]}$ = -0.0092), and the populations are effectively 'rescued' by periods of elevated recruitment in which population growth is extremely rapid ($r_{rec[sus-el]}$) = 0.42, $r_{col[sus-el]}$) = 0.44).

6.3.3 Age effects

Decreasing mortality in the youngest reproductive age classes can lead to a $P_{rec[50]}$ of 50% if mortality declines to 0.28. This is approximately 40% above the historic assumed natural mortality of the adults in this population (Fig. 6.3b) and represents a decline of 45% over the average mortality in these age classes. To reduce $P_{col[50]}$ to 10%, the mortality in the young age classes must decline to 0.23. The PPIs are essentially identical to the sustainable case (i.e. the case in which mortality changes across all age classes; Fig. 6.5).

A decline in mortality of fish aged 7-9 to near the background natural mortality levels increases $P_{rec[50]}$ to only 46% and $P_{col[50]}$ falls to 26% (Fig. 6.3c). The PPIs suggest that in the most common scenarios (i.e. the 25-75% PPIs), the population does eventually begin to recover but the population remains at or near collapse levels for 10-50 years before this will occur (Fig. 6.6a).

In the oldest age classes, there is very little effect of decreasing the mortality to near the background natural mortality rates (Fig. 6.3d). $P_{rec[50]}$ increases to just 15% and $P_{col[50]}$ falls slightly to 61%. The PPIs suggest that in the most common scenarios the population will persist at an abundance near (more likely below) the collapse threshold for the next 100 years (Fig. 6.6b).

6.3.4 Recruitment variability

There is an approximately linear relationship between the average total number of years with elevated recruitment (shown as percentage of total number of years) and both $P_{rec[50]}$ and $P_{col[50]}$ (Fig. 6.7). When the total time with elevated recruitment rates declines by 25% (from 20.5% to 15.2%) $P_{rec[50]}$ declines from 50% to 33% and $P_{col[50]}$ increases to 36%. $P_{rec[50]}$ never reaches 50% in the 25% decline scenario, it asymptotes at 41% after 100 years (Fig. 6.7b). $P_{col[50]}$ also never reaches 10%, although it declines steadily ($P_{col[100]}$) =23%) after an initial spike (Fig. 6.7c).

Small declines in the duration of elevated recruitment periods (down to approximately 5 years) have little effect on the $P_{rec[50]}$, but further declines lead to a rapid increase in $P_{rec[50]}$ (Fig. 6.8). Since the total time spent at elevated recruitment is unchanged it appears that numerous small elevated recruitment events have a greater positive impact on recovery than fewer long duration events.

A decline in the mean fertility rates of 25% during the periods of unusually elevated recruitment results in reduction in $P_{rec[50]}$ from 50% to 37% and a concomitant increase in $P_{col[50]}$ to 30% (Fig. 6.9). As the mean fertility of the elevated recruitment events declines by greater than 25%, both $P_{rec[50]}$ and $P_{col[50]}$ change rapidly (Fig. 6.9a). A 50% decline in mean fertility during elevated recruitment events (mean fertility is still approximately 2.5 times stronger than a year with typical recruitment) results in a decline of $P_{rec[50]}$ to just 12% and $P_{col[50]}$ increases to 50%.

If both the mean fertility and frequency of the elevated recruitment events were to decline by 25% the sustainable mortality necessary to return $P_{rec[50]}$ to 50% is 0.37 (Fig. 6.10), while declines in the strength and frequency of these events by 50% would lower the sustainable mortality rate down to 0.34. These represent declines in mortality of 27% and 33% respectively, from the historical average mortality in the population.

6.4 Discussion

Recovery in SGSL cod is highly unlikely primarily because of the high rate of decline during typical recruitment periods (10% annually). This result is consistent with both the recent trajectory of the population and other projections [106–108]. Swain [108] developed a stochastic model which utilized the most recent 5 years of data (rather than using the entire data-set) and incorporated a more complex fisheries model. Their results suggest that the population will collapse (their collapse threshold occurs at an abundance approximately an order of magnitude lower than the collapse threshold I have utilized) with near certainty within 40 years. Interestingly, Swain [108] argue that the period of elevated recruitment in the 1970's is an anomaly which is not likely to reoccur, whereas I have taken the view that these periods of elevated recruitment are critical to the recovery of this population irrespective of what happens to survival rates. This modelling framework also enabled us to look at how large the changes in the survival and fertility vital rates have to be to significantly alter the probability of collapse and recovery.

A decline in mortality of 19% results in a 50% probability of recovery by 2060, but this recovery is dependent on periods in which recruitment rates are elevated, since the population growth rate during typical recruitment periods remains negative. In addition, there remains a 50% probability that there will be no evidence of recovery in this population for almost two decades in this scenario. Even if mortality rates were cut in half ($r = 0.13$), it would take approximately 20 years to return to 1980s abundance levels without the aid of an unusually high recruitment episode. While lowering mortality rates and attempting to maximize recruitment rates is likely to, in the long run, result in recovery for this population, there is little that can be done to precisely determine when this population may recover given its dependence on rapid growth during periods of elevated recruitment and the uncertainty surrounding their frequency and strength.

This highlights the critical role periods of elevated recruitment have on recovery. During the elevated recruitment event that occurred in the late 1970's, the population grew rapidly ($r = 0.35$), from what was at that time a historical low abundance level, and increased by almost an order of magnitude within a decade. A similar period of rapid growth is also evident in the 1950s, but again a rapid increase in the harvest

capacity lead to a steady decline in the population abundance [108]. Given the historic trends, another period of elevated recruitment seems likely to occur in the near term, but unless mortality can be reduced significantly even this would only provide a short-term buffer from collapse.

While periods of elevated recruitment appear to be relatively common, there have been none in this population since it collapsed. In this population, there is just one example of what constitutes a elevated recruitment event. This makes it difficult to ascertain whether this parameterization accurately depicts: (a) the frequency with which elevated recruitment will occur over long periods of time; (b) the duration of these events; and (c) the strength of recruitment when recruitment is elevated. In Atlantic cod, there is considerable evidence that large declines in abundance may impair recruitment, likely due to changes in the role that cod play within ecosystems altered by harvesting [29,56,116]. A 25% decline in either the frequency or strength of the elevated recruitment period decreases the likelihood of recovery by approximately 30%. Given the uncertainty surrounding the frequency, duration, and strength of these periods, mortality must be minimized in the short term to ensure the population abundance does not drop to exceedingly low levels during the current period of typical recruitment.

6.4.1 Grey seals and cod recovery

The model was parameterized based on historic harvesting pressure and natural mortality rates and includes the recent spikes in natural mortality rates thought to be caused by an increase in grey seal (*Halichoerus grypus*) predation [7, 106, 107]. For a cull of seals in SGSL to prove effective the total mortality in the cod population must decrease to at least 0.41, which represents a 19% decline from the average mortality rate. Grey seals in the SGSL have been estimated to account for between 20% and 70% of adult mortality in Atlantic cod [7]. If seal-induced mortality is at the low end of this range and the seals do not favour a particular size of cod, to achieve a 50% probability of recovery within 50 years, 95% of the population would have to be killed in order to reduce mortality to achieve $P_{rec[50]}$. On the other hand, if seal-induced mortality accounted for 70% of the total mortality the seal population would only have to be reduced by 27% to achieve $P_{rec[50]}$.

Thus, the greater the impact of grey seals on cod mortality the fewer the number of grey seals that must be removed to achieve the sustainability targets. Clearly, if seals are having a large impact on the population, even a small reduction in their numbers should have a large impact on the population dynamics, whereas if the seals are not having a large impact their complete eradication may not lead to recovery in cod. This might suggest that a limited cull be implemented to determine the effect of seals on the cod population. Unfortunately, because it can take decades before a noticeable change in the population trajectory occurs, it will be difficult to determine the true effect of a grey seal cull. In addition, a decline in mortality will be most effective if it targets either all ages evenly or the youngest adults (less than 6 years old). However, there is some evidence to suggest that grey seal mortality might increase with the age(size) of cod, at least during part of the year [7]. If a cull does not significantly influence the mortality of the younger spawners, than these results suggest that even the complete removal the seal population might not have a significant effect on cod recovery.

In the neighbouring Eastern Scotian Shelf (ESS) ecosystem, the lack of cod recovery has been linked to predation of juvenile cod by forage fish [110]. In this ecosystem, the key to recovery is not just a reduction in adult mortality but it is an increase in recruitment through a reduction in juvenile mortality [29]. A forage fish induced reduction in the strength of large recruitment events in SGSL by just 25% would result in the cull being ineffective (in terms of obtaining a 50% probability of recovery by year 50) if seals account for less than 27% of cod mortality. If an ecosystem shift has occurred in SGSL a reduction in grey seal predation on forage fish could result in an increase in forage fish abundance, further reducing the recruitment in Atlantic cod and inhibiting the population's recovery. It is highly likely that both seal predation of adults and forage fish predation of juveniles play a role in cod recovery in SGSL and understanding how these two factors interact may be the key to realizing the path to recovery [29, 109].

6.5 Conclusions

The long-term sustainability of this population may be achievable with moderate reductions in mortality across all adult age classes. Given the current low rates

of harvest mortality management must focus on reducing natural mortality. If the mortality rates attributed to grey seals in this population are correct, it does appear that, under a limited set of circumstances, a cull could be effective in reducing the cod mortality to levels at which recovery is likely in the long term. However, if mortality is lower than estimated, or recruitment is limited due to a cultivation-depensation scenario, the removal of the grey seals could result in depressed recruitment rates within the population and could slow recovery or lead to further declines. To better predict recovery in marine fishes we require a more complete picture of the factors (and their variability) that lead to periods with unusually elevated recruitment.

6.6 Figures and Tables

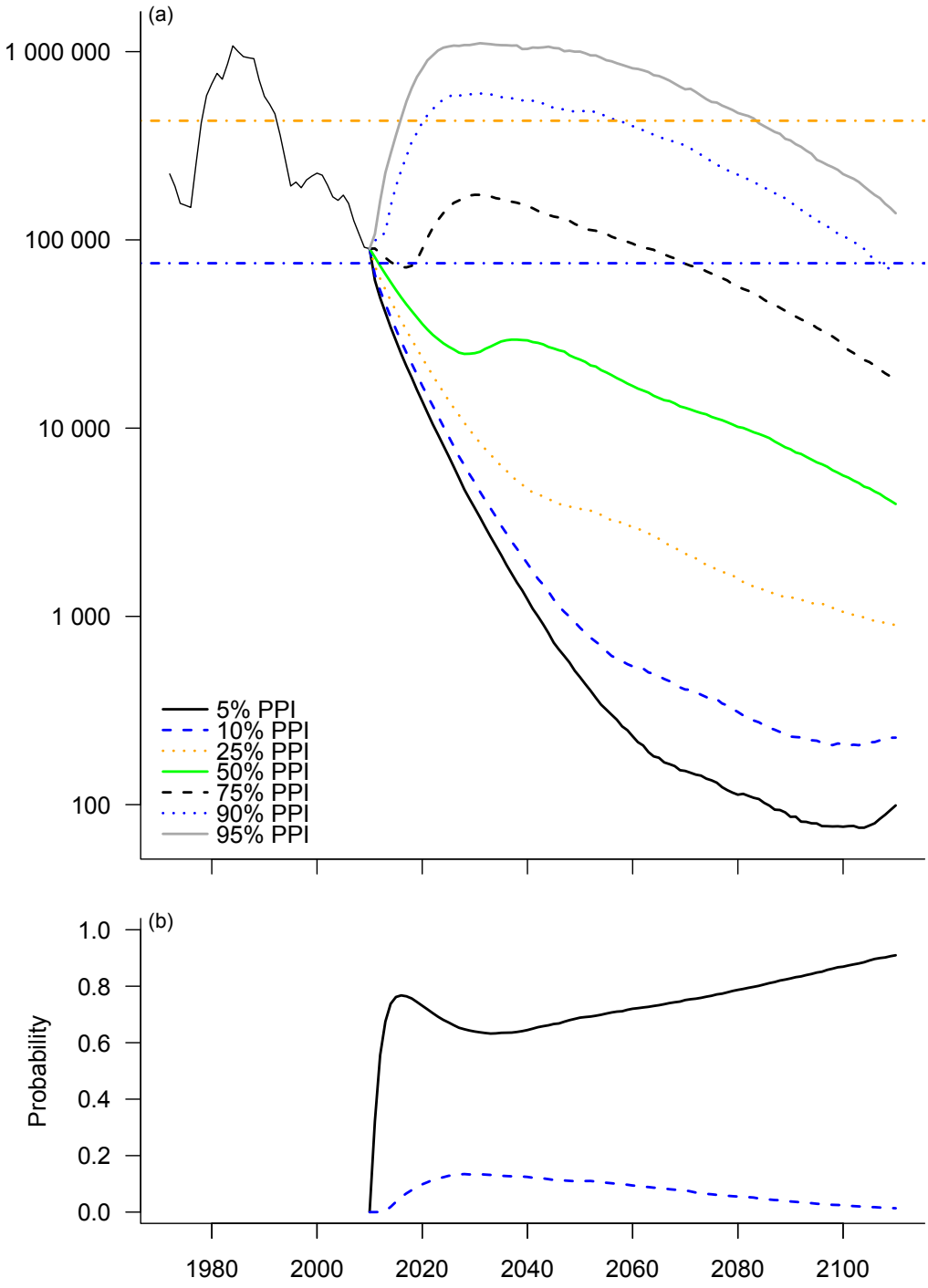

Figure 6.1: (a) The population trajectory given historic recruitment and mortality rates for the base case, the lines are the 5-95 population prediction intervals (PPI's); (b) The probability of collapse (black) and recovery (dashed blue) at year 50 for the base case.

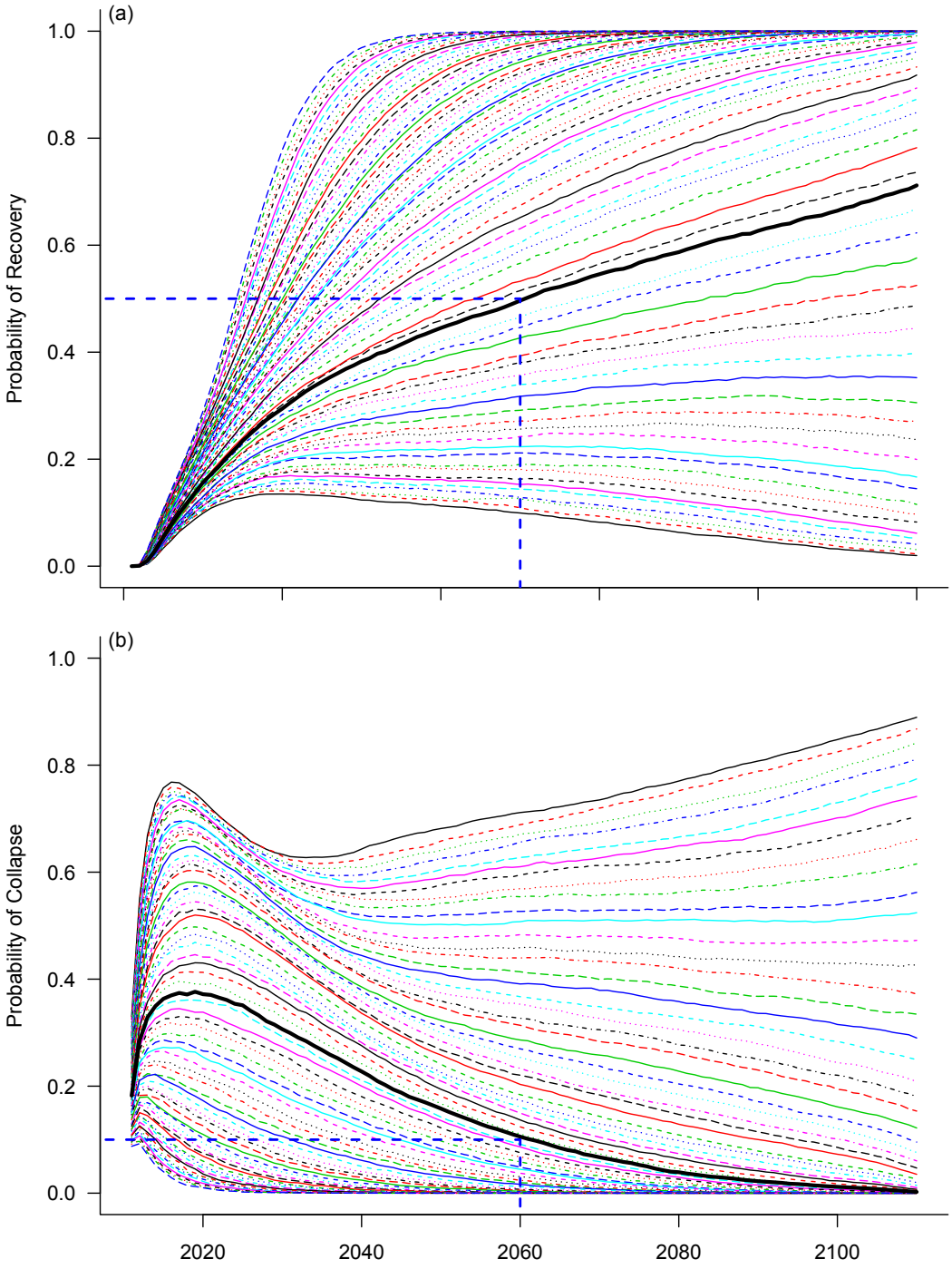

Figure 6.2: The probability of (a) recovery and (b) collapse for the incremental changes in mortality between the base case and the "natural mortality" case. The thick black line represents the simulation in which the target likelihood of recovery (a) or collapse (b) was reached.

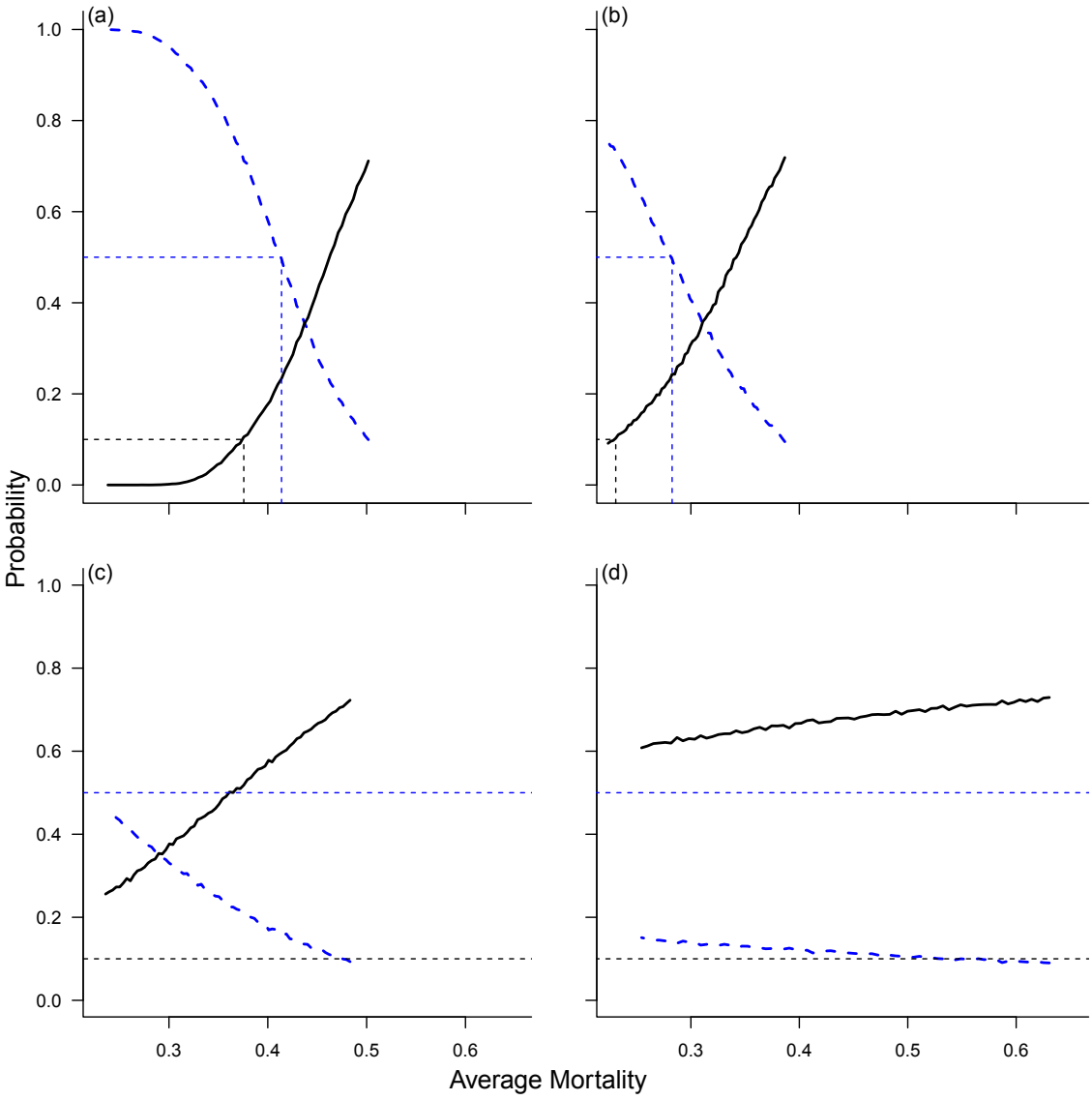

Figure 6.3: Probability of recovery (blue dashed) and collapse (black) in year 50 as a function of mean mortality for (a) all ages classes; (b) ages 4-6; (c) ages 7-9; (d) Ages 11-13.

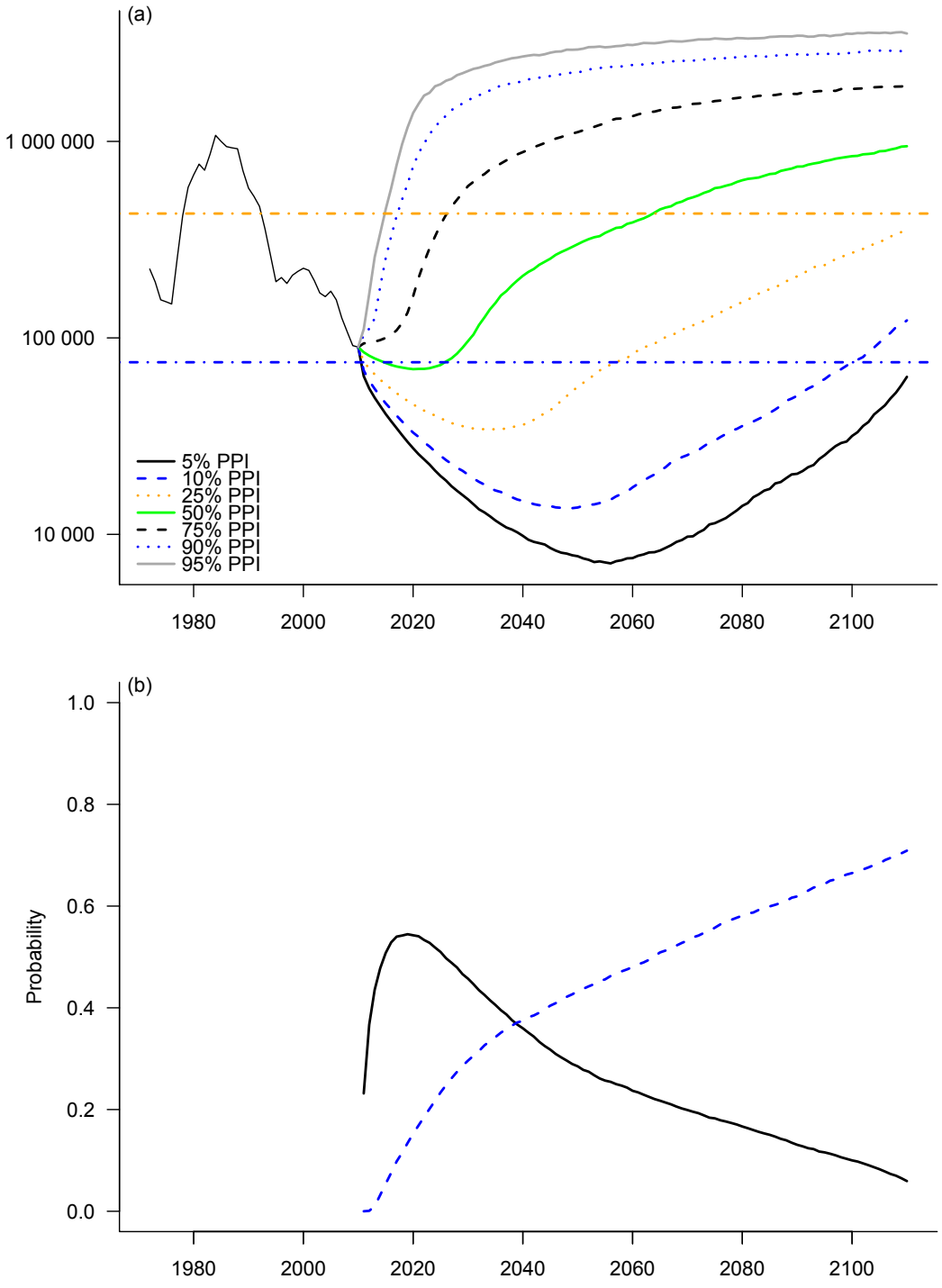

Figure 6.4: (a) The PPI's for the sustainable mortality case; (b) The probability of collapse (black) and recovery (dashed blue) at year 50 for the base case.

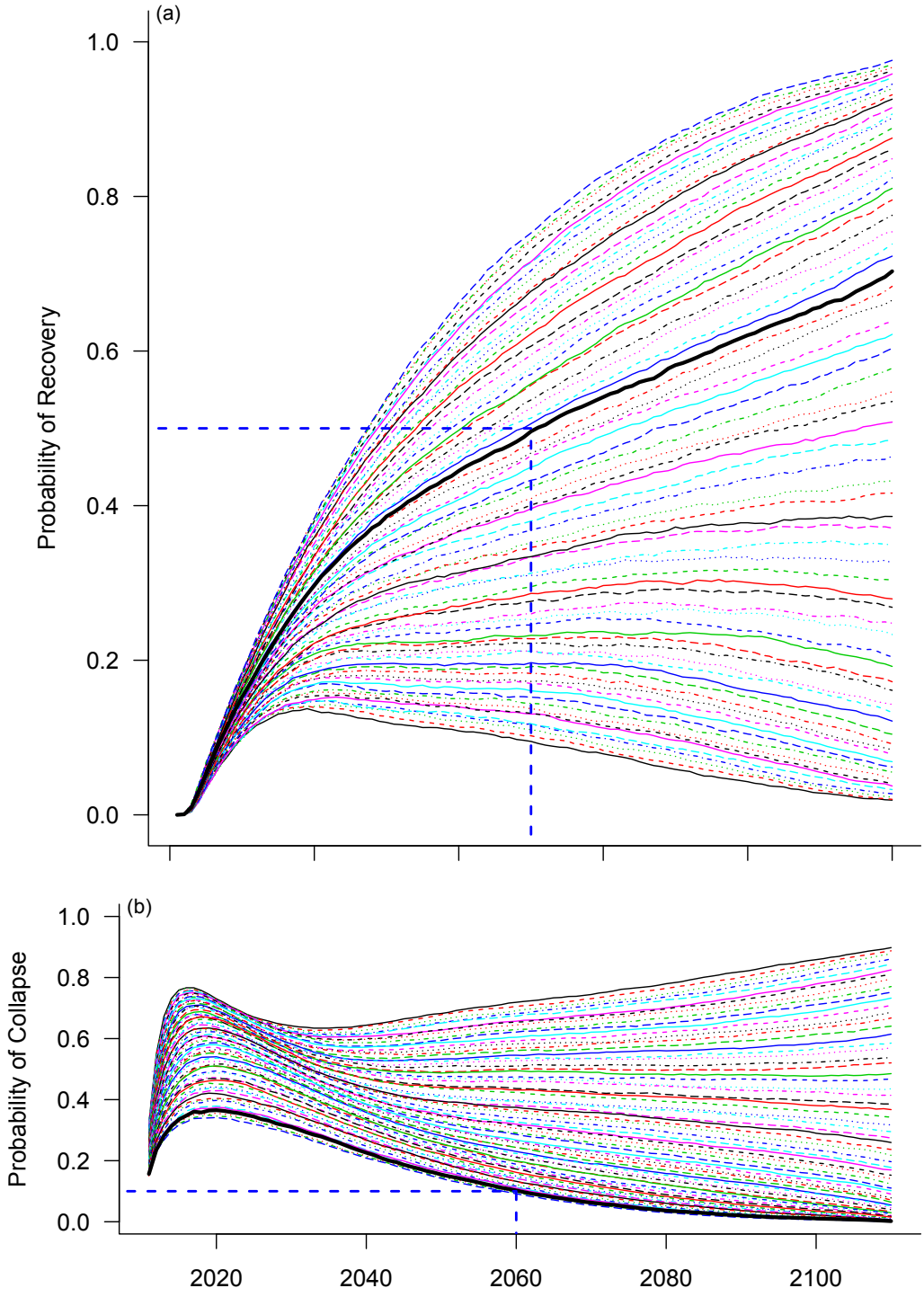

Figure 6.5: The probability of (a) recovery and (b) collapse for the incremental changes in mortality between the base case and the "natural mortality" case when changing mortality of the 4-6 year old fish only.

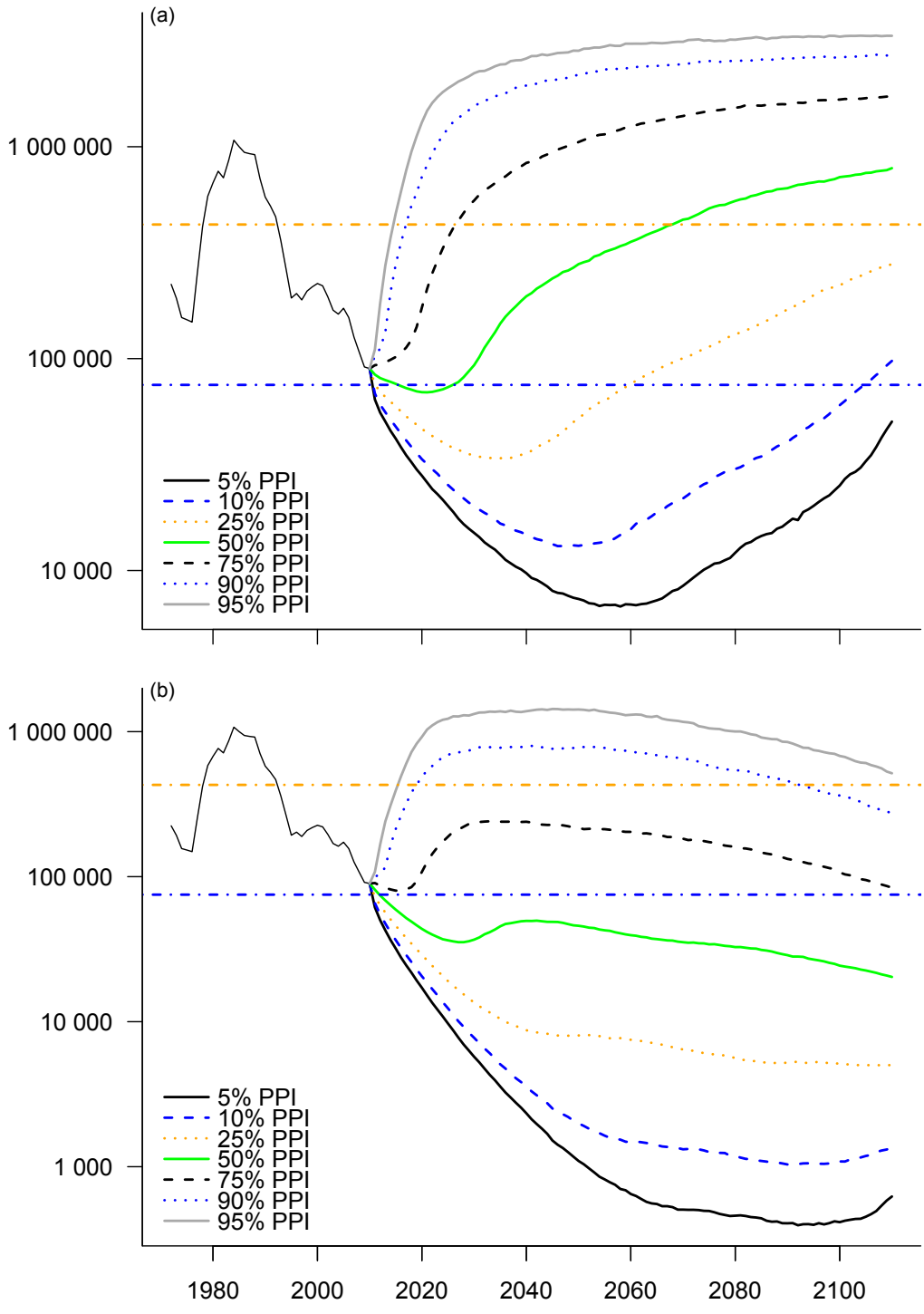

Figure 6.6: (a) The population trajectory given historic recruitment and mortality rates for changes in mortality for 7-9 year old age classes; (b) for the 11-13 year old age classes

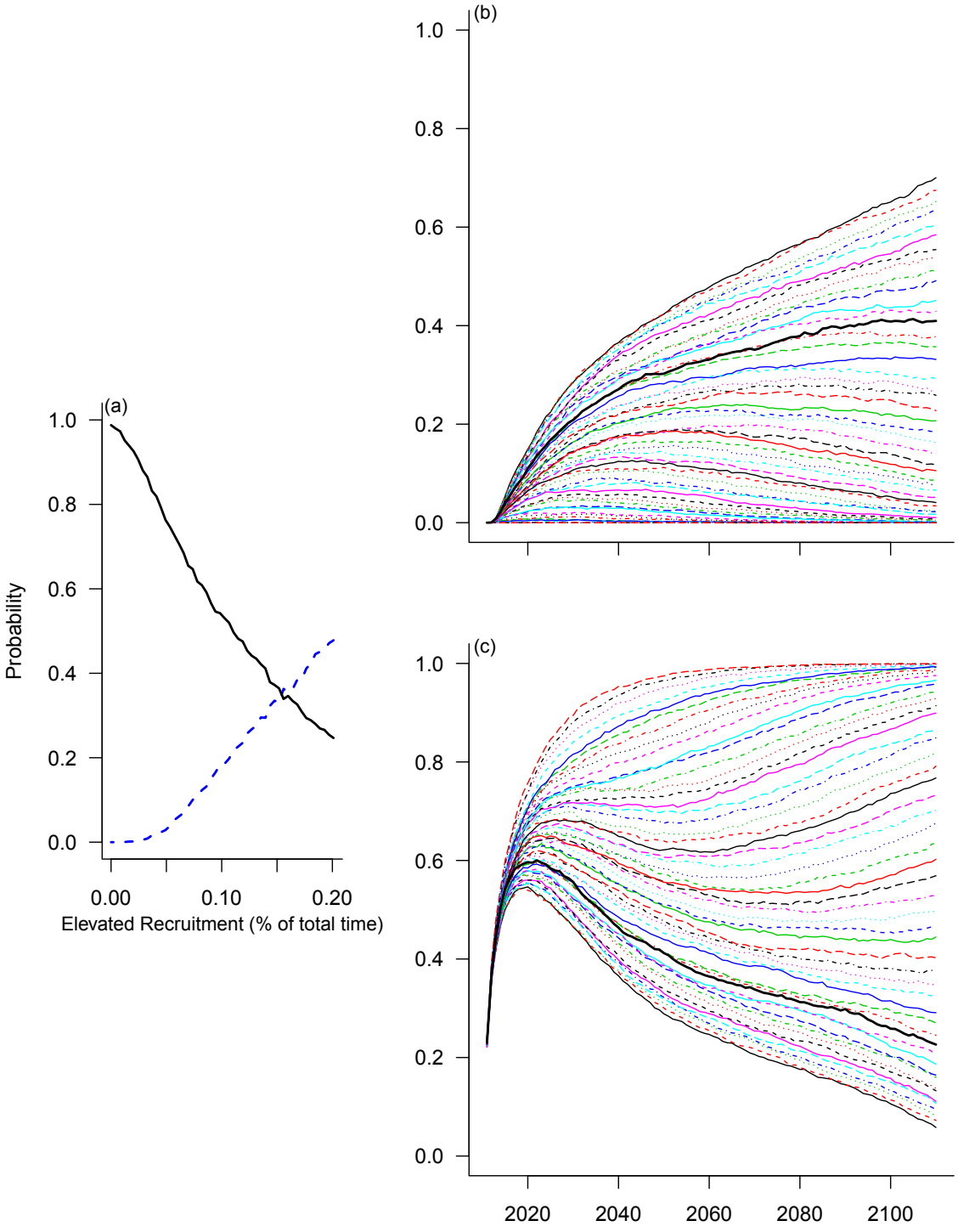

Figure 6.7: The effect of percentage of total time spent in periods of elevated recruitment on; (a) probability of recovery (solid line) and collapse (dashed line) in year 50; (b) Time series of the probability of recovery for a step-wise decline (1 % increments down to 0) in the average percent time spent in periods of elevated recruitment; (c) probability of collapse in year 50. In (b) and (c) the thick black line represents the 25% decline in mortality scenario.

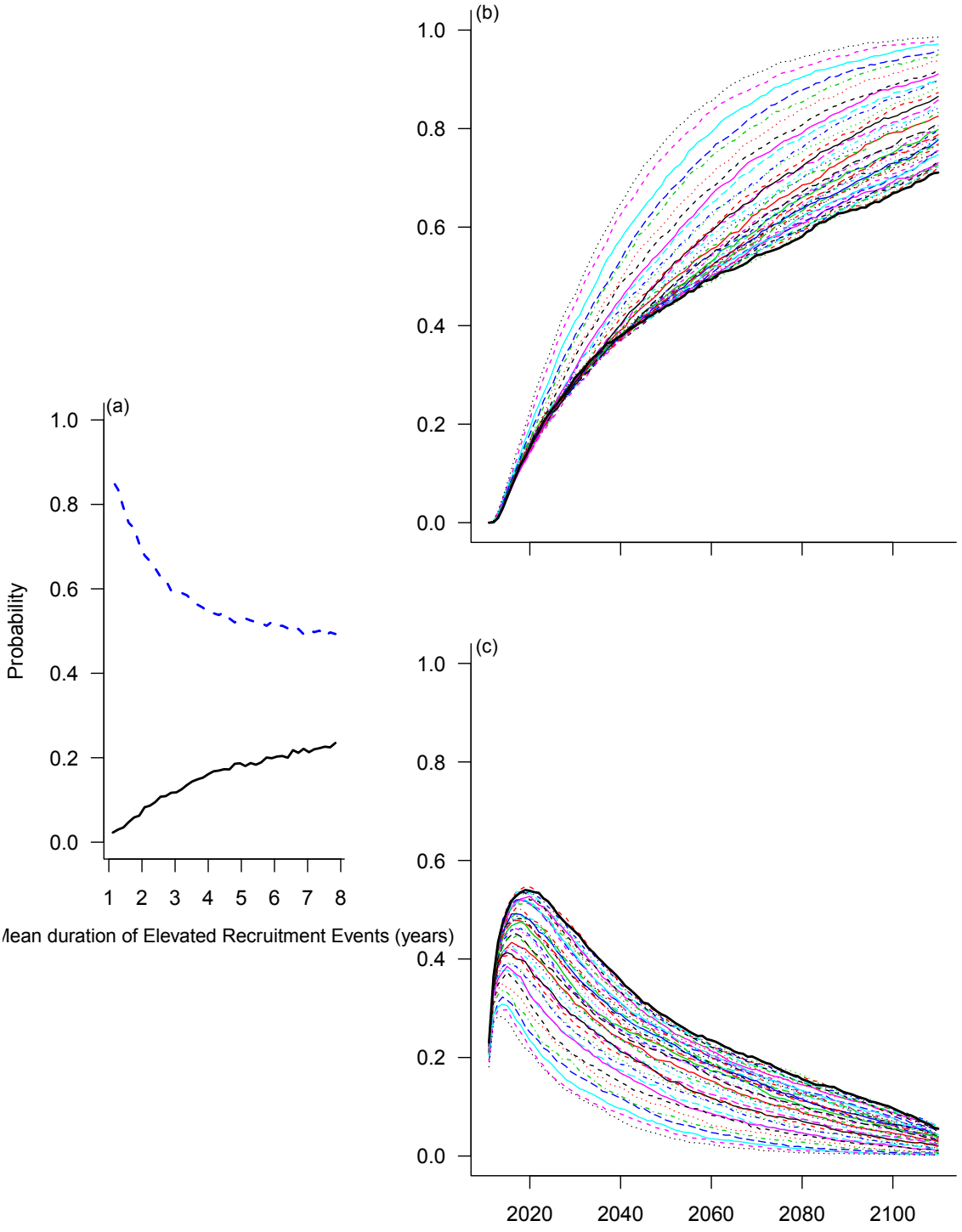

Figure 6.8: The effect of the average duration of a elevated recruitment events on (a) probability of recovery and collapse in year 50; (b) Time series of the probability of recovery for a step-wise decline (1 % increments down to an average duration of 1 year) in the average duration of a ; (c) probability of collapse in year 50. In (b) and (c) the thick black line represents the 25% decline in mortality scenario.

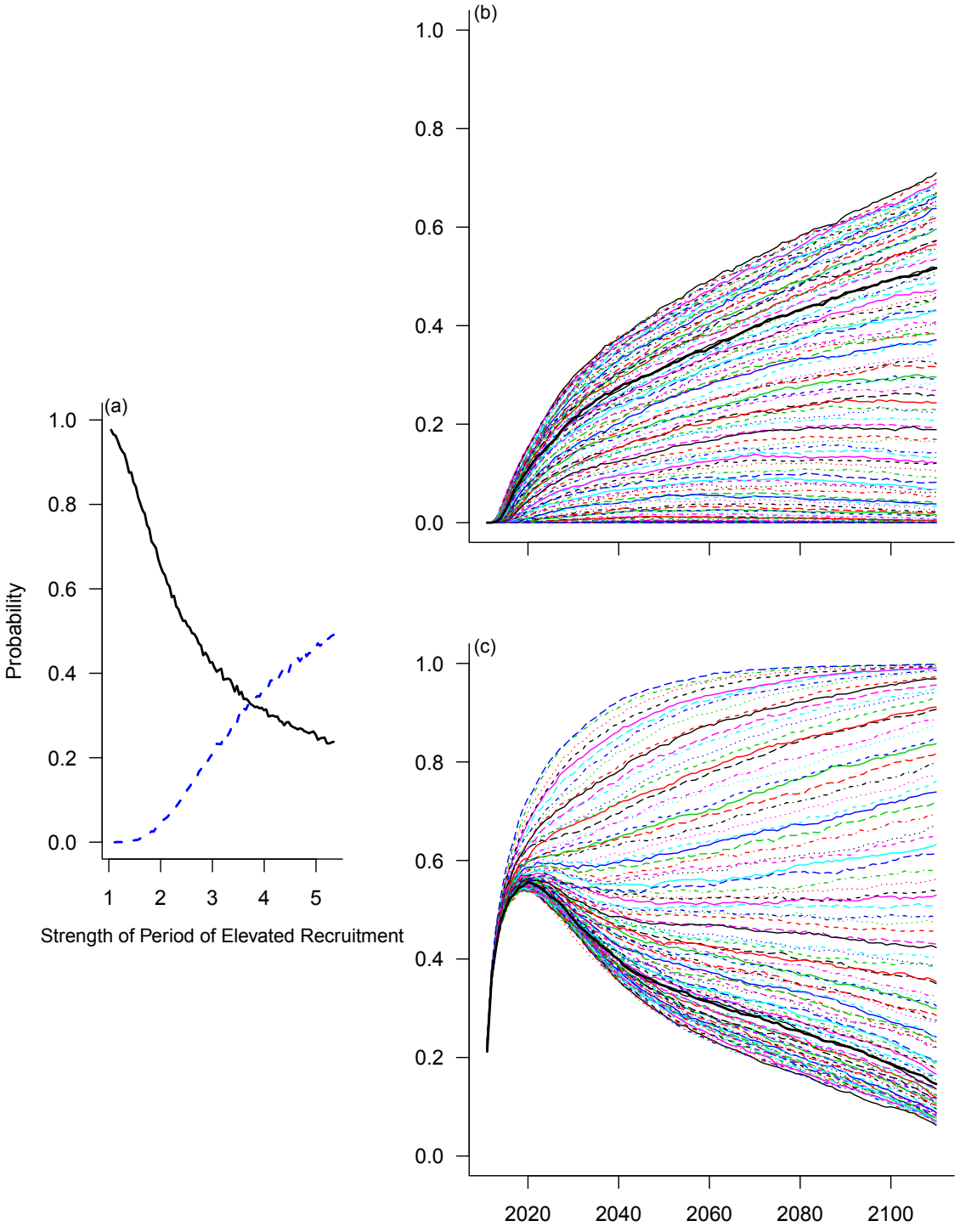

Figure 6.9: The effect of declines in the average strength of the elevated recruitment period on (a) probability of recovery in year 50; (b) Time series of the probability of recovery for a step-wise decline (1 % increments down to an average strength of periods in which recruitment is not elevated) strength of the elevated recruitment period; (c) probability of collapse in year 50. In (a) the 'strength of period of elevated recruitment' is relative to a period of normal recruitment (e.g. 5 represents a period in which recruitment is 5 times larger than a normal recruitment event). In (b) and (c) the thick black line represents the 25% decline in mortality scenario.

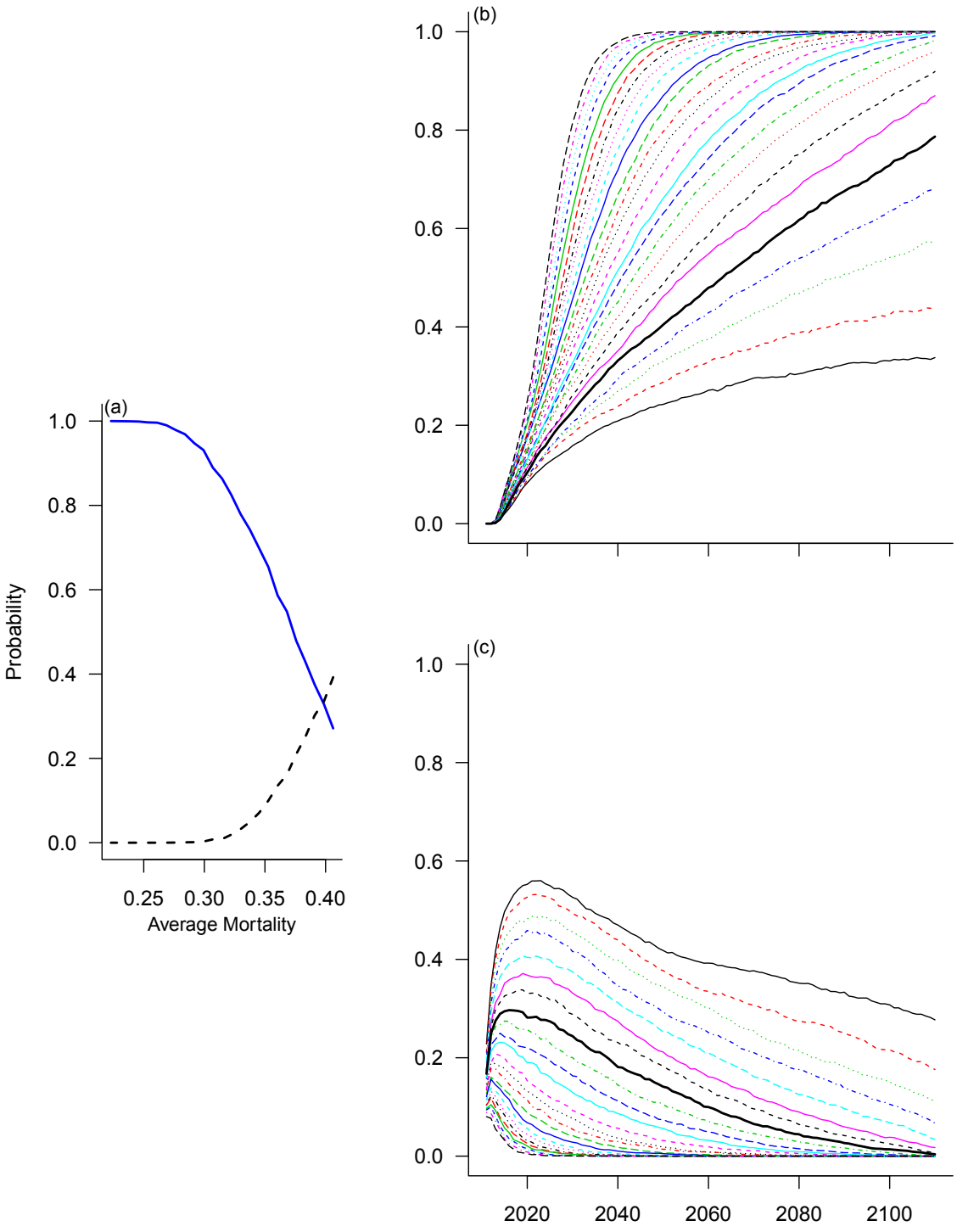

Figure 6.10: For the scenario in which the frequency and average strength of elevated recruitment periods declined by 25%; (a) The effect of declines in mortality on the probability of recovery and collapse in year 50; (b) Time series of the probability of recovery for a step-wise decline (2 % increments in mortality down to the natural mortality rate) in mortality; (c) probability of collapse in year 50. In (b) and (c) the thick black line represents the 25% decline in mortality scenario.

Chapter 7

Conclusion

7.1 Age-specific data

The database constructed as part of this thesis, containing more than 20 years of high quality demographic data for over 100 populations, could greatly improve our understanding of age effects on population dynamics in both marine and terrestrial ecosystems. The lack of long-term demographic data, such as these, in terrestrial systems has been recognized as a major hindrance to understanding long-term population dynamics and the effects of environmental variability [14, 73]. However, even longer time-series are likely required to truly dis-entangle the biological and environmental processes driving the dynamics in these populations [11].

There is a wealth of potential questions that could be addressed with these data. The first steps in the development of a new class of models that incorporate the effects of age structure on recruitment, have already been initiated using this database [98] and I anticipate that more such studies will be forthcoming. A number of questions surrounding the speed, strength, and prevalence of fisheries-induced evolution [60] could be addressed for many populations using these data. How natural mortality rates are impacted by changes to the abundance and mass (size) of the largest individuals is also an area ripe for further investigation. In many regions I also have information for multiple species at different trophic levels (e.g. cod and herring). Using these data, we may be able to determine whether trophic interactions have been altered as the age structure of these populations change with time. In general, the data indicate there is a homogenization of the size of adults between species. Publication of these data will enable researchers from around the world to better understand the effect of age on population dynamics in both marine and terrestrial species.

There are some caveats to anyone using these data. First, these data are, in large part, collected from populations for which the primary source of mortality is harvesting. Thus, the dynamics in these systems are dominated by how the population has

been harvested. This data-set could not easily be used to understand environmental stochasticity given the influence of harvesting. In addition, these data are the output from model results that combine rather different field measures (i.e. landings and survey data) into an estimate of population size, rather than being a direct population census. Clearly, there is some measure of observation error in these data that has not been accounted for in this thesis, but it is worth noting that few field studies directly census a population and many times population estimates, even from detailed field studies, are estimated using some type of model [57]. In Chapters 2-4, this source of error should result in an inflated variance and would make determining the relationship between variables more difficult to detect. In Chapters 5 and 6 this observational error will typically result in the models being somewhat conservative in the estimation of collapse and persistence probability. Following on this, the development of state-space models in which this uncertainty is partitioned into process (biological) and observation (measurement) error may be the best method by which the estimation of model parameters, probability of collapse, and likelihood of recovery could be improved.

7.2 Ecology vs. Fisheries Science

Throughout this thesis, I have attempted to address problems in fisheries science from a more ecological perspective than that traditionally used in fisheries science. This decision was a conscious effort to examine fisheries data from a different point of view than that typified by most studies. Below, I summarize the results of each chapter and discuss the benefits and limitations of this approach.

7.2.1 Allee effects and depensation

In chapter 2, I investigated the relationship between per capita (more accurately "per unit mass") reproduction and abundance (adult biomass) across dozens of harvested populations. Unlike almost all previous approaches, I did not imply any functional relationship between these variables but attempted to determine if there was a continual increase in per capita recruitment as abundance declined [62, 78]. Using a Bayesian framework, along with standardizing the metrics, enabled us to partially pool the data between populations of the same species and effectively increase the sample size

of data [33]. Approaching the problem in this fashion enabled the identification of trends in the data that could not have been done using traditional fisheries models (even using hierarchical Bayesian methods). The weakening of the relationship below 40% of historic maximum for a number of species, and the difference between eastern and western Atlantic populations of cod, are the primary examples of insights I have gained from this analysis.

Of course, this method does present difficulties of its own. Since all of the data had to be standardized, interpretation, in terms of predicting actual recruitment levels, is more difficult. The grouping of species together to standardize $\frac{Recruits}{SSB}$, while helpful in many cases, requires careful observation of the data. For example, the differences in the relationship between eastern and western Atlantic cod populations, due in part to differences in their environments was not immediately obvious. Additionally, combining the data into bins was relatively arbitrary; including everything below 10% in one category may be less than ideal given populations that have declined to 1% of historical maximum may have very different dynamics than populations at 9.9%. Fortunately, the relative consistency within categories for a species suggests this is not a serious problem. Finally, using historic maxima may also be problematic in that the actual maximum abundance for these populations may be much higher depending upon the time between the beginning of the fishery and the available data. However, given the length of the time series used, I believe that this method is superior to attempts to estimate the unfished biomass using surplus production models for which the maximum abundance is highly dependent on a stock-recruitment relationship; as I show, this can problematic, given the weakening of recruitment at low abundance.

7.2.2 Density dependent mortality

In chapter 3, I use functional response curves to determine the shape of the relationship between harvesting and abundance. While the functional response is commonly used in ecological circumstances, it had not been used to determine the shape of the relationship between harvesting rates and abundance in marine species. The results indicate that, in the majority of species, there is an increase in harvest mortality as abundance declines, and very often this mortality peaks when abundances drop below what fisheries scientist would consider MSY levels. When analyzing the age-specific

data, I find that per capita mortality rates for the oldest component of many populations approach 50% per year and this usually occurs when their abundance is near an historic low.

When high exploitation rates are coupled with a functional response (FR) that is fundamentally destabilizing, as occurs in the majority of these fish populations examined here, it should come as little surprise that many of the populations being harvested are either over-exploited or have collapsed. There are a myriad of social, political and economic factors that seem to lead to our fisheries being managed unsustainably [27]. Whether using single-stock models, or multi-species ecosystem models, forecasting in these highly dynamic systems for which the measurements and initial conditions are, at best, measured with substantial error will be fraught with uncertainties. When faced with uncertainty, it appears that most fisheries are not managed following a precautionary biological approach, but instead quotas are maintained at elevated levels, likely to ensure minimal short-term economic impact on the fishers themselves. How scientists can balance socio-economic forces, with ever-changing biological realities (uncertainty) to ensure that the long-term viability of both the fish (ecosystem) and the fishery are maintained, are questions of paramount importance.

This analysis does not attempt to incorporate the effect that increases in effort may have on these populations and it violates some of the assumptions of classic functional response theory [43]. Here I am using functional response curves simply to indicate the shape of the relationship between per capita mortality and abundance. I am interested in whether per capita mortality declines with abundance and I am not concerned whether all of the functional response theoretical assumptions are satisfied. Additionally, if these data came from a developing fishery, one would expect that per capita mortality would be low at high abundance, and increase with declines in abundance, as I have found. The functional response curves provide no evidence that this is what is happening and many of the stocks in this database had been harvested for decades to centuries before these data began to be collected. Finally, even if these data came from a developing fishery, a manager should not allow harvest mortality to continue to increase when abundance drops below MSY levels, as is found in many of these populations.

Taken together, Chapters 2 and 3 provide compelling evidence that both collapse

and slow recovery in harvested marine populations could easily be driven by the overly optimistic view of recruitment built in to many fishery models coupled with the difficulty managers have in lowering per capita harvest rates at low abundances.

7.2.3 Recruitment, spawner age, and size

In chapter 4 I attempt to determine whether there are metrics of age structure that may effect recruitment. My aim was to look at the relationship between density dependence, fecundity (individual mass), and age on $\frac{Recruits}{SSB}$. Here I find that the typical assumption that one kg of adult biomass is equivalent irrespective of the age of the fish is likely incorrect. The contribution to per capita recruitment appears to vary with the age of the fish; the most obvious influence appears to be related to virgin spawners [9, 112]. While traditional fisheries models do not attempt to disentangle the impact of age, size, and mass, the Ricker stock-recruitment model has recently been adapted to look for an effect of age [98].

While the models did result in significantly improved fits over a standard Ricker stock-recruit model, even our best model (which was relatively complex) explained less than 30% of the variability in per capita recruitment. There remains a great deal of unexplained variation in these data, undoubtedly a combination of real variability and observation error. In addition, no single term in the model explained a large amount of the total variation. Thus, while I believe this model is an improvement over traditional fisheries models, there is a need for more advanced techniques to further elucidate the importance of age, abundance, and size on per capita recruitment using these data.

7.2.4 Population viability

Utilizing PVA in fisheries management should be viewed as a potential tool to help generate additional information about both current and long-term population health. Caswell [14] suggests that these models can be fruitfully used in conservation biology to (a) assess the current status of the population, (b) diagnose what is affecting populations deemed to be in an unhealthy state, (c) prescribe an intervention based on which component of the life cycle is most sensitive to change, and (d) determine the fate of the population given a specific intervention.

In fisheries science (a) is largely subsumed by stock assessment models, while for (b) there is often debate whether fishing or environmental change, or some combination therein has negatively influenced the population [35]. This is not a particular focus of chapter 5, but I show that these types of questions can be profitably addressed using PVA and elasticity analysis (e.g. the difference between population growth rates during periods of unusually elevated recruitment and normal recruitment events). In chapter 6 I perform a more specific analysis that looks directly at the impacts of environmental variation. The results suggest that increasing survival of younger fish would be most likely to increase the long-term viability of Southern Gulf of St. Lawrence cod.

While traditional fisheries models do not typically address (c), in both Chapter 5 and 6 I show that PVAs can be used to determine which vital rates most influence population trajectories and how these can change with time. In chapter 5, I see that while there are commonalities between populations and species, there are also differences that may result in specific optimal management strategies for each population (e.g. the low population growth rate during periods of elevated recruitment in some populations). Finally, (d) can be achieved by developing experimental simulations, such as what was performed in chapter 6, to determine what effect altering one or more vital rates would have on the probability of sustainability, collapse, or any other metrics of interest. These types of simulations could also be used to inform an adaptive management strategy, which would lead to valuable insights into the factors that influence population dynamics, and result in the development of more sustainable fisheries [118].

The necessity of placing an arbitrary ceiling ($2 \times$ maximum historic abundance) on the abundance that could be reached during periods of unusually elevated recruitment also could have some influence on the model results. I explored this effect, using a range of maximum abundances between maximum and three times maximum, and found that changing the ceiling had some minor influence on the results obtained, but in general the patterns observed were largely unchanged across this range of maximum allowed abundances.

The incorporation of probabilistic models such as PVA should become a central part of the management of data-rich fisheries. data available in marine ecosystems.

Utilizing these models would enable fishery managers to (i) perform risk assessment of various management strategies, (ii) understand both the short- and long-term implications of harvesting policy on population health, (iii) quantify the influence of environmental variability, and (iv) ascertain which vital rates contribute most to population sustainability.

These models could also be constructed to incorporate the relationships found in chapter 2-4. This may increase the realism of these models. However given the uncertainty surrounding the assumed processes (especially recruitment), the influence of environmental variability, and the increased number of parameters required, I believe that, in many cases, this may be a fool's errand that will do little to increase our forecasting ability. Until we have significantly more data available to understand the processes driving population dynamics in marine ecosystems accurately forecasting population trajectories will remain fraught with error.

7.3 Epilogue

There is much in fisheries science that could be used to inform ecology and much in ecology that can inform fisheries science. To date, the two disciplines have often acted in solitude rather than collaborating together, but I hope this thesis provides fisheries scientists a glimpse of what can be done using more traditional ecological modelling frameworks. Alternatively, it would be very beneficial to see some fisheries science used to help solve non-marine ecological problems. Interaction between fisheries scientists and marine ecologists has already proven very helpful, as evidenced by the collaboration on the problem of estimating the global status of harvested marine fishes [124]. More research in this vein, from scientists on both sides of the shoreline, can only help to improve our understanding of population collapse and recovery in both fisheries and more traditional ecological systems.

Bibliography

[1] P. A. Abrams. Functional responses of optimal foragers. *The American Naturalist*, 120(3):382–390, 1982.

[2] H Akaike. New look at statistical-model identification. *IEEE Transaction on Automatic Control*, AC19(6):716–723, 1974.

[3] H.R. Akcakaya, M.A. Burgman, O. Kindvall, C.C. Wood, P. Sjogren-Gluve, J.S. Hatfield, and M.A. McCarthy. *Species conservation and management: case studies*. Oxford University Press, USA, 2004.

[4] A. Audzijonyte, A. Kuparinen, R Gorton, and E. A. Fulton. Ecological consequences of body size decline in harvested fish species: positive feedback loops in trophic interactions amplify human impact. *Biology Letters*, 9(2), 2013.

[5] J. K. Baum and B. Worm. Cascading top-down effects of changing oceanic predator abundances. *Journal of Animal Ecology*, 78(4):699–714, 2009.

[6] G. Beaugrand, M. Edwards, and L. Legendre. Marine biodiversity, ecosystem functioning, and carbon cycles. *Proceedings of the National Academy of Sciences of the United States of America*, 107(22):10120–10124, 2010.

[7] H. P. Benoît, D. P. Swain, D. W. Bowen, G. A. Breed, M. O. Hammill, and V. Harvey. Evaluating the potential for grey seal predation to explain elevated natural mortality in three fish species in the southern gulf of st. lawrence. *Marine Ecology Progress Series*, 442:149–167, 2011.

[8] L. Berec, D. S. Boukal, and M. Berec. Linking the allee effect, sexual reproduction, and temperature-dependent sex determination via spatial dynamics. *The American Naturalist*, 157(2):217–230, 2001.

[9] S. A. Berkeley, C. Chapman, and S. M. Sogard. Maternal age as a determinant of larval growth and survival in a marine fish, *Sebastes melanops*. *Ecology*, 85(5):1258–1264, 2004.

[10] RJH Beverton and SJ Holt. *On the dynamics of exploited Fish Populations*, volume 19 of Fishery Investigations Series II. UK Ministry of Agriculture, Fisheries and Food, London U.K., 1957.

[11] B. M. Bolker. *Ecological Models and Data in R*. Princeton University Press, Princeton, NJ, 2008.

[12] B. W. Brook, J. J. O'Grady, A. P. Chapman, M. A. Burgman, H. R. Akcakaya, and R. Frankham. Predictive accuracy of population viability analysis in conservation biology. *Nature*, 404(6776):385–387, 2000.

[13] K.P. Burnham and D. R. Anderson. *Model selection and multimodel inference: A practical information-theoretic approach*. Springer-Verlag, New York, 2nd edition, 2002.

[14] H. Caswell. *Matrix Population Models: construction, analysis, and interpretation*. Sinauer Associates, Sunderland, MA, 2nd edition, 2001.

[15] W. M. Chapman. United states policy on high seas fisheries. *Department of State Bulletin*, 20:67–80, 1949.

[16] N. L. Christensen, A. M. Bartuska, J. H. Brown, S. Carpenter, C. D'Antonio, R. Francis, J. F. Franklin, J. A. MacMahon, R. F. Noss, D. J. Parsons, C. H. Peterson, M. G. Turner, and R. G. Woodmansee. The report of the ecological society of america committee on the scientific basis for ecosystem management. *Ecological Applications*, 6(3):665–691, 1996.

[17] V. Christensen and C. J. Walters. Ecopath with ecosim: methods, capabilities and limitations. *Ecological Modelling*, 172:109 – 139, 2004.

[18] D. W. Coltman, P. O'Donoghue, J. T. Jorgenson, J. T. Hogg, C. Strobeck, and M. Festa-Bianchet. Undesirable evolutionary consequences of trophy hunting. *Nature*, 426(6967):655–658, 2003.

[19] F. Courchamp, L. Berec, and J. Gascoigne. *Allee effects in ecology and conservation*. Oxford University Press, New York, New York, 2008.

[20] D. T. Crouse, L. B. Crowder, and H. Caswell. A stage-based population model for loggerhead sea turtles and implications for conservation. *Ecology*, 68(5):1412–1423, 1987.

[21] L. B. Crowder, D. T. Crouse, S. S. Heppell, and T. H. Martin. Predicting the impact of turtle excluder devices on loggerhead sea turtle populations. *Ecological Applications*, 4(3):437–445, 1994.

[22] J.-F. Pulvenis de Sligny, R. Grainger, and A. Gumy. The state of world fisheries and aquaculture (sofia) 2010. food and agriculture organization of the united nations (un fao). rome, 2010.

[23] E. J. Dick. Modeling the reproductive potential of rockfishes (sebastes spp.). ph.d. dissertation,. 2009.

[24] D. L. Dixson, P. L. Munday, and G. P. Jones. Ocean acidification disrupts the innate ability of fish to detect predator olfactory cues. *Ecology Letters*, 13(1):68–75, 2010.

[25] W. F. Fagan, C. Cosner, E. A. Larsen, and J. M. Calabrese. Reproductive asynchrony in spatial population models: How mating behavior can modulate allee effects arising from isolation in both space and time. *The American Naturalist*, 175:362–373, 2010.

[26] S. H. Ferguson and F. Messier. Can human predation of moose cause population cycles? In Lankester, MW and Timmermann, HR, editor, *ALCES 32 - Including papers from the 32nd North American moose conference and workshop*, volume 32, pages 149–161, 1996.

[27] C. Finley. *All the fish in the sea*. The University of Chicago Press, Chicago, 2011.

[28] K. T. Frank and D. Brickman. Allee effects and compensatory population dynamics within a stock complexg. *Canadian Journal of Fisheries and Aquatic Sciences*, 57(3):513–517, 2000.

[29] K. T. Frank, B. Petrie, J. A. D. Fisher, and W. C. Leggett. Transient dynamics of an altered large marine ecosystem. *Nature*, 477(7362):86–89, 2011.

[30] J. C. Gascoigne and R. C. Lipcius. Allee effects driven by predation. *Journal of Applied Ecology*, 41(5):801–810, 2004.

[31] J. C. Gascoigne and R. C. Lipcius. Conserving populations at low abundance: delayed functional maturity and allee effects in reproductive behaviour of the queen conch strombus gigas. *Marine Ecology-Progress Series*, 284:185–194, 2004.

[32] A. Gelman. Analysis of variance - Why it is more important than ever. *Annals of Statistics*, 33(1):1–31, 2005.

[33] A. Gelman and J. Hill. *Data analysis using regression and multilevel/hierarchical models*. Cambridge University Press, New York, 2007.

[34] A. Gelman, J. Hill, and M. Yajima. Why we (usually) don't have to worry about multiple comparisons. *Journal of Research on Educational Effectiveness*, 5:189–211, 2012.

[35] D. J. Gilbert. Towards a new recruitment paradigm for fish stocks. *Canadian Journal of Fisheries and Aquatic Sciences*, 54(4):969–977, 1997.

[36] M. E. Gilpin and M. E. Soule. *Conservation biology: the science of scarcity and diversity*, chapter Minimum viable populations: processes of species extinction, pages 19–34. Sinauer Associates, Sunderland, Massachusetts, USA, 1986.

[37] R. Hilborn. The frequency and severity of fish stock declines and increases. In D. A. Hancock, D. C. Smith, A. Grant, and J. P. Beumer, editors, *Developing and sustaining world fisheries resources*, pages 36–38. CSIRO Publishing, Victoria, 1997.

[38] R. Hilborn and K. Stokes. Defining overfished stocks: have we lost the plot? *Fisheries*, 35(3):113–120, 2010.

[39] R. Hilborn and C. J. Walters, editors. *Quantitative Fisheries Stock Assessment: Choice, Dynamics and Uncertainty*. Chapman and Hall, New York, New York, 1992.

[40] C. L. Hitchcock and C. Gratto-Trevor. Diagnosing a shorebird local population decline with a stage-structured population model. *Ecology*, 78(2):522–534, 1997.

[41] F. Hoelker, D. Beare, H. Doerner, A. di Natale, H.-J. Raetz, A. Temming, and J. Casey. Comment on "Impacts of biodiversity loss on ocean ecosystem services". *Science*, 316(5829):1285, 2007.

[42] C. S. Holling. The components of predation as revealed by a study of small-mammal predation of the european pine sawfly. *The Canadian Entomologist*, 91:293–320, 1959.

[43] C. S. Holling. The functional response of predators to prey density and its role in mimicry and population regulation. *Memoirs of the Entomological Society of Canada*, 97(Supplement S45):5–60, 1965.

[44] J. A. Hutchings. Collapse and recovery of marine fishes. *Nature*, 406(6798):882–885, 2000.

[45] J. A. Hutchings. Conservation biology of marine fishes: perceptions and caveats regarding assignment of extinction risk. *Canadian Journal of Fisheries and Aquatic Sciences*, 58(1):108–121, 2001.

[46] J. A. Hutchings. Life history consequences of overexploitation to population recovery in northwest atlantic cod (gadus morhua). *Canadian Journal of Fisheries and Aquatic Sciences*, 62:824–832, 2005.

[47] J. A. Hutchings and J. K. Baum. Measuring marine fish biodiversity: temporal changes in abundance, life history and demography. *Philosophical Transactions of the Royal Society B-Biological Sciences*, 360(1454):315–338, 2005.

[48] J A Hutchings, I. M Côté, J. J. Dodson, I. A. Fleming, S. Jennings, N. J. Mantua, R. M. Peterman, B. E. Riddell, A. J. Weaver, and D. L. VanderZwaag. Sustaining canadian marine biodiversity: responding to the challenges posed by climate change, fisheries, and aquaculture. expert panel report prepared for the royal society of canada, ottawa. http://www.rsc.ca/documents/rscmarinebiodiversity2012_enfinal.pdf, 2012.

[49] J. A. Hutchings and D. J. Fraser. The nature of fisheries- and farming-induced evolution. *Molecular Ecology*, 17(1):294–313, 2008.

[50] J. A Hutchings, C. Minto, D. Ricard, J. K. Baum, and O. P. Jensen. Trends in the abundance of marine fishes. *Canadian Journal of Fisheries and Aquatic Sciences*, 67:1205–1210, 2010.

[51] J. A. Hutchings and R. A. Myers. Effect of age on the seasonality of maturation and spawning of atlantic cod, *Gadus morhua*, in the northwest atlantic. *Canadian Journal of Fisheries and Aquatic Sciences*, 50(11):2468–2474, 1993.

[52] J. A. Hutchings and R. A. Myers. The evolution of alternative mating strategies in variable environments. *Evolutionary Ecology*, 8(3):256–268, 1994.

[53] J. A. Hutchings and R. W. Rangeley. Correlates of recovery for Canadian Atlantic cod *(Gadus morhua)*. *Canadian Journal of Zoology*, 89(5, SI):386–400, 2011.

[54] J. A. Hutchings and J. D. Reynolds. Marine fish population collapses: Consequences for recovery and extinction risk. *Bioscience*, 54(4):297–309, 2004.

[55] B. Jonsson and N. Jonsson. A review of the likely effects of climate change on anadromous Atlantic salmon Salmo salar and brown trout Salmo trutta, with particular reference to water temperature and flow. *Journal of Fish Biology*, 75(10):2381–2447, 2009.

[56] D. M. Keith and J. A. Hutchings. Population dynamics of marine fishes at low abundance. *Canadian Journal of Fisheries and Aquatic Sciences*, 69:1150–1163, 2012.

[57] M. Kèry. *Introduction to WinBUGS for ecologists: A Bayesian approach to regression, ANOVA, mixed models and related analyses*. Academic Press, Burlington, MA, 2010.

[58] R. Lande, S. Engen, and B. E. Saether. *Stochastic population dynamics in ecology and conservation*. Oxford Series in Ecology and Evolution. Oxford University Press, 2003.

[59] P. A. Larkin. An epitaph for the concept of maximum sustained yield. *Transactions of the American Fisheries Society*, 106(1):1–11, 1977.

[60] R. Law. Fishing, selection, and phenotypic evolution. *ICES Journal of Marine Science*, 57(3):659–668, 2000.

[61] R. Law. Fisheries-induced evolution: present status and future directions. *Marine Ecology-Progress Series*, 335:271–277, 2007.

[62] M. Liermann and R. Hilborn. Depensation in fish stocks: A hierarchic Bayesian meta-analysis. *Canadian Journal of Fisheries and Aquatic Sciences*, 54(9):1976–1984, 1997.

[63] M. Liermann and R. Hilborn. Depensation: evidence, models and implications. *Fish and Fisheries*, 2(1):33–58, 2001.

[64] H. K. Lotze, M. Coll, A. M. Magera, C. Ward-Paige, and L. Airoldi. Recovery of marine animal populations and ecosystems. *Trends Ecol Evol*, 26(11):595–605, 2011.

[65] D. J. Lunn, A. Thomas, N. Best, and D. Spiegelhalter. Winbugs - a bayesian modelling framework: concepts, structure, and extensibility. *Statistics and Computing*, 10:325–337, 2000.

[66] A. D. MacCall. *Dynamic Geography of Marine Fish Populations*. University of Washington Press, Seattle, WA, 1990.

[67] P. M. Mace. Relationships between common biological reference points used as thresholds and targets of fisheries management strategies. *Canadian Journal of Fisheries and Aquatic Sciences*, 51(1):110–122, 1994.

[68] M. Marmontel, S. R. Humphrey, and T. J. O'Shea. Population viability analysis of the florida manatee (trichechus manatus latirostris), 1976-1991. *Conservation Biology*, 11(2):467–481, 1997.

[69] C. T. Marshall, C. L. Needle, A. Thorsen, O. S. Kjesbu, and N. A. Yaragina. Systematic bias in estimates of reproductive potential of an Atlantic cod *(Gadus morhua)* stock: implications for stock-recruit theory and management. *Canadian Journal of Fisheries and Aquatic Sciences*, 63(5):980–994, 2006.

[70] G. Marteinsdottir and G. A. Begg. Essential relationships incorporating the influence of age, size and condition on variables required for estimation of reproductive potential in atlantic cod gadus morhua. *Marine Ecology-Progress Series*, 235:235–256, 2002.

[71] S. J. McNaughton and L. J. Wolf. *General Ecology*. Holt, Rinehard, and Winston Inc., 1979.

[72] S. Mogensen and J.A. Hutchings. Maternal fitness consequences of interactions among agents of mortality in early life of salmonids. *Canadian Journal of Fisheries and Aquatic Sciences*, 69(9):1539–1555, 2012.

[73] W. F. Morris and D. F. Doak. *Quantitative Conservation Biology*. Sinauer Associates, Sunderland, Mass, USA, 2002.

[74] S. B. Munch, A. Kottas, and M. Mangel. Bayesian nonparametric analysis of stock-recruitment relationships. *Canadian Journal of Fisheries and Aquatic Sciences*, 62(8):1808–1821, 2005.

[75] S. Murawski, R. Methot, and G. Tromble. Biodiversity loss in the ocean: How bad is it? *Science*, 316(5829):1281–1284, 2007.

[76] W.W. Murdoch and A. Oaten. Predation and population stability. *Advances in ecological research*, 9:1–131, 1975.

[77] R. A. Myers and N. J. Barrowman. Is fish recruitment related to spawner abundance? *Fishery Bulletin*, 94(4):707–724, 1996.

[78] R. A. Myers, N. J. Barrowman, J. A. Hutchings, and A. A. Rosenberg. Population-dynamics of exploited fish stocks at low population-levels. *Science*, 269(5227):1106–1108, 1995.

[79] R. A. Myers, K. G. Bowen, and N. J. Barrowman. Maximum reproductive rate of fish at low population sizes. *Canadian Journal of Fisheries and Aquatic Sciences*, 56(12):2404–2419, 1999.

[80] R. D. M. Nash and M. Dickey-Collas. The influence of life history dynamics and environment on the determination of year class strength in North Sea herring *(Clupea harengus L.)*. *Fisheries Oceanography*, 14(4):279–291, 2005.

[81] R. D. M. Nash, M. Dickey-Collas, and L. T. Kell. Stock and recruitment in North Sea herring *(Clupea harengus)*; compensation and depensation in the population dynamics. *Fisheries Research*, 95(1):88–97, 2009.

[82] P. Neubauer, O. P. Jensen, J. A. Hutchings, and J. K. Baum. Resilience and recovery of overexploited marine populations. *Science*, In Press, 2013.

[83] R. T. Paine and R. L. Vadas. The effects of grazing by sea urchins, strongylocentrotus spp., on benthic algal populations. *Limnology and Oceanography*, 14(5):pp. 710–719, 1969.

[84] R. M. Peterman. Dynamics of native indian food fisheries on salmon in british columbia. *Canadian Journal of Fisheries and Aquatic Sciences*, 37(4):561–566, 1980.

[85] J. R. Post, M. Sullivan, S. Cox, N. P. Lester, C. J. Walters, E. A. Parkinson, A. J. Paul, L. Jackson, and B. J. Shuter. Canada's recreational fisheries: The invisible collapse? *Fisheries*, 27(1):6–17, 2002.

[86] T. J. Quinn and R. B. Deriso. *Quantitative fish dynamics*. Oxford University Press, 1999.

[87] R Development Core Team. R: A language and environment for statistical computing. ISBN 3-900051-07-0 URL: http://www.R-project.org/, 2012.

[88] D. Ricard, C. Minto, O. P. Jensen, and J. K. Baum. Examining the knowledge base and status of commercially exploited marine species with the ram legacy stock assessment database. *Fish and Fisheries*, 2011.

[89] W. E. Ricker. Stock and recruitment. *Journal of the Fisheries Research Board of Canada*, 11:559–623, 1954.

[90] W. E. Ricker. Maximum sustained yield from fluctuating environments and mixed stocks. *Journal of the Fisheries Research Board of Canada*, 15(5):991–1006, 1958.

[91] L. A. Rogers, L. C. Stige, E. M. Olsen, H. Knutsen, K.-S. Chan, and N. C. Stenseth. Climate and population density drive changes in cod body size throughout a century on the Norwegian coast. *Proceedings of the National Academy of Sciences of the United States of America*, 108(5):1961–1966, 2011.

[92] G. A. Rose. Reconciling overfishing and climate change with stock dynamics of Atlantic cod (Gadus morhua) over 500 years. *Canadian Journal of Fisheries and Aquatic Sciences*, 61(9):1553–1557, 2004.

[93] S. Rowe, J. A. Hutchings, D. Bekkevold, and A. Rakitin. Depensation, probability of fertilization, and the mating system of Atlantic cod *(Gadus morhua L.)*. *ICES Journal of Marine Science*, 61(7):1144–1150, 2004.

[94] Senate. Standing senate committee on fisheries and oceans. the sustainable management of grey seal populations: A path toward the recovery of cod and other groudfish stocks. 1-27, 2012.

[95] N. L. Shackell, K. T. Frank, J. A. D. Fisher, B. Petrie, and W. C. Leggett. Decline in top predator body size and changing climate alter trophic structure in an oceanic ecosystem. *Proceedings of the Royal Society B-Biological Sciences*, 277(1686):1353–1360, 2010.

[96] M. L. Shaffer. Minimum population sizes for species conservation. *BioScience*, 31(2):131–134, 1981.

[97] D. M. T. Sharpe and A. P. Hendry. Synthesis: Life history change in commercially exploited fish stocks: an analysis of trends across studies. *Evolutionary Applications*, 2(3):260–275, 2009.

[98] A. O. Shelton, S.B. Munch, D. M. Keith, and M. Mangel. Maternal age, fecundity, egg quality, and recruitment: linking stock structure to recruitment using an age-structured ricker model. *Canadian Journal of Fisheries and Aquatic Sciences*, 69(10):1631–1641, 2012.

[99] P. A. Shelton and B. P. Healey. Should depensation be dismissed as a possible explanation for the lack of recovery of the northern cod *(Gadus morhua)* stock? *Canadian Journal of Fisheries and Aquatic Sciences*, 56(9):1521–1524, 1999.

[100] J. Short and B. Turner. Control of feral cats for nature conservation. IV. Population dynamics and morphological attributes of feral cats at Shark Bay, Western Australia. *Wildlife Research*, 32(6):489–501, 2005.

[101] M. E. Solomon. The natural control of animal populations. *Journal of Animal Ecology*, 18(1):pp. 1–35, 1949.

[102] D. E. Spalinger and N. T. Hobbs. Mechanisms of foraging in mammalian herbivores: New models of functional response. *The American Naturalist*, 140(2):pp. 325–348, 1992.

[103] P. D. Spencer and M. W. Dorn. Incorporation of weight-specific relative fecundity and maternal effects in larval survival into stock assessments. *Fisheries Research*, 138:159 – 167, 2013.

[104] P. A. Stephens and W. J. Sutherland. Consequences of the Allee effect for behaviour, ecology and conservation. *Trends in Ecology and Evolution*, 14(10):401–405, 1999.

[105] P. A. Stephens, W. J. Sutherland, and R. P. Freckleton. What is the Allee effect? *Oikos*, 87(1):185–190, 1999.

[106] D. P. Swain. Natural mortality and projected biomass of southern gulf of st. lawrence cod (gadus morhua). Technical report, Canadian Science Advisory Secretariat Research Document 2011/040, 2011.

[107] D. P. Swain, H.P Benoit, and M. O. Hammill. Grey seal reduction scenarios to restore the southern gulf of st. lawrence cod population. Technical report, DFO Canadian Science Advisory Secretariat Research Document 2011/035., 2011.

[108] D. P. Swain and G. A. Chouinard. Predicted extirpation of the dominant demersal fish in a large marine ecosystem: Atlantic cod (Gadus morhua) in the southern Gulf of St. Lawrence. *Canadian Journal of Fisheries and Aquatic Sciences*, 65(11):2315–2319, 2008.

[109] D. P. Swain and R. K. Mohn. Forage fish and the factors governing recovery of atlantic cod (gadus morhua) on the eastern scotian shelf. *Canadian Journal of Fisheries and Aquatic Sciences*, 69(6):997–1001, 2012.

[110] D. P. Swain and A. F. Sinclair. Pelagic fishes and the cod recruitment dilemma in the northwest atlantic. *Canadian Journal of Fisheries and Aquatic Sciences*, 57(7):1321–1325, 2000.

[111] D. P. Swain, A. F. Sinclair, and J. M. Hanson. Evolutionary response to size-selective mortality in an exploited fish population. *Proceedings of the Royal Society B-Biological Sciences*, 274(1613):1015–1022, 2007.

[112] E. A. Trippel. Egg size and viability and seasonal offspring production of young Atlantic cod. *Transactions of the American Fisheries Society*, 127:339–359, 1998.

[113] S. Tuljapurkar and H. Caswell. *Structured-population models in marine, terrestrial, and freshwater systems*. Population and community biology series 18. Chapman and Hall, New York, NY, 1997.

[114] L. Vallin and A. Nissling. Maternal effects on egg size and egg buoyancy of baltic cod, gadus morhua - implications for stock structure effects on recruitment. *Fisheries Research*, 49(1):21–37, 2000.

[115] T. van Kooten, J. Andersson, P. Bystrom, L. Persson, and A. M. de Roos. Size at hatching determines population dynamics and response to harvesting in cannibalistic fish. *Canadian Journal of Fisheries and Aquatic Sciences*, 67(2):401–416, 2010.

[116] A. Van Leeuwen, A. M. De Roos, and L. Persson. How cod shapes its world. *Journal of Sea Research*, 60(1-2, Sp. Iss. SI):89–104, 2008.

[117] P. A. Venturelli, B. J. Shuter, and C. A. Murphy. Evidence for harvest-induced maternal influences on the reproductive rates of fish populations. *Proceedings of the Royal Society B-Biological Sciences*, 276(1658):919–924, 2009.

[118] C. J. Walters and R. Hilborn. Adaptive control of fishing systems. *Journal of the Fisheries Research Board of Canada*, 33(1):145–159, 1976.

[119] C. J. Walters, R. Hilborn, and V. Christensen. Surplus production dynamics in declining and recovering fish populations. *Canadian Journal of Fisheries and Aquatic Sciences*, 65(11):2536–2551, 2008.

[120] C. J. Walters and J. F. Kitchell. Cultivation/depensation effects on juvenile survival and recruitment: implications for the theory of fishing. *Canadian Journal of Fisheries and Aquatic Sciences*, 58(1):39–50, 2001.

[121] C. J. Walters and J. D. Martell. *Fisheries Ecology and Management*. Princeton University Press, Princeton, 2004.

[122] C.J. Walters and J.-J. Maguire. Lessons for stock assessment from the northern cod collapse. *Reviews in Fish Biology and Fisheries*, 6(2):125–137, 1996.

[123] B. Worm, E. B. Barbier, N. Beaumont, J. E. Duffy, C. Folke, B. S. Halpern, J. B. C. Jackson, H. K. Lotze, F. Micheli, S. R. Palumbi, E. Sala, K. A. Selkoe, J. J. Stachowicz, and R. Watson. Impacts of biodiversity loss on ocean ecosystem services. *Science*, 314(5800):787–790, 2006.

[124] B. Worm, R. Hilborn, J. K. Baum, T. A. Branch, J. S. Collie, C. Costello, M. J. Fogarty, E. A. Fulton, J. A. Hutchings, S. Jennings, O. P. Jensen, H. K. Lotze, P. M. Mace, T. R. McClanahan, C. Minto, S. R. Palumbi, A. M. Parma, D. Ricard, A. A. Rosenberg, R. Watson, and D. Zeller. Rebuilding Global Fisheries. *Science*, 325(5940):578–585, 2009.

[125] A. F. Zuur, E. N. Ieno, N. J. Walker, A. A. Saveliev, and G. M. Smith. *Mixed Effects Models and Extensions in Ecology with R*. Springer, New York, New York USA, 2009.

Appendix A

Chapter 2 supplemental tables and figures

Table A.1: Stocks used in the analysis, including scientific name, common name, order, stock ID, and assessment method.

Stock ID	Common Name	Scientific Name	Order	Assess Method
ADFG-HERRPWS-1980-2006-COLLIE	Pacific herring	Clupea pallasii	Clupeiformes	AD-CAM
ADFG-HERRSITKA-1978-2007-COLLIE	Pacific herring	Clupea pallasii	Clupeiformes	AD-CAM
AFSC-ALPLAICBSAI-1972-2008-MELNYCHUK	Alaska plaice	Pleuronectes quadrituberculatus	Pleuronectiformes	AD-CAM
AFSC-ARFLOUNDBSAI-1970-2008-STANTON	Arrowtooth flounder	Reinhardtius stomias	Pleuronectiformes	AD-CAM
AFSC-ARFLOUNDGA-1958-2010-STANTON	Arrowtooth flounder	Reinhardtius stomias	Pleuronectiformes	AD-CAM
AFSC-ATKABSAI-1976-2009-STANTON	Atka mackerel	Pleurogrammus monopterygius	Scorpaeniformes	AD-CAM
AFSC-CABEZNCAL-1916-2005-STANTON	Cabezon	Scorpaenichthys marmoratus	Scorpaeniformes	SS2
AFSC-CABEZSCAL-1932-2005-STANTON	Cabezon	Scorpaenichthys marmoratus	Scorpaeniformes	SS2
AFSC-DSOLEGA-1978-2010-STANTON	Dover sole	Microstomus pacificus	Pleuronectiformes	AD-CAM
AFSC-DUSROCKGA-1973-2008-MELNYCHUK	Dusky rockfish	Sebastes variabilis	Scorpaeniformes	AD-CAM
AFSC-FLSOLEBSAI-1977-2008-STANTON	Flathead sole	Hippoglossoides elassodon	Pleuronectiformes	AD-CAM
AFSC-FLSOLEGA-1978-2010-Stachura	Flathead sole	Hippoglossoides elassodon	Pleuronectiformes	AD-CAM
AFSC-NROCKBSAI-1974-2009-STANTON	Northern rockfish	Sebastes polyspinis	Scorpaeniformes	AD-CAM
AFSC-NROCKGA-1959-2008-MELNYCHUK	Northern rockfish	Sebastes polyspinis	Scorpaeniformes	AD-CAM
AFSC-PCODBSAI-1964-2008-MELNYCHUK	Pacific cod	Gadus macrocephalus	Gadiformes	SS2
AFSC-PCODGA-1964-2008-MELNYCHUK	Pacific cod	Gadus macrocephalus	Gadiformes	SS2
AFSC-PERCHEBSAI-1974-2009-STANTON	Pacific ocean perch	Sebastes alutus	Scorpaeniformes	AD-CAM
AFSC-POPERCHGA-1959-2010-Stachura	Pacific ocean perch	Sebastes alutus	Scorpaeniformes	AD-CAM
AFSC-REXSOLEGA-1979-2008-STANTON	Rex sole	Glyptocephalus zachirus	Pleuronectiformes	AD-CAM
AFSC-REYEROCKBSAI-1974-2009-STANTON	Rougheye rockfish	Sebastes aleutianus	Scorpaeniformes	AD-CAM
AFSC-REYEROCKGA-1974-2007-MELNYCHUK	Rougheye rockfish	Sebastes aleutianus	Scorpaeniformes	AD-CAM
AFSC-SABLEFEBSAIGA-1956-2008-MELNYCHUK	Sablefish	Anoplopoma fimbria	Scorpaeniformes	AD-CAM
AFSC-WPOLLAI-1976-2008-MELNYCHUK	Walleye pollock	Theragra chalcogramma	Gadiformes	AD-CAM
AFSC-WPOLLEBS-1963-2008-MELNYCHUK	Walleye pollock	Theragra chalcogramma	Gadiformes	AD-CAM
AFSC-WPOLLGA-1964-2008-MELNYCHUK	Walleye pollock	Theragra chalcogramma	Gadiformes	AD-CAM
AFSC-YSOLEBSAI-1959-2008-MELNYCHUK	Yellowfin sole	Limanda aspera	Pleuronectiformes	AD-CAM
AFWG-CODCOASTNOR-1982-2006-MINTO	Atlantic cod	Gadus morhua	Gadiformes	VPA
AFWG-CODNEAR-1943-2006-MINTO	Atlantic cod	Gadus morhua	Gadiformes	VPA
AFWG-GHALNEAR-1959-2007-JENNINGS	Greenland halibut	Reinhardtius hippoglossoides	Pleuronectiformes	XSA

Table A.1: Stocks used in the analysis, including scientific name, common name, order, stock ID, and assessment method.

Stock ID	Common Name	Scientific Name	Order	Assess Method
AFWG-GOLDREDNEAR-1986-2006-MINTO	Golden Redfish	Sebastes norvegicus	Scorpaeniformes	GADGET
AFWG-HADNEAR-1947-2006-MINTO	Haddock	Melanogrammus aeglefinus	Gadiformes	VPA
AFWG-POLLNEAR-1957-2006-MINTO	Pollock	Pollachius virens	Gadiformes	XSA
ASMFC-ATLCROAKMATLC-1973-2002-STANTON	Atlantic croaker	Micropogonias undulatus	Perciformes	AD-CAM
CCSBT-SC-SBT-1931-2009-Parma	Southern bluefin tuna	Thunnus maccoyii	Perciformes	IA
CSIRO-BIGHTREDSE-1958-2007-FULTON	Bight redfish	Centroberyx gerrardi	Beryciformes	SS2
CSIRO-DEEPFLATHEADSE-1978-2007-FULTON	Deepwater flathead	Platycephalus conatus	Scorpaeniformes	SS2
CSIRO-GEMFISHSE-1966-2007-FULTON	common gemfish	Rexea solandri	Perciformes	SS2
CSIRO-MORWONGSE-1913-2007-FULTON	Hawaiian morwong	Nemadactylus macropterus	Perciformes	SS2
CSIRO-OROUGHYCASCADE-1987-2006-FULTON	Orange roughy	Hoplostethus atlanticus	Beryciformes	SS2
CSIRO-PTOOTHFISHMI-1975-2010-FAY	Patagonian toothfish	Dissostichus eleginoides	Perciformes	SS3
CSIRO-SILVERFISHSE-1978-2006-FULTON	Silverfish	Seriolella punctata	Perciformes	SS2
CSIRO-SWHITSE-1945-2007-FULTON	School whiting	Sillago flindersi	Perciformes	SS2
CSIRO-WAREHOUESE-1984-2006-FULTON	whario	Seriolella brama	Perciformes	SS2
CSIRO-WAREHOUWSE-1984-2006-FULTON	whario	Seriolella brama	Perciformes	SS2
DFO-COD5Zjm-1978-2003-PREFONTAINE	Atlantic cod	Gadus morhua	Gadiformes	ADAPT
DFO-HAD5Zejm-1968-2003-PREFONTAINE	Haddock	Melanogrammus aeglefinus	Gadiformes	ADAPT
DFO-HERR4VWX-1964-2006-PREFONTAINE	Herring	Clupea harengus	Clupeiformes	ADAPT
DFO-MAR-HAD4X5Y-1960-2003-PREFONTAINE	Haddock	Melanogrammus aeglefinus	Gadiformes	SPA-ADAPT
DFO-NFLD-AMPL23K-1960-2004-PREFONTAINE	American plaice	Hippoglossoides platessoides	Pleuronectiformes	Survey indices
DFO-NFLD-COD2J3KLIS-1959-2006-PREFONTAINE	Atlantic cod	Gadus morhua	Gadiformes	ADAPT
DFO-NFLD-COD3Ps-1959-2004-PREFONTAINE	Atlantic cod	Gadus morhua	Gadiformes	B-ADAPT
DFO-PAC-HERRCC-1951-2007-COLLIE	Pacific herring	Clupea pallasii	Clupeiformes	AD-CAM
DFO-PAC-HERRPRD-1951-2007-COLLIE	Pacific herring	Clupea pallasii	Clupeiformes	AD-CAM
DFO-PAC-HERRQCI-1951-2007-COLLIE	Pacific herring	Clupea pallasii	Clupeiformes	AD-CAM
DFO-PAC-HERRSOG-1951-2007-COLLIE	Pacific herring	Clupea pallasii	Clupeiformes	AD-CAM
DFO-PAC-HERRWCVANI-1951-2007-COLLIE	Pacific herring	Clupea pallasii	Clupeiformes	AD-CAM
DFO-PAC-RSOLEHSTR-1945-2001-COLLIE	Rock sole	Lepidopsetta bilineata	Pleuronectiformes	TSA
DFO-POLL4X5YZ-1980-2006-PREFONTAINE	Pollock	Pollachius virens	Gadiformes	ADAPT

Table A.1: Stocks used in the analysis, including scientific name, common name, order, stock ID, and assessment method.

Stock ID	Common Name	Scientific Name	Order	Assess Method
DFO-QUE-COD3Pn4RS-1964-2007-PREFONTAINE	Atlantic cod	Gadus morhua	Gadiformes	ADAPT
DFO-QUE-HERR4RFA-1971-2003-PREFONTAINE	Herring	Clupea harengus	Clupeiformes	SPA-ADAPT
DFO-QUE-HERR4RSP-1963-2004-PREFONTAINE	Herring	Clupea harengus	Clupeiformes	SPA-ADAPT
DFO-SG-COD4TVn-1965-2009-RICARD	Atlantic cod	Gadus morhua	Gadiformes	ADAPT
DFO-SG-HERR4TFA-1974-2007-PREFONTAINE	Herring	Clupea harengus	Clupeiformes	SPA-ADAPT
DFO-SG-HERR4TSP-1974-2007-PREFONTAINE	Herring	Clupea harengus	Clupeiformes	SPA-ADAPT
HAWG-HERR2224IIIa-1991-2006-MINTO	Herring	Clupea harengus	Clupeiformes	ICA
HAWG-HERRNIRS-1960-2006-JENNINGS	Herring	Clupea harengus	Clupeiformes	ICA
HAWG-HERRNS-1960-2007-MINTO	Herring	Clupea harengus	Clupeiformes	ICA
HAWG-HERRVIa-1957-2006-MINTO	Herring	Clupea harengus	Clupeiformes	ICA
HAWG-HERRVIaVIIbc-1969-2000-MINTO	Herring	Clupea harengus	Clupeiformes	VPA
ICCAT-ALBANATL-1929-2005-WORM	Albacore tuna	Thunnus alalunga	Perciformes	VPA
ICCAT-ATBTUNAEATL-1969-2007-WORM	Atlantic bluefin tuna	Thunnus thynnus	Perciformes	VPA
ICCAT-ATBTUNAWATL-1969-2007-WORM	Atlantic bluefin tuna	Thunnus thynnus	Perciformes	VPA
ICCAT-BIGEYEATL-1950-2005-JENSEN	Bigeye tuna	Thunnus obesus	Perciformes	ASPIC
ICCAT-SWORDNATL-1978-2007-JENSEN	Swordfish	Xiphias gladius	Perciformes	ASPIC
ICCAT-YFINATL-1970-2006-JENSEN	Yellowfin tuna	Thunnus albacares	Perciformes	VPA
IMARPE-PANCHPERUNC-1963-2004-RICARD	Peruvian anchoveta	Engraulis ringens	Clupeiformes	VPA
INIDEP-ARGANCHONARG-1989-2007-Parma	Argentine anchoita	Engraulis anchoita	Clupeiformes	ADAPT
INIDEP-ARGANCHOSARG-1992-2007-Parma	Argentine anchoita	Engraulis anchoita	Clupeiformes	ASPM
INIDEP-ARGHAKENARG-1985-2007-Parma	Argentine hake	Merluccius hubbsi	Gadiformes	VPA
INIDEP-ARGHAKESARG-1985-2008-Parma	Argentine hake	Merluccius hubbsi	Gadiformes	VPA
INIDEP-PATGRENADIERSARG-1983-2006-Parma	Patagonian grenadier	Macruronus magellanicus	Gadiformes	VPA
INIDEP-SBWHITARGS-1985-2007-Parma	Southern blue whiting	Micromesistius australis	Gadiformes	VPA
IPHC-PHALNPAC-1988-2009-Parma	Pacific halibut	Hippoglossus stenolepis	Pleuronectiformes	AD-CAM
MARAM-ANCHOSA-1984-2006-deMoor	Anchovy	Engraulis encrasicolus	Clupeiformes	SCA
MARAM-CHAKESA-1917-2008-DEDECKER	Shallow-water cape hake	Merluccius capensis	Gadiformes	ASPM
MARAM-CTRACSA-1950-2007-Johnston	Cape horse mackerel	Trachurus capensis	Perciformes	ASPM
MARAM-DEEPCHAKESA-1917-2008-DEDECKER	Deep-water cape hake	Merluccius paradoxus	Gadiformes	ASPM

Table A.1: Stocks used in the analysis, including scientific name, common name, order, stock ID, and assessment method.

Stock ID	Common Name	Scientific Name	Order	Assess Method
MARAM-SARDSA-1984-2006-deMoor	Sardine	Sardinops sagax	Clupeiformes	SCA
NAFO-SC-AMPL3LNO-1955-2007-BAUM	American plaice	Hippoglossoides platessoides	Pleuronectiformes	VPA
NAFO-SC-AMPL3M-1960-2007-BAUM	American plaice	Hippoglossoides platessoides	Pleuronectiformes	XSA
NAFO-SC-COD3M-1959-2008-BAUM	Atlantic cod	Gadus morhua	Gadiformes	hybrid
NAFO-SC-COD3NO-1953-2007-BAUM	Atlantic cod	Gadus morhua	Gadiformes	SPA
NAFO-SC-GHAL23KLMNO-1960-2006-PREFONTAINE	Greenland halibut	Reinhardtius hippoglossoides	Pleuronectiformes	XSA
NAFO-SC-REDFISHSPP3M-1985-2006-PREFONTAINE	Sebastes species	Sebastes spp	Scorpaeniformes	XSA
NEFSC-ACADREDGOMGB-1913-2007-MILLER	Acadian redfish	Sebastes fasciatus	Scorpaeniformes	ASAP
NEFSC-AMPL5YZ-1960-2008-OBRIEN	American plaice	Hippoglossoides platessoides	Pleuronectiformes	ADAPT
NEFSC-BLUEFISHATLC-1981-2007-SHEPHERD	Bluefish	Pomatomus saltatrix	Perciformes	ASAP
NEFSC-BSBASSMATLC-1968-2007-SHEPHERD	Black sea bass	Centropristis striata	Perciformes	SCALE
NEFSC-CODGB-1960-2008-BAUM	Atlantic cod	Gadus morhua	Gadiformes	ADAPT
NEFSC-CODGOM-1893-2008-BAUM	Atlantic cod	Gadus morhua	Gadiformes	ADAPT
NEFSC-HAD5Y-1956-2008-BAUM	Haddock	Melanogrammus aeglefinus	Gadiformes	NFT-ADAPT
NEFSC-HADGB-1930-2008-BAUM	Haddock	Melanogrammus aeglefinus	Gadiformes	NFT-ADAPT
NEFSC-HERRNWATLC-1960-2005-OVERHOLTZ	Herring	Clupea harengus	Clupeiformes	AD-CAM
NEFSC-MACKGOMCHATT-1960-2005-OVERHOLTZ	Mackerel	Scomber scombrus	Perciformes	VPA
NEFSC-SCUPNWATLC-1960-2007-TERCEIRO	Scup	Stenotomus chrysops	Perciformes	ASAP
NEFSC-SFLOUNMATLC-1940-2007-BAUM	Summer flounder	Paralichthys dentatus	Pleuronectiformes	ASAP
NEFSC-STRIPEDBASSGOMCHATT-1982-2006-SHEPHERD	Striped bass	Morone saxatilis	Perciformes	AD-CAM
NEFSC-WHAKEGBGOM-1963-2007-SOSEBEE	White hake	Urophycis tenuis	Gadiformes	ASPM
NEFSC-WINFLOUN5Z-1982-2007-HENDRICKSON	Winter flounder	Pseudopleuronectes americanus	Pleuronectiformes	ADAPT
NEFSC-WINFLOUNSNEMATL-1940-2007-TERCEIRO	Winter flounder	Pseudopleuronectes americanus	Pleuronectiformes	NFT-ADAPT
NEFSC-WITFLOUN5Y-1982-2008-WIGLEY	Witch flounder	Glyptocephalus cynoglossus	Pleuronectiformes	VPA
NEFSC-YELLCCODGOM-1935-2008-LEGAULT	Yellowtail flounder	Limanda ferruginea	Pleuronectiformes	VPA
NEFSC-YELLGB-1935-2008-BAUM	Yellowtail flounder	Limanda ferruginea	Pleuronectiformes	VPA
NEFSC-YELLSNEMATL-1935-2008-BAUM	Yellowtail flounder	Limanda ferruginea	Pleuronectiformes	VPA
NIWA-AUSSALMONNZ-1975-2006-JENSEN	Australian salmon	Arripis trutta	Perciformes	CASAL
NWFSC-ARFLOUNDPCOAST-1916-2007-BRANCH	Arrowtooth flounder	Reinhardtius stomias	Pleuronectiformes	SS2

Table A.1: Stocks used in the analysis, including scientific name, common name, order, stock ID, and assessment method.

Stock ID	Common Name	Scientific Name	Order	Assess Method
NWFSC-BGROCKPCOAST-1950-2005-STANTON	Blackgill rockfish	Sebastes melanostomus	Scorpaeniformes	SS2
NWFSC-BLACKROCKNPCOAST-1914-2006-BRANCH	Black rockfish	Sebastes melanops	Scorpaeniformes	SS2
NWFSC-CHILISPCOAST-1892-2007-BRANCH	Chilipepper rockfish	Sebastes goodei	Scorpaeniformes	SS2
NWFSC-CROCKPCOAST-1916-2009-Stachura	Canary rockfish	Sebastes pinniger	Scorpaeniformes	SS2
NWFSC-ESOLEPCOAST-1876-2007-BRANCH	English sole	Parophrys vetulus	Pleuronectiformes	SS2
NWFSC-KELPGREENLINGORECOAST-1979-2005-STANTON	Kelp greenling	Hexagrammos decagrammus	Scorpaeniformes	SS2
NWFSC-PHAKEPCOAST-1966-2008-BRANCH	Pacific hake	Merluccius productus	Gadiformes	SS2
NWFSC-POPERCHPCOAST-1953-2007-BRANCH	Pacific ocean perch	Sebastes alutus	Scorpaeniformes	AD-CAM
NWFSC-PSOLENPCOAST-1910-2005-STANTON	Petrale sole	Eopsetta jordani	Pleuronectiformes	SS2
NWFSC-PSOLESPCOAST-1874-2005-STANTON	Petrale sole	Eopsetta jordani	Pleuronectiformes	SS2
NWFSC-SABLEFPCOAST-1900-2007-BRANCH	Sablefish	Anoplopoma fimbria	Scorpaeniformes	SS2
NWFSC-WROCKPCOAST-1955-2006-BRANCH	Widow rockfish	Sebastes entomelas	Scorpaeniformes	AD-CAM
NWFSC-YTROCKNPCOAST-1967-2005-STANTON	Yellowtail rockfish	Sebastes flavidus	Scorpaeniformes	SS1
NWWG-CODFAPL-1959-2006-MINTO	Atlantic cod	Gadus morhua	Gadiformes	VPA
NWWG-CODICE-1952-2006-MINTO	Atlantic cod	Gadus morhua	Gadiformes	SCA
NWWG-HADFAPL-1955-2006-MINTO	Haddock	Melanogrammus aeglefinus	Gadiformes	VPA
NWWG-HADICE-1977-2007-MINTO	Haddock	Melanogrammus aeglefinus	Gadiformes	VPA
NWWG-POLLFAPL-1958-2006-MINTO	Pollock	Pollachius virens	Gadiformes	VPA
NZMFishDEEPWATER-SMOOTHOREOCR-1979-2006-JENSEN	Smooth oreo	Pseudocyttus maculatus	Zeiformes	CASAL
NZMFishHOKIWG-HOKIENZ-1972-2007-FRANCIS	Hoki	Macruronus novaezelandiae	Gadiformes	CASAL
NZMFishHOKIWG-HOKIWNZ-1972-2007-FRANCIS	Hoki	Macruronus novaezelandiae	Gadiformes	CASAL
NZMFishINSHOREWG-NZSNAPNZ8-1931-2005-JENSEN	New Zealand snapper	Chrysophrys auratus	Perciformes	CASAL
NZMFishINSHOREWG-TREVALLYTRE7-1944-2005-JENSEN	Trevally	Pseudocaranx dentex	Perciformes	CASAL
NZMFishMIDDEPTHSWG-GEMFISHNZ-1952-2007-JENSEN	common gemfish	Rexea solandri	Perciformes	CASAL
NZMFishMIDDEPTHSWG-SBWHITACIR-1979-2006-JENSEN	Southern blue whiting	Micromesistius australis	Gadiformes	CASAL
NZMFishMIDDEPTHSWG-SOUTHHAKECR-1975-2006-JENSEN	Southern hake	Merluccius australis	Gadiformes	CASAL
NZMFishMIDDEPTHSWG-SOUTHHAKESA-1975-2007-JENSEN	Southern hake	Merluccius australis	Gadiformes	CASAL
PFMC-LINGCODNPCOAST-1956-2005-STANTON	Lingcod	Ophiodon elongatus	Scorpaeniformes	SS2
PFMC-LINGCODSPCOAST-1956-2005-STANTON	Lingcod	Ophiodon elongatus	Scorpaeniformes	SS2

Table A.1: Stocks used in the analysis, including scientific name, common name, order, stock ID, and assessment method.

Stock ID	Common Name	Scientific Name	Order	Assess Method
SEFSC-GAGGM-1963-2004-JENSEN	Gag	Mycteroperca microlepis	Perciformes	Unknown
SEFSC-GAGSATLC-1962-2005-JENSEN	Gag	Mycteroperca microlepis	Perciformes	AD-CAM
SEFSC-GRAMBERSATLC-1946-2006-JENSEN	Greater amberjack	Seriola dumerili	Perciformes	SCA
SEFSC-MUTSNAPSATLCGM-1981-2006-JENSEN	Mutton snapper	Lutjanus analis	Perciformes	SCA
SEFSC-RPORGYSATLC-1972-2004-JENSEN	Common seabream	Pagrus pagrus	Perciformes	SCA
SEFSC-RSNAPSATLC-1945-2006-JENSEN	Red snapper	Lutjanus campechanus	Perciformes	SCA
SEFSC-SNOWGROUPSATLC-1961-2002-STANTON	Snowy grouper	Epinephelus niveatus	Perciformes	SCA
SEFSC-SPANMACKSATLC-1950-2008-JENSEN	Spanish mackerel	Scomberomorus maculatus	Perciformes	SCA
SEFSC-TILESATLC-1961-2002-STANTON	Tilefish	Lopholatilus chamaeleonticeps	Perciformes	SCA
SEFSC-YTSNAPSATLC-1962-2001-STANTON	Yellowtail snapper	Ocyurus chrysurus	Perciformes	SCA
SPC-ALBASPAC-1959-2006-JENSEN	Albacore tuna	Thunnus alalunga	Perciformes	MULTIFAN-CL
SPC-BIGEYEWPO-1952-2006-JENSEN	Bigeye tuna	Thunnus obesus	Perciformes	MULTIFAN-CL
SPC-SKJCWPAC-1972-2006-JENSEN	Skipjack tuna	Katsuwonus pelamis	Perciformes	MULTIFAN-CL
SPC-STMARLINSWPO-1950-2003-JENSEN	Striped marlin	Kajikia audax	Perciformes	MULTIFAN-CL
SPC-YFINCWPAC-1952-2005-JENSEN	Yellowfin tuna	Thunnus albacares	Perciformes	MULTIFAN-CL
SPRFMO-CHTRACCH-1950-2010-RICARD	Chilean jack mackerel	Trachurus murphyi	Perciformes	JJM
SWFSC-CALSCORPSCAL-1990-2005-STANTON	California scorpionfish	Scorpaena guttata	Scorpaeniformes	AD-CAM
SWFSC-CMACKPCOAST-1929-2008-PINSKY	Chub mackerel	Scomber japonicus	Perciformes	ASAP
SWFSC-DSOLEPCOAST-1910-2005-STANTON	Dover sole	Microstomus pacificus	Pleuronectiformes	SS2
SWFSC-GOPHERSPCOAST-1965-2005-STANTON	Gopher rockfish	Sebastes carnatus	Scorpaeniformes	SS2
SWFSC-SARDPCOAST-1981-2007-PINSKY	Sardine	Sardinops sagax	Clupeiformes	SS2
SWFSC-SBELLYROCKPCOAST-1950-2005-BRANCH	Shortbelly rockfish	Sebastes jordani	Scorpaeniformes	SS2
SWFSC-STFLOUNNPCOAST-1970-2005-STANTON	Starry flounder	Platichthys stellatus	Pleuronectiformes	SS2
SWFSC-STFLOUNSPCOAST-1970-2005-STANTON	Starry flounder	Platichthys stellatus	Pleuronectiformes	SS2
WGBFAS-CODBA2224-1969-2007-JENNINGS	Atlantic cod	Gadus morhua	Gadiformes	XSA
WGBFAS-CODBA2532-1964-2007-JENNINGS	Atlantic cod	Gadus morhua	Gadiformes	XSA
WGBFAS-CODKAT-1970-2006-MINTO	Atlantic cod	Gadus morhua	Gadiformes	B-ADAPT
WGBFAS-HERR2532-1973-2006-JENNINGS	Herring	Clupea harengus	Clupeiformes	XSA
WGBFAS-HERR30-1972-2007-JENNINGS	Herring	Clupea harengus	Clupeiformes	XSA

Table A.1: Stocks used in the analysis, including scientific name, common name, order, stock ID, and assessment method.

Stock ID	Common Name	Scientific Name	Order	Assess Method
WGBFAS-HERR31-1979-2006-JENNINGS	Herring	Clupea harengus	Clupeiformes	XSA
WGBFAS-HERRIsum-1983-2007-JENNINGS	Herring	Clupea harengus	Clupeiformes	NFT-ADAPT
WGBFAS-HERRRIGA-1976-2007-JENNINGS	Herring	Clupea harengus	Clupeiformes	XSA
WGBFAS-SOLEIIIa-1982-2007-JENNINGS	common European sole	Solea vulgaris	Pleuronectiformes	XSA
WGBFAS-SPRAT22-32-1973-2007-JENNINGS	Sprat	Sprattus sprattus	Clupeiformes	XSA
WGHMM-FMEG8c9a-1986-2006-JENNINGS	Fourspotted megrim	Lepidorhombus boscii	Pleuronectiformes	XSA
WGHMM-HAKENRTN-1977-2007-JENNINGS	Hake	Merluccius merluccius	Gadiformes	XSA
WGHMM-HAKESOTH-1982-2007-JENNINGS	Hake	Merluccius merluccius	Gadiformes	XSA
WGHMM-MEG8c9a-1985-2007-JENNINGS	Megrim	Lepidorhombus whiffiagonis	Pleuronectiformes	XSA
WGHMM-SOLEVIII-1982-2006-JENNINGS	common European sole	Solea vulgaris	Pleuronectiformes	XSA
WGMHSA-MACKNEICES-1972-2007-JENNINGS	Mackerel	Scomber scombrus	Perciformes	ICA
WGMHSA-SARDPVIIIc-IXa-1978-2007-JENNINGS	European pilchard	Sardina pilchardus	Clupeiformes	AMCI
WGNPBW-BWHITNEA-1980-2007-JENNINGS	Blue whiting	Micromesistius poutassou	Gadiformes	SMS
WGNSDS-CODIS-1968-2006-MINTO	Atlantic cod	Gadus morhua	Gadiformes	B-ADAPT
WGNSDS-CODVIa-1977-2006-MINTO	Atlantic cod	Gadus morhua	Gadiformes	TSA
WGNSDS-HADVIa-1977-2006-MINTO	Haddock	Melanogrammus aeglefinus	Gadiformes	TSA
WGNSDS-PLAICIS-1962-2006-MINTO	European Plaice	Pleuronectes platessa	Pleuronectiformes	ICA
WGNSDS-SOLEIS-1968-2006-MINTO	common European sole	Solea vulgaris	Pleuronectiformes	XSA
WGNSSK-CODNS-1962-2007-MINTO	Atlantic cod	Gadus morhua	Gadiformes	B-ADAPT
WGNSSK-HADNS-IIIa-1963-2006-MINTO	Haddock	Melanogrammus aeglefinus	Gadiformes	XSA
WGNSSK-HADROCK-1990-2007-JENNINGS	Haddock	Melanogrammus aeglefinus	Gadiformes	XSA
WGNSSK-NPOUTNS-1983-2007-MINTO	Norway Pout	Trisopterus esmarkii	Gadiformes	XSA
WGNSSK-PLAIC7d-1979-2006-MINTO	European Plaice	Pleuronectes platessa	Pleuronectiformes	XSA
WGNSSK-PLAICIIIa-1976-2006-MINTO	European Plaice	Pleuronectes platessa	Pleuronectiformes	XSA
WGNSSK-PLAICNS-1956-2006-MINTO	European Plaice	Pleuronectes platessa	Pleuronectiformes	XSA
WGNSSK-POLLNS-VI-IIIa-1964-2006-MINTO	Pollock	Pollachius virens	Gadiformes	XSA
WGNSSK-SEELNS-1983-2007-MINTO	Sand eel	Ammodytes marinus	Perciformes	XSA
WGNSSK-SOLENS-1956-2006-MINTO	common European sole	Solea vulgaris	Pleuronectiformes	XSA
WGNSSK-SOLEVIId-1981-2006-MINTO	common European sole	Solea vulgaris	Pleuronectiformes	XSA

Table A.1: Stocks used in the analysis, including scientific name, common name, order, stock ID, and assessment method.

Stock ID	Common Name	Scientific Name	Order	Assess Method
WGNSSK-WHITNS-VIId-IIIa-1979-2006-MINTO	Whiting	Merlangius merlangus	Gadiformes	XSA
WGSSDS-HADVIIb-k-1993-2006-JENNINGS	Haddock	Melanogrammus aeglefinus	Gadiformes	XSA
WGSSDS-PLAICCELT-1976-2006-JENNINGS	European Plaice	Pleuronectes platessa	Pleuronectiformes	XSA
WGSSDS-PLAICECHW-1975-2006-JENNINGS	European Plaice	Pleuronectes platessa	Pleuronectiformes	XSA
WGSSDS-SOLECS-1970-2006-JENNINGS	common European sole	Solea vulgaris	Pleuronectiformes	XSA
WGSSDS-SOLEVIIe-1968-2006-JENNINGS	common European sole	Solea vulgaris	Pleuronectiformes	XSA
WGSSDS-WHITVIIek-1982-2007-JENNINGS	Whiting	Merlangius merlangus	Gadiformes	XSA

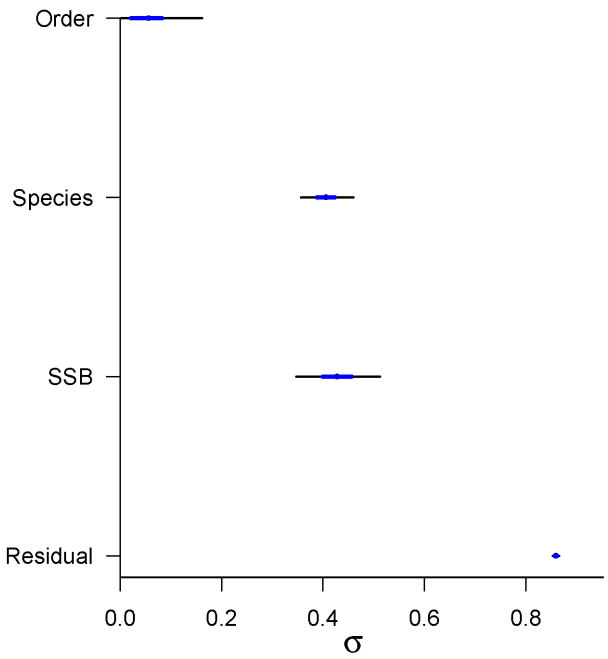

Figure A.1: The variance explained (σ) by the fixed effect (γ_{ssb}), random effects ($\delta_{ssb,species}, \eta_{ssb,order}$), and residual error ($\epsilon_i$) terms in the hierarchical model. Analysis excluding statistical catch at age data (non-SCA analysis).

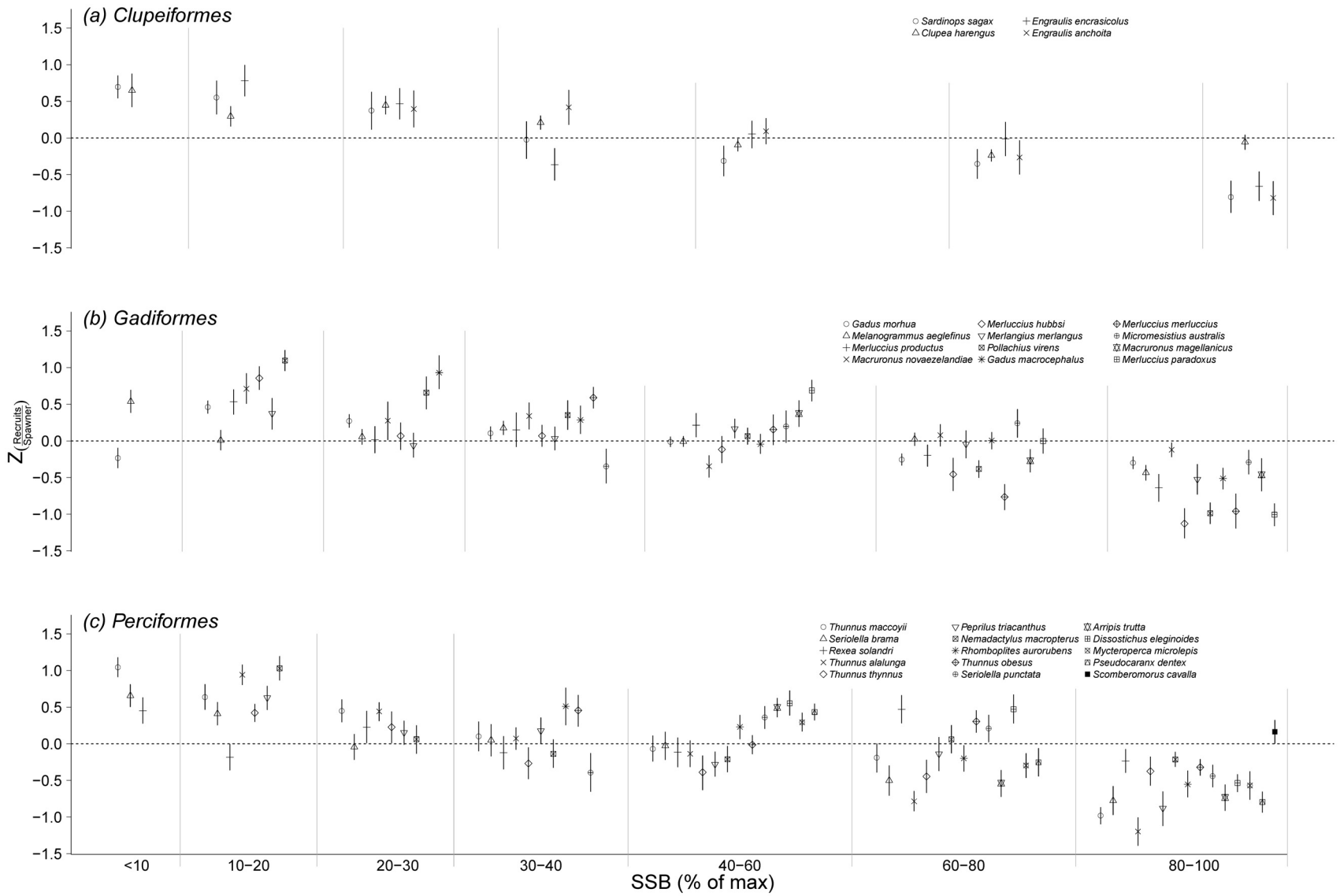

Figure A.2a: Estimated model coefficients of the term $\delta_{ssb,species} + \gamma_{ssb}$ with 50% Bayesian credible intervals sorted by order. a: Clupeiformes, b: Gadiformes, c: Perciformes, d: Pleuronectiformes, e: Scorpaeniformes. This figure excludes the orders for which there is data for 2 or fewer species (i.e. the Beryciformes and Zeiformes). Analysis excluding statistical catch at age data (non-SCA analysis).

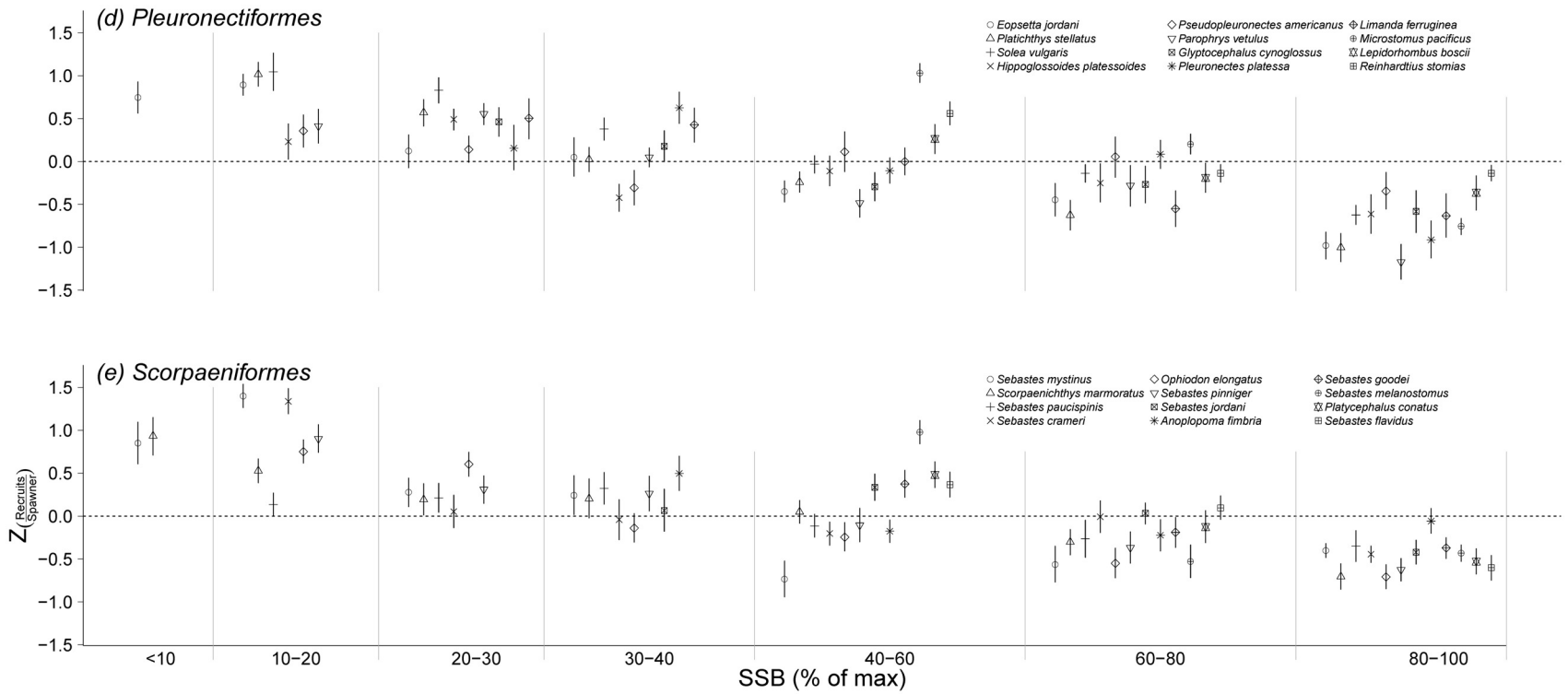

Figure A.2b: Estimated model coefficients of the term $\delta_{ssb,species} + \gamma_{ssb}$ with 50% Bayesian credible intervals sorted by order. a: Clupeiformes, b: Gadiformes, c: Perciformes, d: Pleuronectiformes, e: Scorpaeniformes. This figure excludes the orders for which there is data for 2 or fewer species (i.e. the Beryciformes and Zeiformes). Analysis excluding statistical catch at age data (non-SCA analysis).

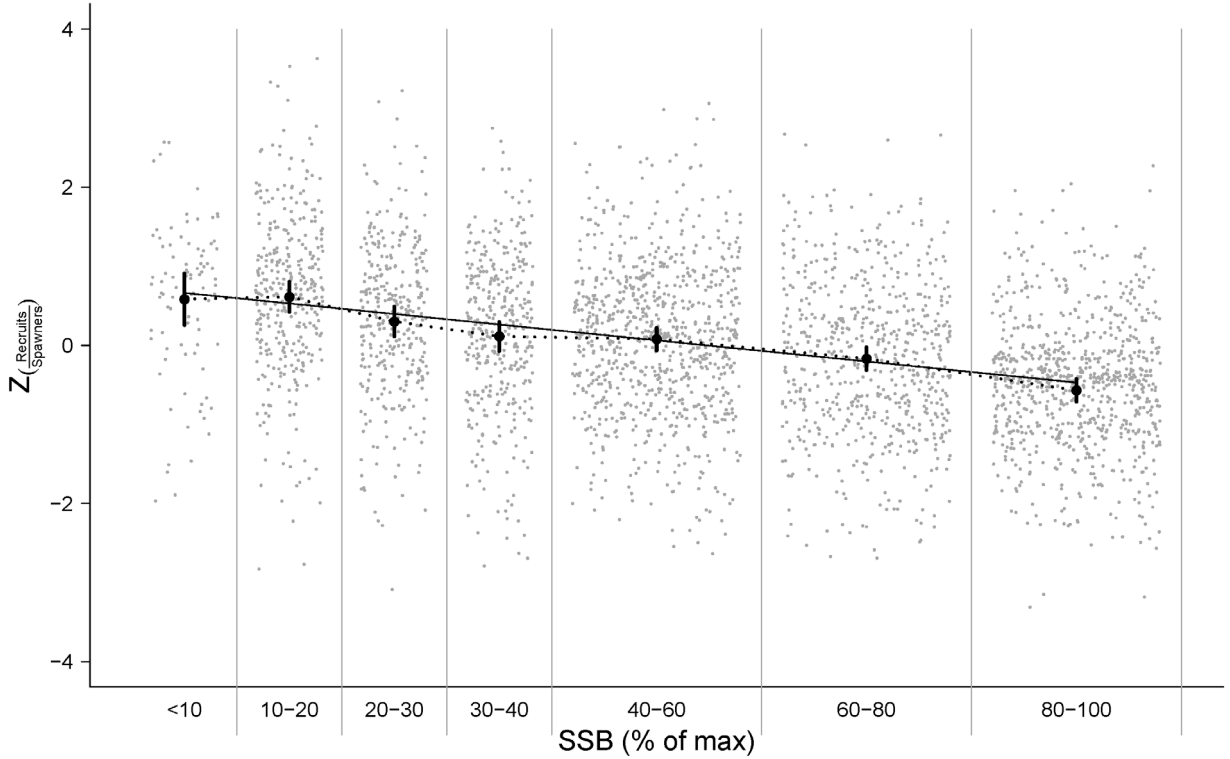

Figure A.3: Modelled relationship between $Z_{\ln\left(\frac{Rec}{SSB}\right)}$ and SSB. Grey points represent individual data points. Model means with 95% Bayesian credible intervals connected with dotted line. A Ricker model based on the entire dataset is shown with the solid black line. Analysis excluding statistical catch at age data (non-SCA analysis).

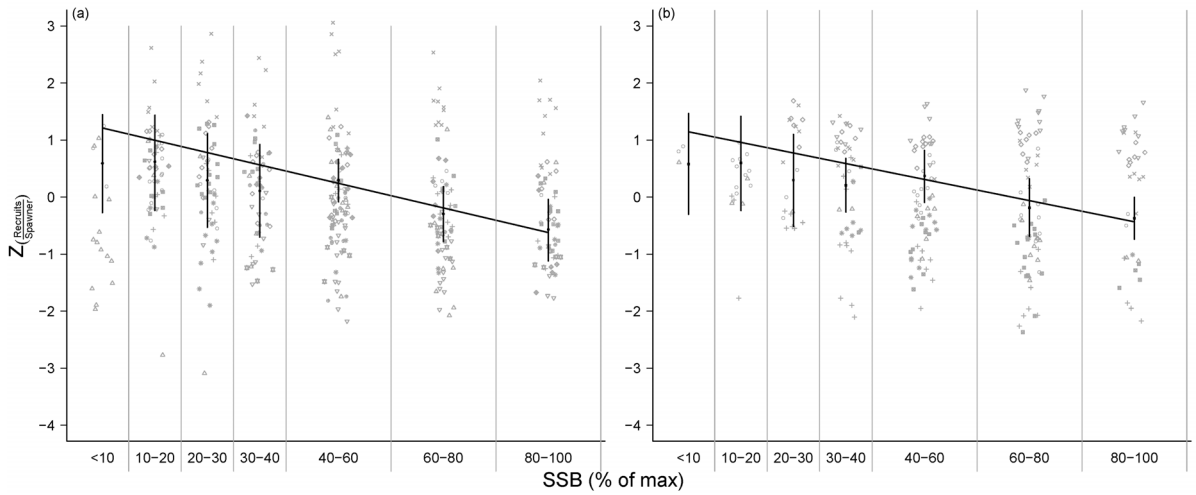

Figure A.4: Estimated model coefficients of the terms $\delta_{ssb,species} + \gamma_{ssb}$ for a: Atlantic cod (*Gadus morhua*) and b: Atlantic herring (*Clupea harengus*). Symbols represent individual data points for individual stocks. Model means with 95% Bayesian credible intervals connected with dotted line. A Ricker model based on the data $> 40\%$ of maximum historic SSB is shown with the solid black line for each species. Analysis excluding statistical catch at age data (non-SCA analysis).

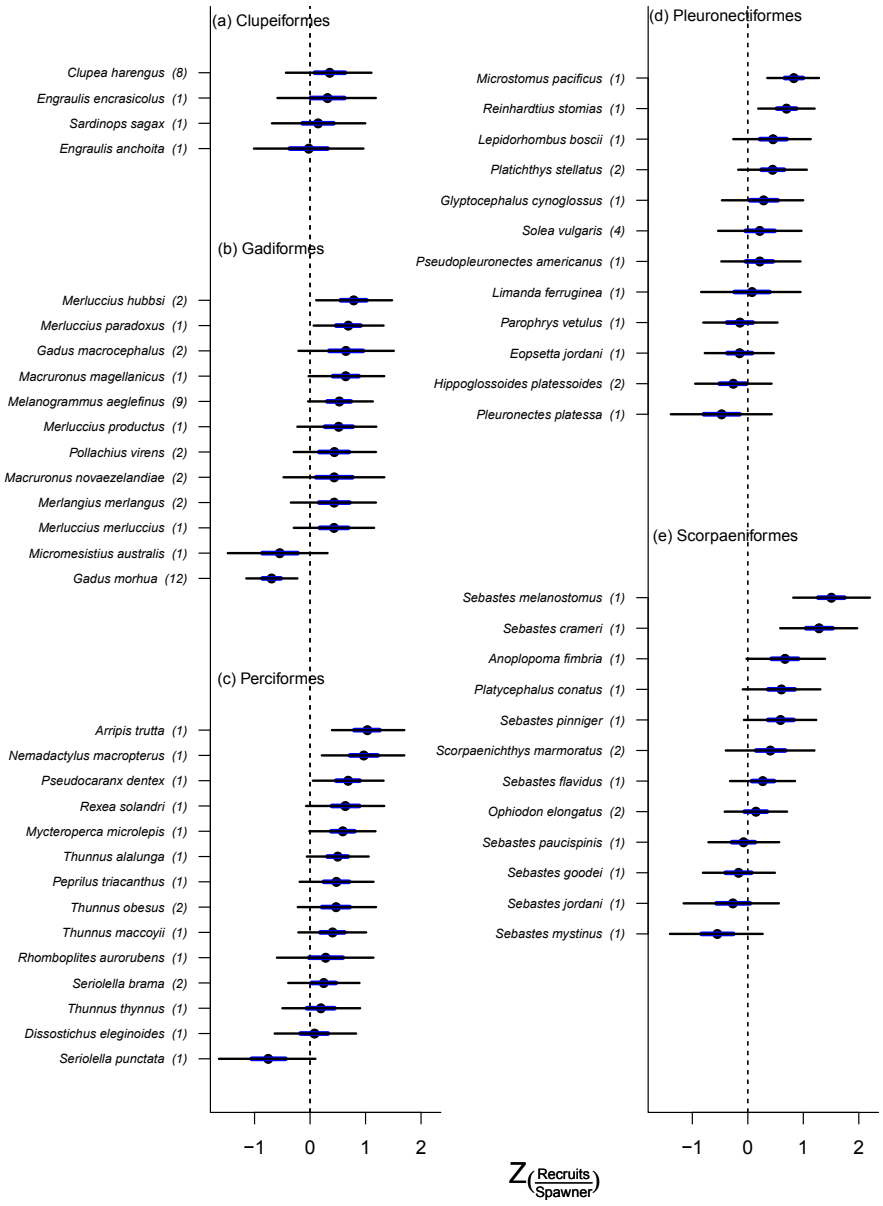

Figure A.5: Contrast of $Z_{\ln\left(\frac{Rec}{SSB}\right)}$ between lowest and second lowest SSB category for each species, sorted by order. Negative values represent a lower $\mathrm{Z}_{\frac{\mathrm{Recruits}}{\mathrm{SSB}}}$ in the lowest SSB category. Thick lines represent 50% Bayesian credible intervals, thin lines represent 95% BCI. a: Clupeiformes, b: Gadiformes, c: Perciformes, d: Pleuronectiformes, e: Scorpaeniformes. Number of stocks included in analysis for each species in brackets after species name. This figure excludes the orders for which there is data for 2 or fewer species (i.e. the Beryciformes and Zeiformes). Analysis excluding statistical catch at age data (non-SCA analysis).

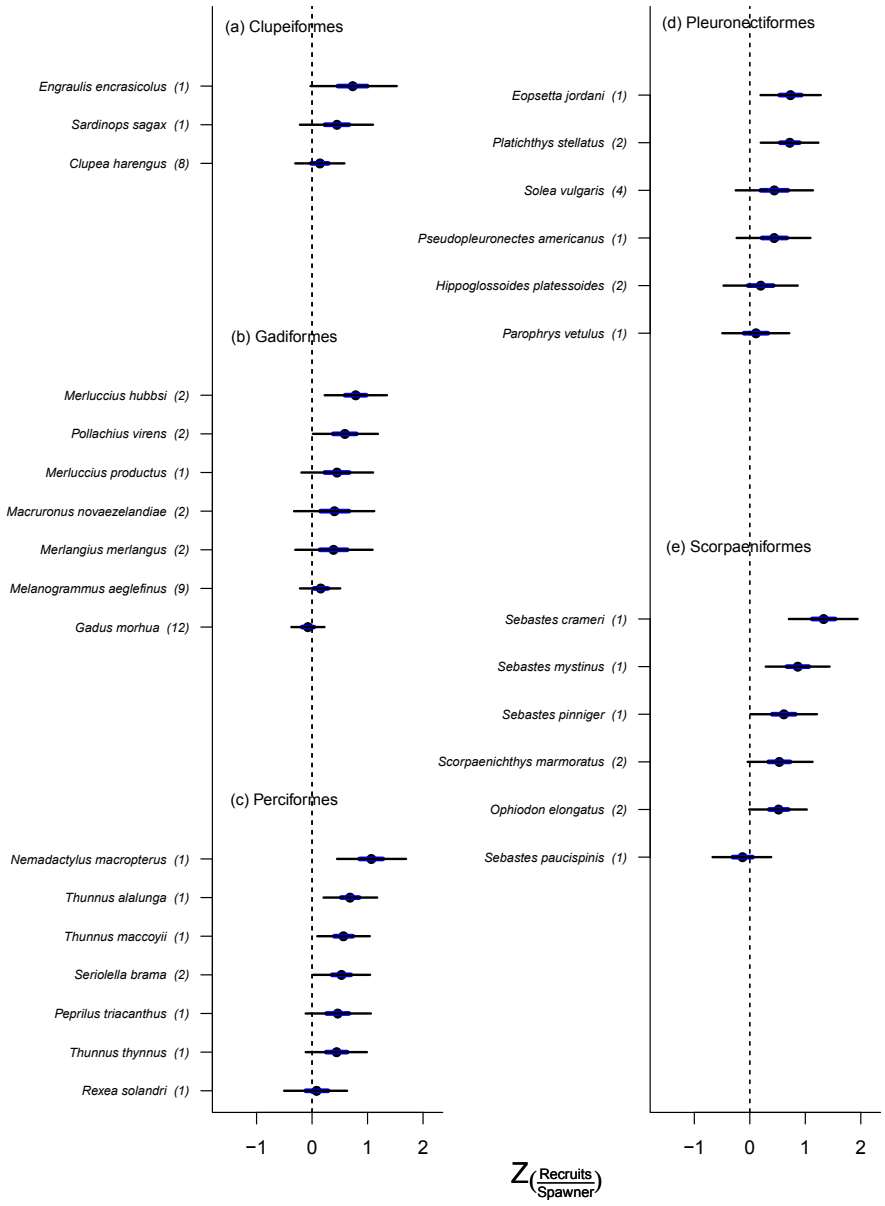

Figure A.6: Contrast of $Z_{\ln\left(\frac{Rec}{SSB}\right)}$ between SSB $< 20\%$ and SSB between 20-40% for each species sorted by order. Negative values represent a lower $Z_{\frac{\text{Recruits}}{\text{SSB}}}$ in the $<$ 20% SSB category. Thick lines represent 50% Bayesian credible intervals, thin lines represent 95% BCI. a: Clupeiformes, b: Gadiformes, c: Perciformes, d: Pleuronectiformes, e: Scorpaeniformes. Number of stocks included in analysis for each species in brackets after species name.This figure excludes the orders for 2 or fewer species (i.e. the Beryciformes and Zeiformes). Analysis excluding statistical catch at age data (non-SCA analysis).

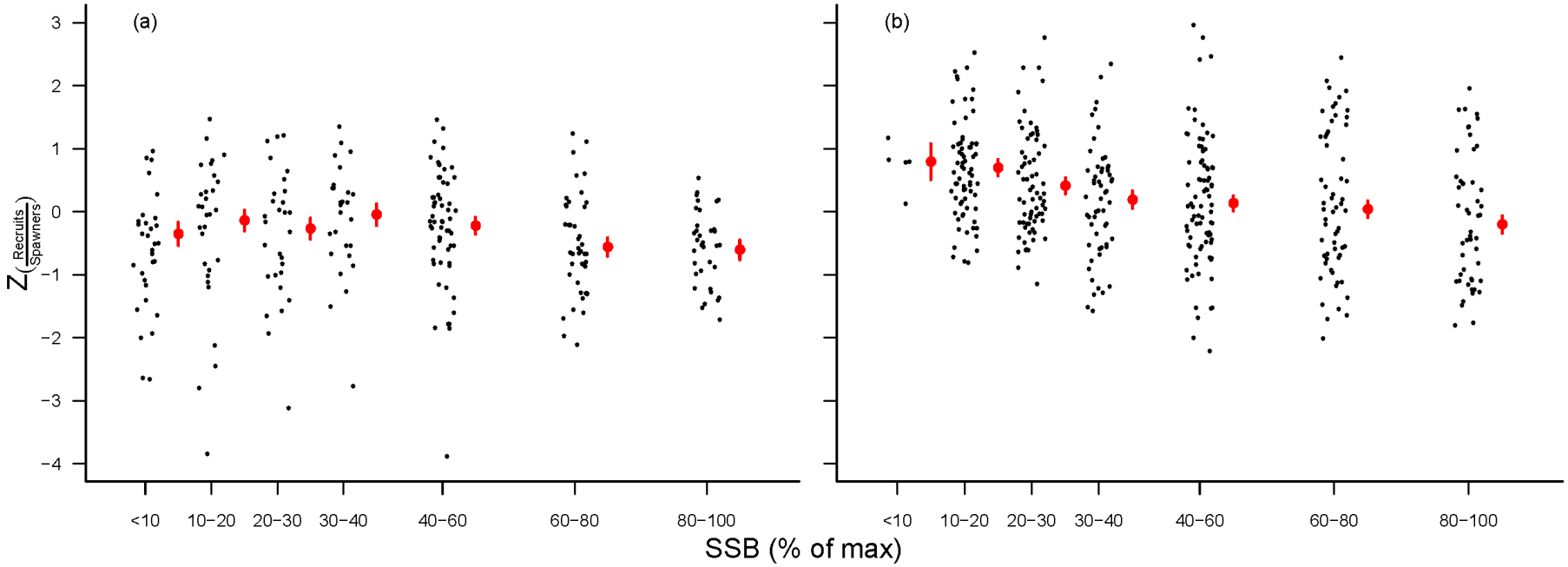

Figure A.7: Modelled relationship between $Z_{\ln\left(\frac{Rec}{SSB}\right)}$ and SSB for (a) Western and (b) Eastern Atlantic cod stocks. Blacks points represent individual data points. Model means with 50% Bayesian credible intervals shown in red.

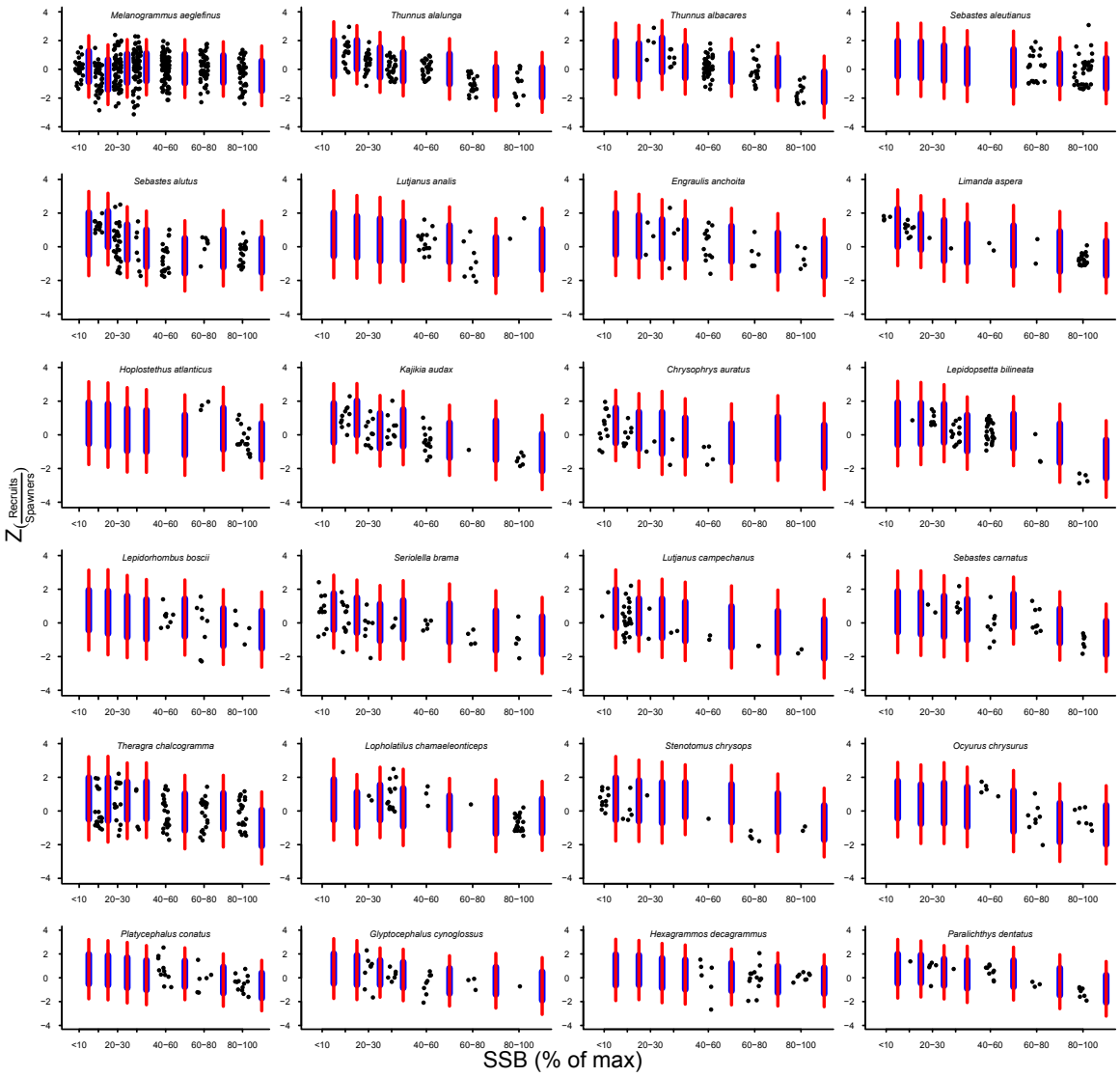

Figure A.8a: Posterior predictive checks (PPC's) were used to visually assess the model fit of the model coefficients of the term $\delta_{ssb,species} + \gamma_{ssb}$ to the raw data for every species in the analysis. Each individual data point is represented by black filled circles. The estimated PPC's include the 50% (thick blue line) and 95% (thin red line) Bayesian credible intervals for each coefficient.

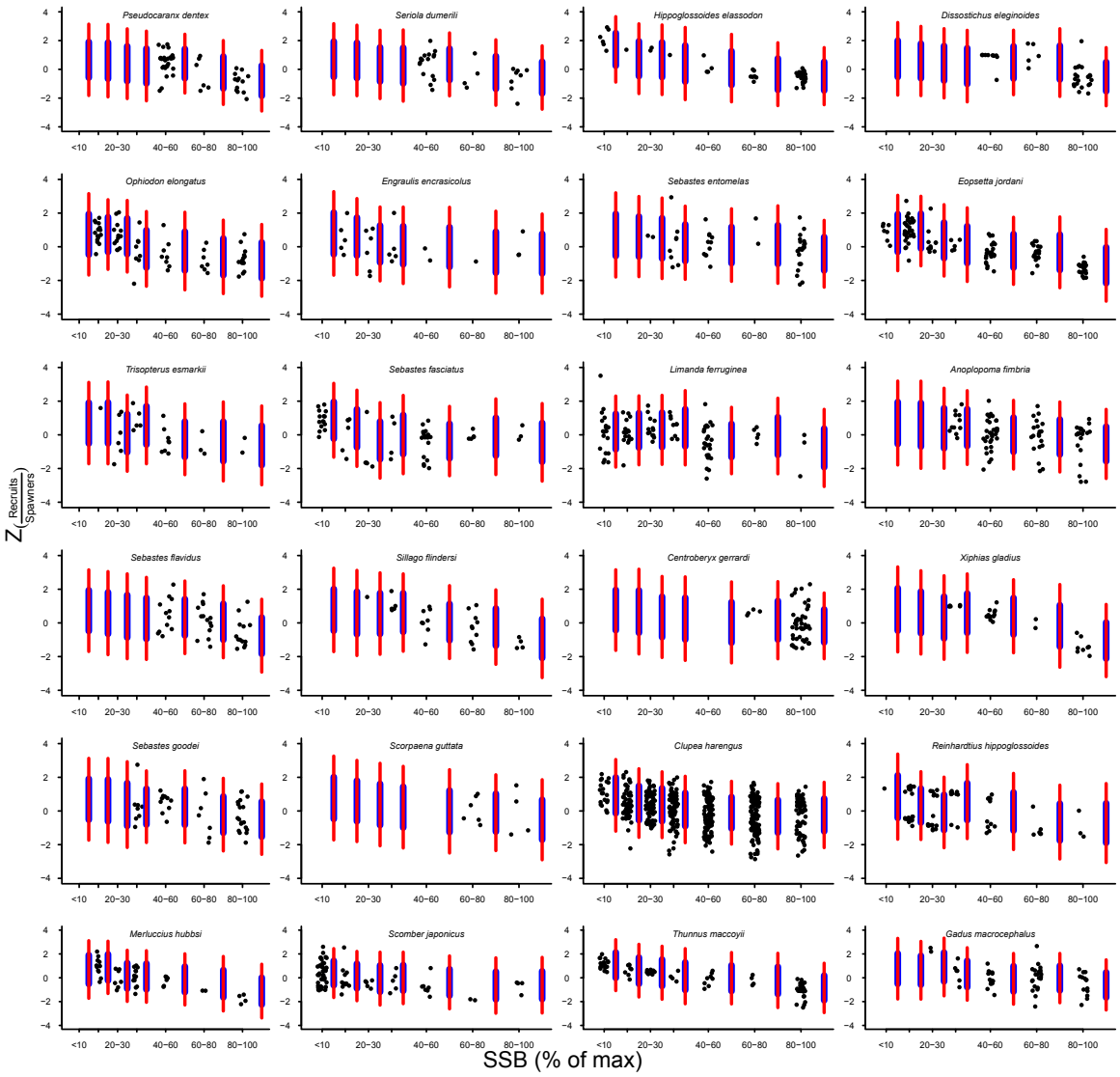

Figure A.8b: Posterior predictive checks (PPC's) were used to visually assess the model fit of the model coefficients of the term $\delta_{ssb,species} + \gamma_{ssb}$ to the raw data for every species in the analysis. Each individual data point is represented by black filled circles. The estimated PPC's include the 50% (thick blue line) and 95% (thin red line) Bayesian credible intervals for each coefficient.

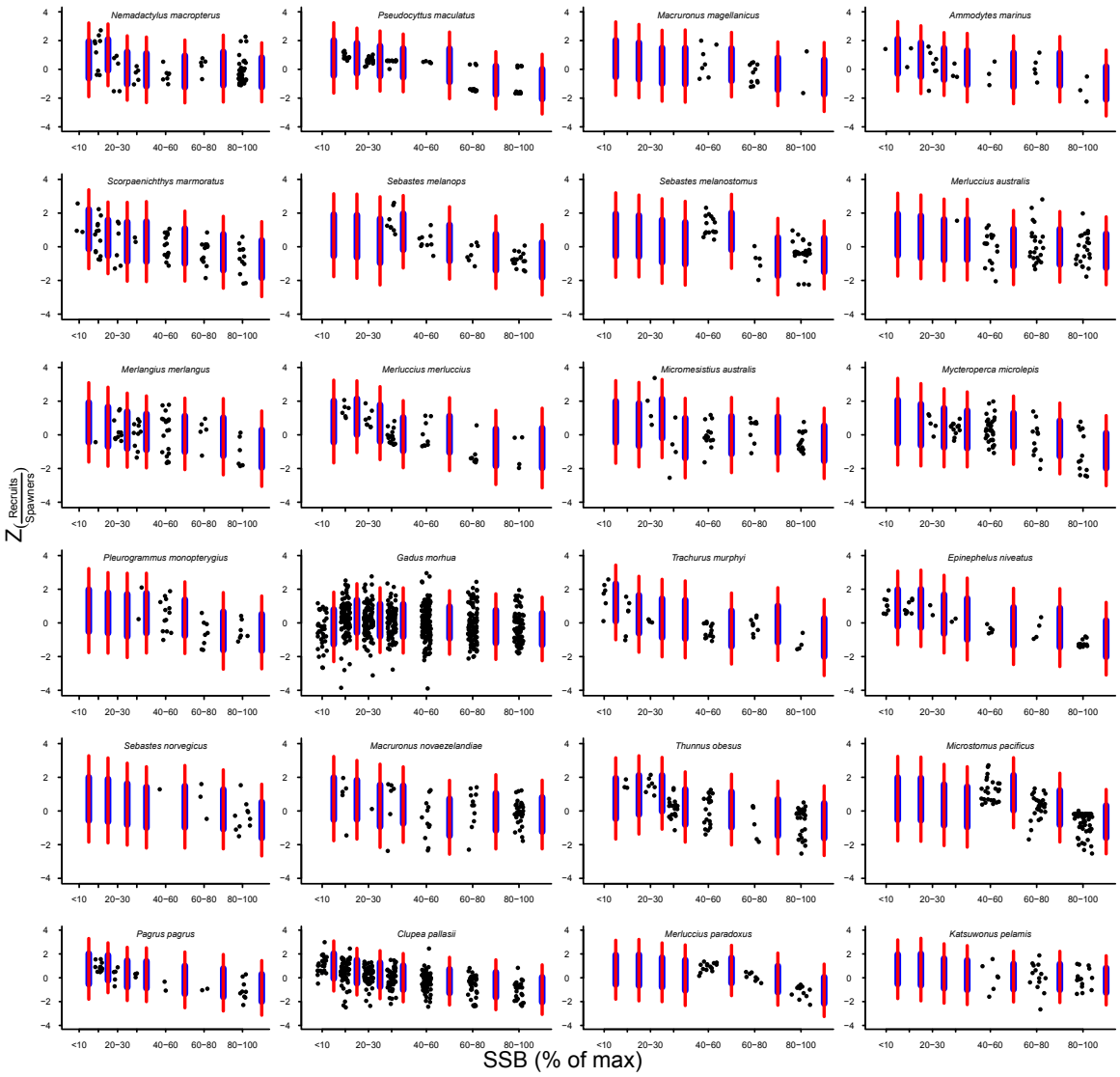

Figure A.8c: Posterior predictive checks (PPC's) were used to visually assess the model fit of the model coefficients of the term $\delta_{ssb,species} + \gamma_{ssb}$ to the raw data for every species in the analysis. Each individual data point is represented by black filled circles. The estimated PPC's include the 50% (thick blue line) and 95% (thin red line) Bayesian credible intervals for each coefficient.

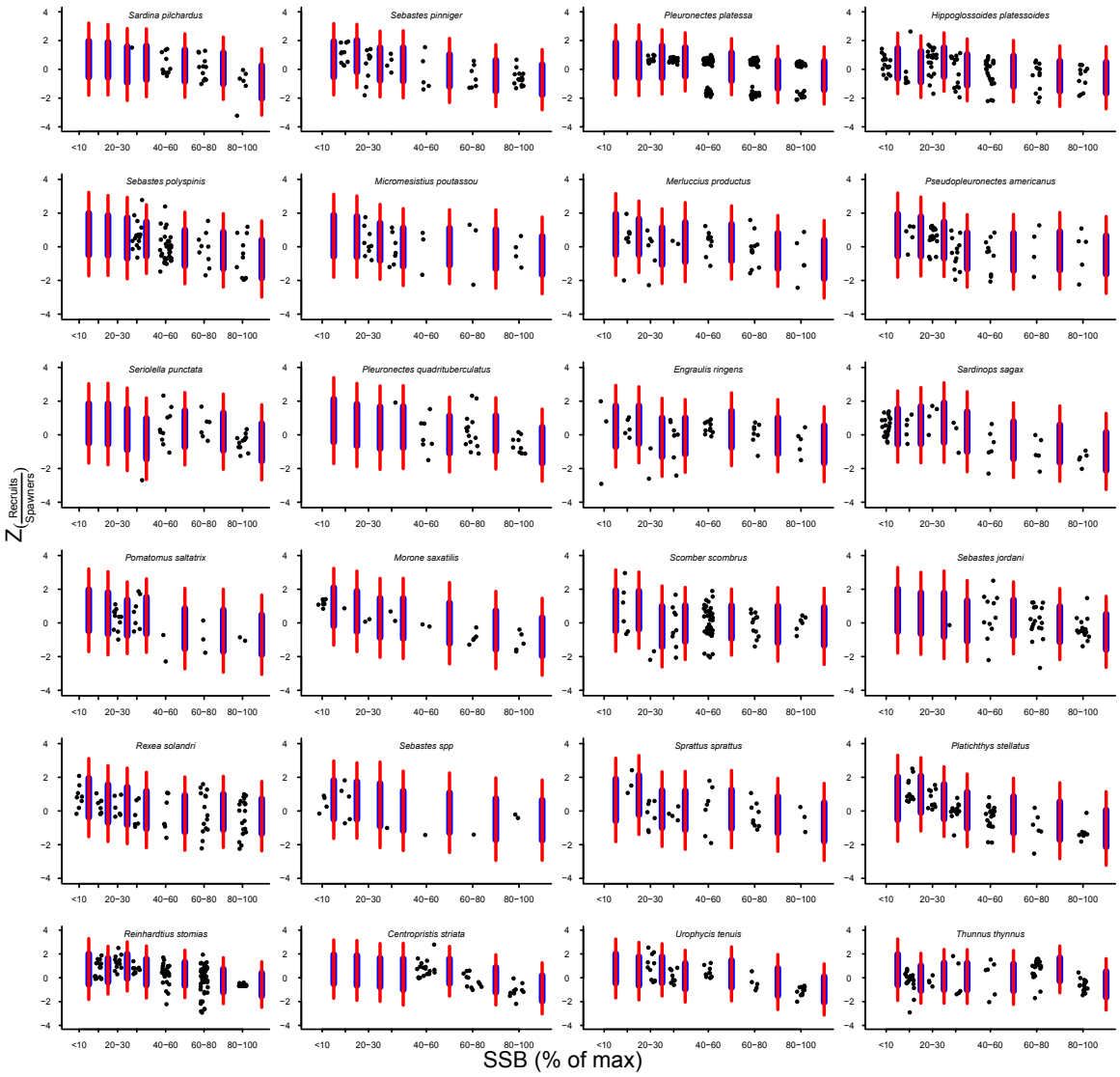

Figure A.8d: Posterior predictive checks (PPC's) were used to visually assess the model fit of the model coefficients of the term $\delta_{ssb,species} + \gamma_{ssb}$ to the raw data for every species in the analysis. Each individual data point is represented by black filled circles. The estimated PPC's include the 50% (thick blue line) and 95% (thin red line) Bayesian credible intervals for each coefficient.

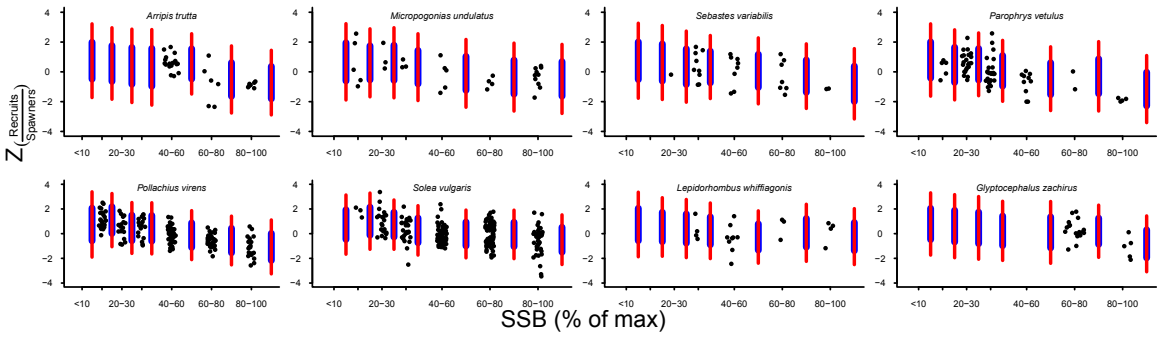

Figure A.8e: Posterior predictive checks (PPC's) were used to visually assess the model fit of the model coefficients of the term $\delta_{ssb,species} + \gamma_{ssb}$ to the raw data for every species in the analysis. Each individual data point is represented by black filled circles. The estimated PPC's include the 50% (thick blue line) and 95% (thin red line) Bayesian credible intervals for each coefficient.

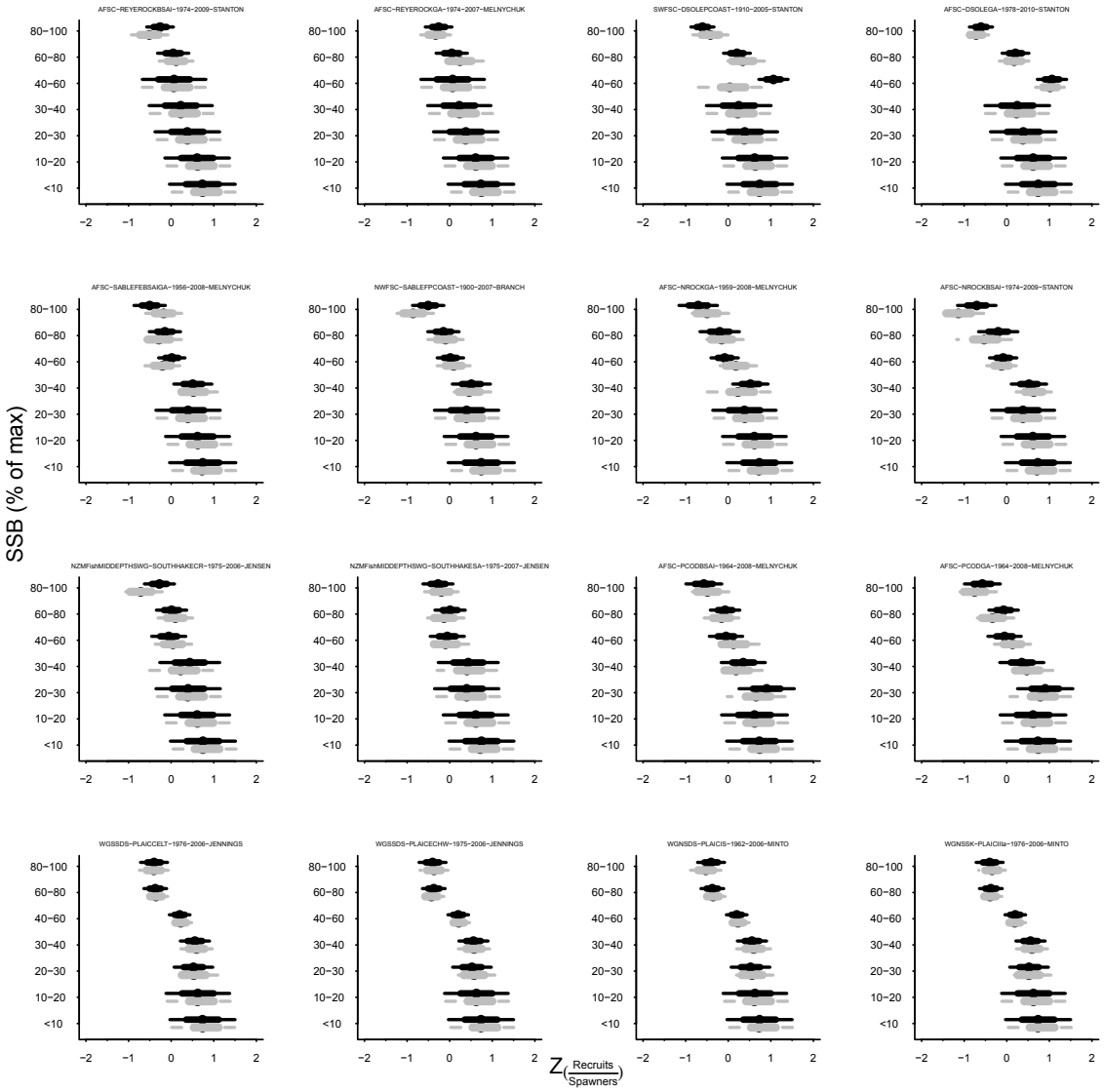

Figure A.9a: Influence of removing a stock from the analysis on the estimated model coefficients of the term $\delta_{ssb,species} + \gamma_{ssb}$ for every species with 2 or more stocks used in the analysis. The black line represent the full model estimate, with 50% (thick line), and 95% (thin line) Bayesian credible intervals. The grey line represents the estimated coefficients with 50% (thick line), and 95% (thin line) Bayesian credible intervals with one stock removed. The ID of the removed stock is given in each panel of the plot.

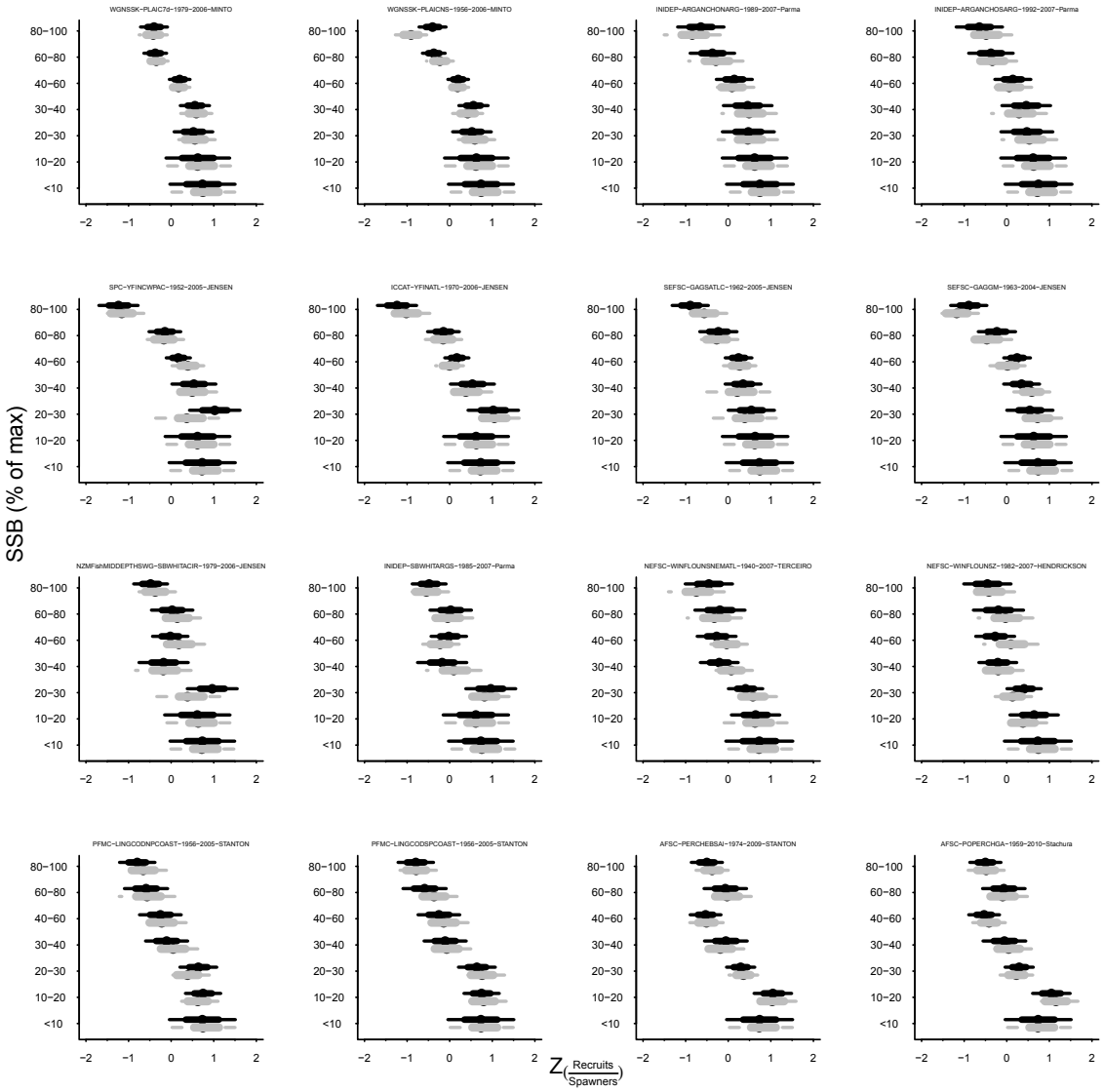

Figure A.9b: Influence of removing a stock from the analysis on the estimated model coefficients of the term $\delta_{ssb,species} + \gamma_{ssb}$ for every species with 2 or more stocks used in the analysis. The black line represent the full model estimate, with 50% (thick line), and 95% (thin line) Bayesian credible intervals. The grey line represents the estimated coefficients with 50% (thick line), and 95% (thin line) Bayesian credible intervals with one stock removed. The ID of the removed stock is given in each panel of the plot.

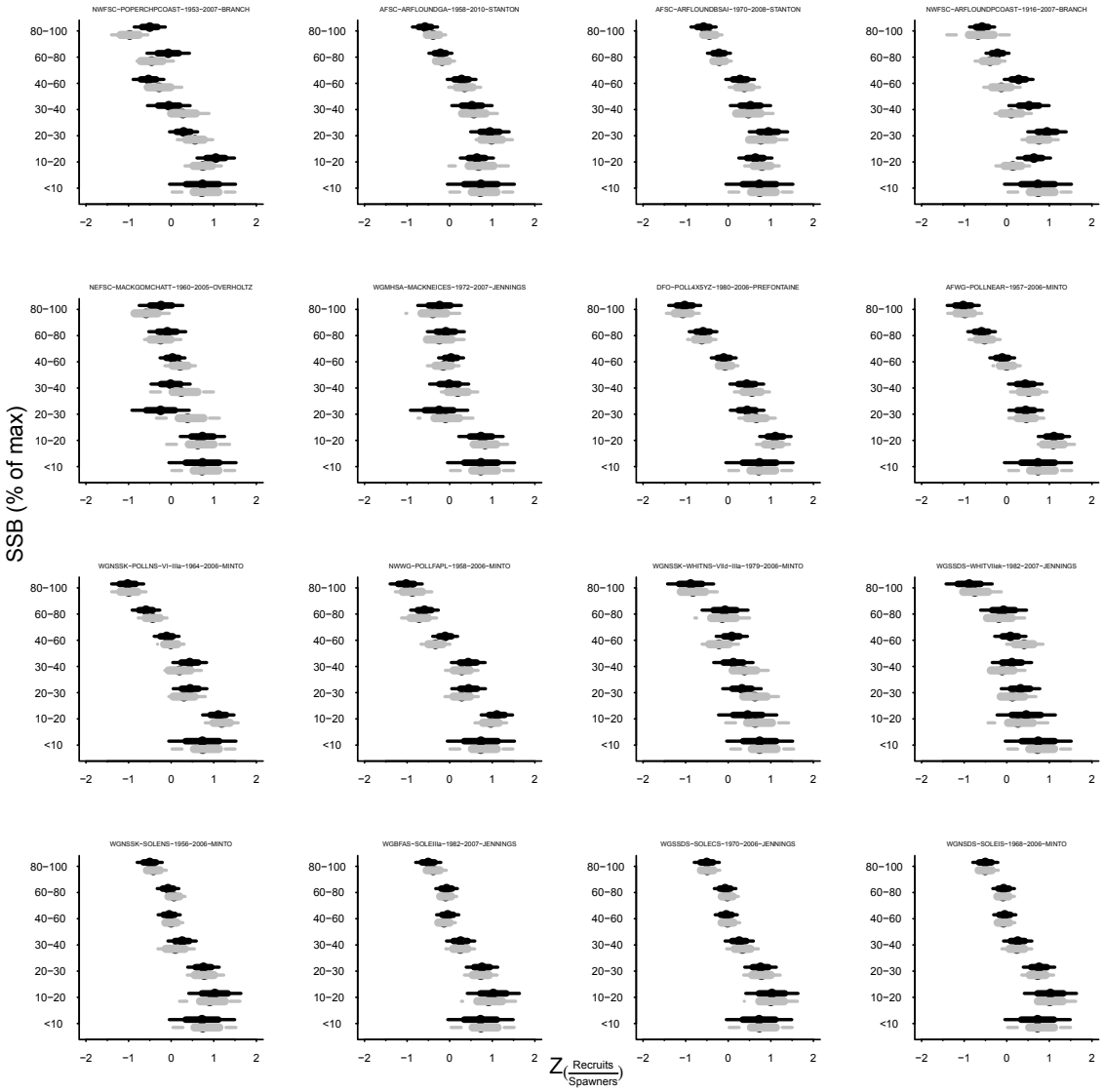

Figure A.9c: Influence of removing a stock from the analysis on the estimated model coefficients of the term $\delta_{ssb,species} + \gamma_{ssb}$ for every species with 2 or more stocks used in the analysis. The black line represent the full model estimate, with 50% (thick line), and 95% (thin line) Bayesian credible intervals. The grey line represents the estimated coefficients with 50% (thick line), and 95% (thin line) Bayesian credible intervals with one stock removed. The ID of the removed stock is given in each panel of the plot.

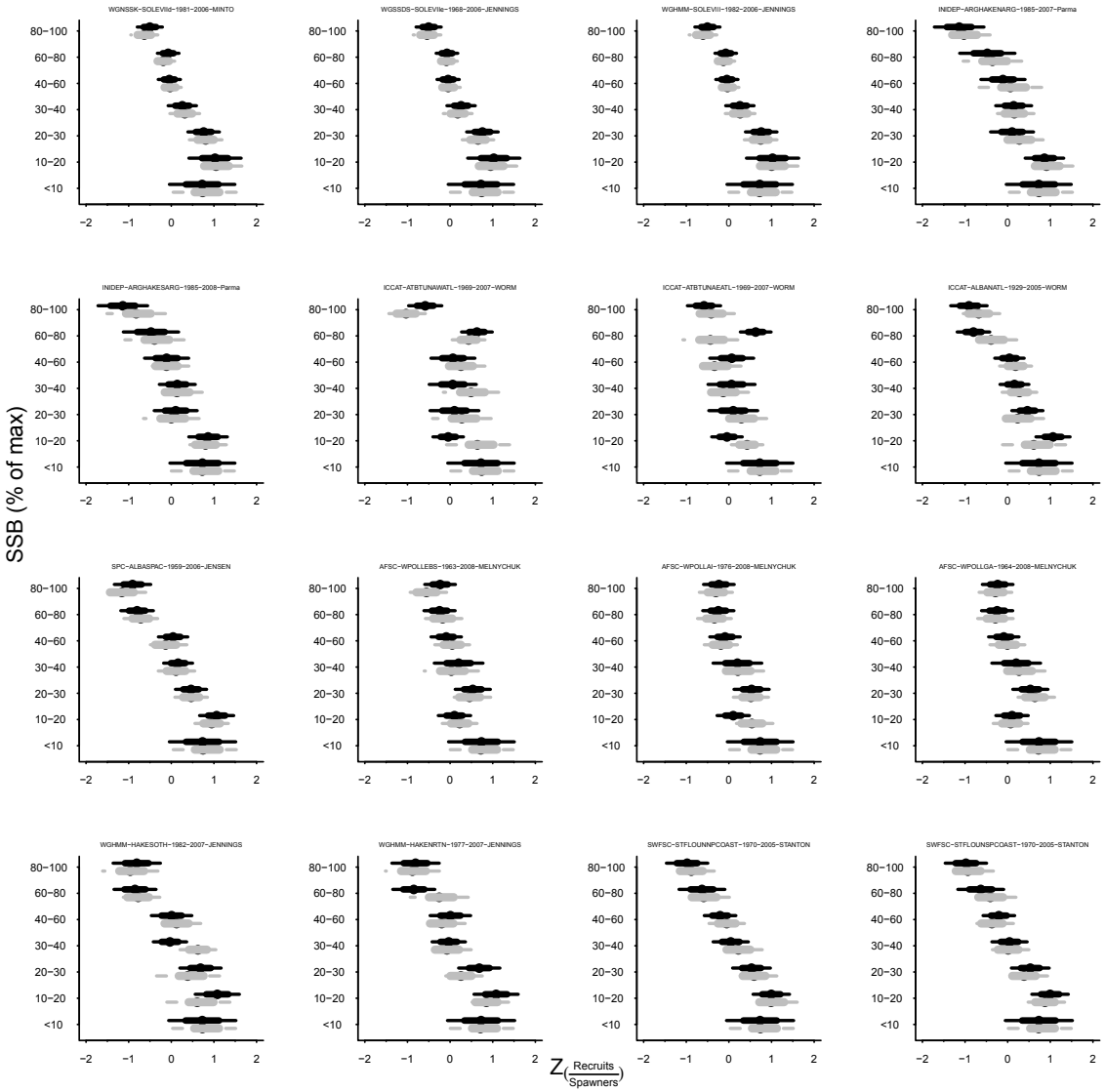

Figure A.9d: Influence of removing a stock from the analysis on the estimated model coefficients of the term $\delta_{ssb,species} + \gamma_{ssb}$ for every species with 2 or more stocks used in the analysis. The black line represent the full model estimate, with 50% (thick line), and 95% (thin line) Bayesian credible intervals. The grey line represents the estimated coefficients with 50% (thick line), and 95% (thin line) Bayesian credible intervals with one stock removed. The ID of the removed stock is given in each panel of the plot.

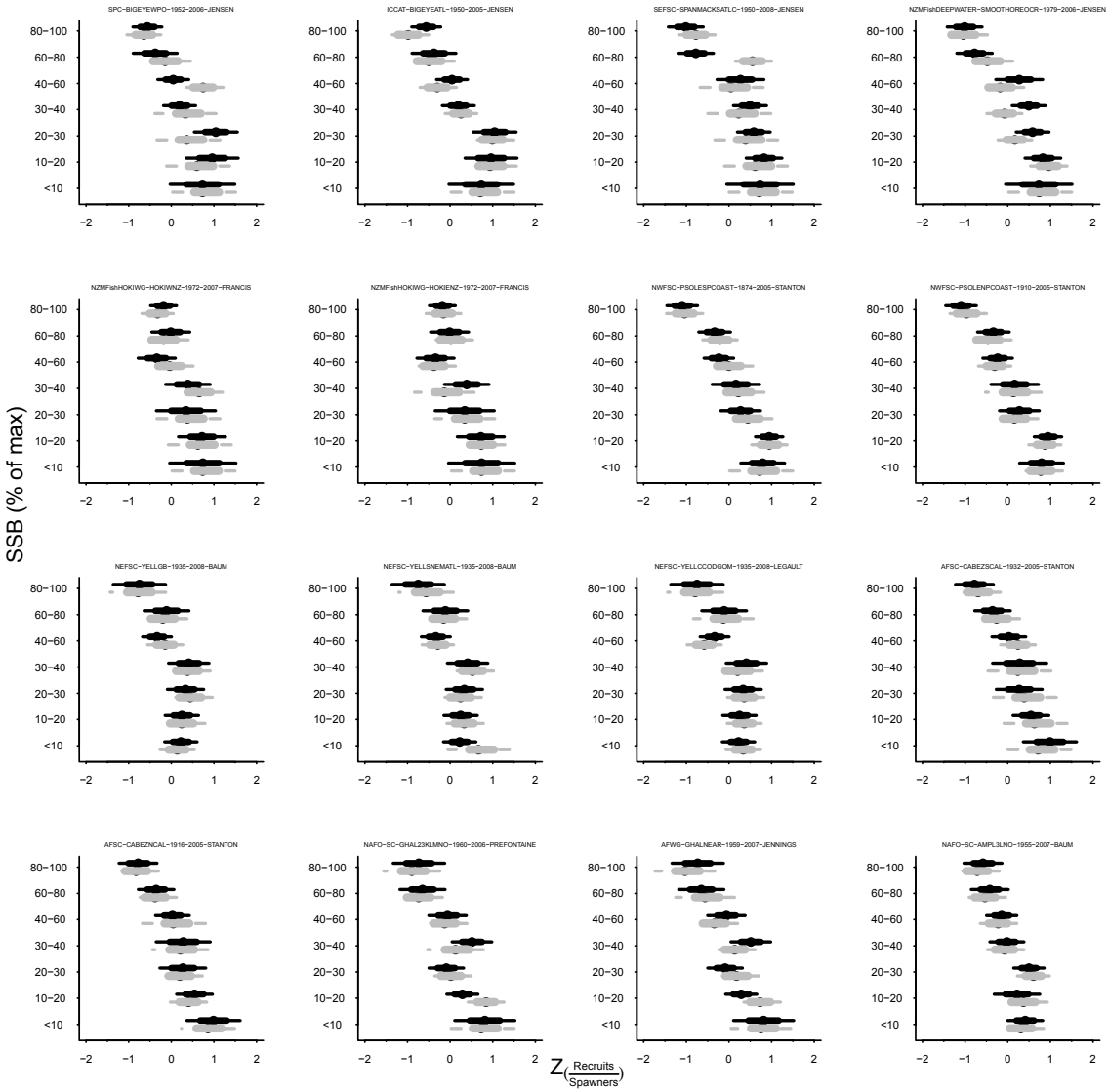

Figure A.9e: Influence of removing a stock from the analysis on the estimated model coefficients of the term $\delta_{ssb,species} + \gamma_{ssb}$ for every species with 2 or more stocks used in the analysis. The black line represent the full model estimate, with 50% (thick line), and 95% (thin line) Bayesian credible intervals. The grey line represents the estimated coefficients with 50% (thick line), and 95% (thin line) Bayesian credible intervals with one stock removed. The ID of the removed stock is given in each panel of the plot.

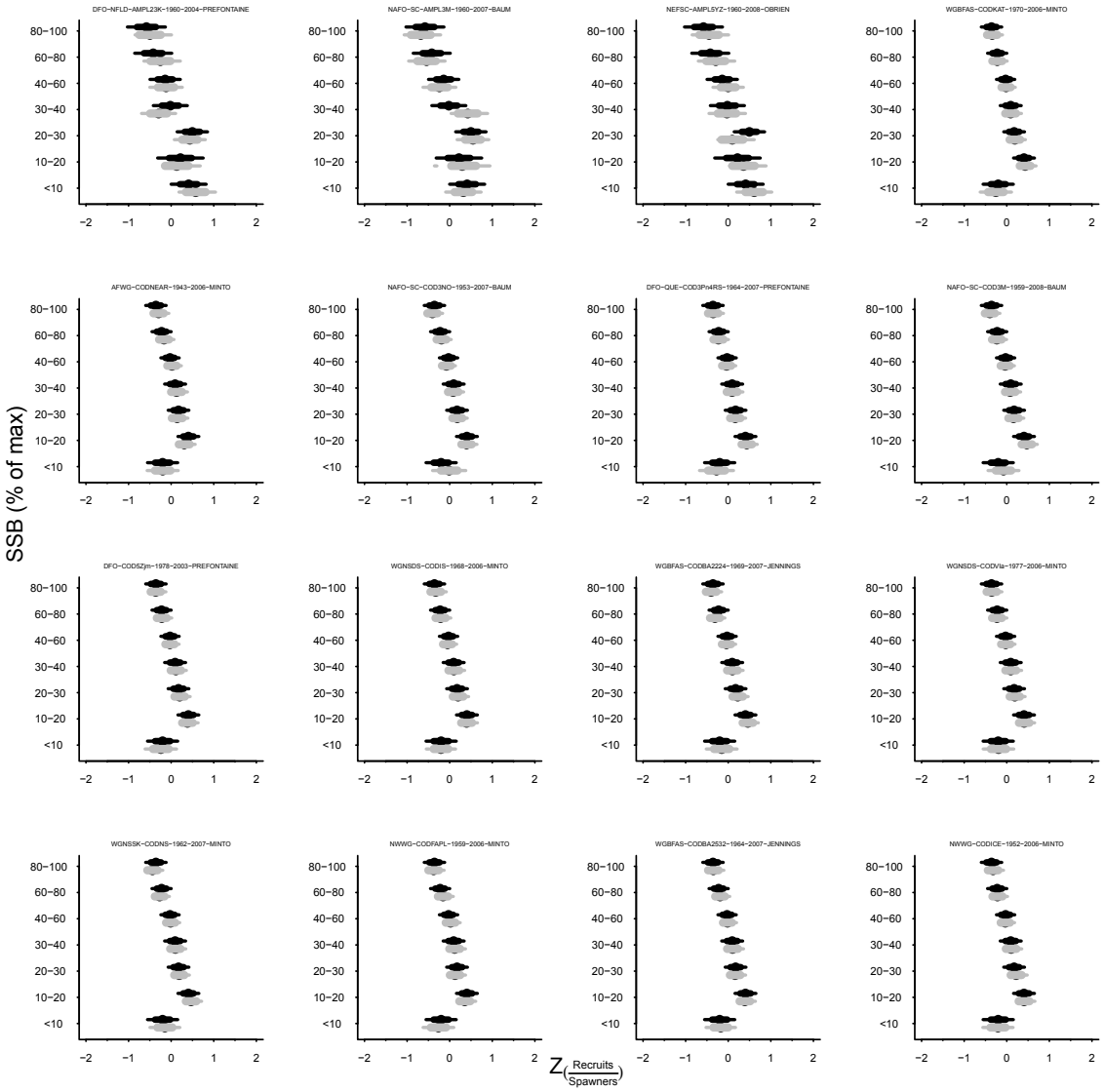

Figure A.9f: Influence of removing a stock from the analysis on the estimated model coefficients of the term $\delta_{ssb,species} + \gamma_{ssb}$ for every species with 2 or more stocks used in the analysis. The black line represent the full model estimate, with 50% (thick line), and 95% (thin line) Bayesian credible intervals. The grey line represents the estimated coefficients with 50% (thick line), and 95% (thin line) Bayesian credible intervals with one stock removed. The ID of the removed stock is given in each panel of the plot.

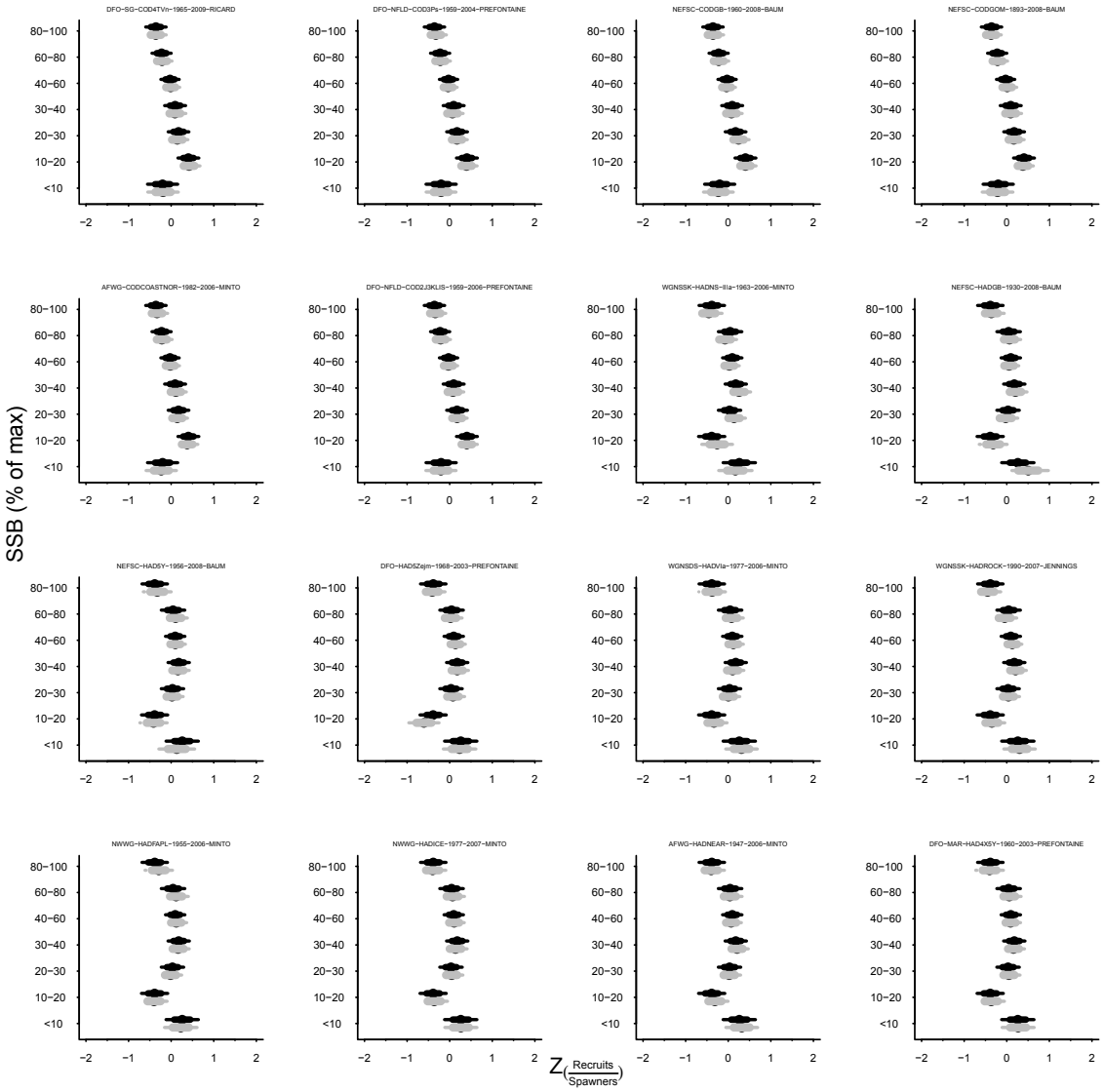

Figure A.9g: Influence of removing a stock from the analysis on the estimated model coefficients of the term $\delta_{ssb,species} + \gamma_{ssb}$ for every species with 2 or more stocks used in the analysis. The black line represent the full model estimate, with 50% (thick line), and 95% (thin line) Bayesian credible intervals. The grey line represents the estimated coefficients with 50% (thick line), and 95% (thin line) Bayesian credible intervals with one stock removed. The ID of the removed stock is given in each panel of the plot.

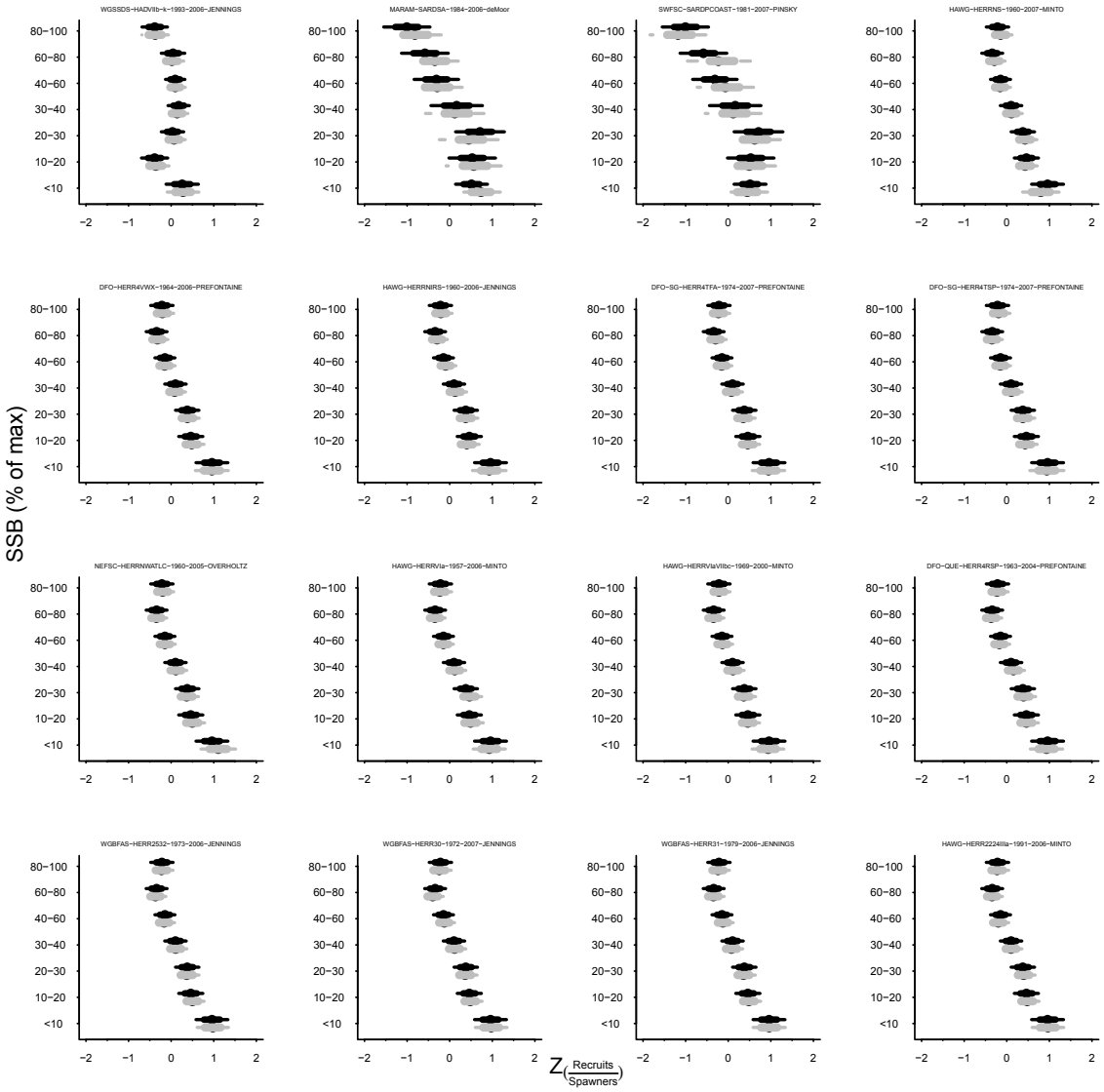

Figure A.9h: Influence of removing a stock from the analysis on the estimated model coefficients of the term $\delta_{ssb,species} + \gamma_{ssb}$ for every species with 2 or more stocks used in the analysis. The black line represent the full model estimate, with 50% (thick line), and 95% (thin line) Bayesian credible intervals. The grey line represents the estimated coefficients with 50% (thick line), and 95% (thin line) Bayesian credible intervals with one stock removed. The ID of the removed stock is given in each panel of the plot.

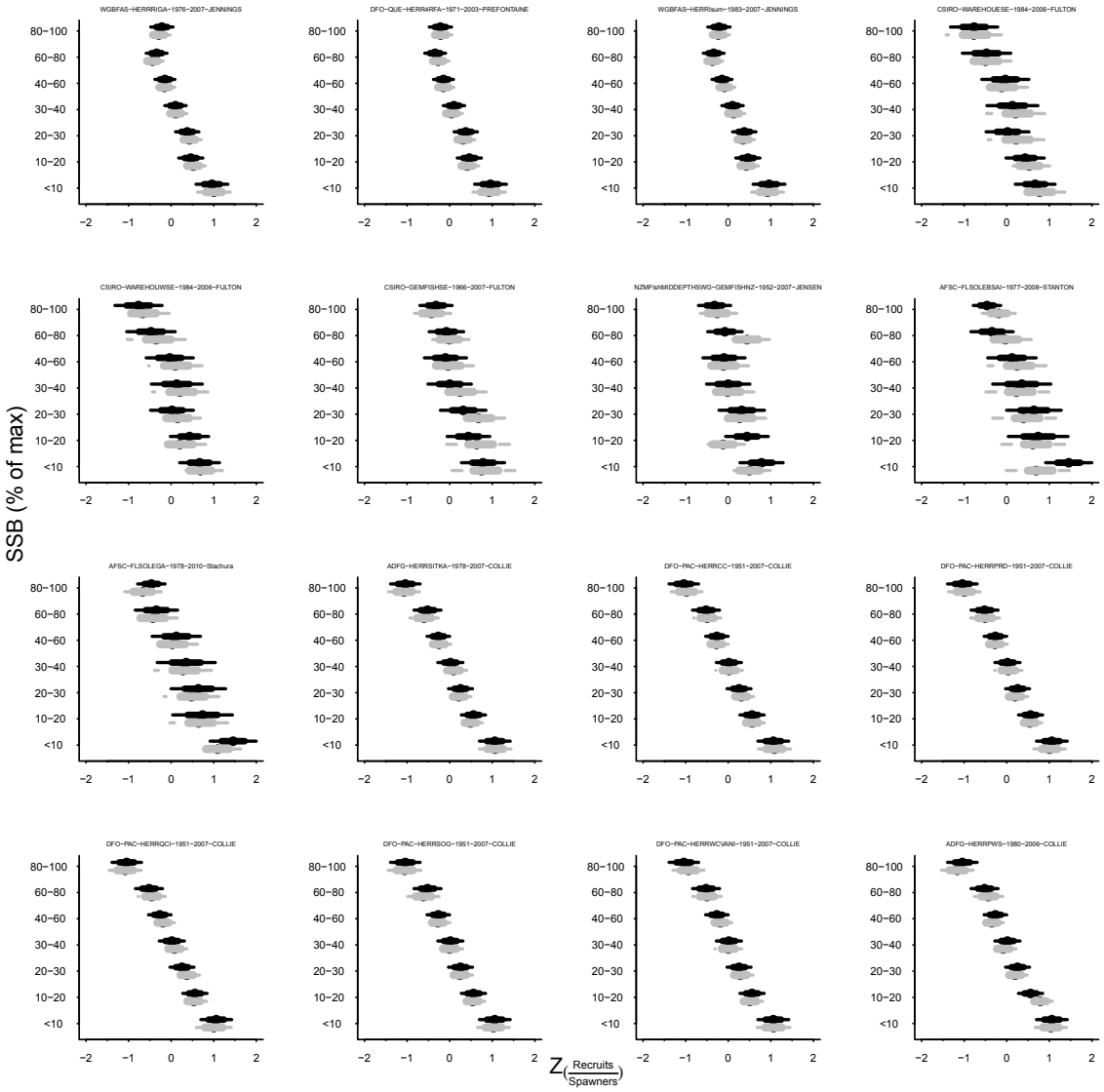

Figure A.9i: Influence of removing a stock from the analysis on the estimated model coefficients of the term $\delta_{ssb,species} + \gamma_{ssb}$ for every species with 2 or more stocks used in the analysis. The black line represent the full model estimate, with 50% (thick line), and 95% (thin line) Bayesian credible intervals. The grey line represents the estimated coefficients with 50% (thick line), and 95% (thin line) Bayesian credible intervals with one stock removed. The ID of the removed stock is given in each panel of the plot.

Appendix B

Chapter 3 supplemental tables and figures

Table B.1: Model selection table with classification (DI, NDD,PDD) as response variable.

Model	K	AICc	Delta AICc	Model Likliehood	AICc Weight	Log Likliehood	Cumulative AICc Weight
Intercept	2	181.3	0.00	1.000	0.94	-88.5	0.94
Order	8	187.5	6.20	0.045	0.04	-83.9	0.98
Manage	8	188.9	7.68	0.021	0.02	-84.6	1.00
Manage+Order	14	200.1	18.88	0.000	0.00	-79.7	1.00
Manage*Order	32	358.0	176.74	0.000	0.00	-76.6	1.00

Table B.2: Model selection table with classification (DI, NDD,PDD) as response variable with ICCAT populations removed.

Model	K	AICc	Delta AICc	Model Likliehood	AICc Weight	Log Likliehood	Cumulative AICc Weight
Intercept	2	174.6	0.00	1.000	0.93	-85.2	0.93
Order	8	179.8	5.16	0.076	0.07	-80.1	1.00
Manage	8	188.9	14.30	0.001	0.00	-84.6	1.00
Manage+Order	14	200.1	25.50	0.000	0.00	-79.7	1.00
Manage*Order	32	358.0	183.37	0.000	0.00	-76.6	1.00

Table B.3: Model selection table with peak exploitation rate ($Peak_{ER}$) as response variable.

Model	K	AICc	Delta AICc	Model Likliehood	AICc Weight	Log Likliehood	Cumulative AICc Weight
Intercept	2	228.5	0.00	1.000	0.77	-112.2	0.77
Manage	5	231.5	3.04	0.219	0.17	-110.4	0.94
Order	5	234.4	5.98	0.050	0.04	-111.9	0.98
Manage*Order	12	236.9	8.46	0.015	0.01	-104.4	0.99
Manage+Order	8	237.8	9.36	0.009	0.01	-110.0	1.00

Table B.4: Model selection table with absolute difference in exploitation rate between minimum and maximum abundance (Abs_{ER}) as response variable.

Model	K	AICc	Delta AICc	Model Likliehood	AICc Weight	Log Likliehood	Cumulative AICc Weight
Intercept	2	-109.1	0.00	1.000	0.75	56.6	0.75
Order	5	-106.3	2.80	0.247	0.19	58.5	0.94
Manage	5	-103.4	5.67	0.059	0.04	57.1	0.98
Manage+Order	8	-101.3	7.75	0.021	0.02	59.6	1.00
Manage*Order	12	-98.9	10.22	0.006	0.00	63.5	1.00

Table B.5: Model selection table with relative change in exploitation rate between minimum and maximum abundance (Rel_{ER}) as response variable.

Model	K	AICc	Delta AICc	Model Likliehood	AICc Weight	Log Likliehood	Cumulative AICc Weight
Order	5	208.9	0.00	1.000	0.57	-99.1	0.57
Intercept	2	210.2	1.26	0.533	0.31	-103.0	0.88
Manage+Order	8	212.7	3.73	0.155	0.09	-97.4	0.97
Manage	5	215.3	6.33	0.042	0.02	-102.3	0.99
Manage*Order	12	217.3	8.33	0.016	0.01	-94.6	1.00

Table B.6: Model selection table with classification (DI, NDD,PDD) as response variable for age-specific data.

Model	K	AICc	Delta AICc	Model Likliehood	AICc Weight	Log Likliehood	Cum. AICc Weight
Order+Age	10	350.5	0.00	1.000	0.74	-163.9	0.74
Age	4	353.9	3.45	0.179	0.13	-172.7	0.87
Order	8	354.3	3.80	0.149	0.11	-168.3	0.98
Intercept	2	357.8	7.34	0.026	0.02	-176.8	1.00
Manage+Age	10	363.0	12.58	0.002	0.00	-170.2	1.00
Manage+Order+Age	16	363.6	13.09	0.001	0.00	-162.3	1.00
Manage	8	366.3	15.87	0.000	0.00	-174.3	1.00
Manage+Order	14	366.7	16.20	0.000	0.00	-166.7	1.00
Order*Age + Manage	22	372.8	22.35	0.000	0.00	-157.5	1.00
Manage*Age + Order	22	378.4	27.89	0.000	0.00	-160.2	1.00
Manage*Age + Order*Age	28	384.1	33.67	0.000	0.00	-151.9	1.00
Manage*Order + Age	34	420.4	69.95	0.000	0.00	-156.7	1.00
Manage*Order + Order*Age	40	443.2	92.74	0.000	0.00	-151.8	1.00
Manage*Order + Manage*Age	40	448.9	98.39	0.000	0.00	-154.6	1.00
Manage*Order + Manage*Age + Order*Age	46	472.4	121.91	0.000	0.00	-146.1	1.00
Manage*Order*Age	64	686.2	335.71	0.000	0.00	-144.9	1.00

Table B.7: Model selection table with peak exploitation rate ($Peak_{ER}$) as response variable for age-specific data.

Model	K	AICc	Delta AICc	Model Likliehood	AICc Weight	Log Likliehood	Cum. AICc Weight
Manage*Order + Order*Age	16	465.2	0.00	1.000	0.55	-214.9	0.55
Manage*Order + Age	13	466.7	1.46	0.481	0.27	-219.2	0.82
Manage*Order + Manage*Age + Order*Age	19	469.1	3.94	0.140	0.08	-213.2	0.90
Manage*Order*Age	23	469.8	4.63	0.099	0.05	-208.4	0.95
Manage+Age	6	471.6	6.39	0.041	0.02	-229.6	0.97
Manage*Order + Manage*Age	16	472.0	6.83	0.033	0.02	-218.4	0.99
Order*Age + Manage	12	474.6	9.36	0.009	0.01	-224.4	1.00
Manage+Order+Age	9	475.5	10.33	0.006	0.00	-228.2	1.00
Manage*Age + Order*Age	15	478.5	13.29	0.001	0.00	-222.8	1.00
Manage*Age + Order	12	480.7	15.53	0.000	0.00	-227.4	1.00
Age	3	489.4	24.20	0.000	0.00	-241.6	1.00
Order+Age	6	492.8	27.57	0.000	0.00	-240.1	1.00
Manage	5	552.2	86.96	0.000	0.00	-270.9	1.00
Manage+Order	8	557.0	91.79	0.000	0.00	-270.1	1.00
Intercept	2	561.6	96.39	0.000	0.00	-278.8	1.00
Order	5	565.9	100.69	0.000	0.00	-277.8	1.00

Table B.8: Model selection table with peak exploitation rate ($Peak_{ER}$) as response variable for age-specific data with the lone NOAA clupeiform population removed.

Model	K	AICc	Delta AICc	Model Likliehood	AICc Weight	Log Likliehood	Cum. AICc Weight
Order*Age + Manage	12	457.9	0.00	1.000	0.27	-216.0	0.27
Manage+Age	6	458.7	0.85	0.652	0.18	-223.1	0.44
Manage*Order + Order*Age	15	458.9	1.01	0.603	0.16	-213.0	0.61
Manage+Order+Age	9	459.0	1.08	0.582	0.16	-220.0	0.76
Manage*Order + Age	12	460.0	2.11	0.349	0.09	-217.1	0.86
Manage*Age + Order*Age	15	461.0	3.13	0.209	0.06	-214.0	0.91
Manage*Order*Age	21	462.1	4.20	0.122	0.03	-207.1	0.95
Manage*Order + Manage*Age + Order*Age	18	462.2	4.27	0.118	0.03	-211.0	0.98
Manage*Age + Order	12	463.7	5.81	0.055	0.01	-218.9	0.99
Manage*Order + Manage*Age	15	464.9	7.02	0.030	0.01	-216.0	1.00
Age	3	481.1	23.26	0.000	0.00	-237.5	1.00
Order+Age	6	483.8	25.93	0.000	0.00	-235.7	1.00
Manage	5	542.9	85.04	0.000	0.00	-266.3	1.00
Manage+Order	8	545.5	87.63	0.000	0.00	-264.3	1.00
Intercept	2	555.0	97.09	0.000	0.00	-275.5	1.00
Order	5	558.9	100.97	0.000	0.00	-274.3	1.00

Table B.9: Model selection table with absolute difference in exploitation rate between minimum and maximum abundance (Abs_{ER}) as response variable for age-specific data.

Model	K	AICc	Delta AICc	Model Likliehood	AICc Weight	Log Likliehood	Cum. AICc Weight
Age	3	-211.2	0.00	1.000	0.66	108.7	0.66
Order+Age	6	-207.7	3.56	0.169	0.11	110.1	0.77
Manage*Order + Order*Age	16	-206.6	4.63	0.099	0.06	121.0	0.84
Manage+Age	6	-205.9	5.37	0.068	0.04	109.2	0.88
Manage*Order + Age	13	-205.8	5.42	0.067	0.04	117.0	0.92
Manage*Order + Manage*Age + Order*Age	19	-205.0	6.28	0.043	0.03	123.8	0.95
Intercept	2	-204.6	6.61	0.037	0.02	104.3	0.98
Order*Age + Manage	12	-202.0	9.27	0.010	0.01	113.9	0.98
Manage+Order+Age	9	-201.4	9.81	0.007	0.00	110.2	0.99
Order	5	-201.0	10.23	0.006	0.00	105.7	0.99
Manage*Order + Manage*Age	16	-200.3	10.89	0.004	0.00	117.8	0.99
Manage*Age + Order*Age	15	-200.2	11.00	0.004	0.00	116.6	1.00
Manage	5	-199.3	11.95	0.003	0.00	104.8	1.00
Manage*Age + Order	12	-196.2	15.07	0.001	0.00	111.0	1.00
Manage*Order*Age	23	-196.1	15.15	0.001	0.00	124.5	1.00
Manage+Order	8	-194.8	16.42	0.000	0.00	105.8	1.00

Table B.10: Model selection table with relative change in exploitation rate between minimum and maximum abundance (Rel_{ER}) as response variable for age-specific data.

Model	K	AICc	Delta AICc	Model Likliehood	AICc Weight	Log Likliehood	Cum. AICc Weight
Manage*Order*Age	23	511.1	0.00	1.000	0.39	-229.1	0.39
Order	5	512.9	1.80	0.407	0.16	-251.3	0.55
Manage*Age + Order*Age	15	513.2	2.01	0.366	0.14	-240.1	0.70
Manage*Order + Manage*Age + Order*Age	19	514.1	3.01	0.222	0.09	-235.7	0.78
Order+Age	6	514.6	3.49	0.175	0.07	-251.1	0.85
Order*Age + Manage	12	515.0	3.90	0.142	0.06	-244.6	0.91
Manage*Order + Order*Age	16	516.1	4.98	0.083	0.03	-240.4	0.94
Manage*Age + Order	12	517.2	6.01	0.050	0.02	-245.7	0.96
Manage+Order	8	517.5	6.32	0.042	0.02	-250.3	0.98
Manage*Order + Manage*Age	16	518.3	7.19	0.028	0.01	-241.5	0.99
Manage+Order+Age	9	519.2	8.08	0.018	0.01	-250.1	1.00
Manage*Order + Age	13	520.5	9.33	0.009	0.00	-246.2	1.00
Intercept	2	523.6	12.43	0.002	0.00	-259.8	1.00
Age	3	525.2	14.08	0.001	0.00	-259.5	1.00
Manage	5	529.6	18.44	0.000	0.00	-259.6	1.00
Manage+Age	6	531.3	20.17	0.000	0.00	-259.4	1.00

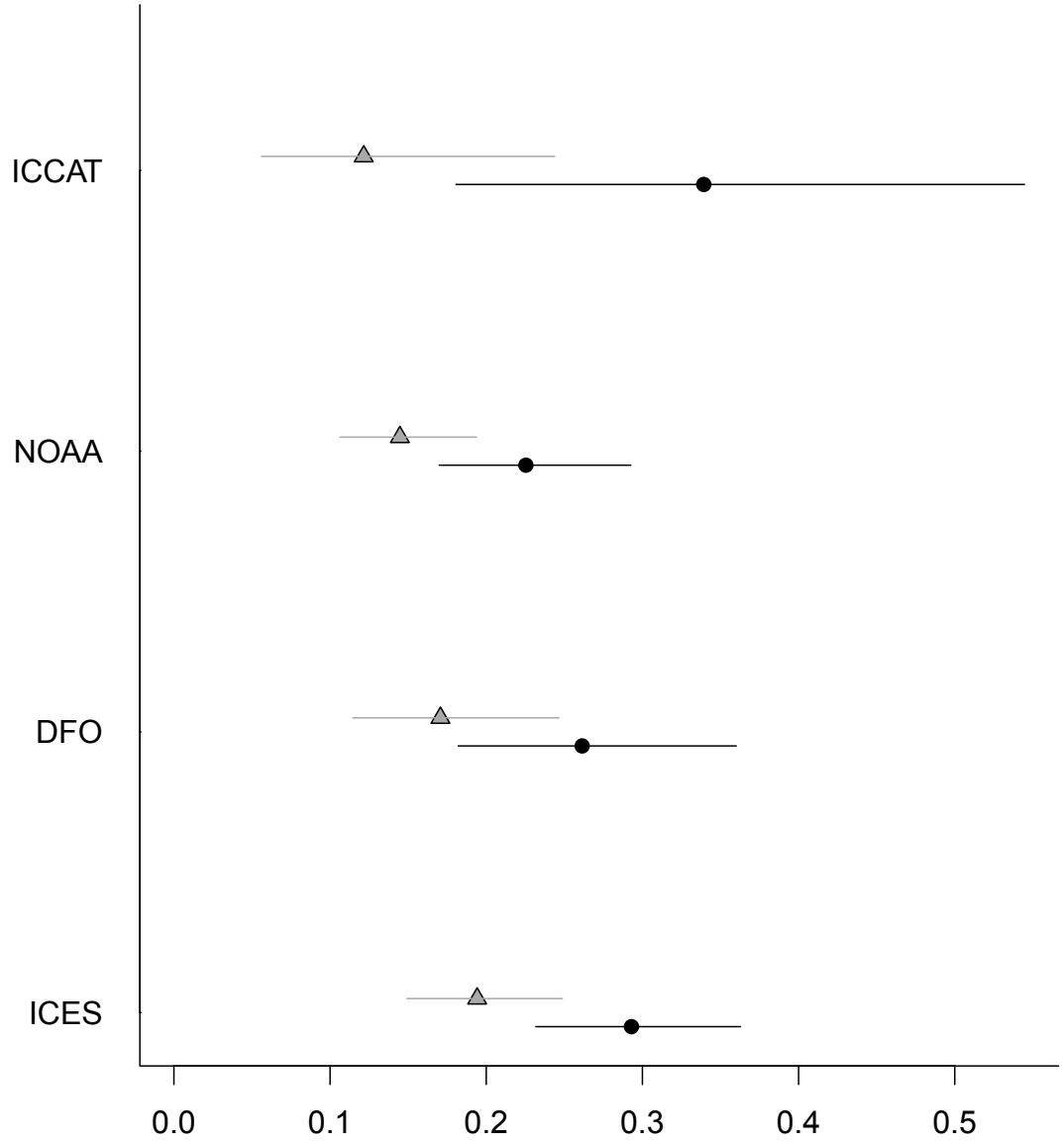

Figure B.1: Model estimated peak exploitation rate ($Peak_{ER}$) with 95% confidence intervals as it varies by taxonomic grouping for old (black circles) and young (grey triangles) age classes with the NOAA clupeiform population removed.

Figure B.2: The functional response model fits for each population are found in electronic supplement A.

Figure B.3: The age-specific functional response model fits for each population are found in electronic supplement B.

Appendix C

Chapter 5 supplemental figures population viability analysis

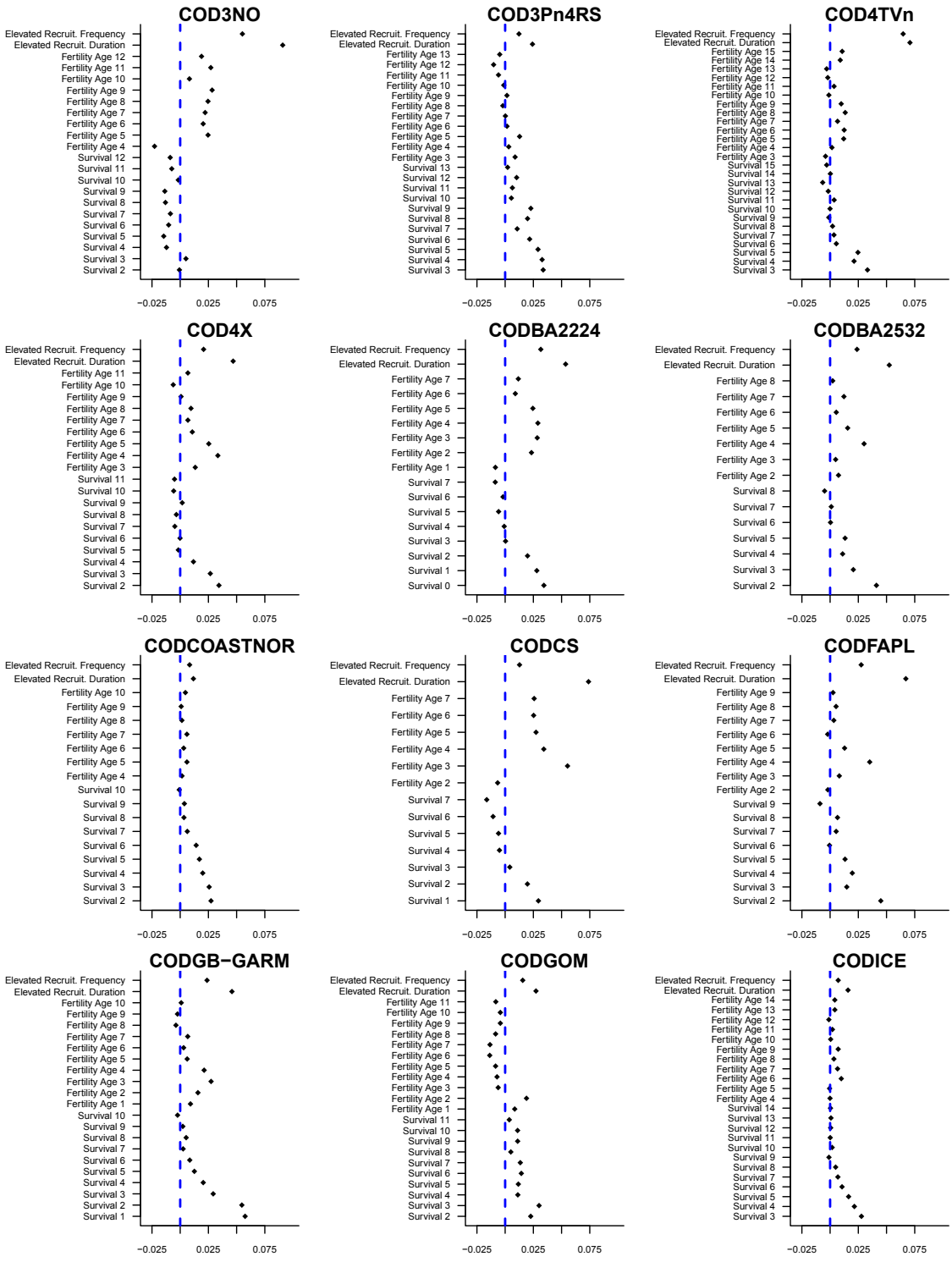

Figure C1a: The elasticity of the population growth rate for each population during a bonanaza

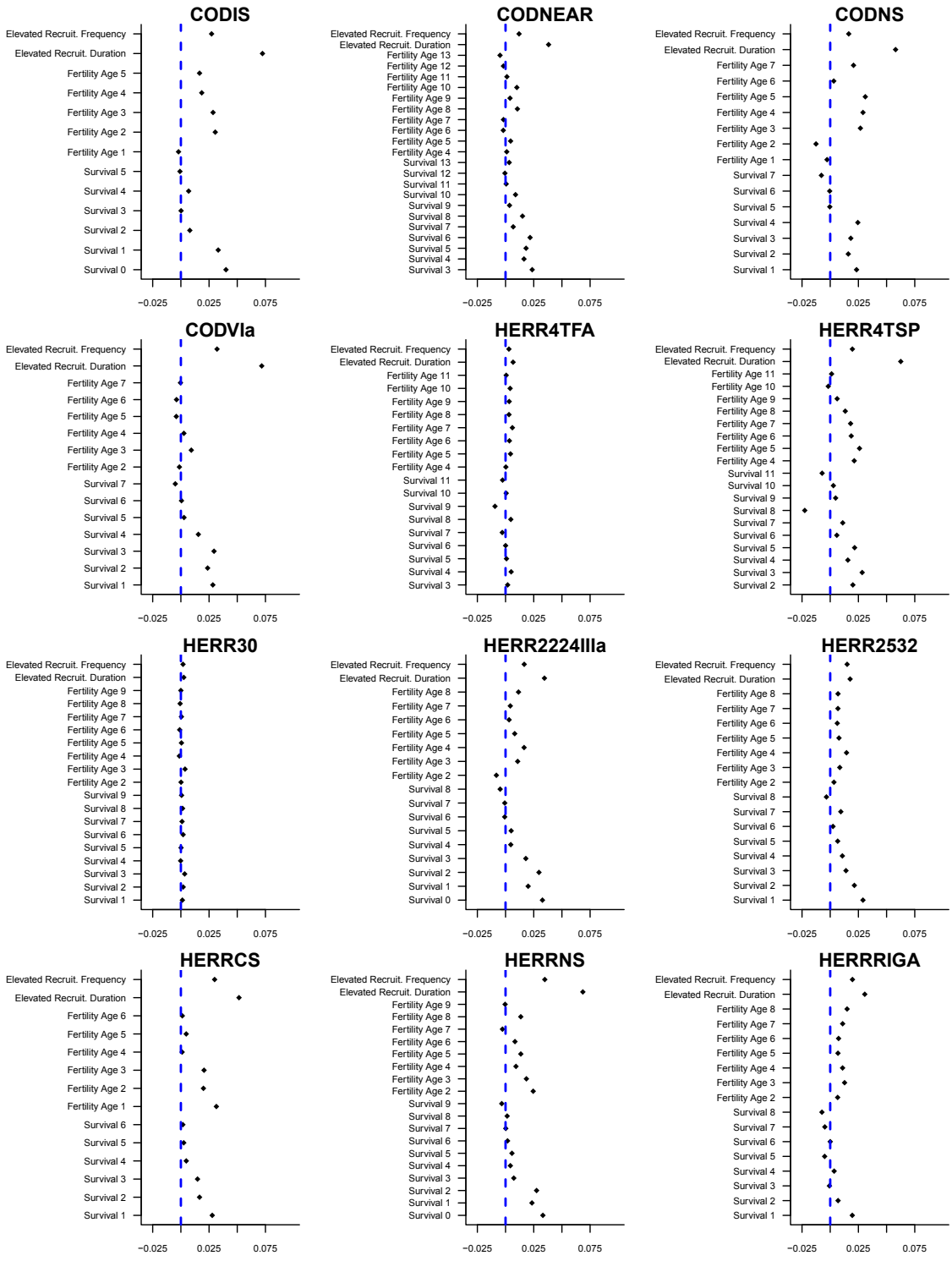

Figure C1b: The elasticity of the population growth rate for each population during a bonanaza

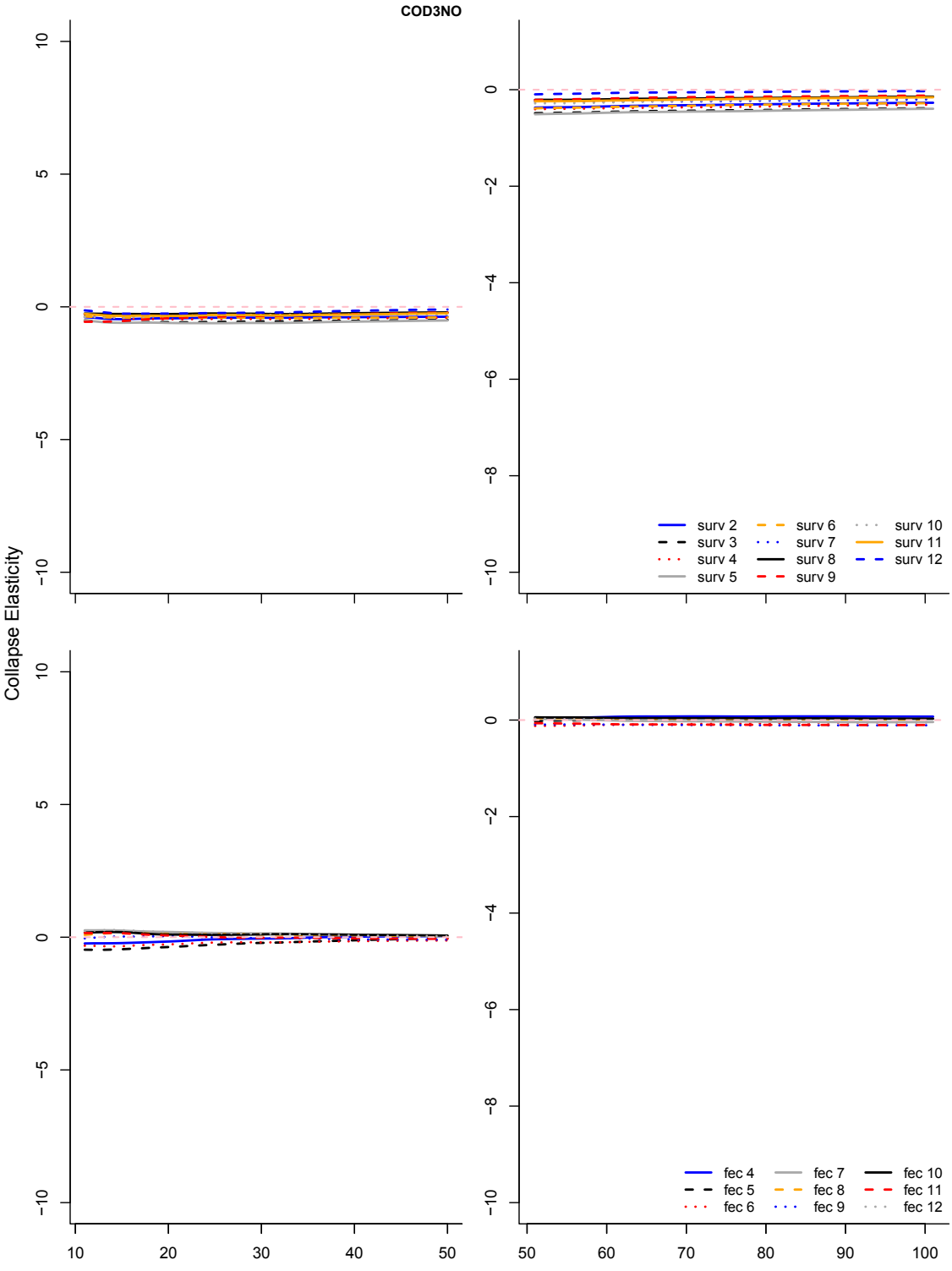

Figure C2a: Time series of the elasticity of the probability of collapse for each survival and fecundity vital rate during a period of typical recruitment for each population (population name at top of figure). Populations with a zero percent probability of collapse after 50 years are excluded from this figure.

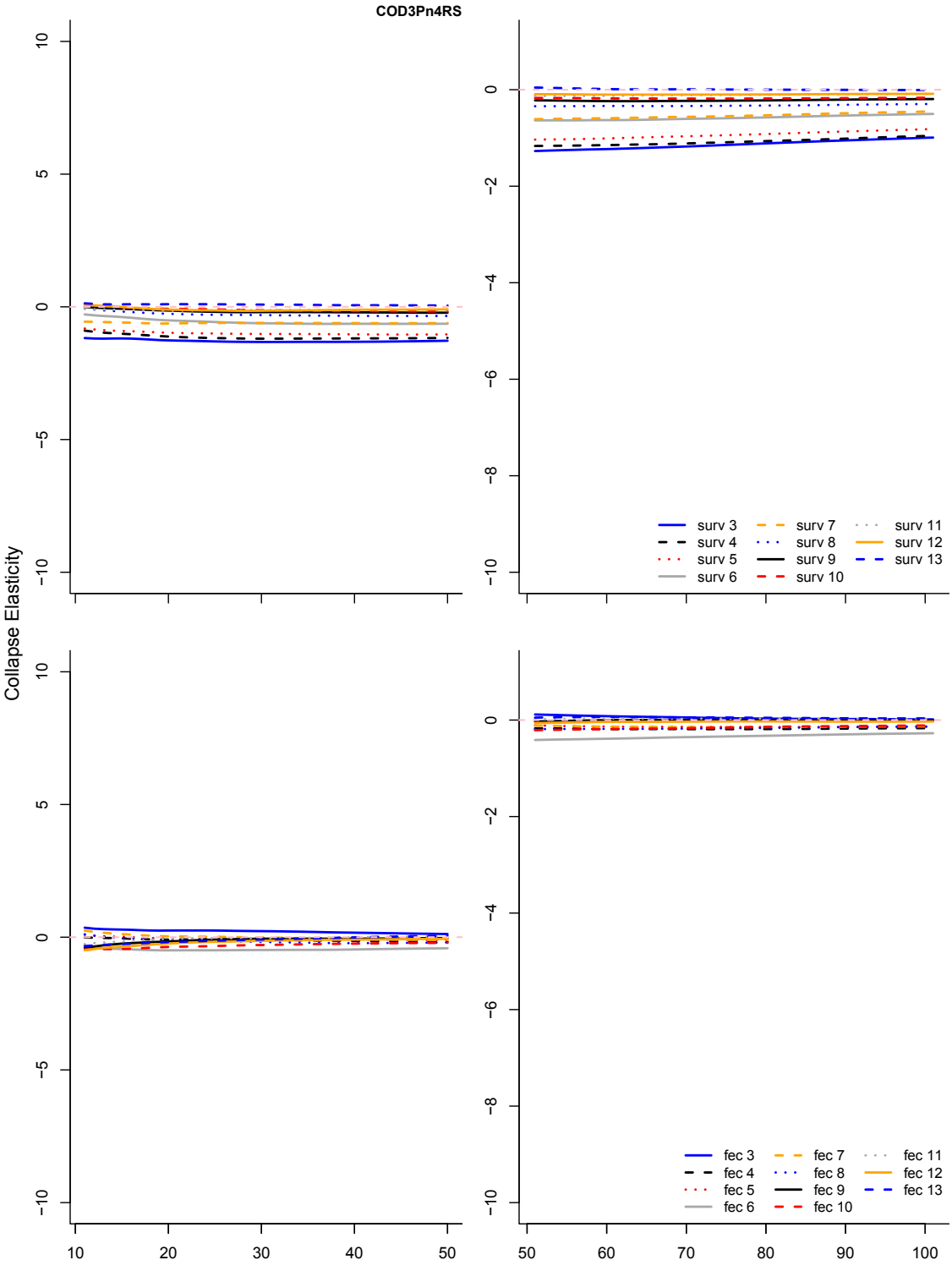

Figure C2b: Time series of the elasticity of the probability of collapse for each survival and fecundity vital rate during a period of typical recruitment for each population (population name at top of figure). Populations with a zero percent probability of collapse after 50 years are excluded from this figure.

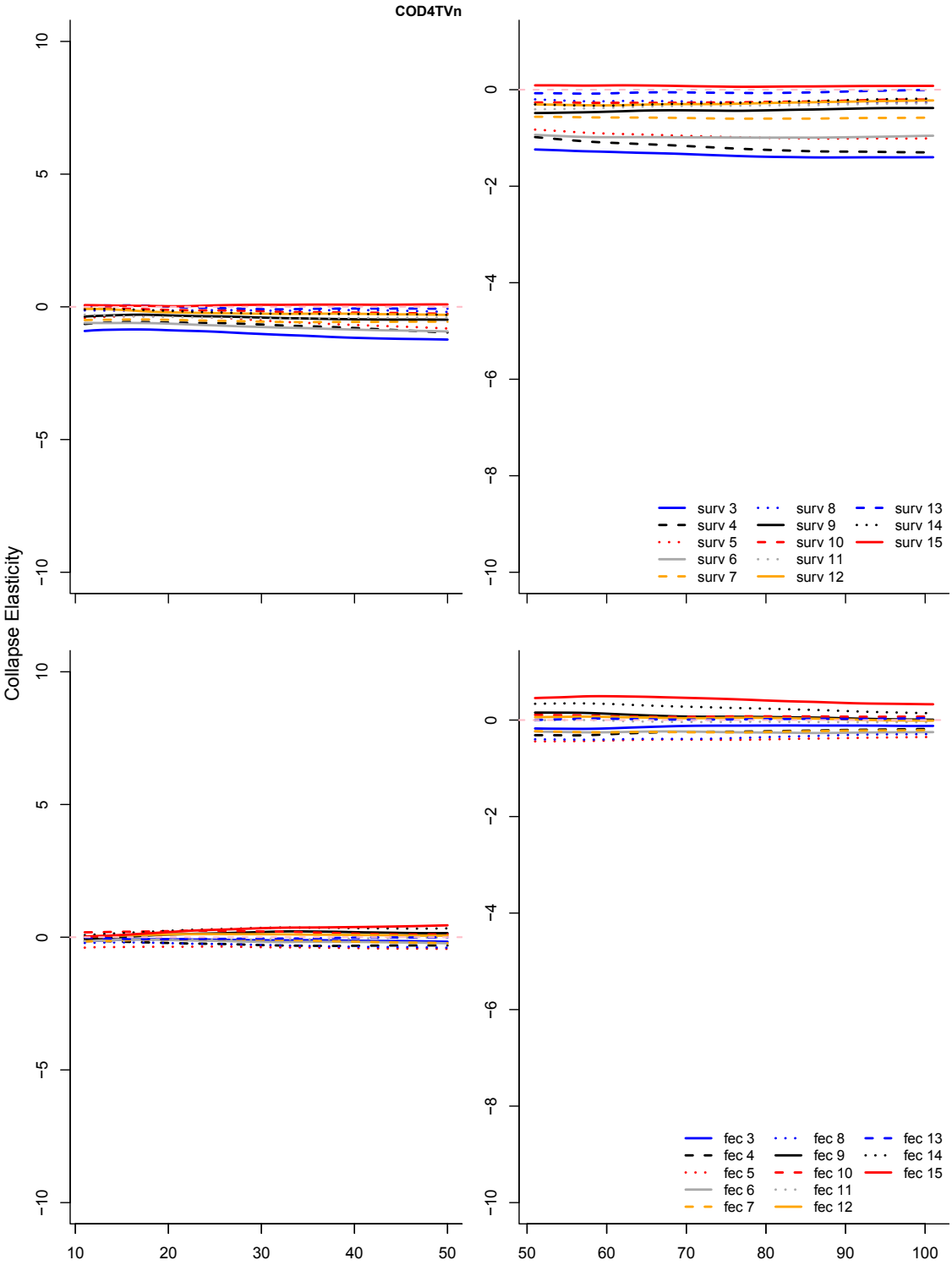

Figure C2c: Time series of the elasticity of the probability of collapse for each survival and fecundity vital rate during a period of typical recruitment for each population (population name at top of figure). Populations with a zero percent probability of collapse after 50 years are excluded from this figure.

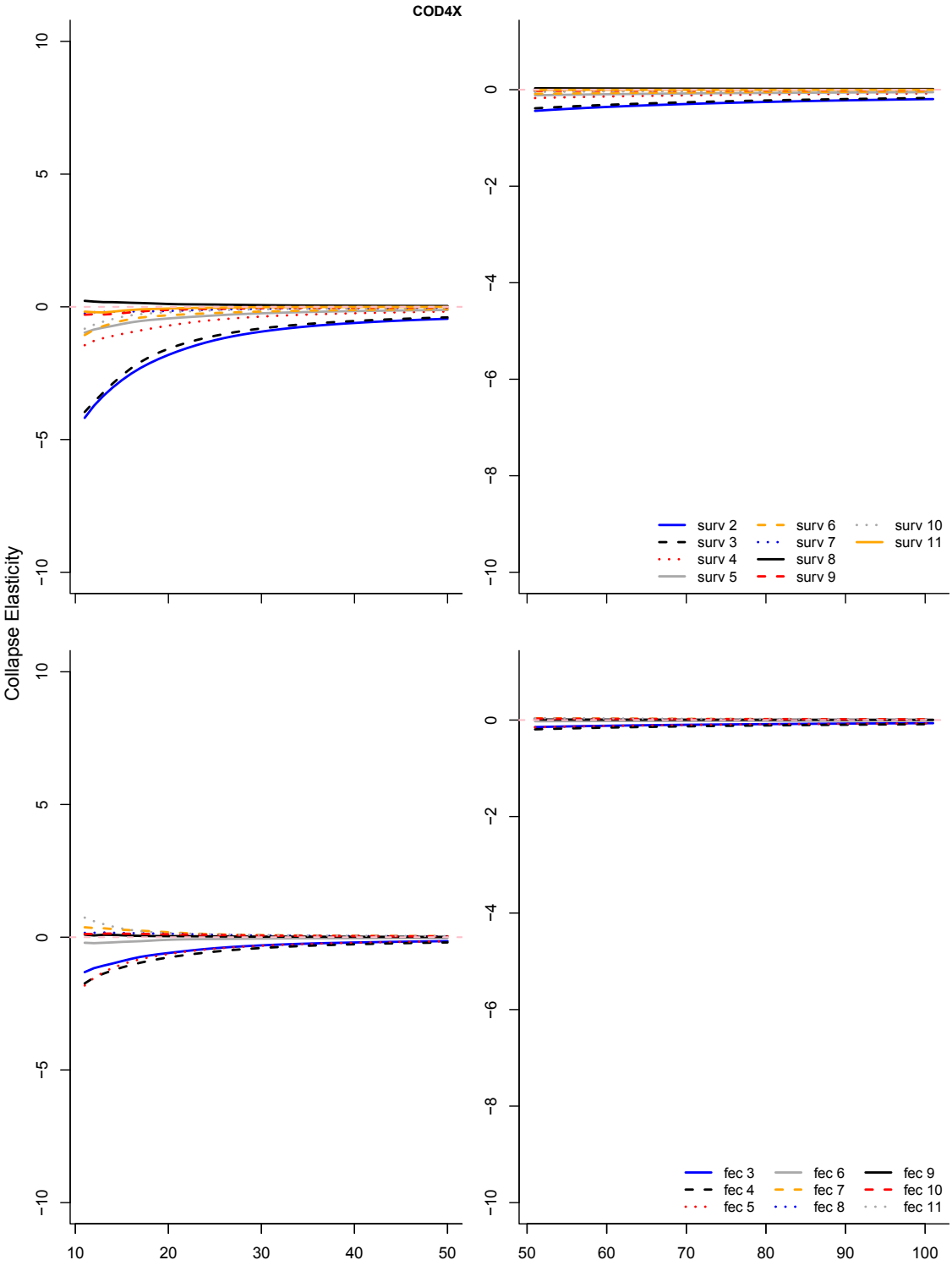

Figure C2d: Time series of the elasticity of the probability of collapse for each survival and fecundity vital rate during a period of typical recruitment for each population (population name at top of figure). Populations with a zero percent probability of collapse after 50 years are excluded from this figure.

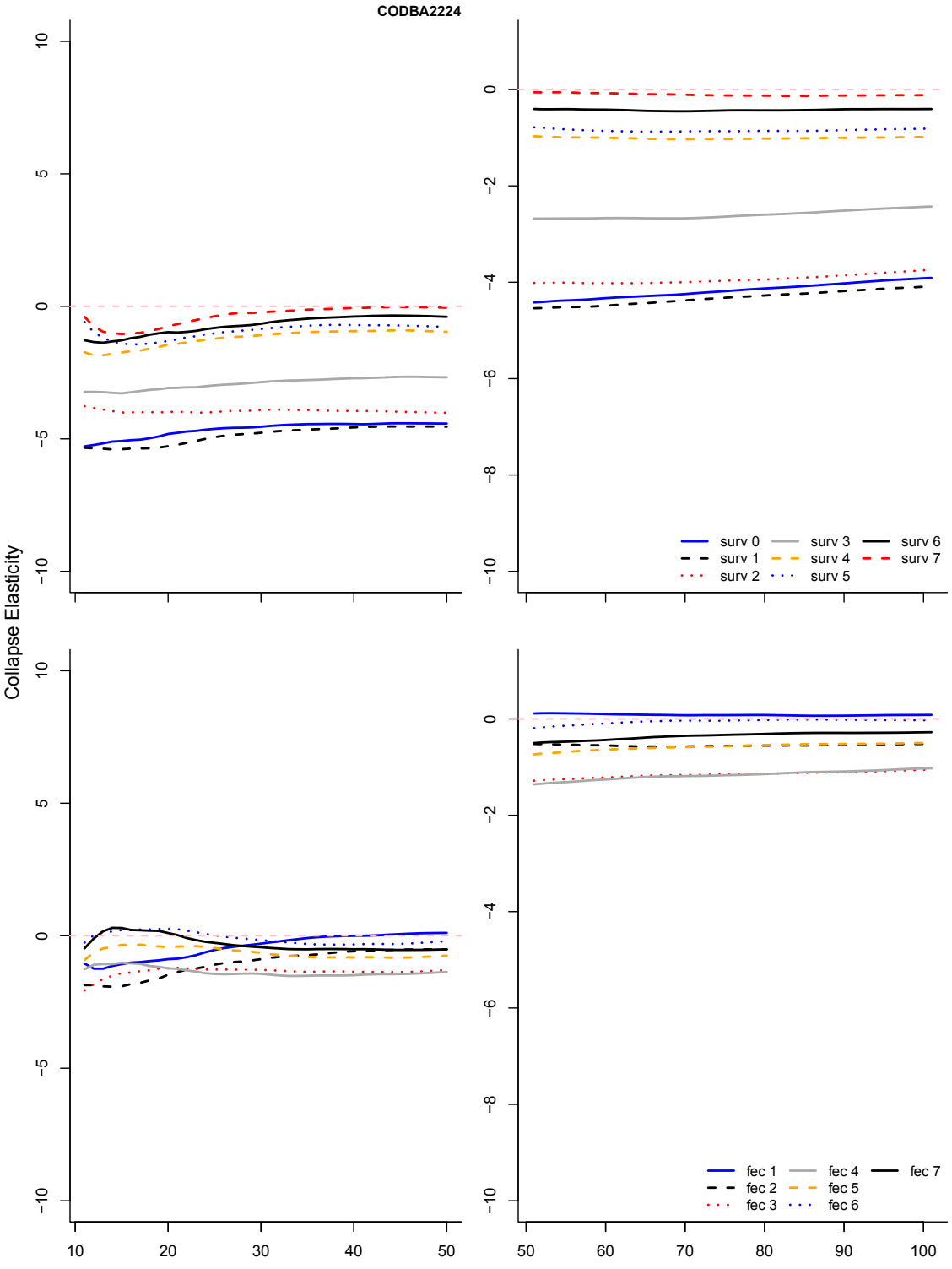

Figure C2e: Time series of the elasticity of the probability of collapse for each survival and fecundity vital rate during a period of typical recruitment for each population (population name at top of figure). Populations with a zero percent probability of collapse after 50 years are excluded from this figure.

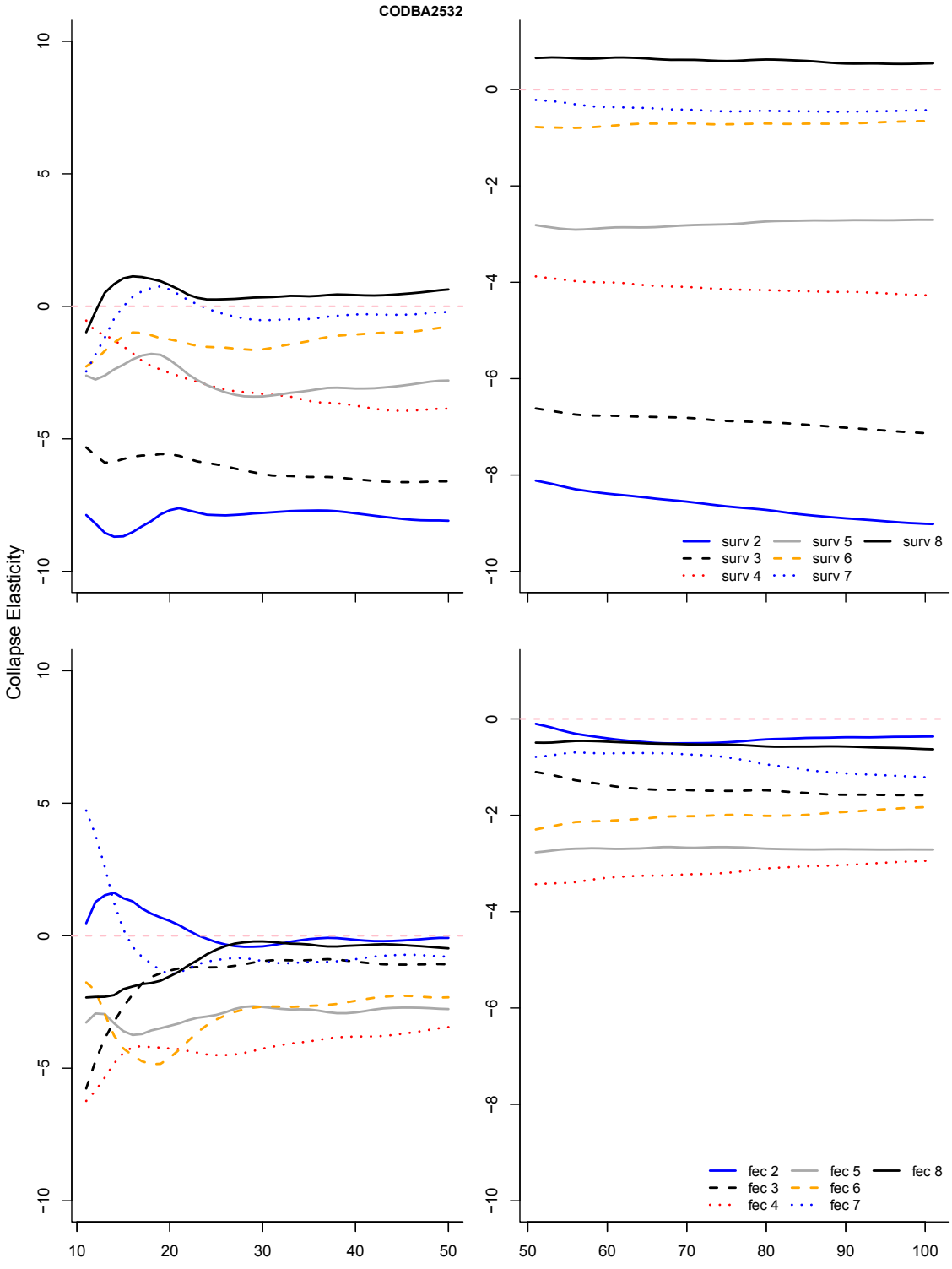

Figure C2f: Time series of the elasticity of the probability of collapse for each survival and fecundity vital rate during a period of typical recruitment for each population (population name at top of figure). Populations with a zero percent probability of collapse after 50 years are excluded from this figure.

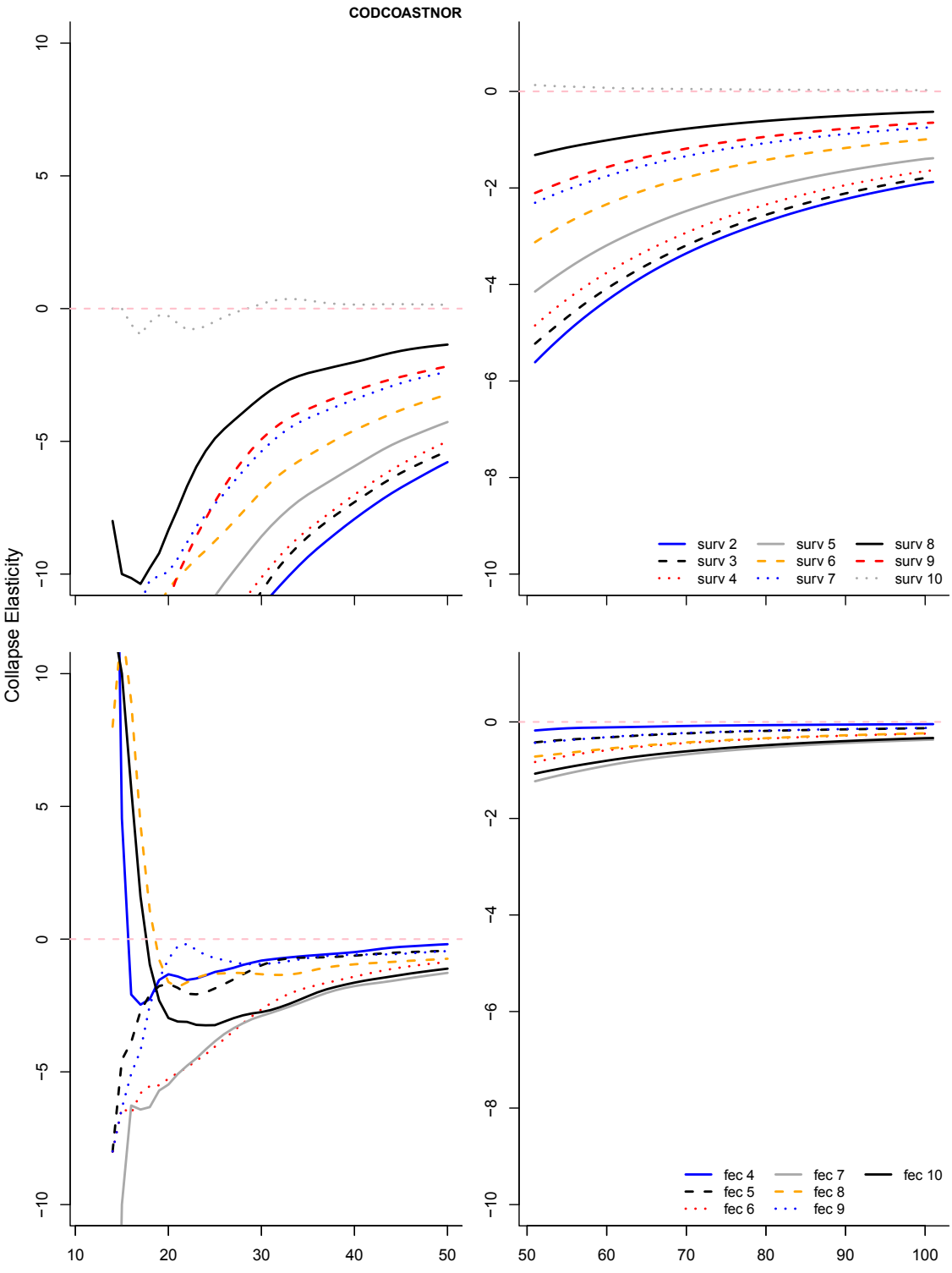

Figure C2g: Time series of the elasticity of the probability of collapse for each survival and fecundity vital rate during a period of typical recruitment for each population (population name at top of figure). Populations with a zero percent probability of collapse after 50 years are excluded from this figure.

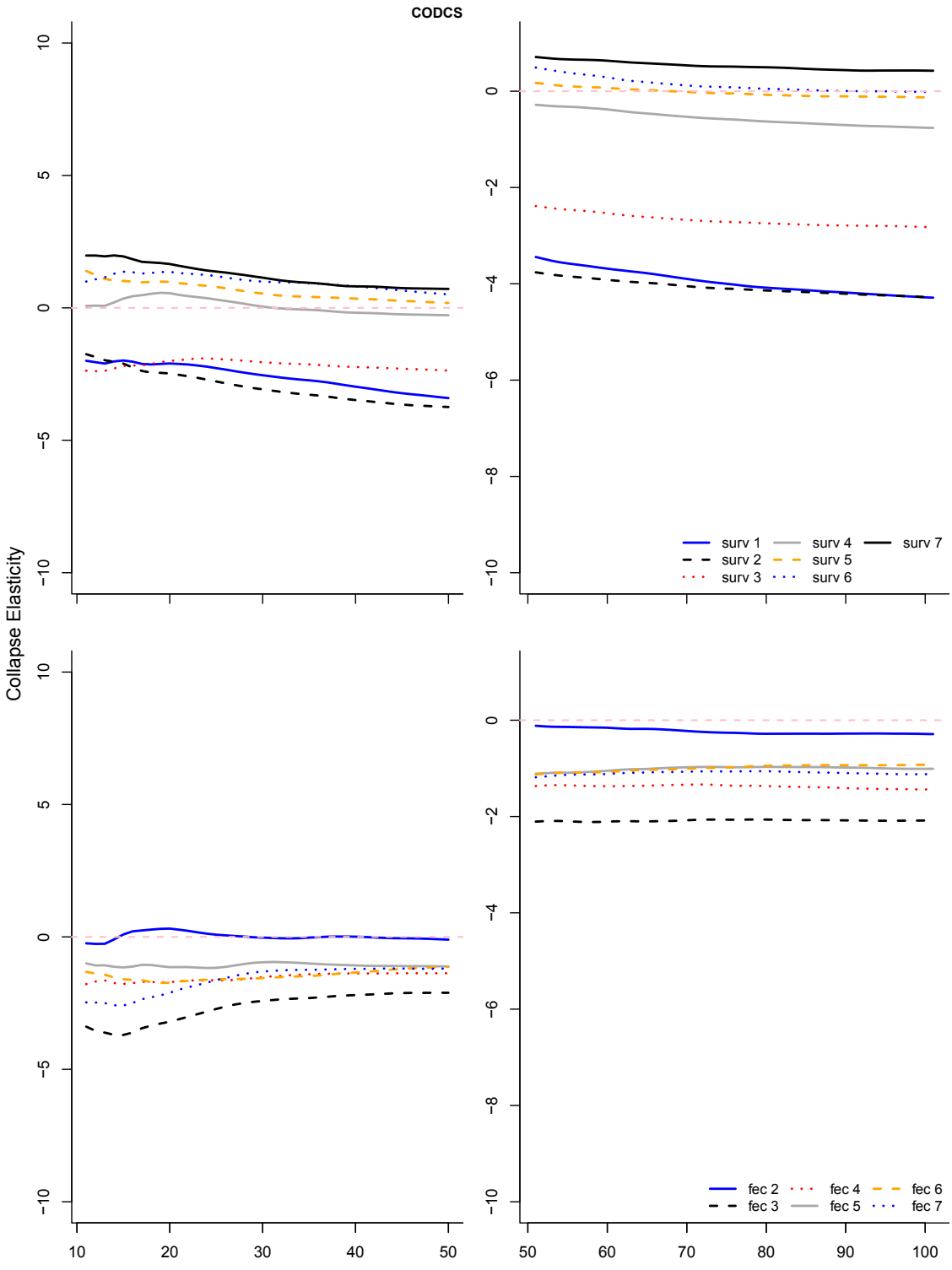

Figure C2h: Time series of the elasticity of the probability of collapse for each survival and fecundity vital rate during a period of typical recruitment for each population (population name at top of figure). Populations with a zero percent probability of collapse after 50 years are excluded from this figure.

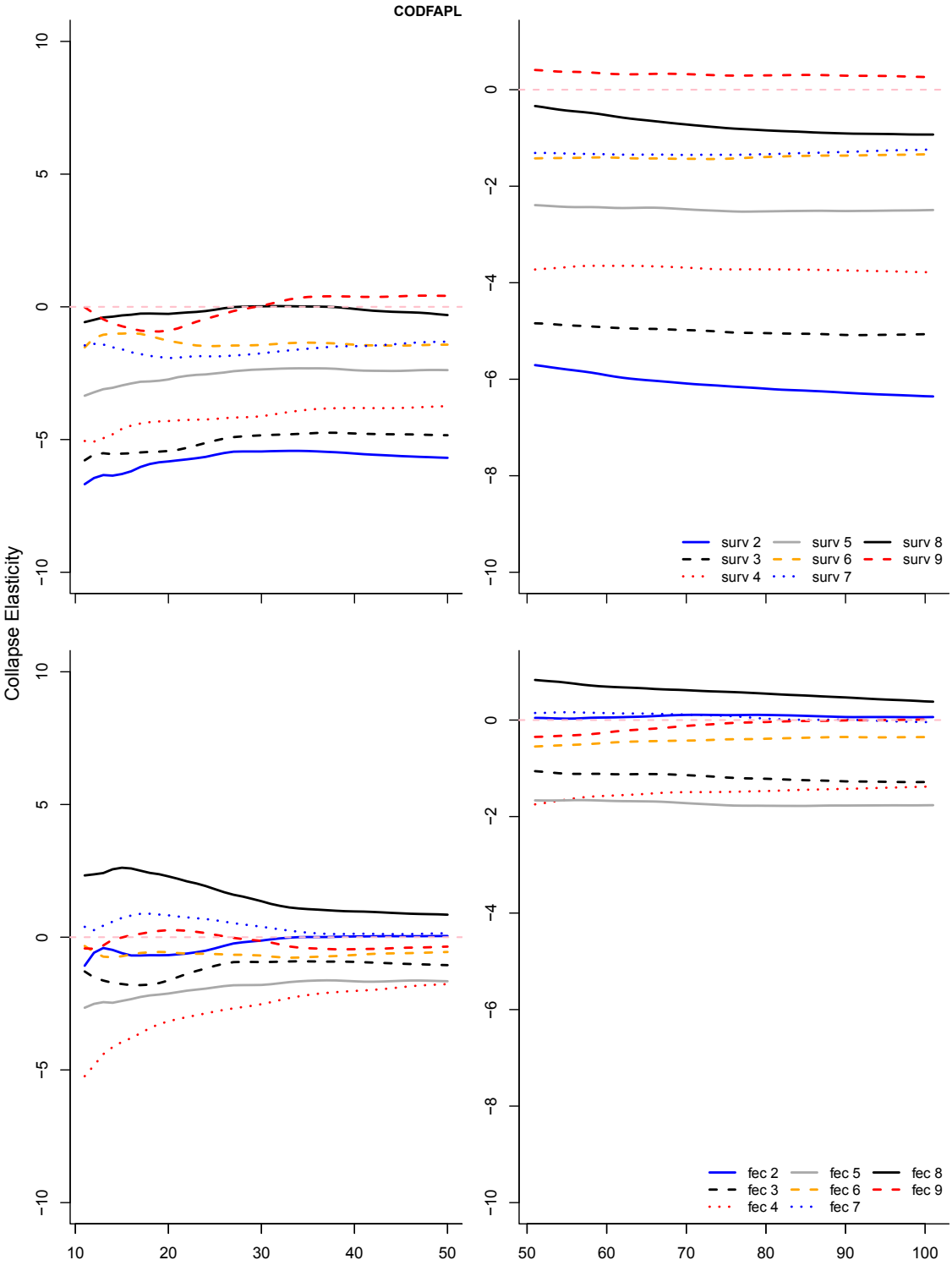

Figure C2i: Time series of the elasticity of the probability of collapse for each survival and fecundity vital rate during a period of typical recruitment for each population (population name at top of figure). Populations with a zero percent probability of collapse after 50 years are excluded from this figure.

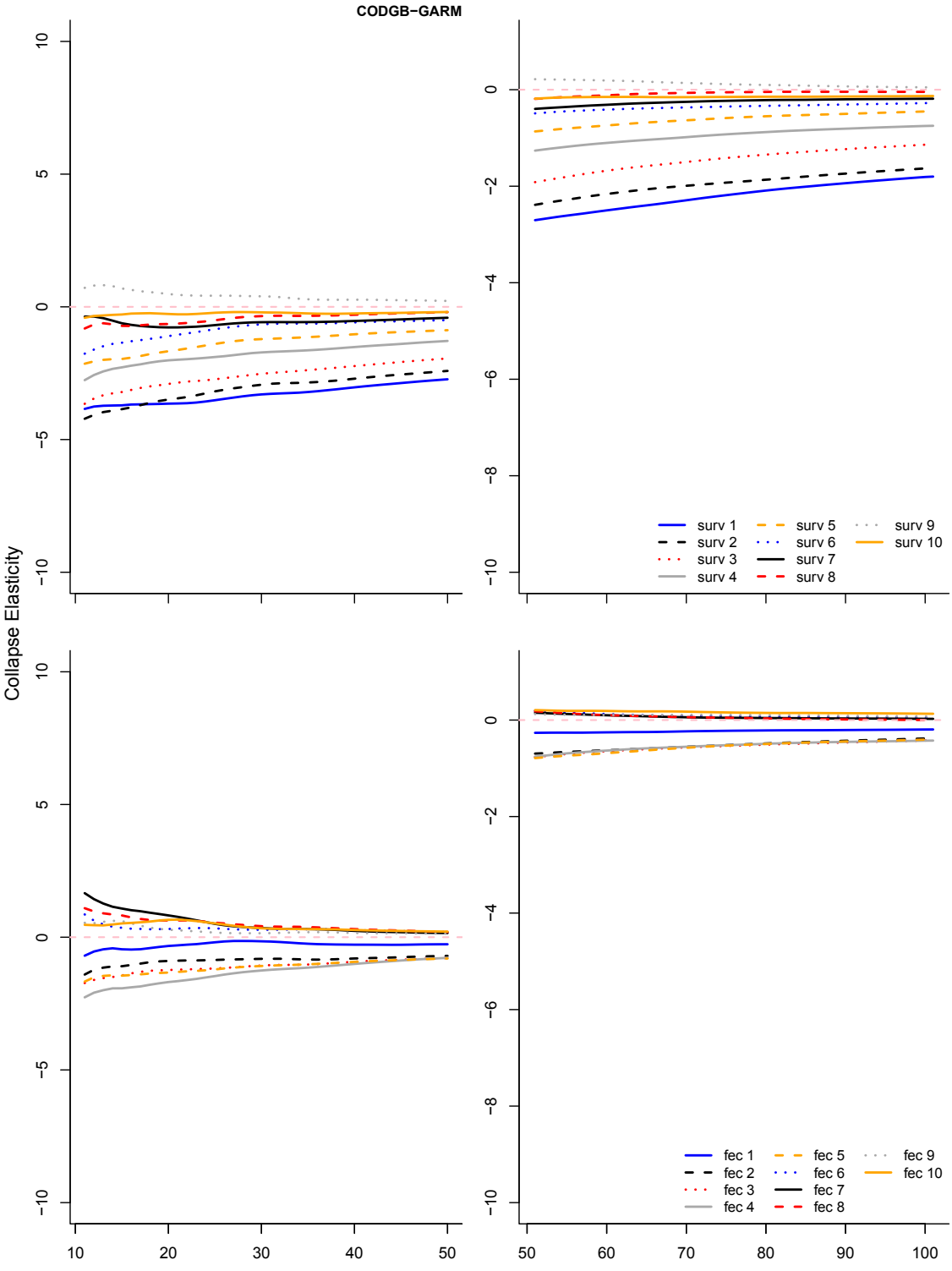

Figure C2j: Time series of the elasticity of the probability of collapse for each survival and fecundity vital rate during a period of typical recruitment for each population (population name at top of figure). Populations with a zero percent probability of collapse after 50 years are excluded from this figure.

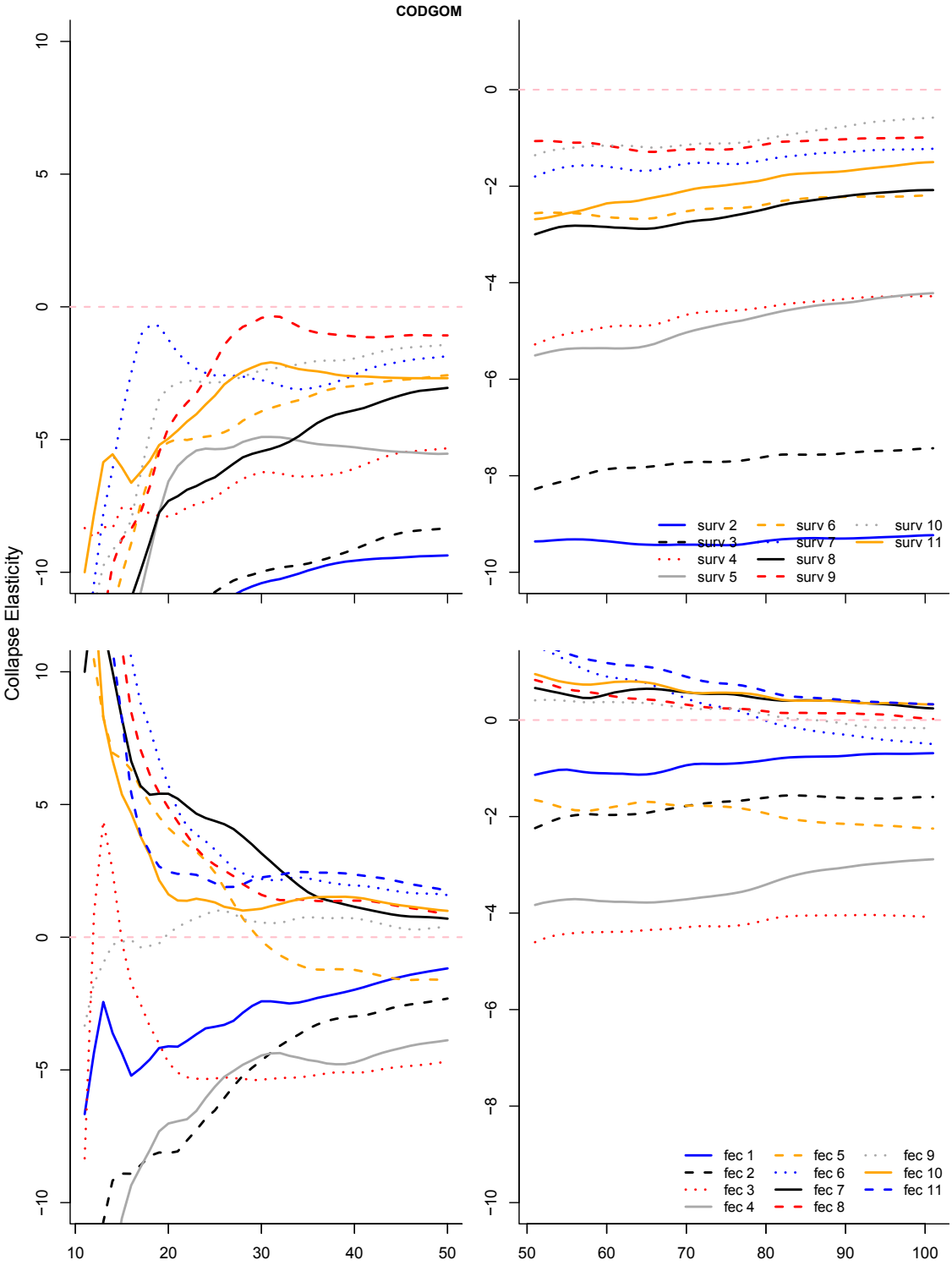

Figure C2k: Time series of the elasticity of the probability of collapse for each survival and fecundity vital rate during a period of typical recruitment for each population (population name at top of figure). Populations with a zero percent probability of collapse after 50 years are excluded from this figure.

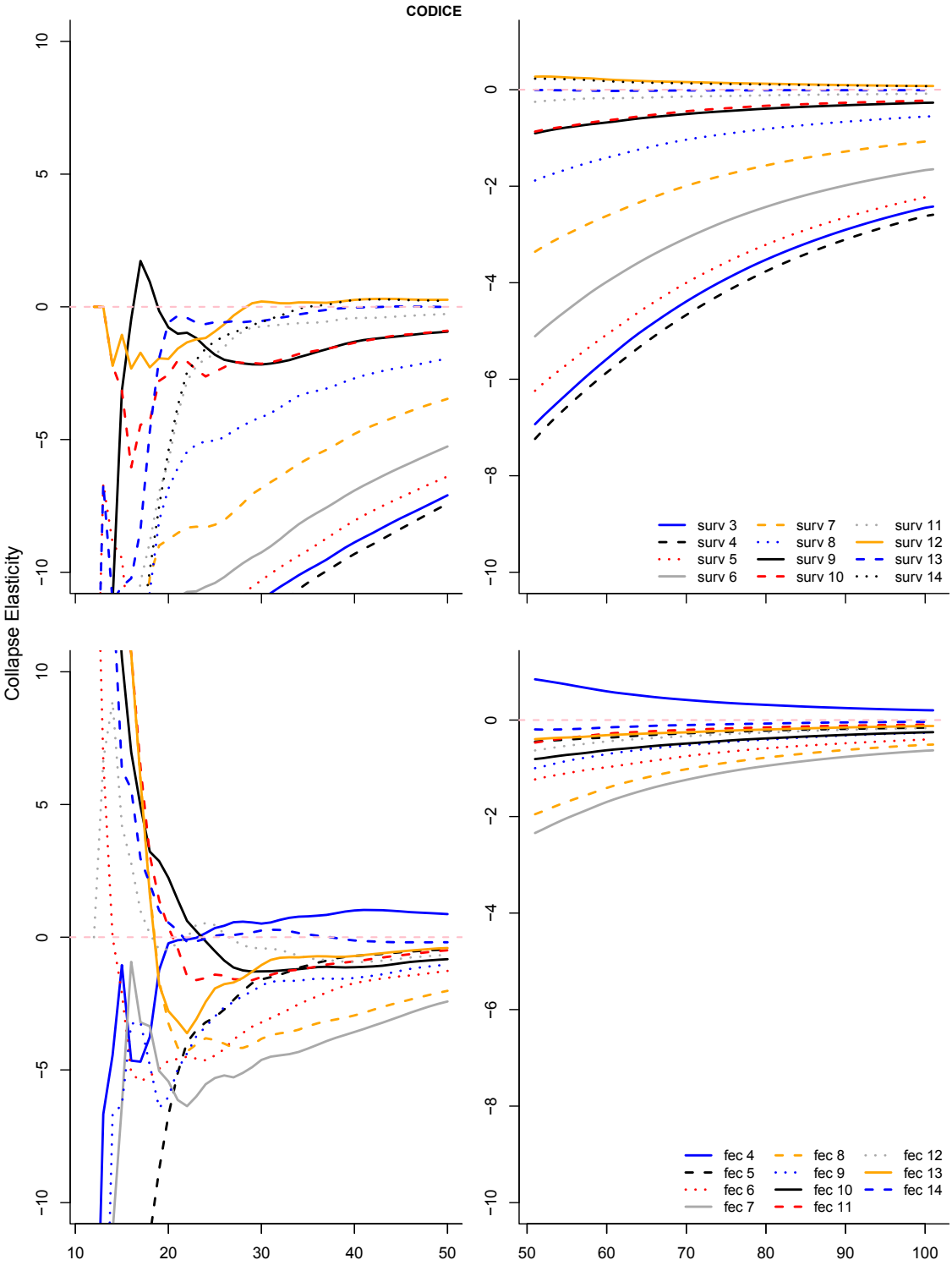

Figure C2l: Time series of the elasticity of the probability of collapse for each survival and fecundity vital rate during a period of typical recruitment for each population (population name at top of figure). Populations with a zero percent probability of collapse after 50 years are excluded from this figure.

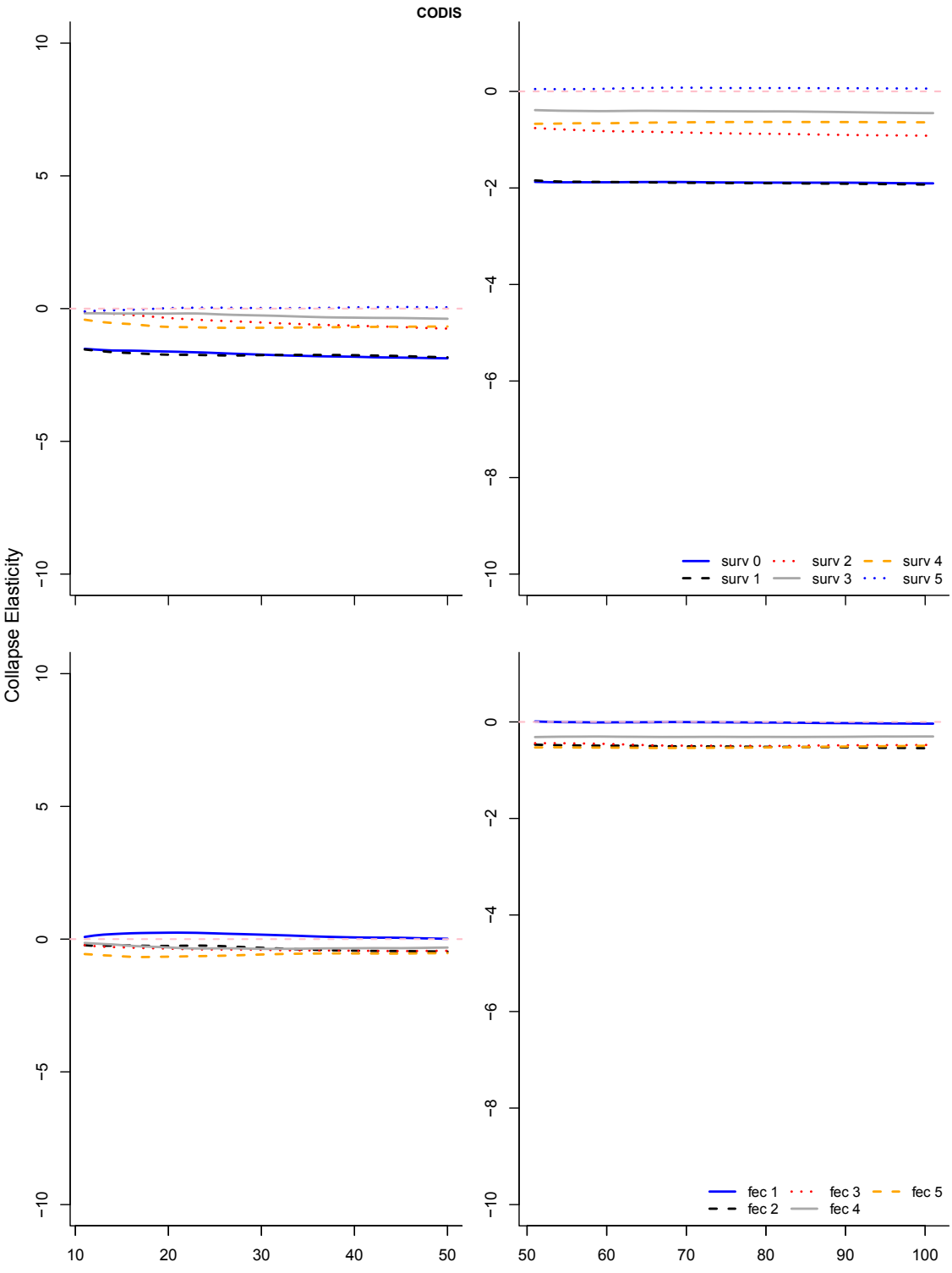

Figure C2m: Time series of the elasticity of the probability of collapse for each survival and fecundity vital rate during a period of typical recruitment for each population (population name at top of figure). Populations with a zero percent probability of collapse after 50 years are excluded from this figure.

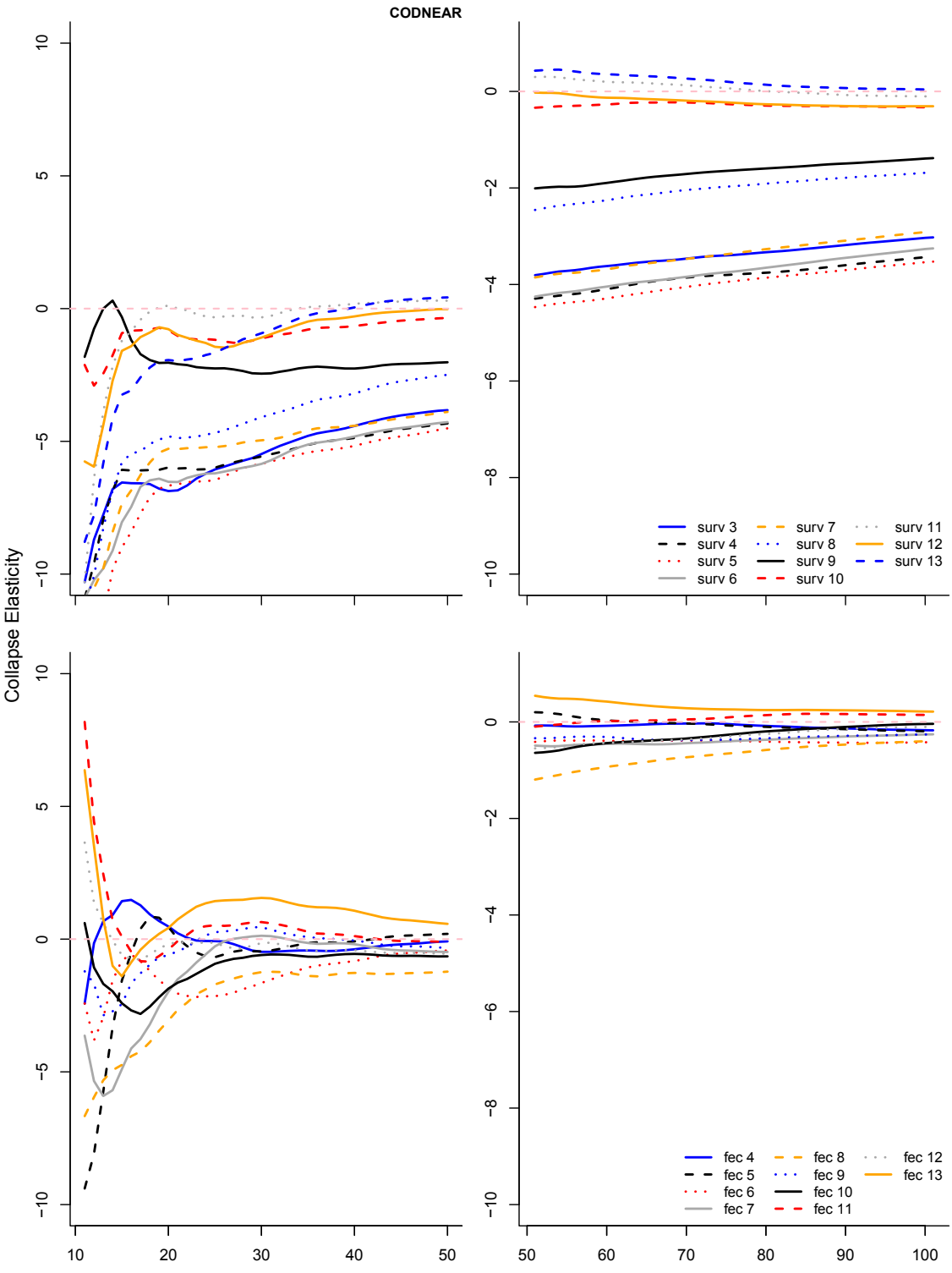

Figure C2n: Time series of the elasticity of the probability of collapse for each survival and fecundity vital rate during a period of typical recruitment for each population (population name at top of figure). Populations with a zero percent probability of collapse after 50 years are excluded from this figure.

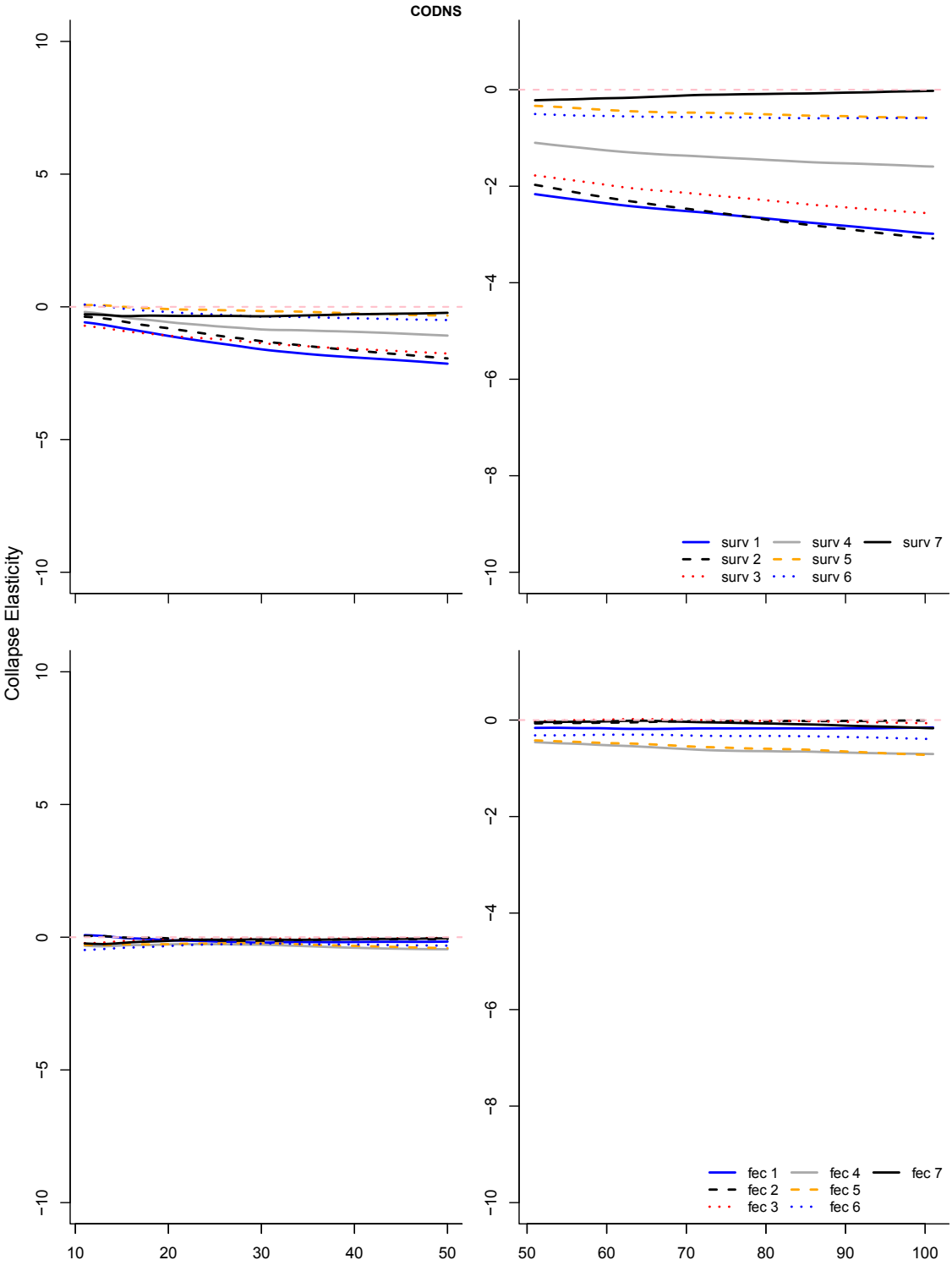

Figure C2o: Time series of the elasticity of the probability of collapse for each survival and fecundity vital rate during a period of typical recruitment for each population (population name at top of figure). Populations with a zero percent probability of collapse after 50 years are excluded from this figure.

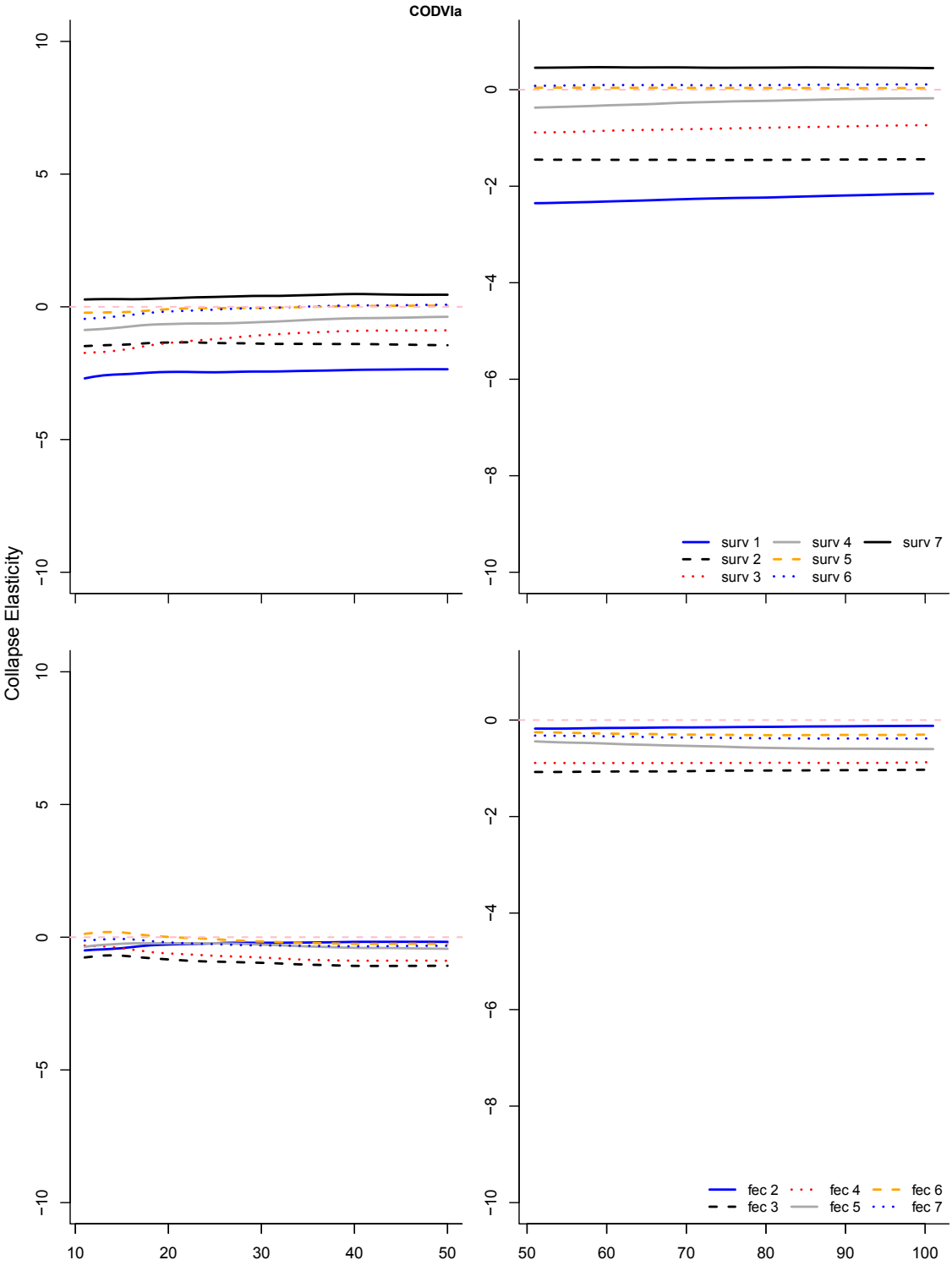

Figure C2p: Time series of the elasticity of the probability of collapse for each survival and fecundity vital rate during a period of typical recruitment for each population (population name at top of figure). Populations with a zero percent probability of collapse after 50 years are excluded from this figure.

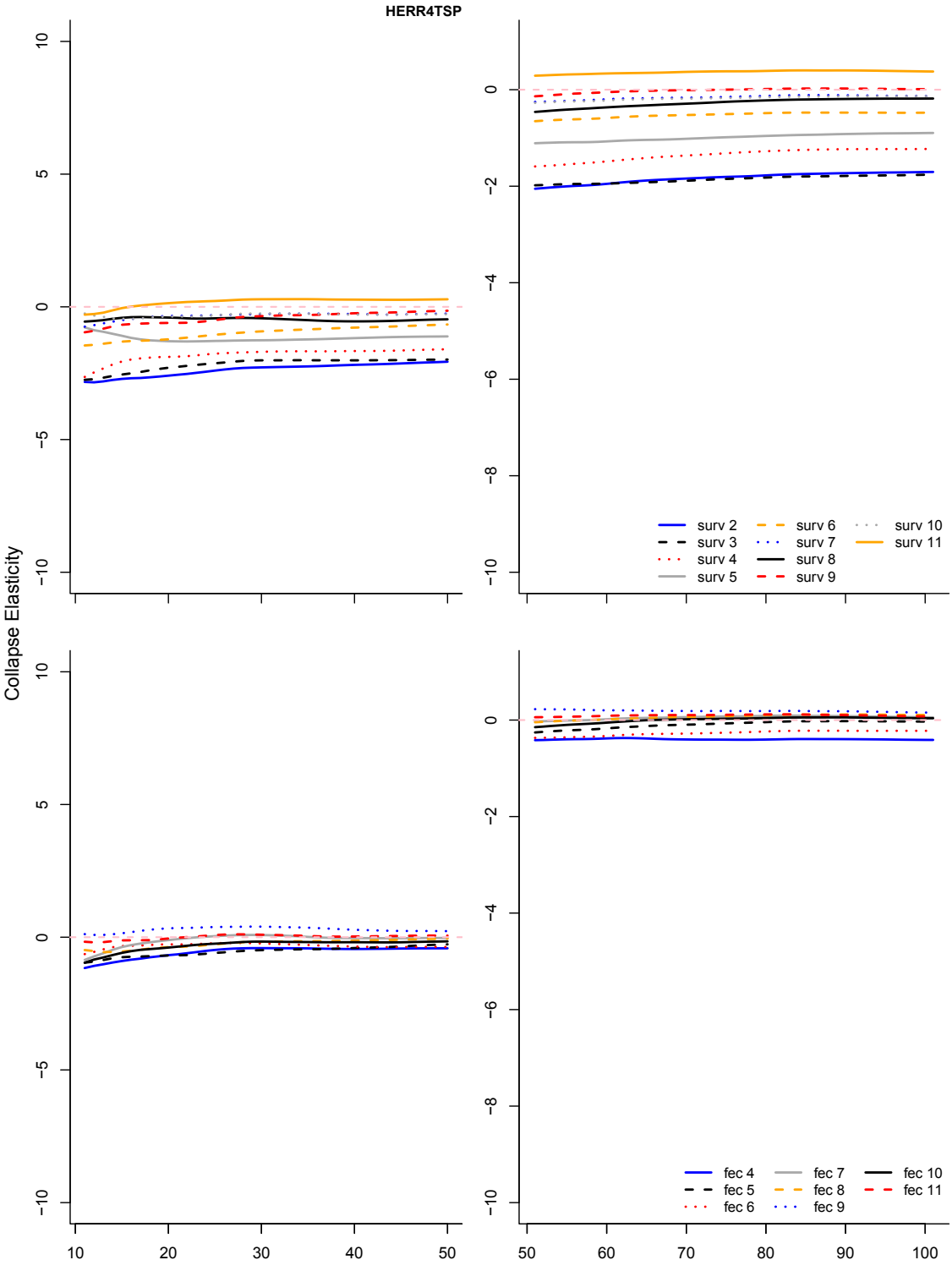

Figure C2q: Time series of the elasticity of the probability of collapse for each survival and fecundity vital rate during a period of typical recruitment for each population (population name at top of figure). Populations with a zero percent probability of collapse after 50 years are excluded from this figure.

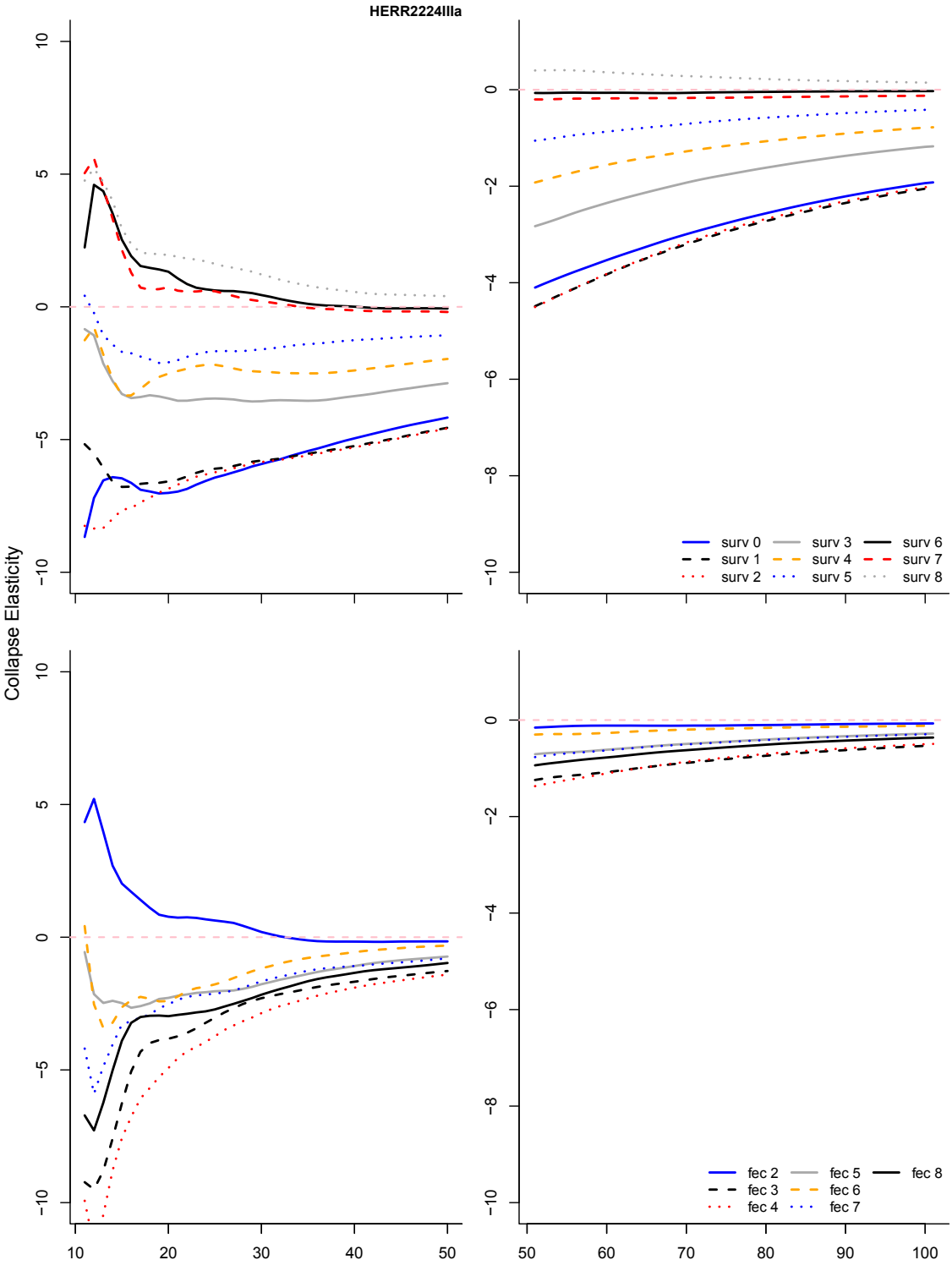

Figure C2r: Time series of the elasticity of the probability of collapse for each survival and fecundity vital rate during a period of typical recruitment for each population (population name at top of figure). Populations with a zero percent probability of collapse after 50 years are excluded from this figure.

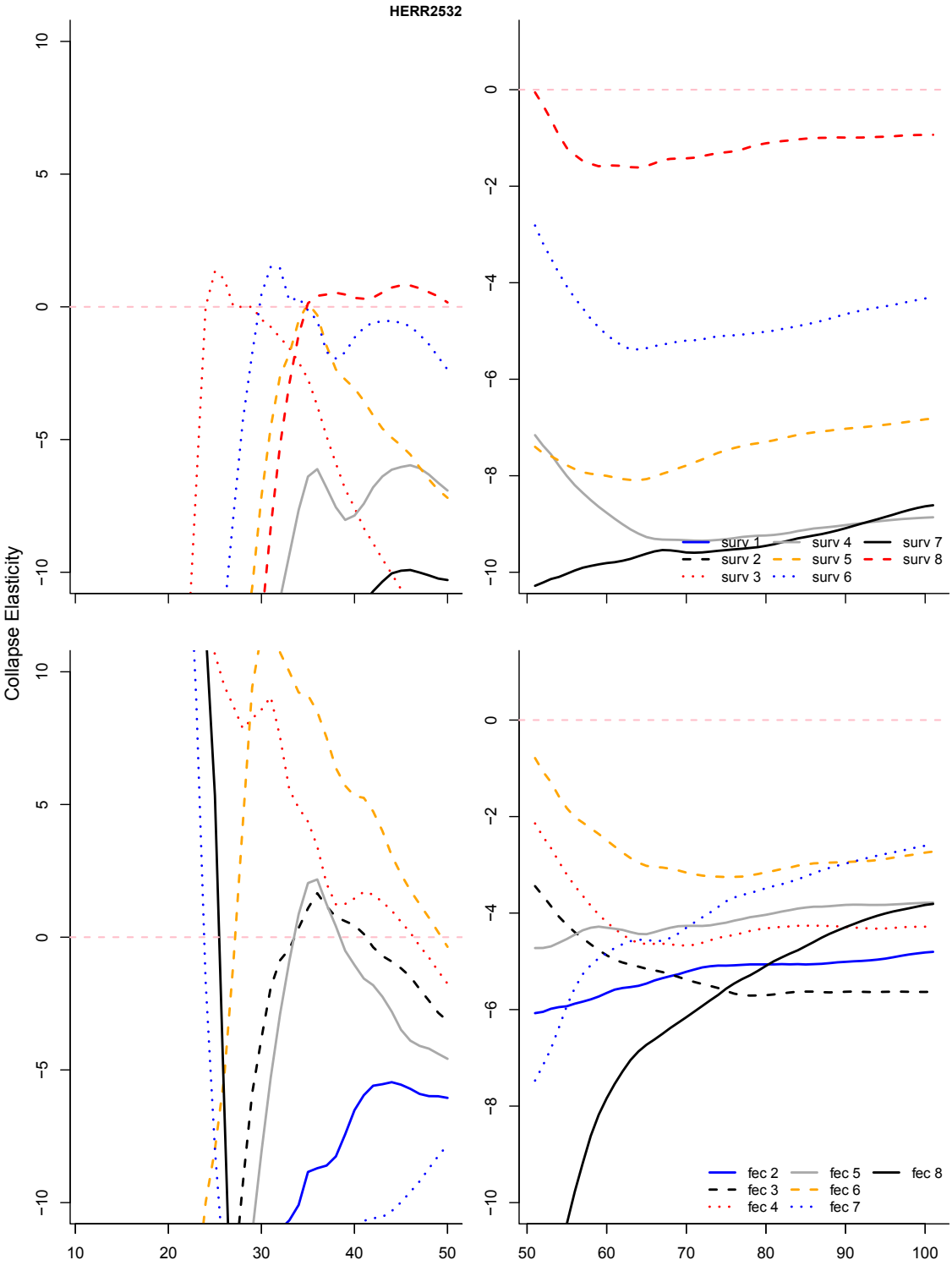

Figure C2s: Time series of the elasticity of the probability of collapse for each survival and fecundity vital rate during a period of typical recruitment for each population (population name at top of figure). Populations with a zero percent probability of collapse after 50 years are excluded from this figure.

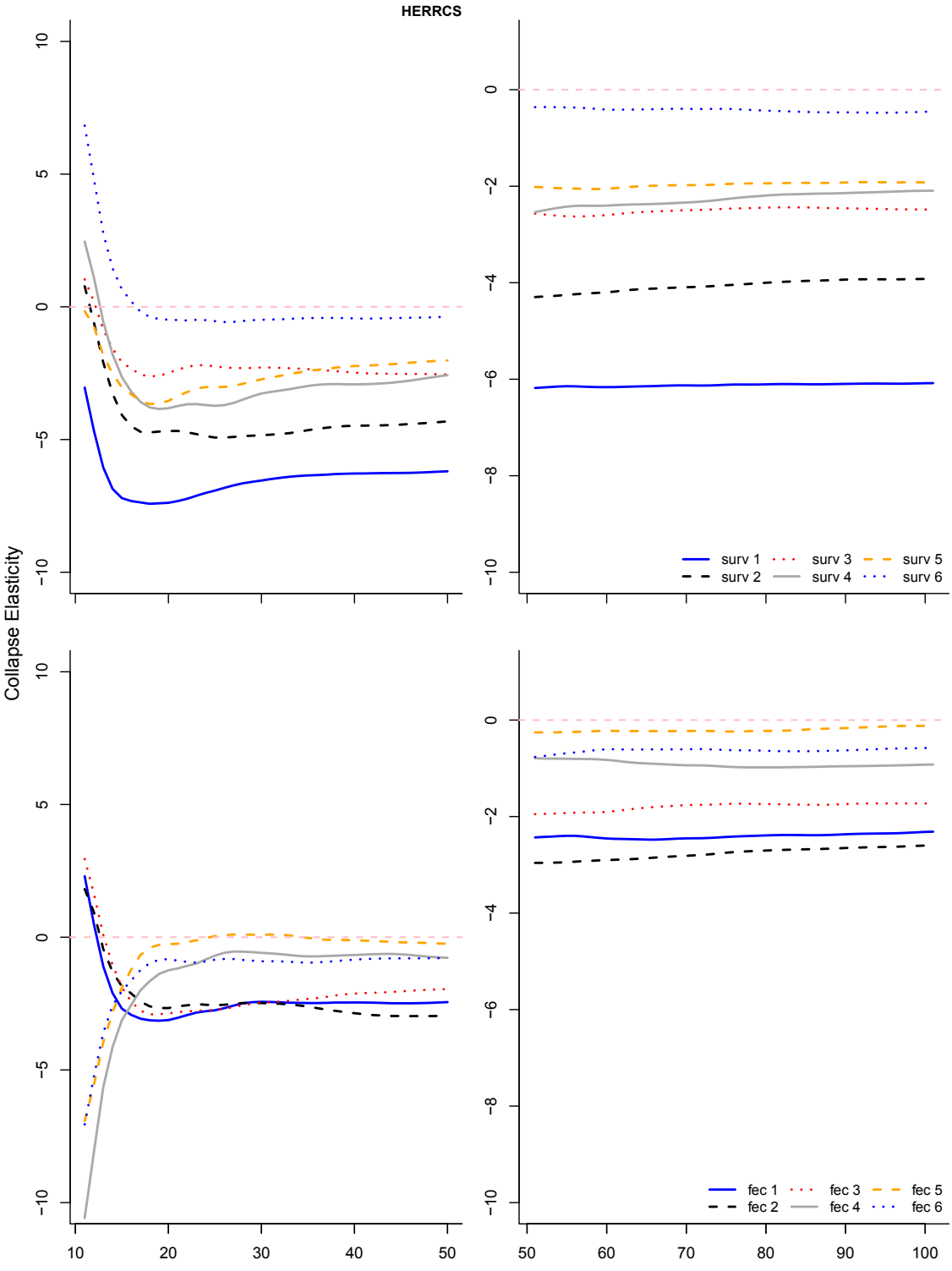

Figure C2t: Time series of the elasticity of the probability of collapse for each survival and fecundity vital rate during a period of typical recruitment for each population (population name at top of figure). Populations with a zero percent probability of collapse after 50 years are excluded from this figure.

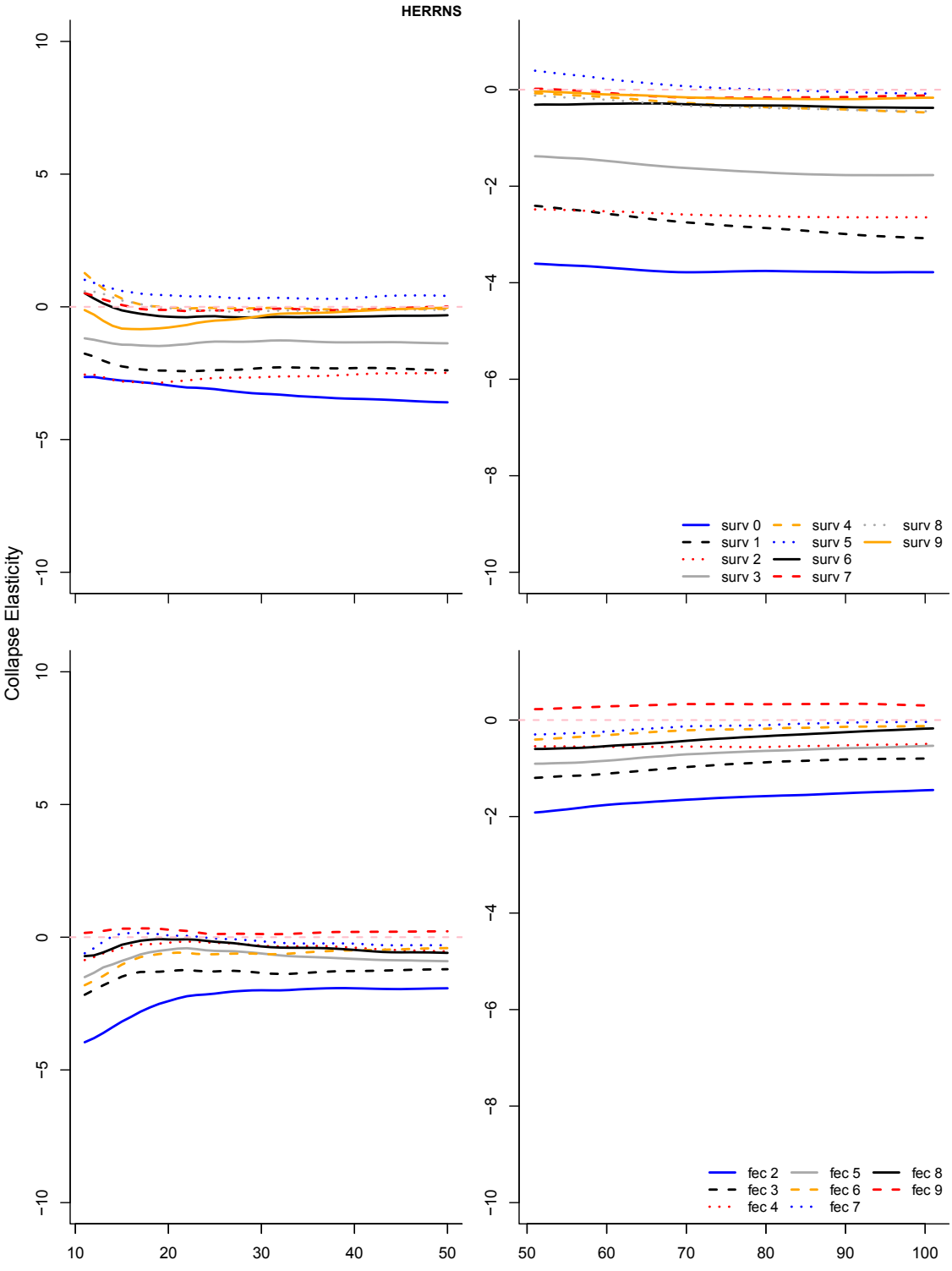

Figure C2u: Time series of the elasticity of the probability of collapse for each survival and fecundity vital rate during a period of typical recruitment for each population (population name at top of figure). Populations with a zero percent probability of collapse after 50 years are excluded from this figure.

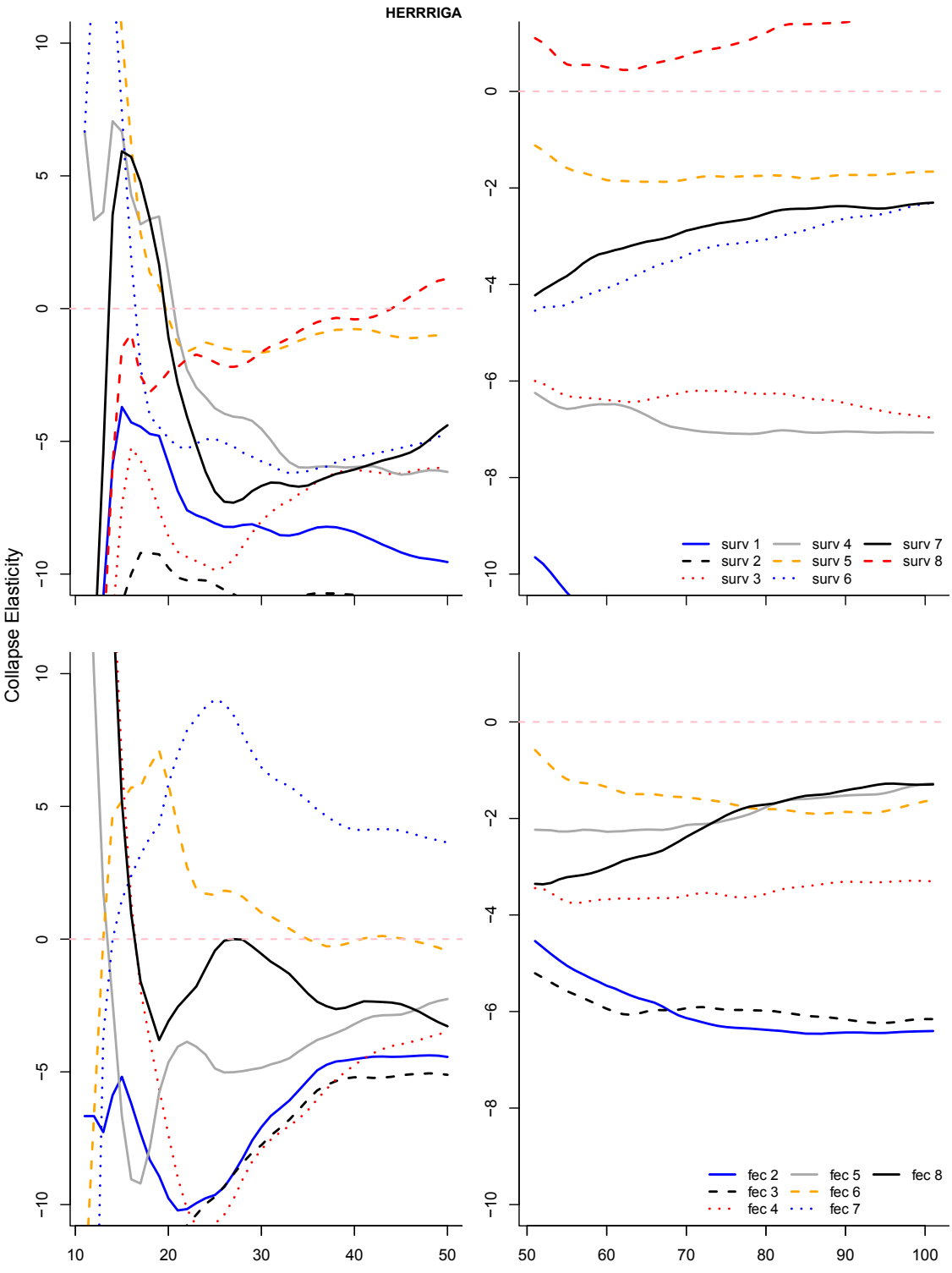

Figure C2v: Time series of the elasticity of the probability of collapse for each survival and fecundity vital rate during a period of typical recruitment for each population (population name at top of figure). Populations with a zero percent probability of collapse after 50 years are excluded from this figure.

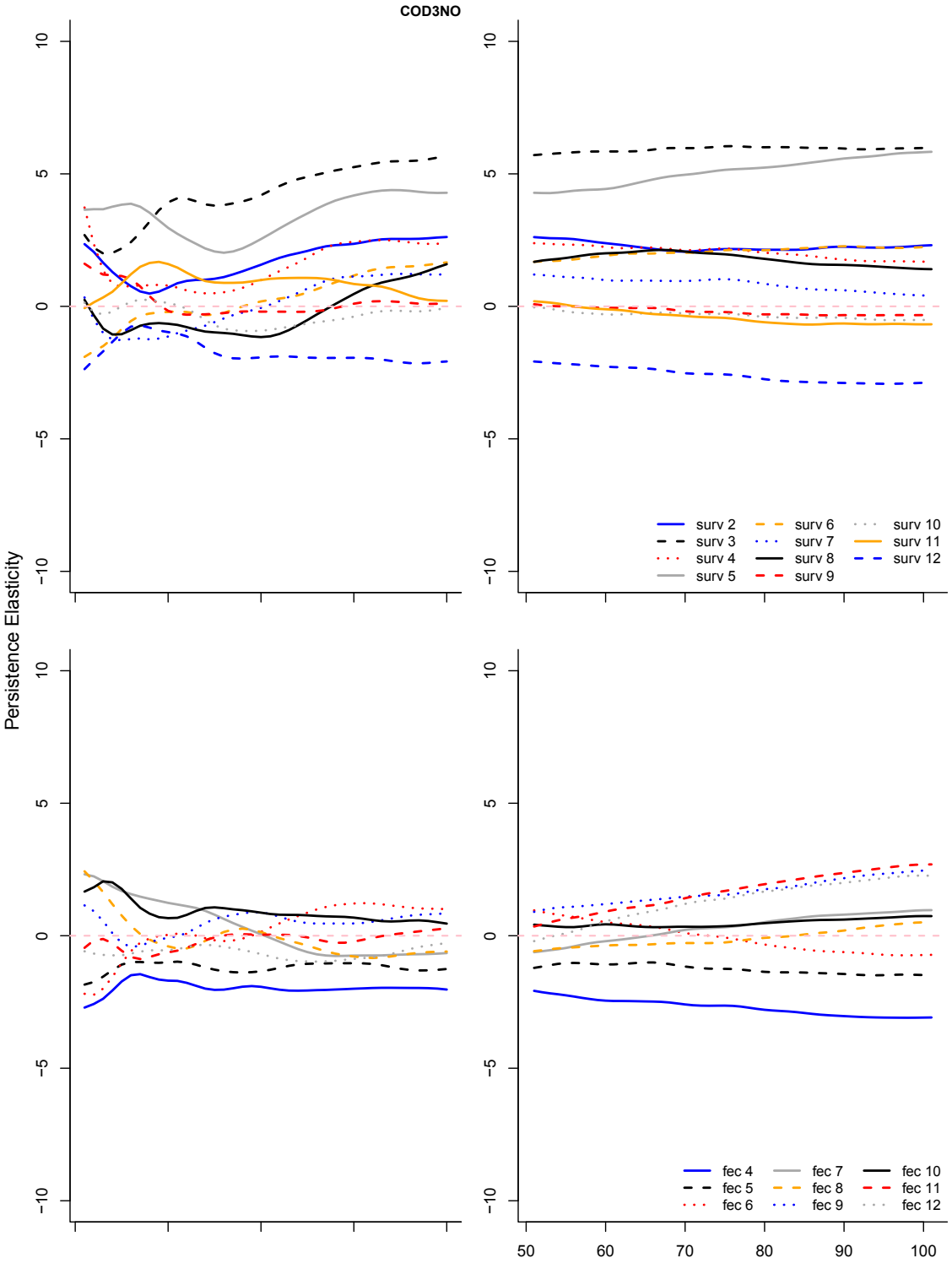

Figure C3a: Time series of the elasticity of the probability of persistence for each survival and fertility vital rate during periods of typical recruitment for each population (population name at top of figure). Populations with a zero percent probability of recovery after 50 years are excluded from this figure.

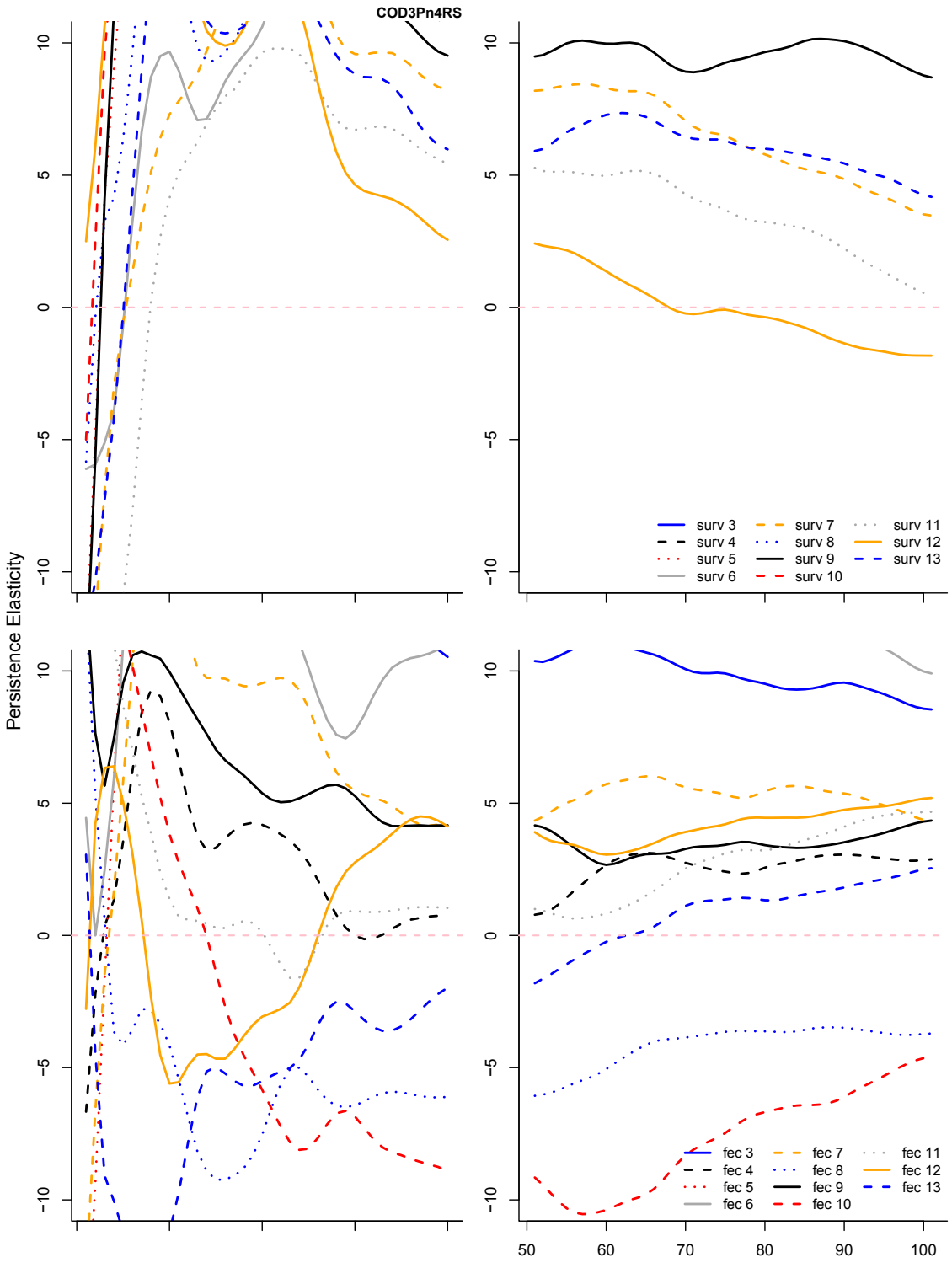

Figure C3b: Time series of the elasticity of the probability of persistence for each survival and fertility vital rate during periods of typical recruitment for each population (population name at top of figure). Populations with a zero percent probability of recovery after 50 years are excluded from this figure.

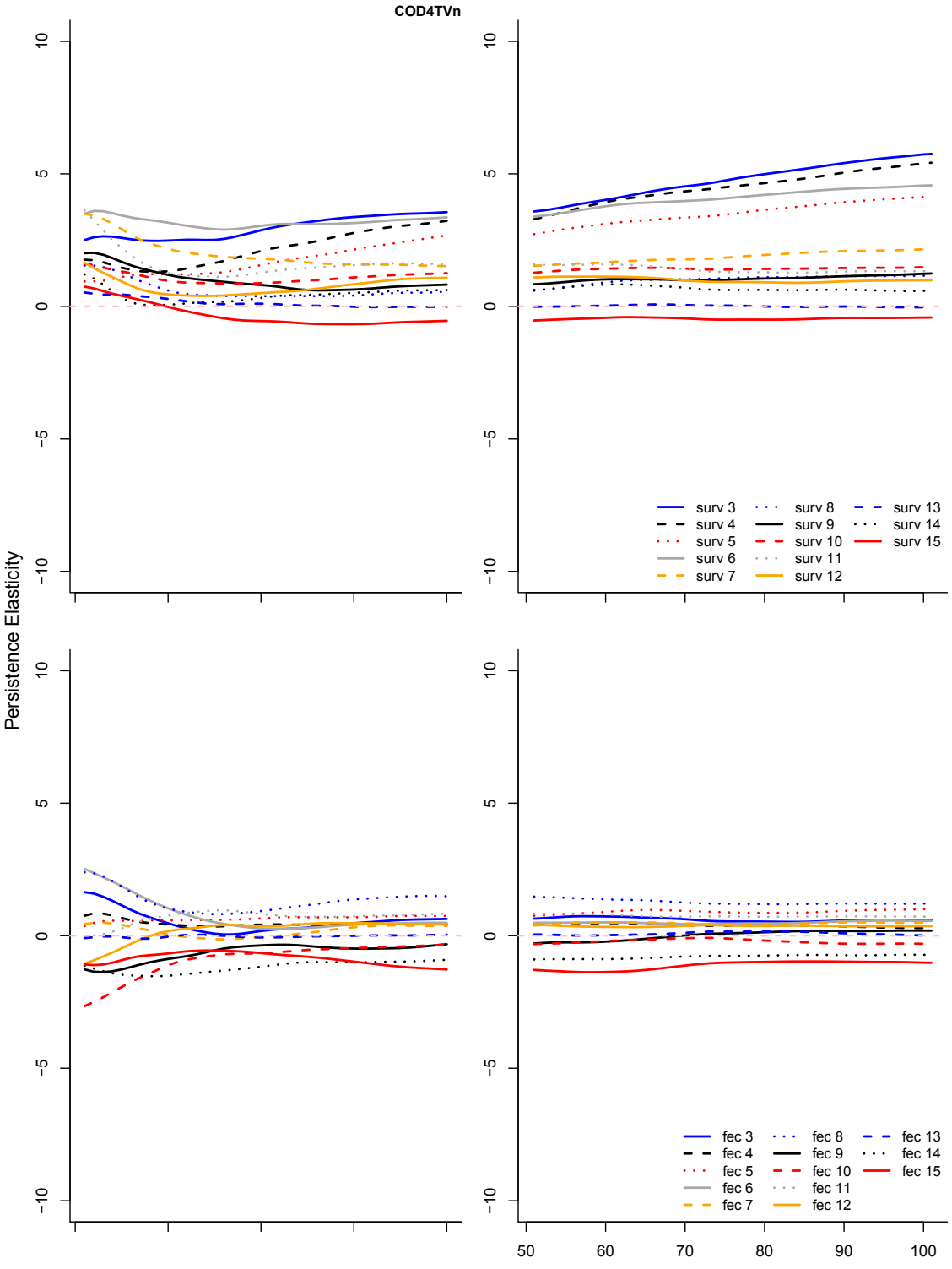

Figure C3c: Time series of the elasticity of the probability of persistence for each survival and fertility vital rate during periods of typical recruitment for each population (population name at top of figure). Populations with a zero percent probability of recovery after 50 years are excluded from this figure.

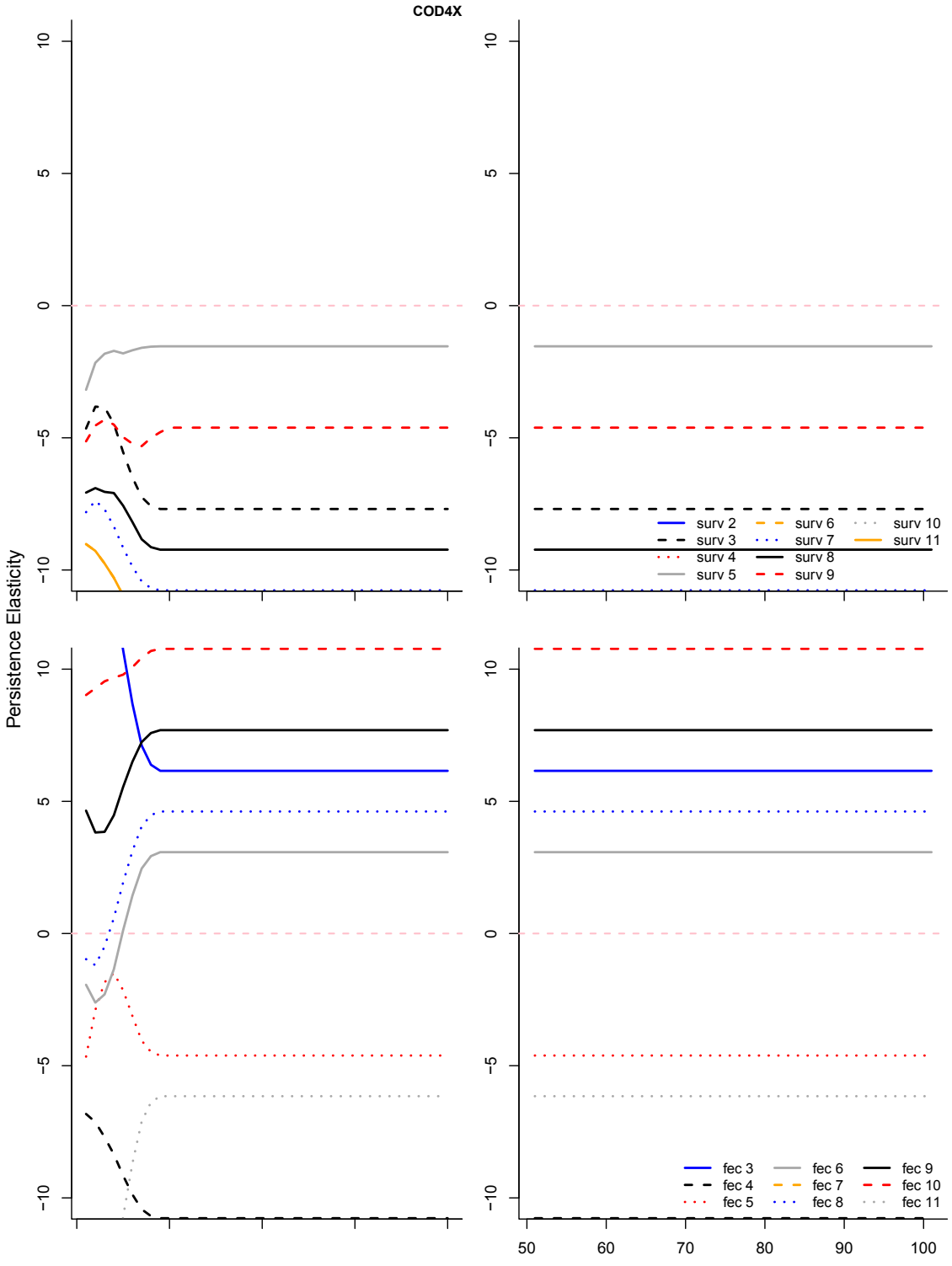

Figure C3d: Time series of the elasticity of the probability of persistence for each survival and fertility vital rate during periods of typical recruitment for each population (population name at top of figure). Populations with a zero percent probability of recovery after 50 years are excluded from this figure.

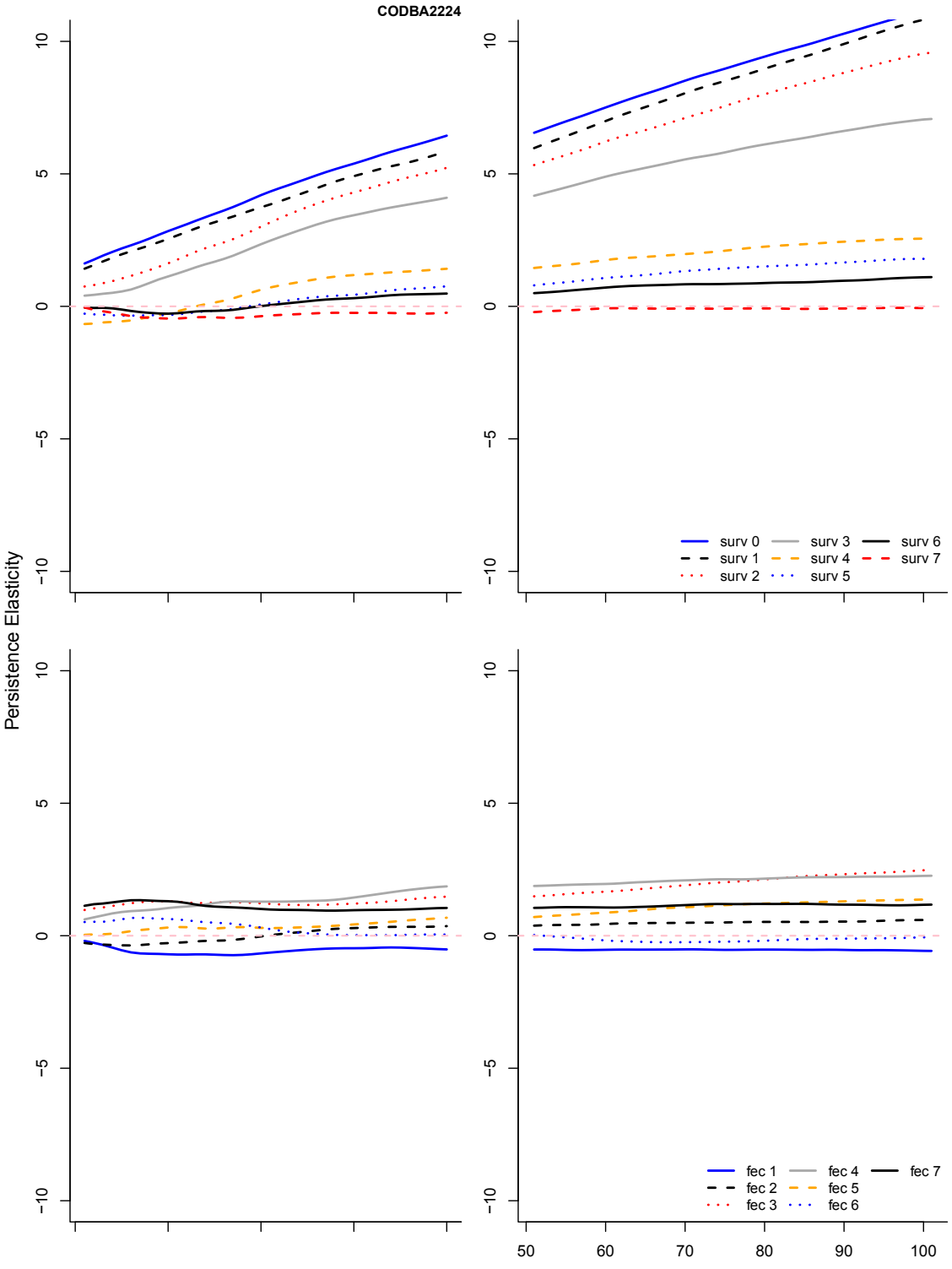

Figure C3e: Time series of the elasticity of the probability of persistence for each survival and fertility vital rate during periods of typical recruitment for each population (population name at top of figure). Populations with a zero percent probability of recovery after 50 years are excluded from this figure.

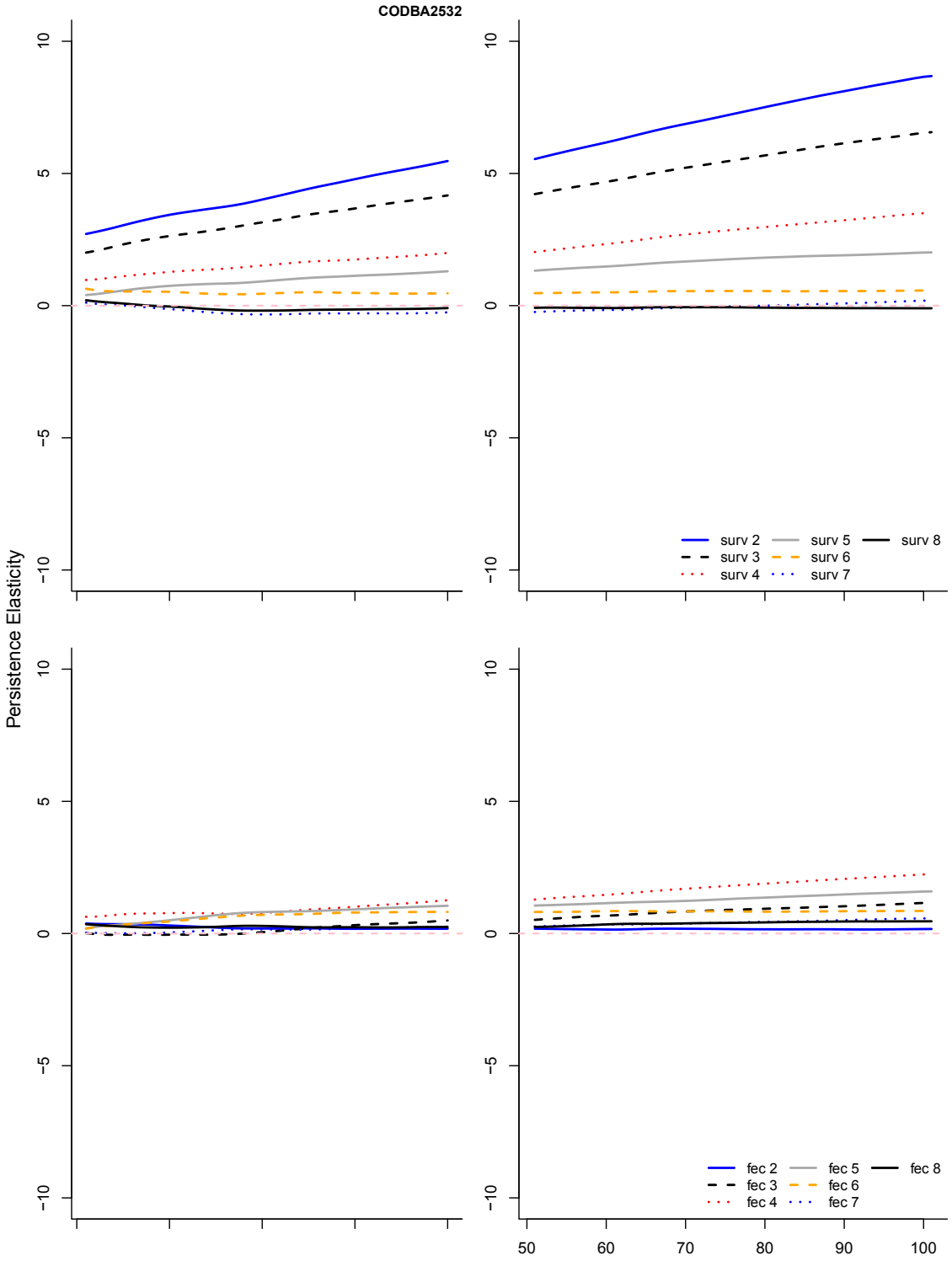

Figure C3f: Time series of the elasticity of the probability of persistence for each survival and fertility vital rate during periods of typical recruitment for each population (population name at top of figure). Populations with a zero percent probability of recovery after 50 years are excluded from this figure.

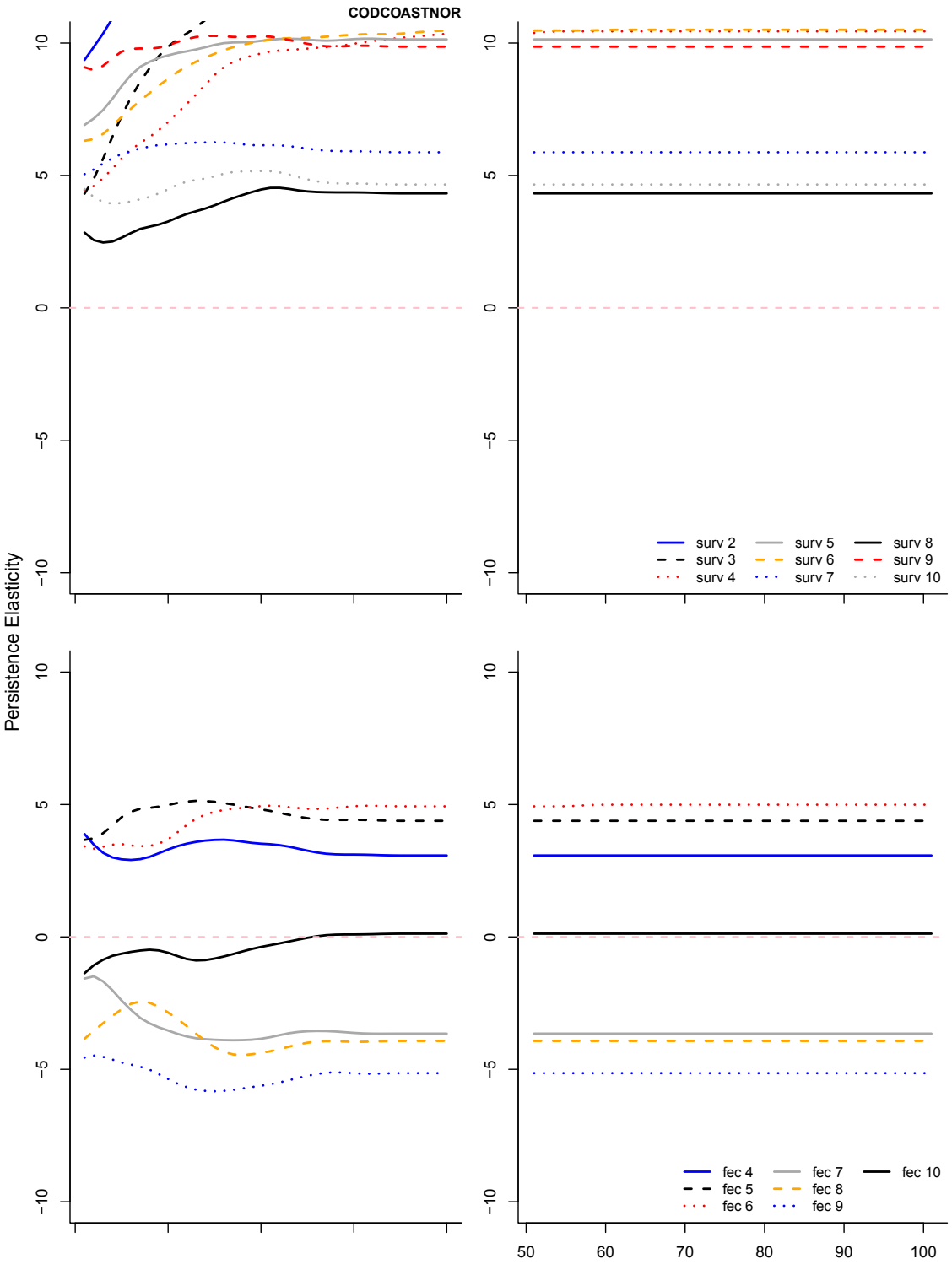

Figure C3g: Time series of the elasticity of the probability of persistence for each survival and fertility vital rate during periods of typical recruitment for each population (population name at top of figure). Populations with a zero percent probability of recovery after 50 years are excluded from this figure.

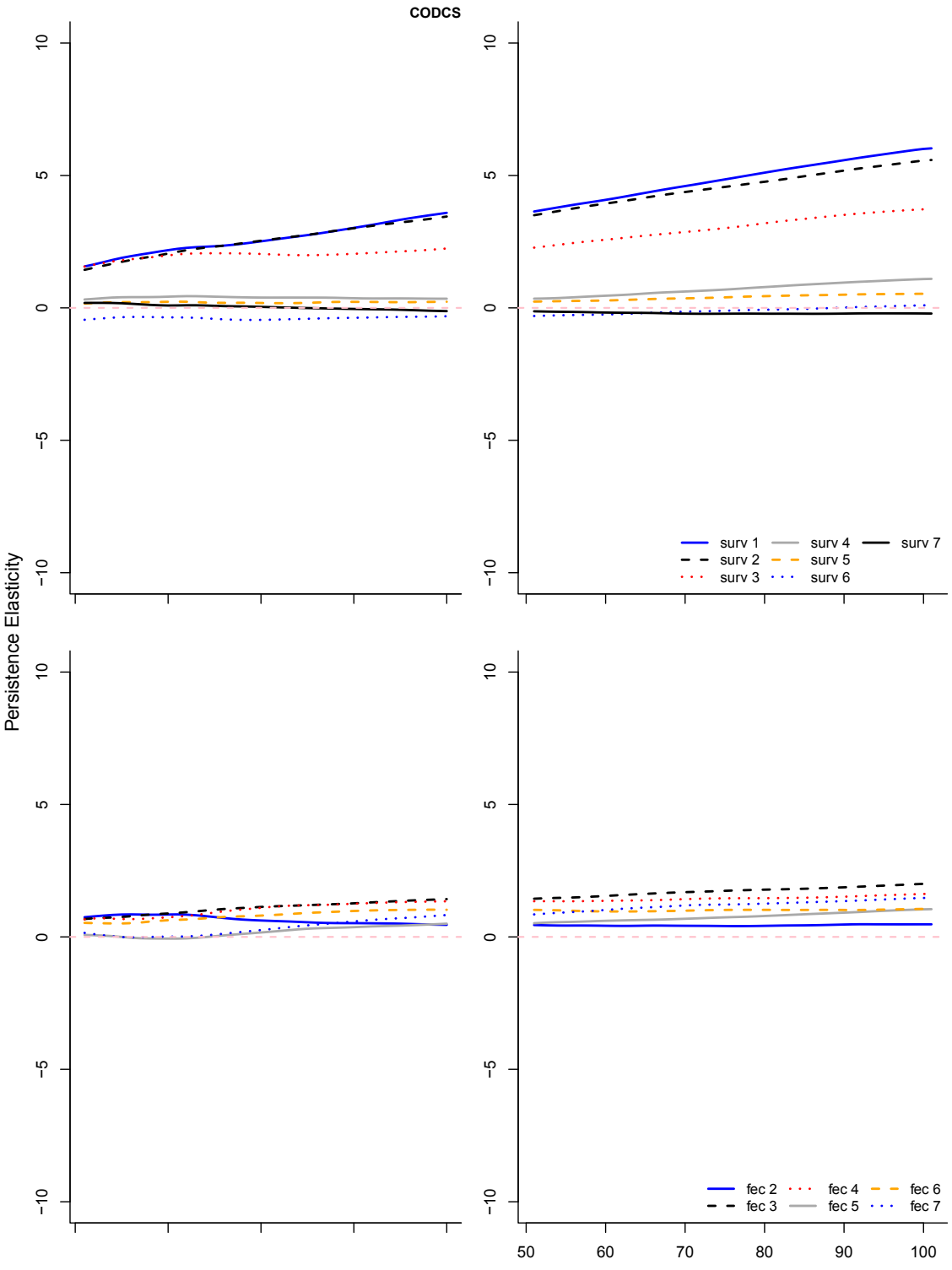

Figure C3h: Time series of the elasticity of the probability of persistence for each survival and fertility vital rate during periods of typical recruitment for each population (population name at top of figure). Populations with a zero percent probability of recovery after 50 years are excluded from this figure.

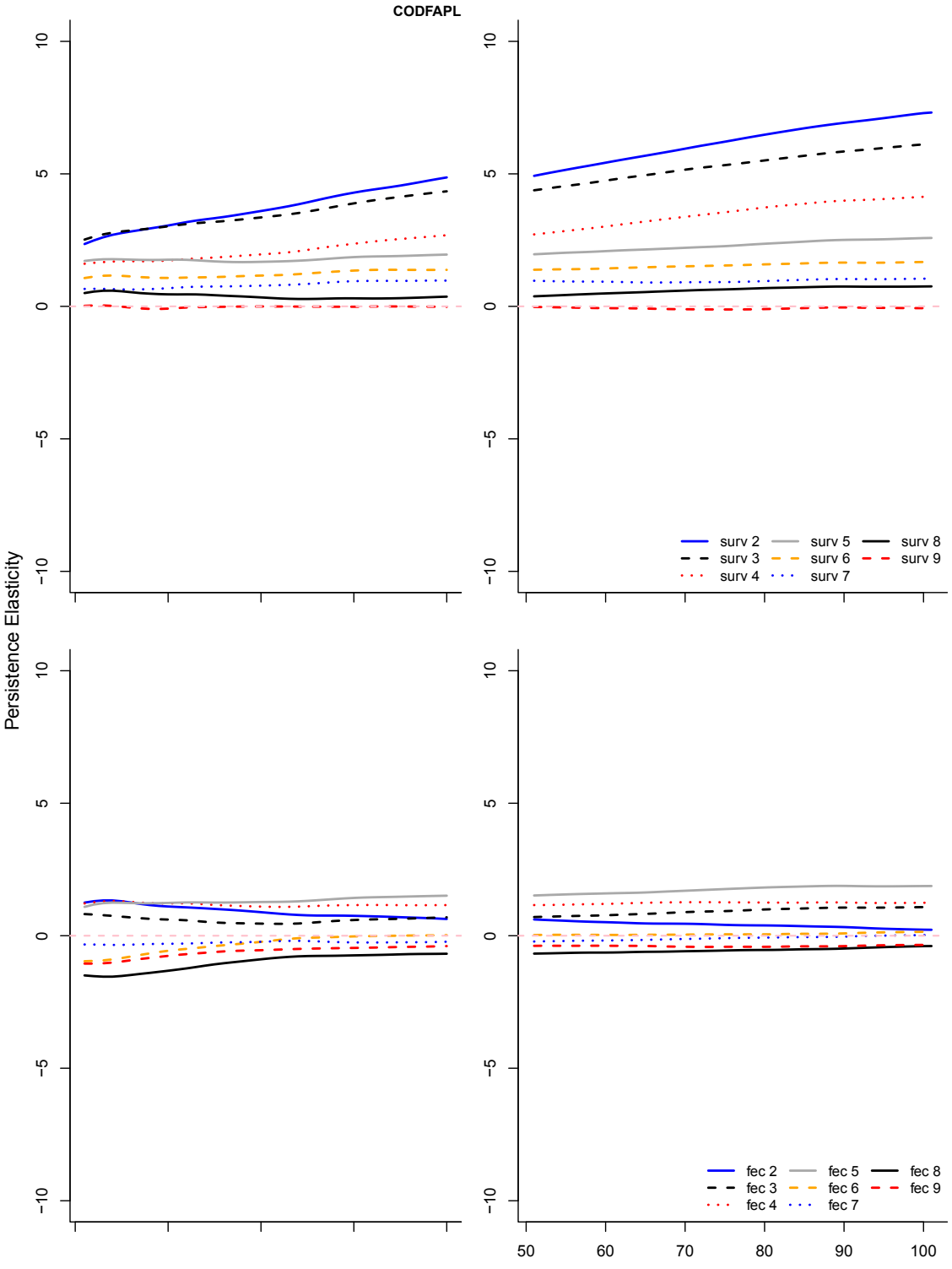

Figure C3i: Time series of the elasticity of the probability of persistence for each survival and fertility vital rate during periods of typical recruitment for each population (population name at top of figure). Populations with a zero percent probability of recovery after 50 years are excluded from this figure.

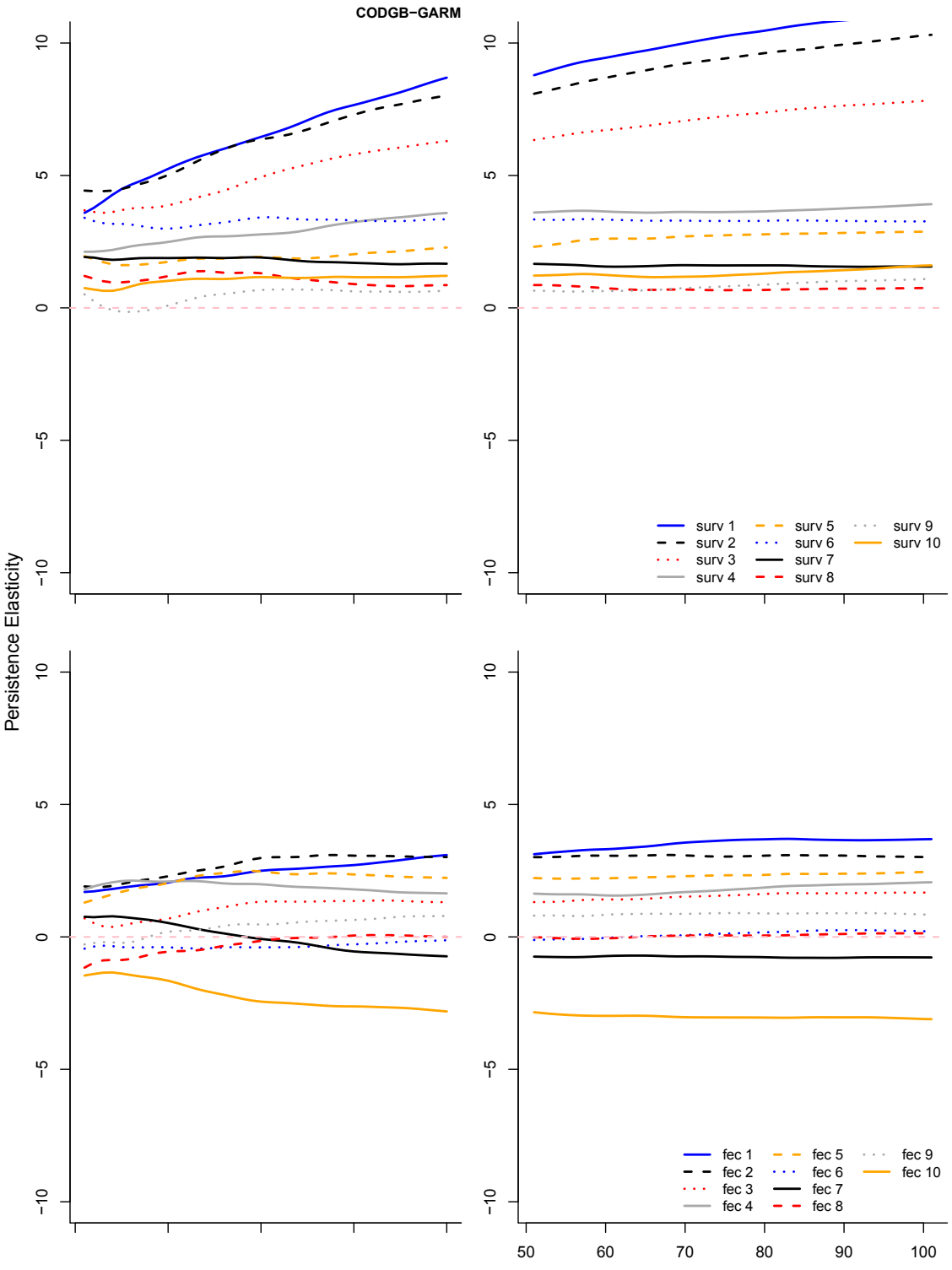

Figure C3j: Time series of the elasticity of the probability of persistence for each survival and fertility vital rate during periods of typical recruitment for each population (population name at top of figure). Populations with a zero percent probability of recovery after 50 years are excluded from this figure.

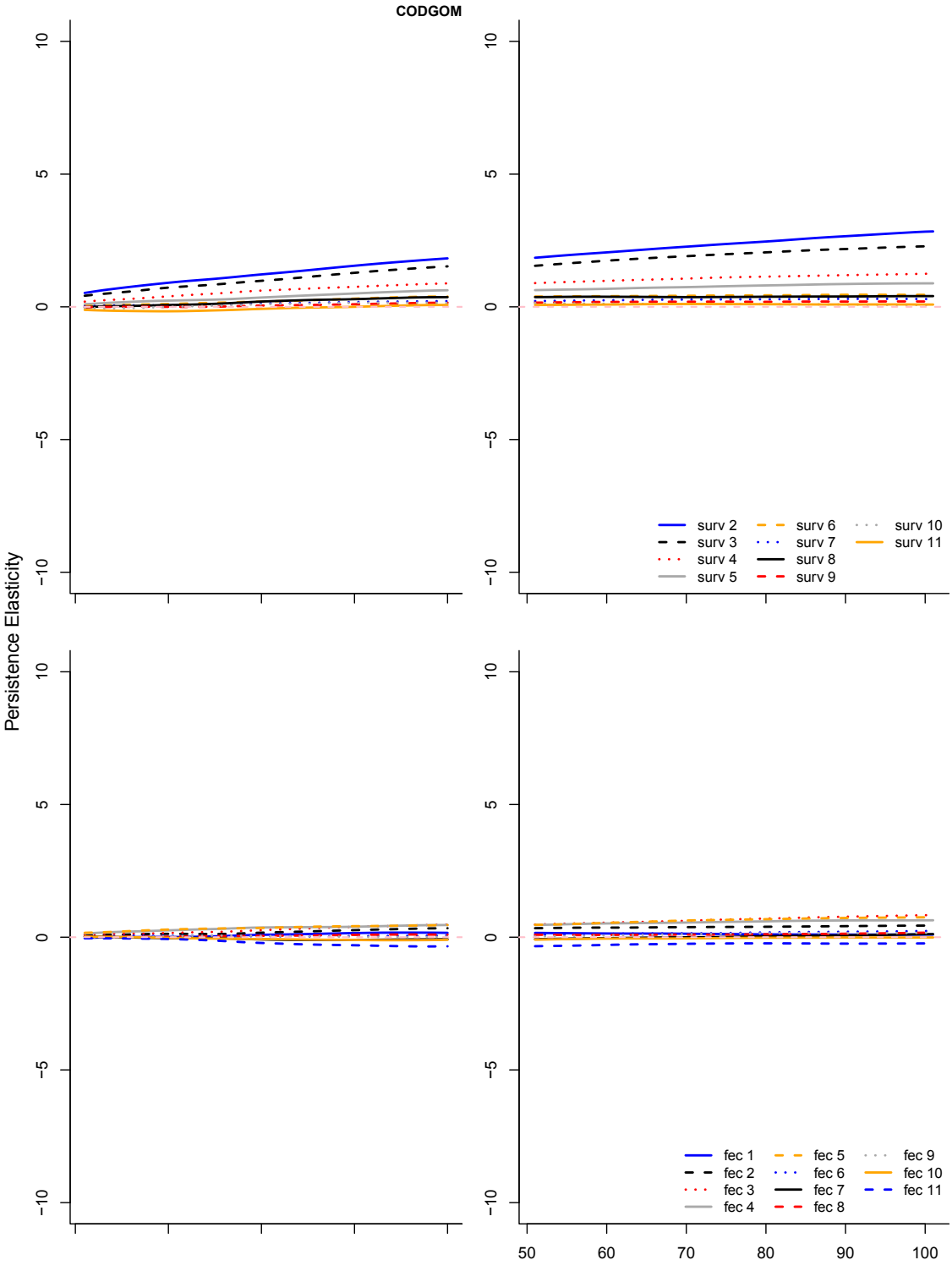

Figure C3k: Time series of the elasticity of the probability of persistence for each survival and fertility vital rate during periods of typical recruitment for each population (population name at top of figure). Populations with a zero percent probability of recovery after 50 years are excluded from this figure.

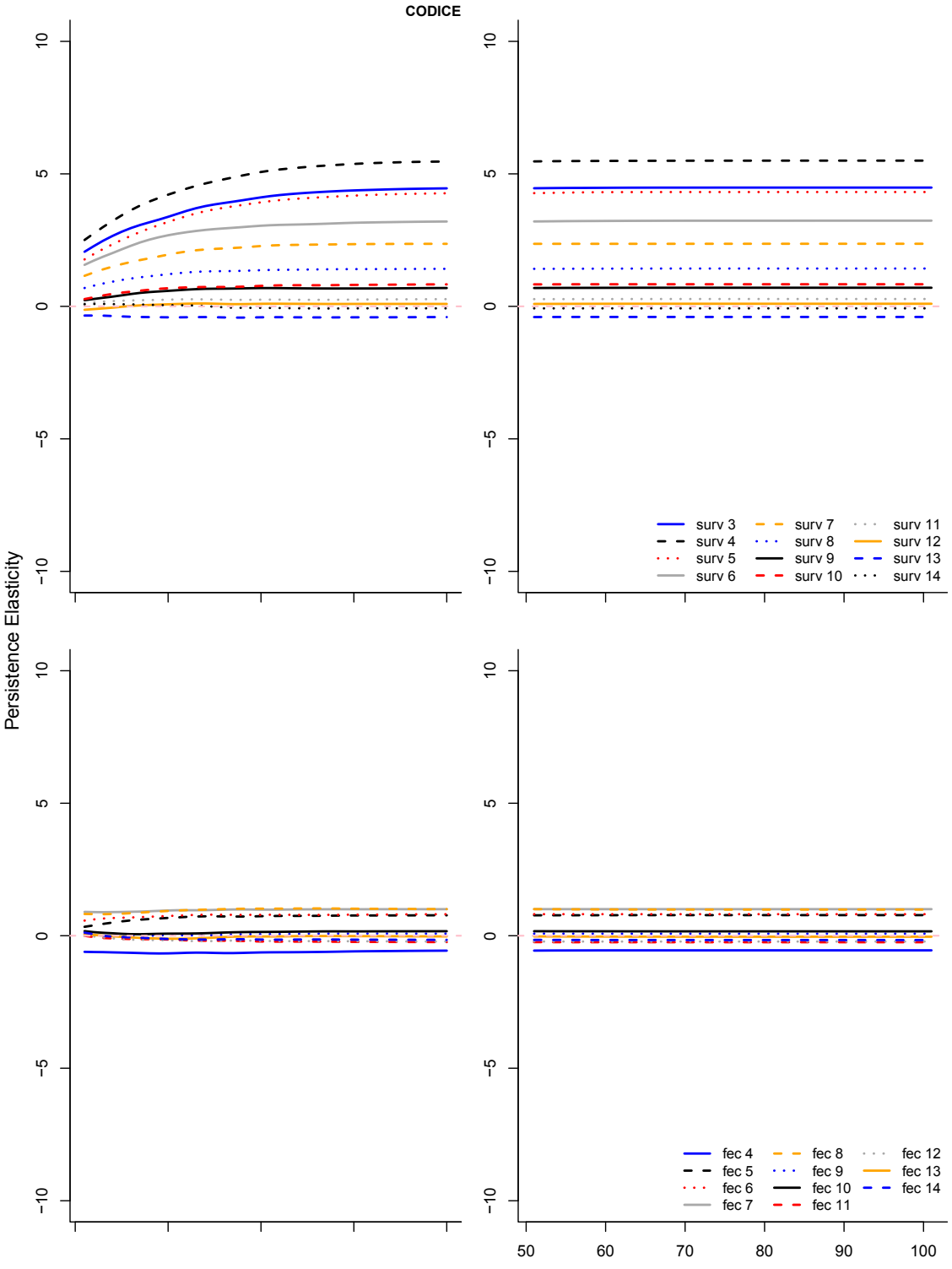

Figure C3l: Time series of the elasticity of the probability of persistence for each survival and fertility vital rate during periods of typical recruitment for each population (population name at top of figure). Populations with a zero percent probability of recovery after 50 years are excluded from this figure.

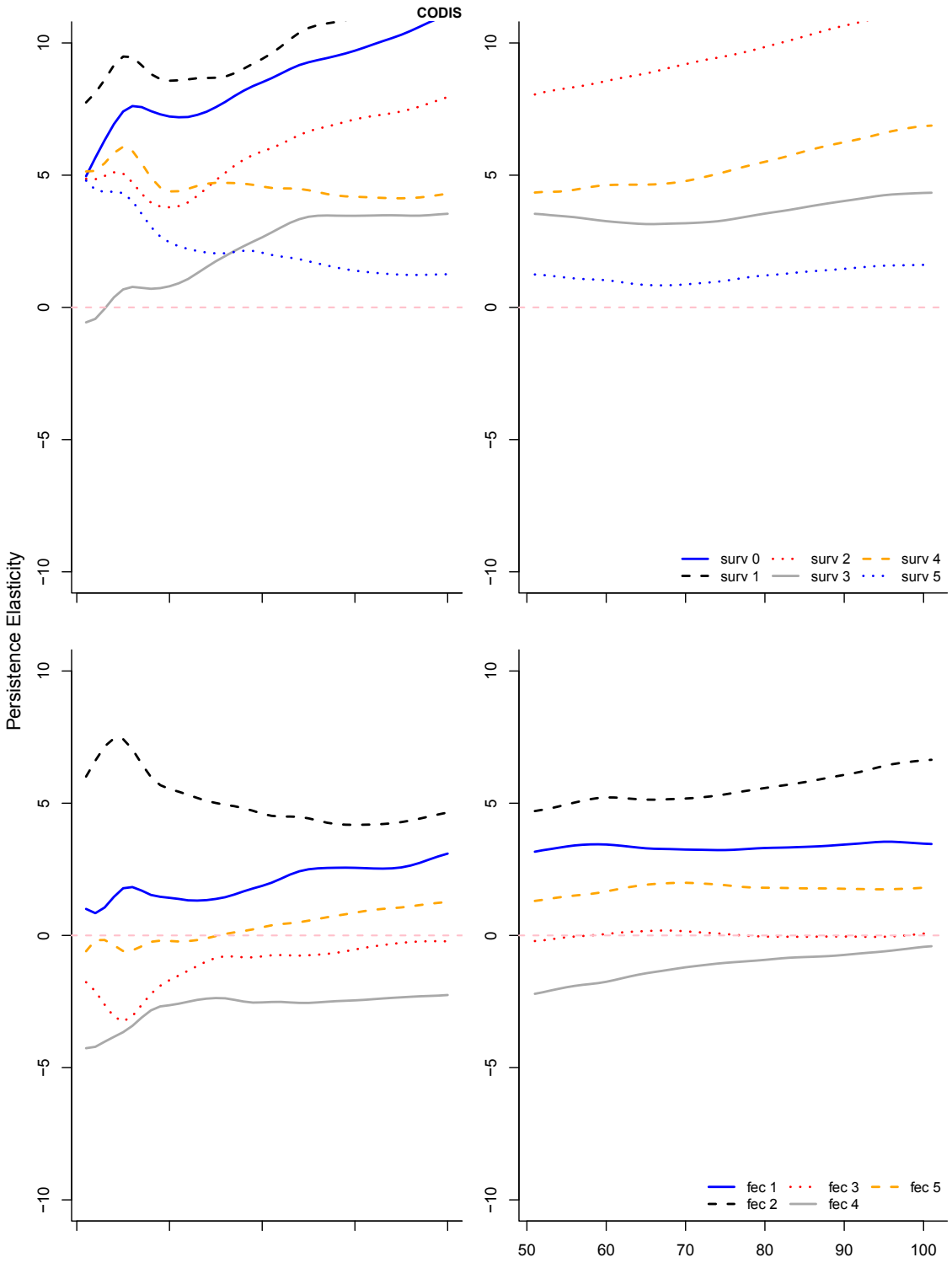

Figure C3m: Time series of the elasticity of the probability of persistence for each survival and fertility vital rate during periods of typical recruitment for each population (population name at top of figure). Populations with a zero percent probability of recovery after 50 years are excluded from this figure.

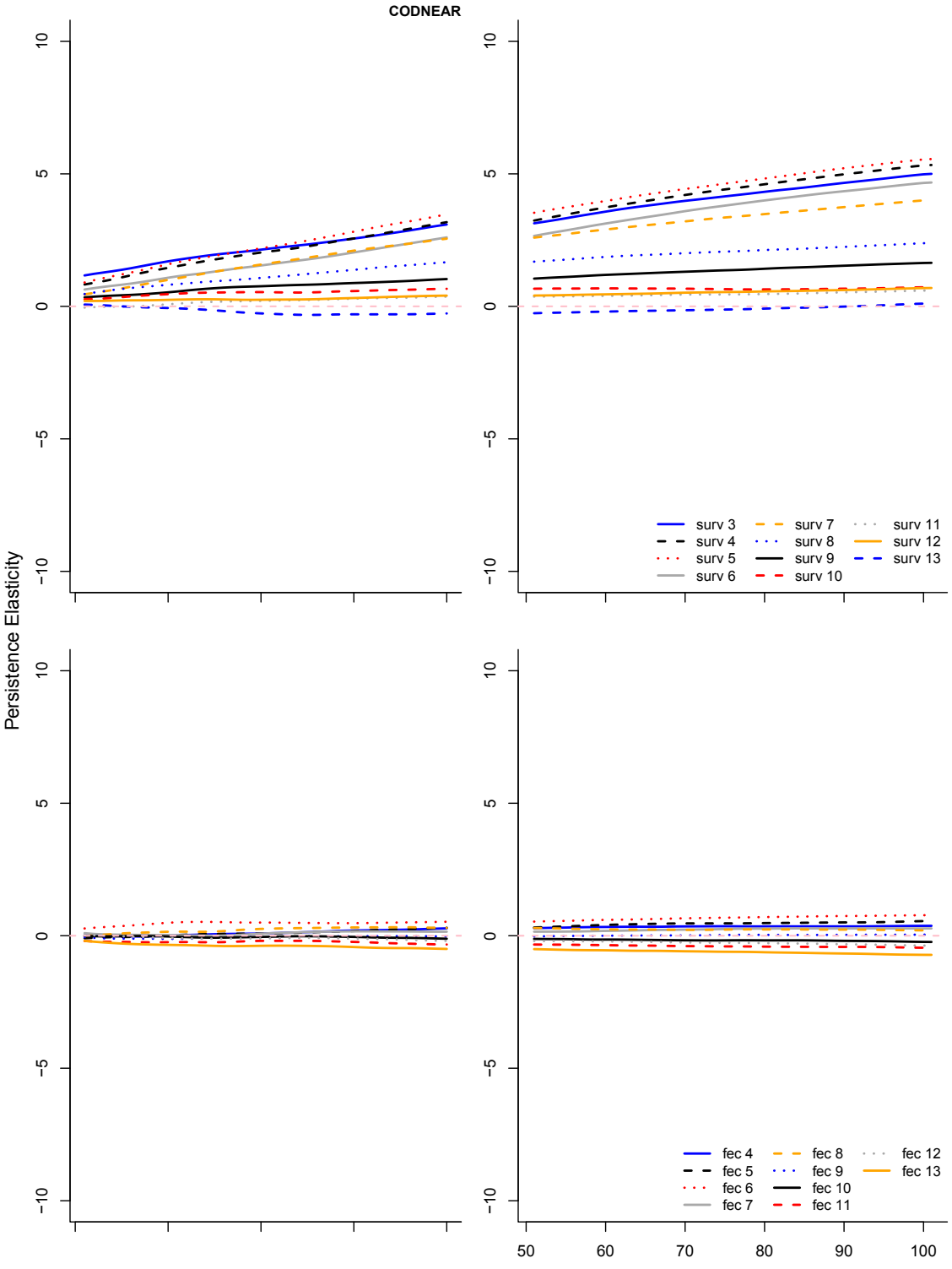

Figure C3n: Time series of the elasticity of the probability of persistence for each survival and fertility vital rate during periods of typical recruitment for each population (population name at top of figure). Populations with a zero percent probability of recovery after 50 years are excluded from this figure.

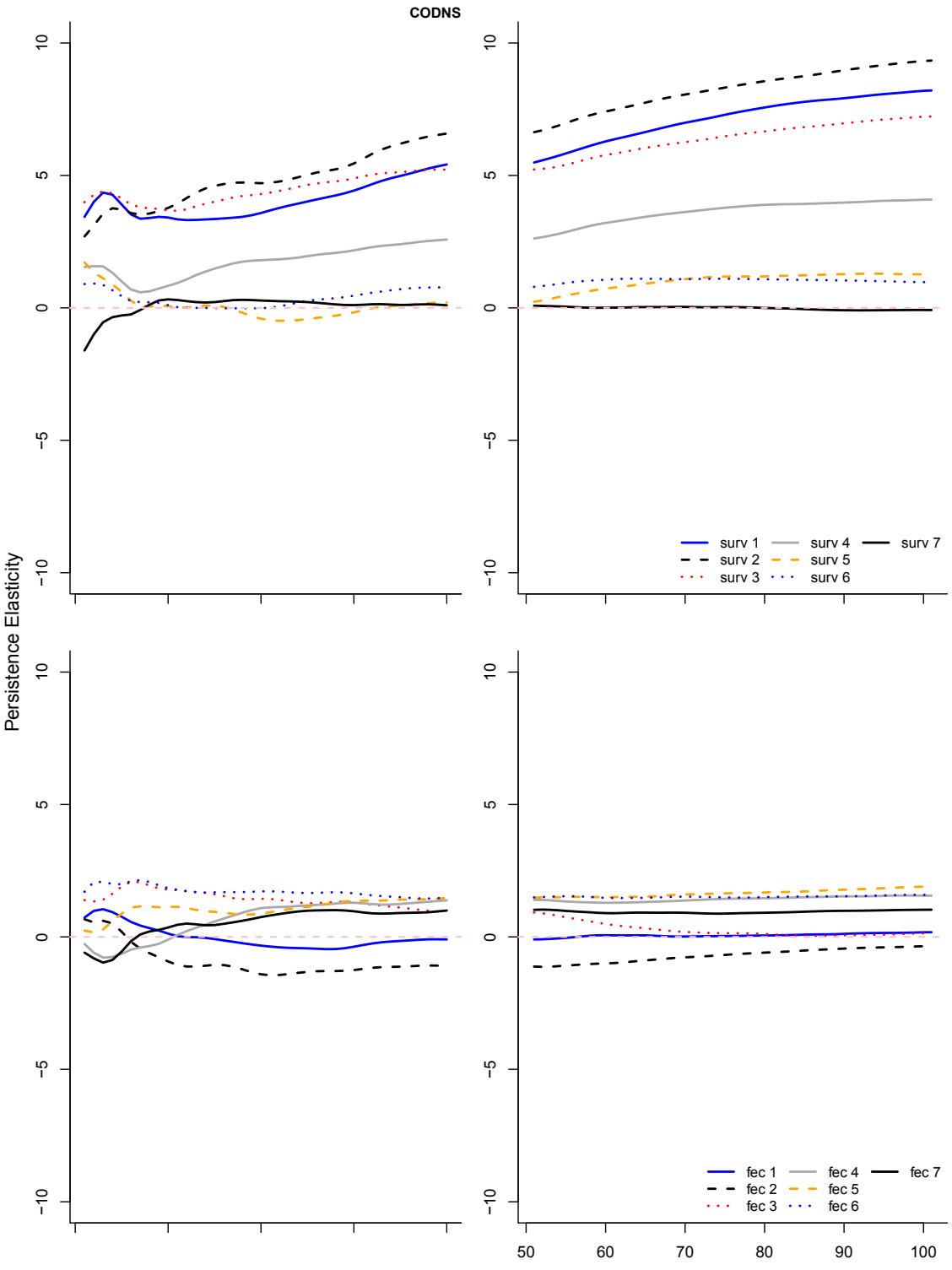

Figure C3o: Time series of the elasticity of the probability of persistence for each survival and fertility vital rate during periods of typical recruitment for each population (population name at top of figure). Populations with a zero percent probability of recovery after 50 years are excluded from this figure.

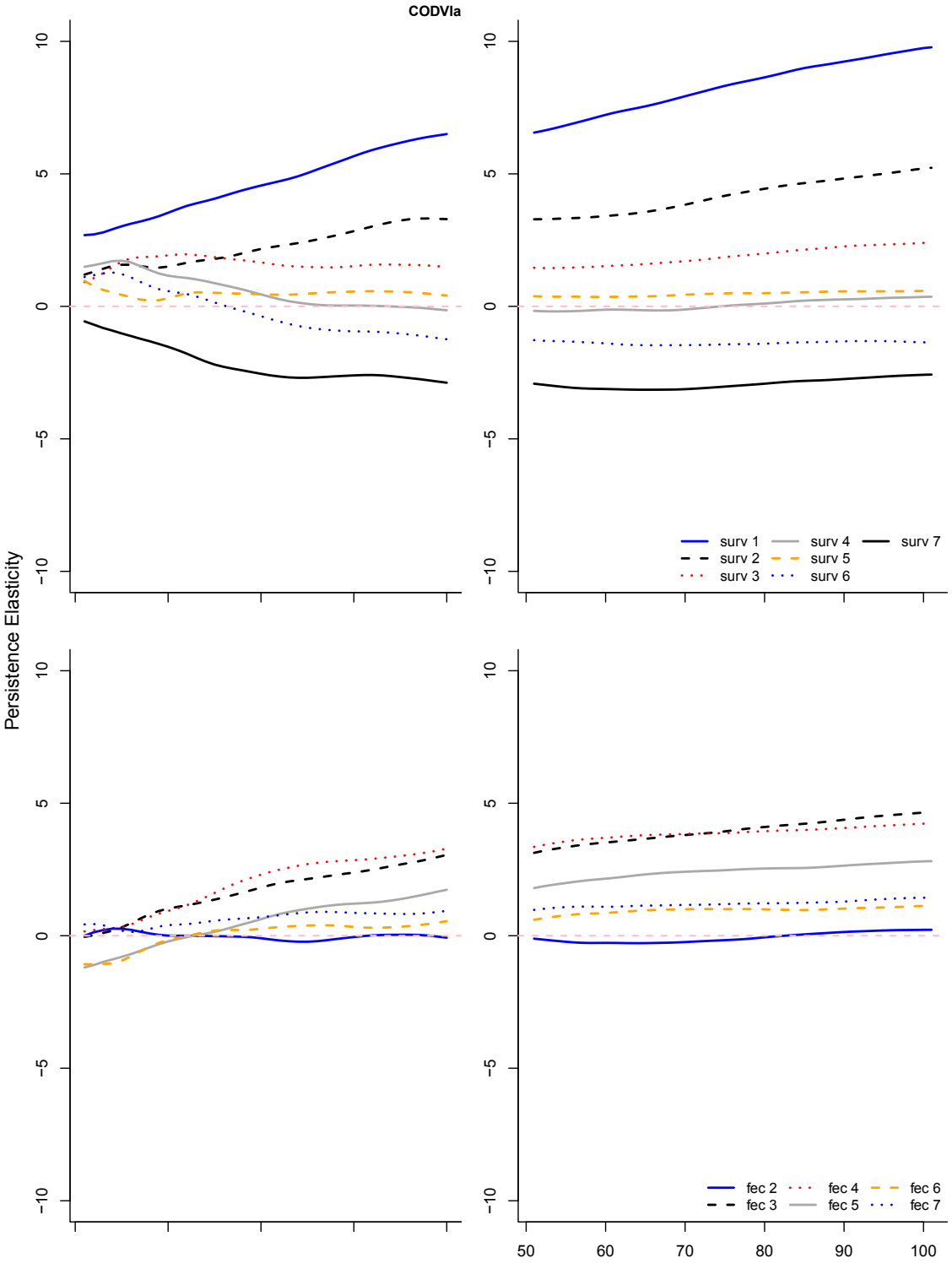

Figure C3p: Time series of the elasticity of the probability of persistence for each survival and fertility vital rate during periods of typical recruitment for each population (population name at top of figure). Populations with a zero percent probability of recovery after 50 years are excluded from this figure.

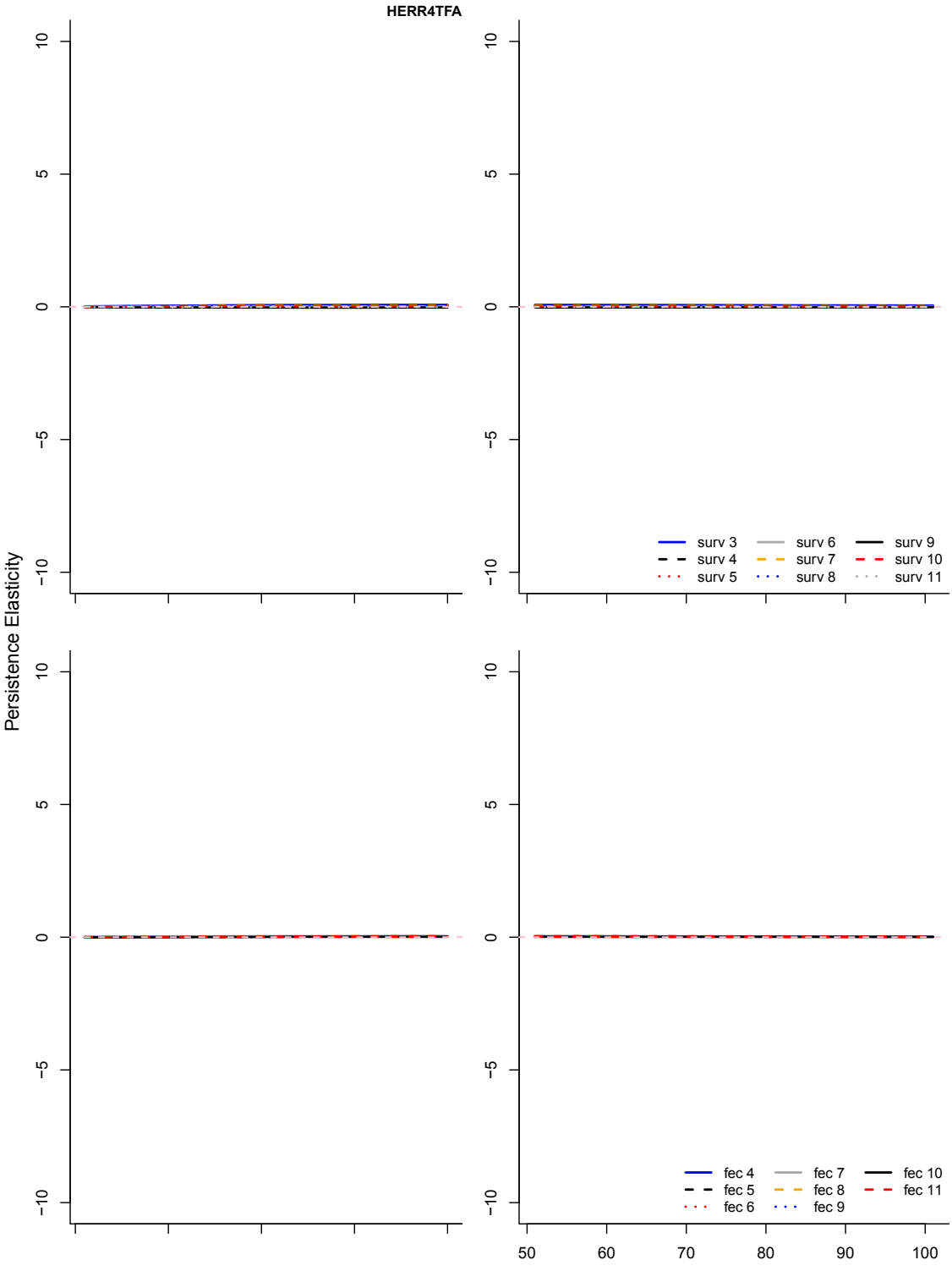

Figure C3q: Time series of the elasticity of the probability of persistence for each survival and fertility vital rate during periods of typical recruitment for each population (population name at top of figure). Populations with a zero percent probability of recovery after 50 years are excluded from this figure.

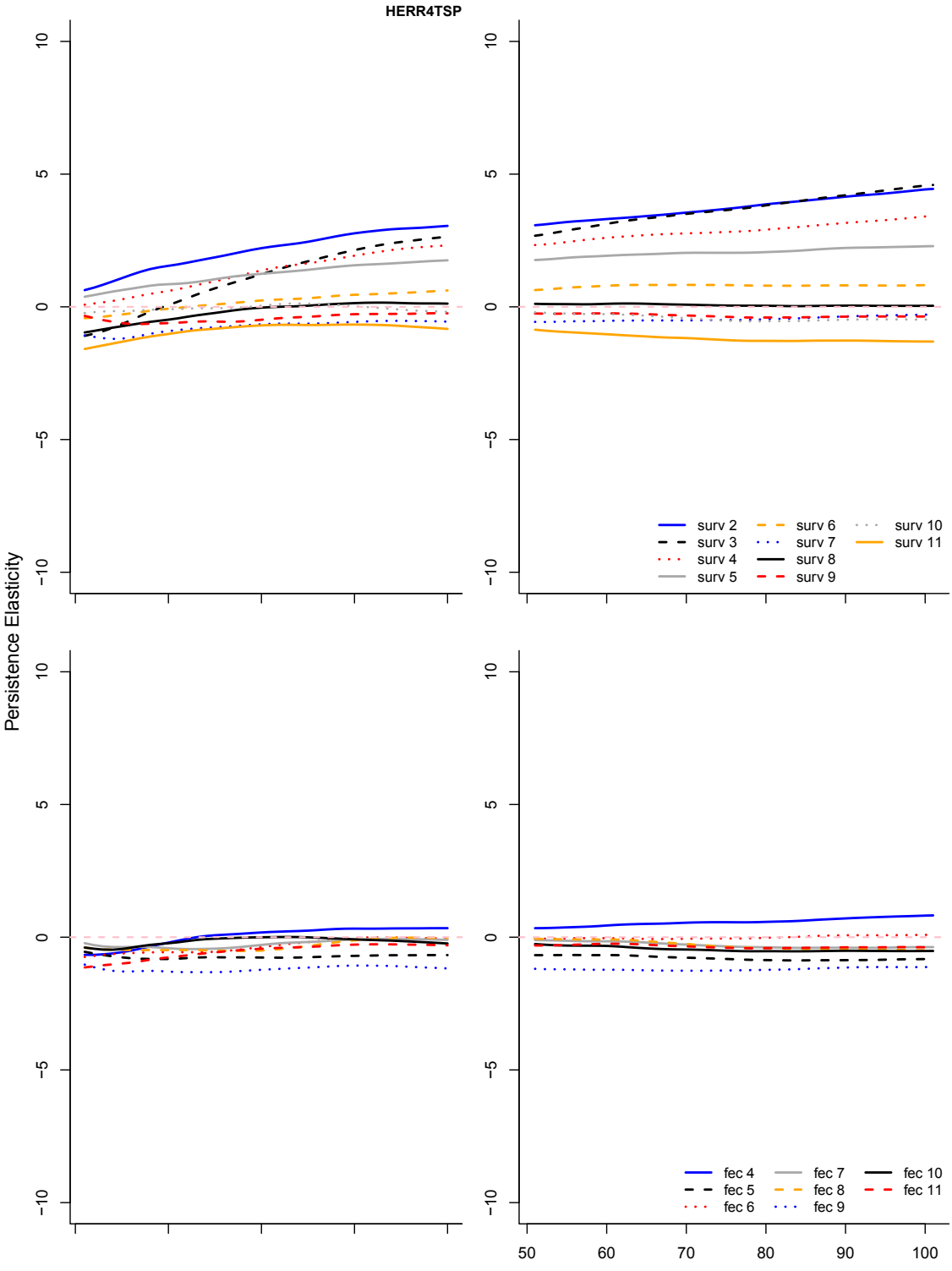

Figure C3r: Time series of the elasticity of the probability of persistence for each survival and fertility vital rate during periods of typical recruitment for each population (population name at top of figure). Populations with a zero percent probability of recovery after 50 years are excluded from this figure.

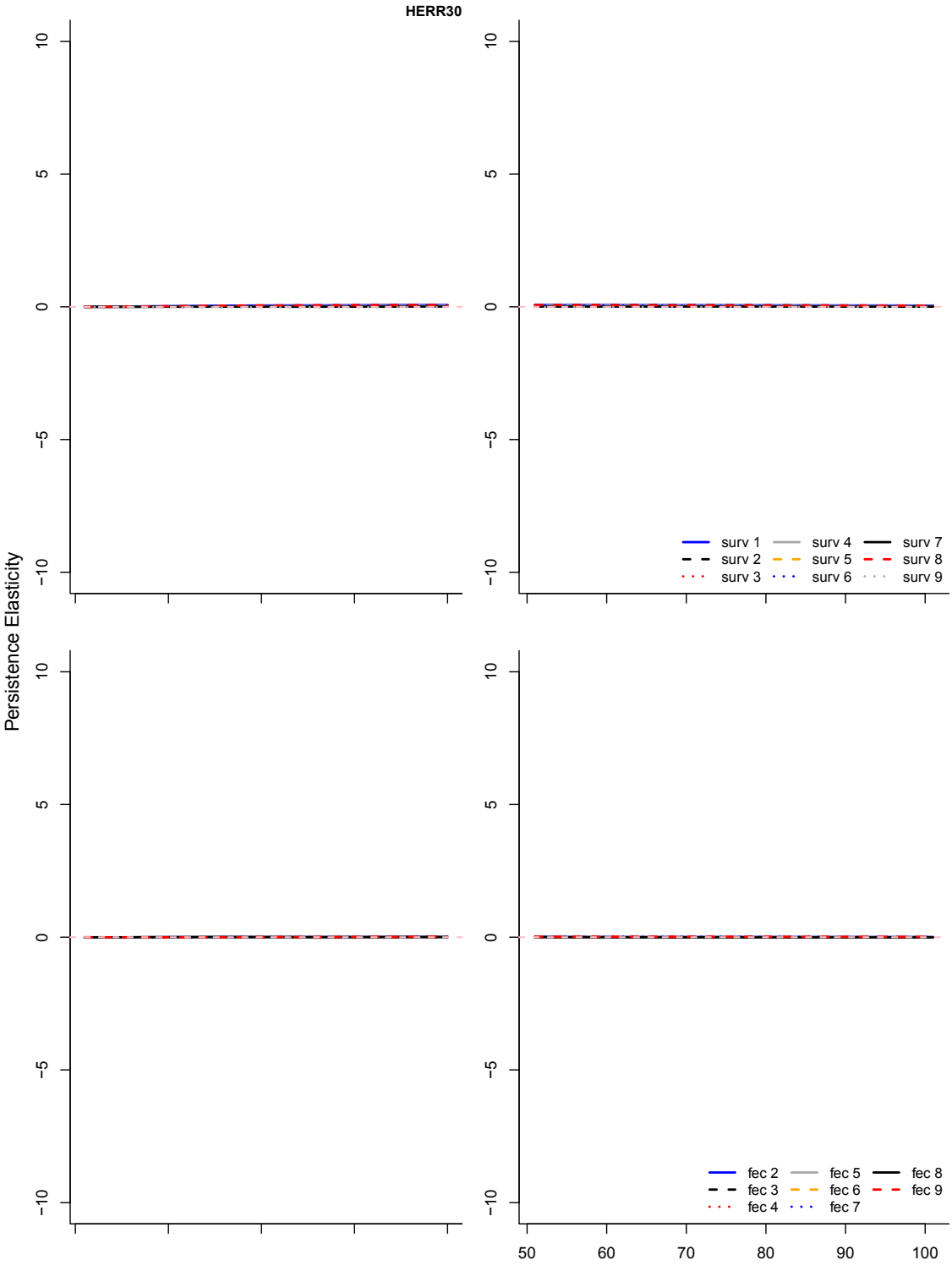

Figure C3s: Time series of the elasticity of the probability of persistence for each survival and fertility vital rate during periods of typical recruitment for each population (population name at top of figure). Populations with a zero percent probability of recovery after 50 years are excluded from this figure.

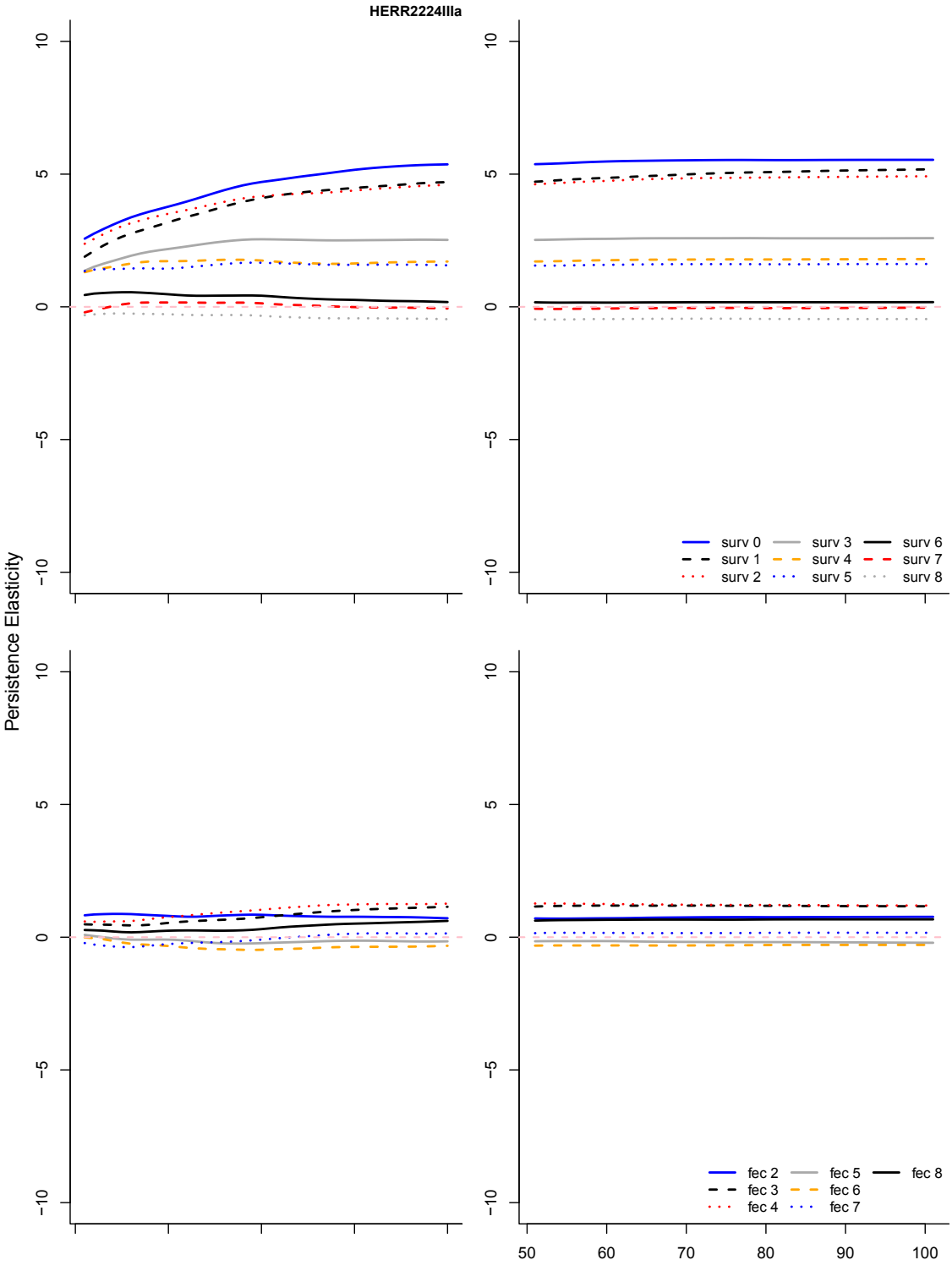

Figure C3t: Time series of the elasticity of the probability of persistence for each survival and fertility vital rate during periods of typical recruitment for each population (population name at top of figure). Populations with a zero percent probability of recovery after 50 years are excluded from this figure.

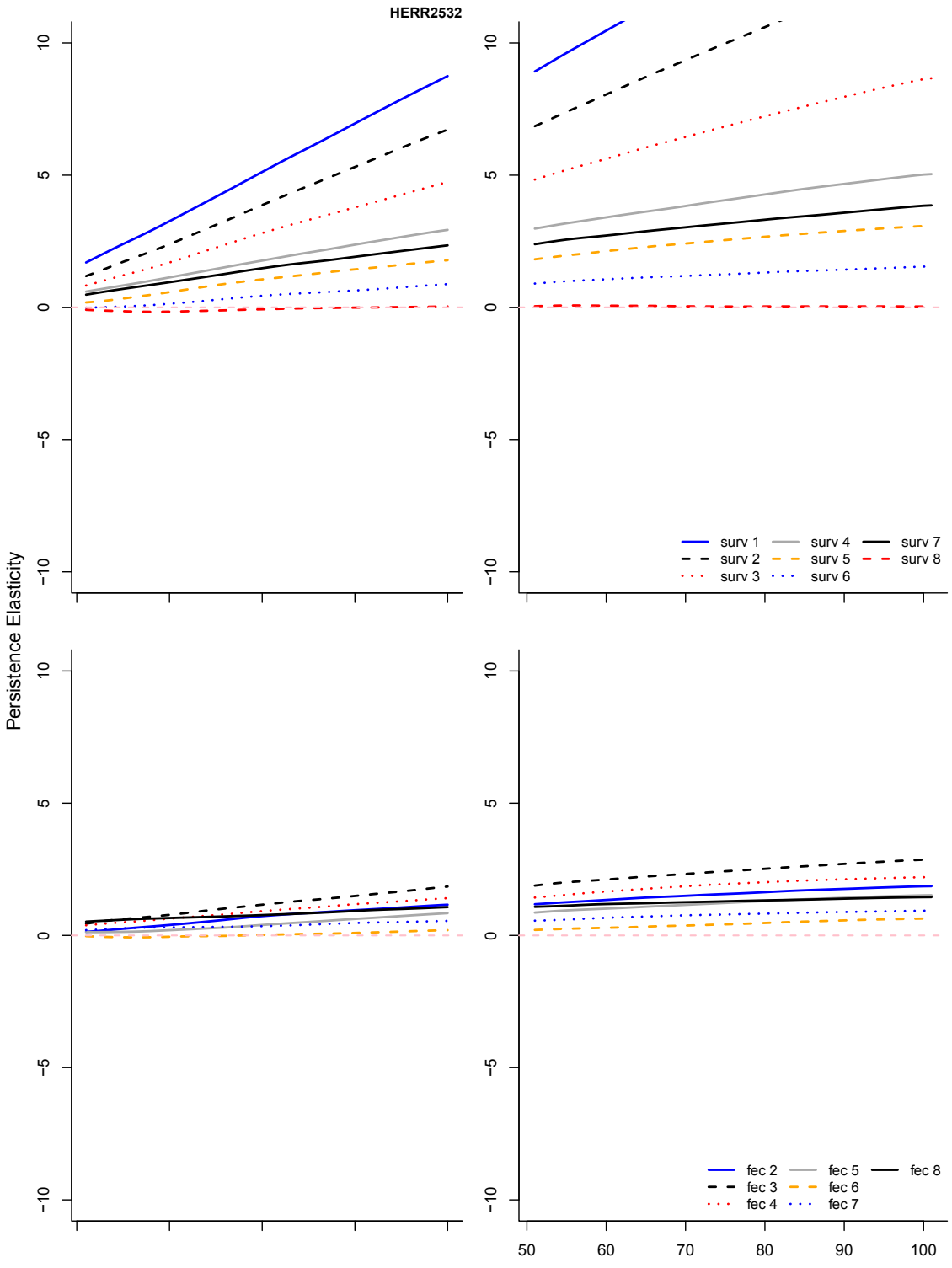

Figure C3u: Time series of the elasticity of the probability of persistence for each survival and fertility vital rate during periods of typical recruitment for each population (population name at top of figure). Populations with a zero percent probability of recovery after 50 years are excluded from this figure.

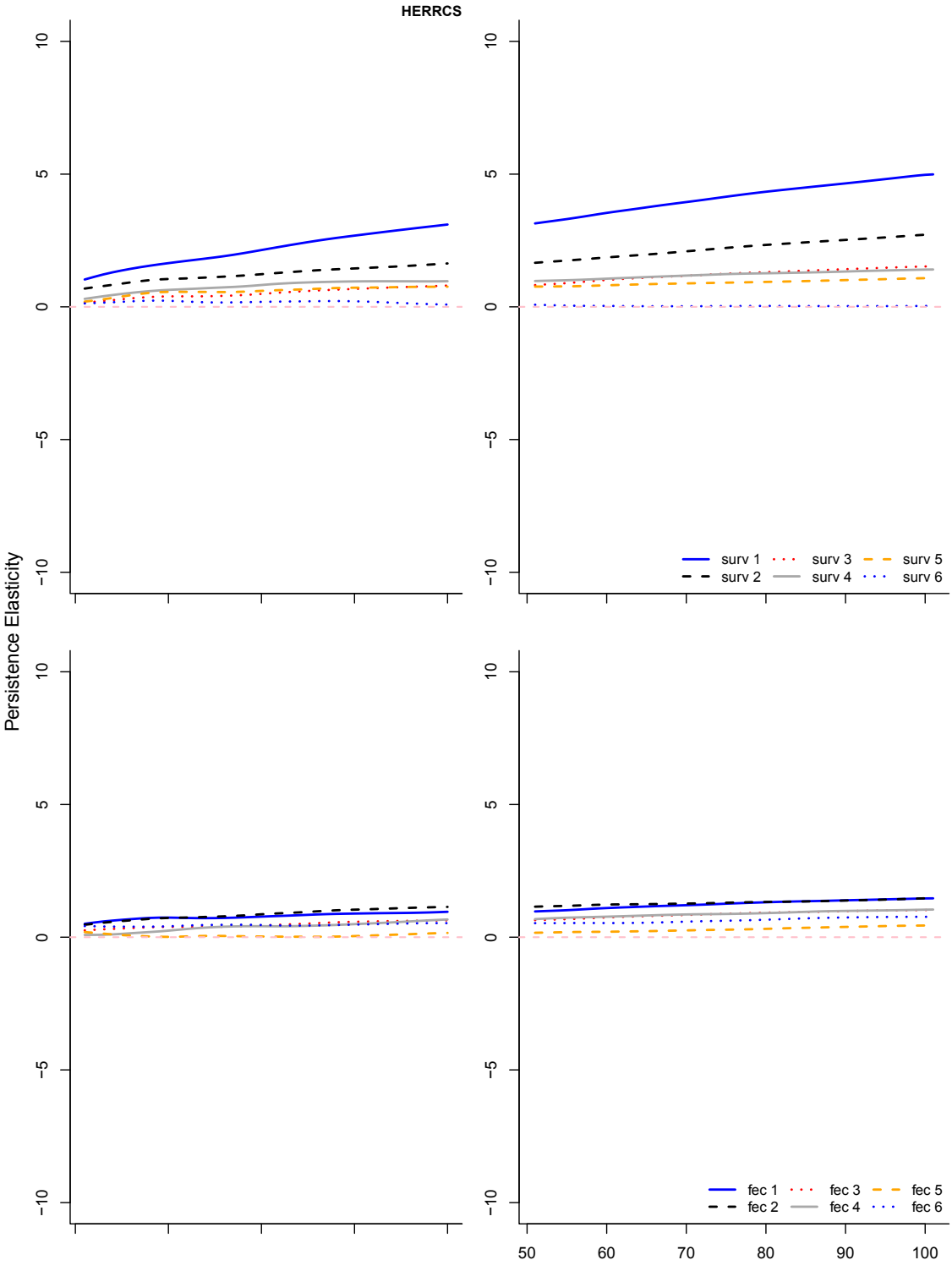

Figure C3v: Time series of the elasticity of the probability of persistence for each survival and fertility vital rate during periods of typical recruitment for each population (population name at top of figure). Populations with a zero percent probability of recovery after 50 years are excluded from this figure.

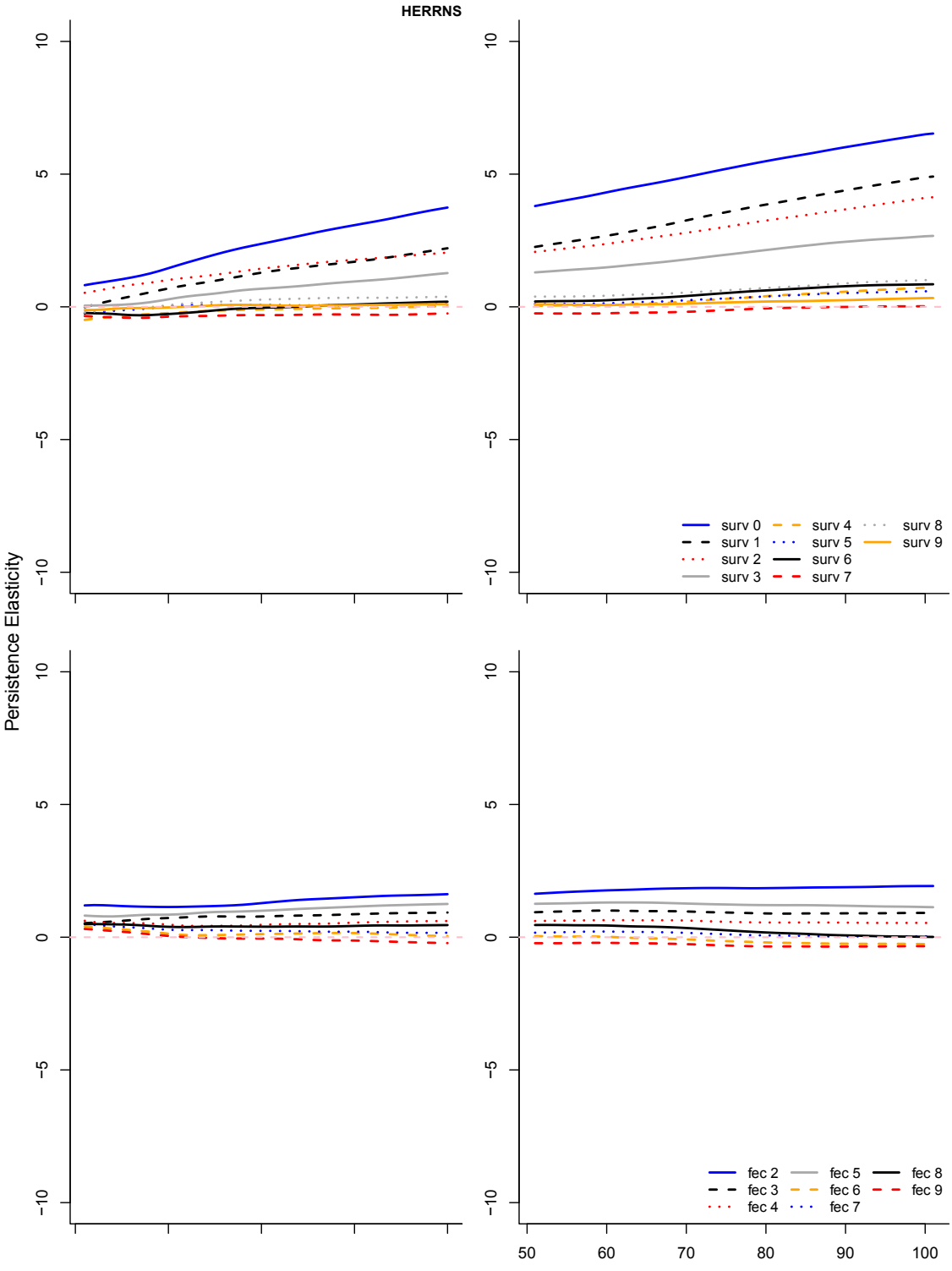

Figure C3w: Time series of the elasticity of the probability of persistence for each survival and fertility vital rate during periods of typical recruitment for each population (population name at top of figure). Populations with a zero percent probability of recovery after 50 years are excluded from this figure.

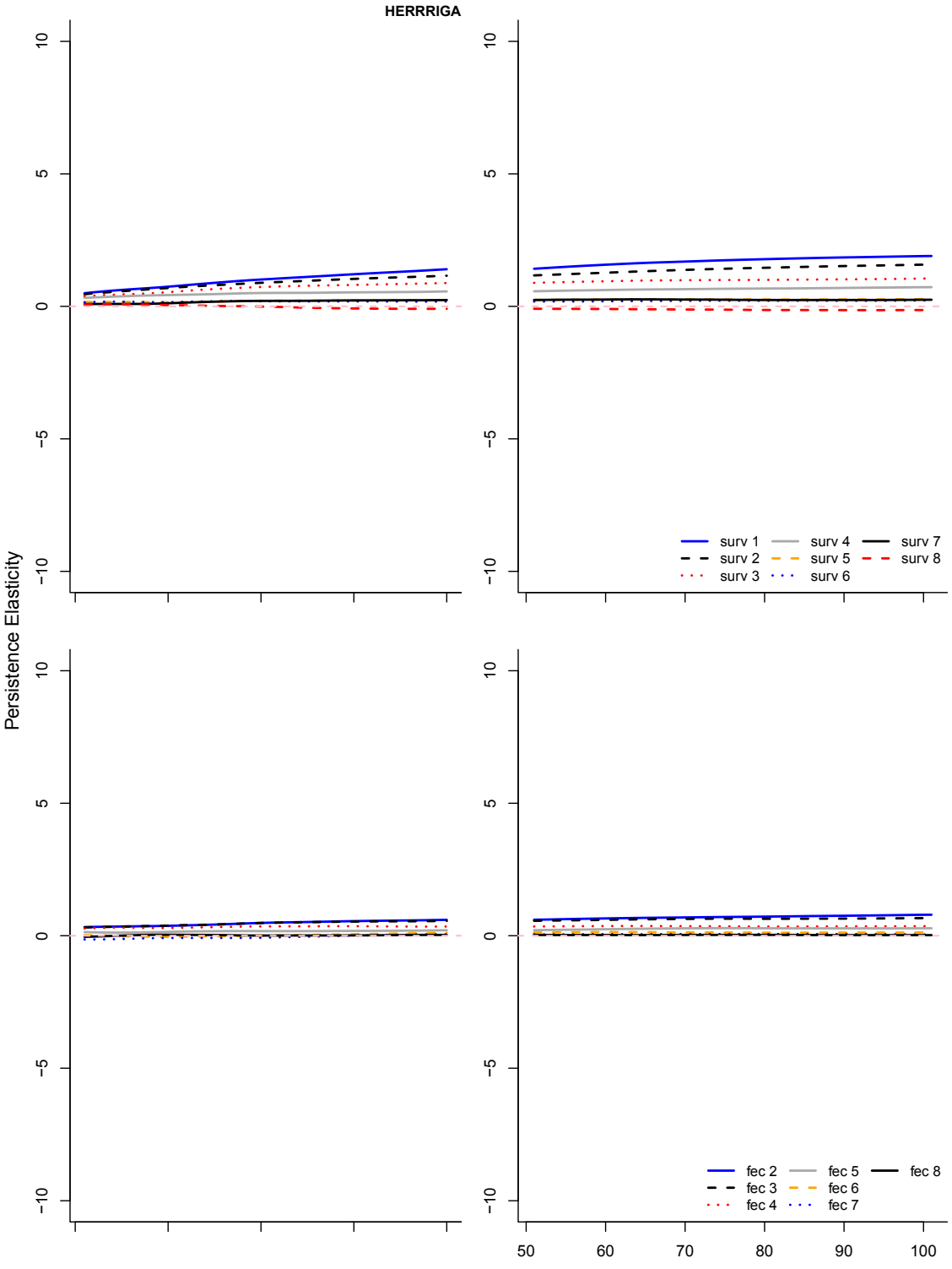

Figure C3x: Time series of the elasticity of the probability of persistence for each survival and fertility vital rate during periods of typical recruitment for each population (population name at top of figure). Populations with a zero percent probability of recovery after 50 years are excluded from this figure.

Appendix D

Electronic Supplement Description

The model fits for each populations functional responses (Chapter 3) can be found in Electronic Supplement A. The age-specific model fits for each population can be found in Electronic Supplement B. The code of the Population Viability Analysis can be found in Electronic Supplement C. These files are available from Dalspace

Appendix E

Copyright Agreement

NRC Research Press

Delivering **quality science** to the world
La **science de qualité** pour le monde entier

LICENCE TO PUBLISH (MANUSCRIPT)

THIS AGREEMENT made in duplicate this 25 (Day) day of April (Month) 2012 (Year) .

BETWEEN:

CANADIAN SCIENCE PUBLISHING (CSP)/ÉDITIONS SCIENCES CANADA (ESC), operating as NRC Research Press (herein referred to as "NRC Press")

AND: David Keith
Department of Biology
Dalhousie University
[illegible]
(name and address of copyright holder or authorized signing officer of institution, government, or corporation)

1. This refers to the manuscript entitled: Population dynamics of marine fishes at low abundance

(the "Manuscript"), manuscript number 2011-0355, written by the following

author(s): David M. Keith
Jeffrey A. Hutchings

for publication in: Canadian Journal of Fisheries and Aquatic Sciences

2. In consideration of NRC Press agreeing to publish the Manuscript, the Author(s) grant to NRC Press for the full term of copyright in the Manuscript and any extensions thereto, subject to clause 3 and 4 below, an irrevocable, royalty-free, exclusive licence in perpetuity *(a)* to publish, reproduce, distribute, display, and store the Manuscript in all forms, formats, and media whether now known or hereafter developed (including without limitation in print, digital or electronic form) throughout the world, *(b)* to translate the Manuscript into other languages, create adaptations, summaries or extracts of the Manuscript or other derivative works based on the contribution and exercise all of the rights set forth in *(a)* above in such translations, adaptations, summaries, extracts, and derivative works, *(c)* to license others to do any or all of the above, and *(d)* to assign this license.

3. Ownership of the copyright in the material contained in the Manuscript ("the Material") remains with the Author(s), and provided that, when reproducing the Manuscript or extracts from it, the Author(s) acknowledge and reference publication in the Journal, the Author(s) retain the following non-exclusive rights:

   (a) To post a copy of their submitted manuscript (pre-print) on their own Web site, an institutional repository, or their funding body's designated archive.

   (b) To post a copy of their accepted manuscript (post-print) on their own Web site, an institutional repository, or their funding body's designated archive. Authors who archive or self-archive accepted articles must provide a hyperlink from the manuscript to the Journal's Web site.

   (c) They and any academic institution where they work at the time may reproduce their Manuscript for the purpose of course teaching.

   (d) To reuse all or part of the Manuscript in other works created by them for noncommercial purposes, provided the original publication in an NRC Press journal is acknowledged through a note or citation in a format acceptable to NRC Press.

NRC Research Press

Delivering **quality science** to the world
La **science de qualité** pour le monde entier

LICENCE TO PUBLISH (MANUSCRIPT)

4. In consideration of the NRC Press agreeing to publish the Manuscript, the Author(s) also grant to NRC Press for the full term of copyright and any extensions thereto the same rights that have been granted in respect of the Manuscript as set out in clause 2 above, in supplementary data submitted with the manuscript to be made available on the Web site, but on a non-exclusive basis.

5. The Author(s) warrant and represent that:

   (a) The Author(s) are the sole authors and owners of the copyright in the Material. If the Material includes materials of others, the Author(s) have obtained the permission of the owners of the copyright in all such materials to enable them to grant the rights contained herein. Copies of all such permissions have been sent to the editorial or publisher's office.

   (b) The Author(s) qualify for authorship, and the manuscript, or its equivalent, has not been submitted for publication elsewhere. If it is accepted for publication by the NRC Press, it, or its equivalent, will not be submitted for publication elsewhere.

   (c) All of the facts contained in the Material are true and accurate.

   (d) Nothing in the Material is obscene, defamatory, libellous, violates any right of privacy or infringes any intellectual property rights (including without limitation copyright, patent or trademark) or any other human, personal or other rights of any kind of any person or entity or is otherwise unlawful.

   (e) Nothing in the Material infringes any duty of confidentiality which any of the Author(s) may owe to anyone else or violates any contract, express or implied, of any of the Author(s), and all of the institutions in which work recorded in the Material was carried out have authorized publication of the Material.

6. The Author(s) authorize NRC Press to take such steps as it considers necessary, in its own absolute discretion and at its own expense, in the Author(s)' name and on their behalf if it believes that a third party is infringing or is likely to infringe copyright in the Manuscript, including but not limited to taking legal proceedings.

7. The Author(s) hereby consent to the inclusion of electronic links from the material to third-party Material wherever it may be located.

8. The Author(s) warrants that he/she is:
   (check only one option)

- ☐ the sole Author of the Manuscript and the sole owner of the copyright in the Material and the Manuscript,
- ☒ a co-author of the Manuscript and a part owner of the copyright in the Material and the Manuscript, in conjunction with interests held by co-authors, or their employers,
- ☐ an agent of my employer with authority to assign the copyright in the Material and the Manuscript owned by the employer, who is:

CANADIAN SCIENCE PUBLISHING | ÉDITIONS SCIENCES CANADA

NRC Research Press

Delivering **quality science** to the world
La **science de qualité** pour le monde entier

LICENCE TO PUBLISH (MANUSCRIPT)

9. Submission of this Manuscript does not guarantee publication. If the Manuscript is withdrawn, rejected, or not published within 2 years after acceptance, the licence is revoked.

Signed at Halifax NS (*City, Province or State*) on 25 April 2012 (*day month year*)

Name & Title: David Keith (*Please print*) Per: David Keith (*Signature*)

Digitally signed by David Keith
DN: cn=David Keith, o=Dalhousie University, ou=Dept. of Biology, email=keithdm@dal.ca, c=CA
Date: 2012.04.25 07:53:18 -03'00'

Reset form Print form and sign